

Development of Biomimetic and Template Assisted Selective C–H activation

**Submitted in partial fulfilment of the requirements
of the Degree of**

DOCTOR OF PHILOSOPHY

by

JYOTI PRASAD BISWAS

(164033017)

Supervisor

Prof. Debabrata Maiti



**DEPARTMENT OF CHEMISTRY
INDIAN INSTITUTE OF TECHNOLOGY BOMBAY**

2022

*Dedicated
to my
Beloved Family*

Approval Sheet

This thesis entitled “*Development of Biomimetic and Template Assisted Selective C-H activation*” by **Jyoti Prasad Biswas** (Roll No. **164033017**) is approved for the degree of Doctor of Philosophy.



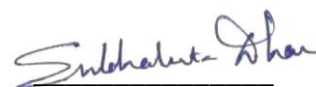
External Examiner



Internal Examiner



Supervisor



Chairperson

Date: 14.03.2023

Place: Department of Chemistry, IIT Bombay

Declaration

I declare that this written submission represents my ideas in my own words and where others' ideas or words have been included, I have adequately cited and referenced the original sources. I also declare that I have adhered to all principles of academic honesty and integrity and have not misrepresented or fabricated or falsified any idea/data/fact/source in my submission. I understand that any violation of the above will cause for disciplinary action by the Institute and can also evoke penal action from the sources which have thus not been properly cited or from whom proper permission has not been taken when needed.

Jyoti Prasad Biswas

Jyoti Prasad Biswas
(Name of the student)

164033017
(Roll No.)

Date: 14.03.2023

Acknowledgement

To start with I would like to express my deepest regards and gratitude towards my supervisor Prof. **Debabrata Maiti** for supporting me and providing me with the necessary guidance throughout my Ph.D. journey. His sincere efforts have made the lab environment extremely friendly and cordial. He has given me full freedom to pursue various projects without any objection and has given many insightful discussions into each and every minute topic. He has given me enough motivation and positive feedback throughout my entire Ph.D. programme. His enthusiasm, knowledge and scientific inputs has helped me to become an independent thinker. Amongst various other things, he has instilled in me the importance of always being technically sound and scientifically ethical and as well as a good human being.

I would like to acknowledge IIT Bombay and Department of Chemistry for providing infrastructure and facilities to carry out my research and CSIR India for providing me fellowship. I would also like to thank my 'Research Progress Committee' members, **Prof. Santosh J. Gharpure** and **Prof. Gopalan Rajaraman** for valuable and constructive suggestions to improve my research work.

I'm thankful to the entire staff of the Department of Chemistry, in particular Mrs. Shweta for processing thesis documents, Mr. Narendra and Mr. Niteen for NMR and ESR spectroscopy, Mr. Rajesh for Mass spectroscopy, Mr. Darshan Mahatre for X-ray Crystallography and Mr. Ratish Sekhar for their kind help and cooperation throughout my research period.

I am very happy to acknowledge all my seniors and labmates especially Dr. Sujoy Rana, Dr. Tapas Kr. Achar and Dr. Srimanta Guin for supporting and guiding me all throughout my research period. Their ideas, knowledge and excellent skills has motivated me.

I sincerely extend my heartfelt gratitude to all graduated seniors Ph. D. students Dr. Naveen Togati, Dr. Soham Maity, Dr. Tuhin Patra, Dr. Atanu Modak, Dr. Argha Deb, Dr. Arun Maji, Dr. Soumitra Agasti, Dr. Sukdev Bag, Dr. Uttam Dutta, Dr. Sandeep Pimparkar, Dr. Sheuli Sasmal senior and current postdoc students Dr. Ramasamy Jayarajan, Dr. Ramakrishna Kankanala, Dr. Anjana Ramesh, Dr. Sadhan Jana, Dr. Wajid Ali, Dr. Sayan Roy, Dr. Prasun Mukherji for mentoring, teaching and encouraging during my studies. I would like to specially mention labmates cum friends Pravas Dolui, Dr. Sandip Porey, Dr. Jayabrata Das, Chandrashekar HB, Tapas Pal for supporting all way possible throughout this journey. I am also thankful to the former and current lab members Soumya Kumar Sinha, Trisha Bhattacharya, Sukumar Pradhan, Sudip Maiti, Nupur Goswami, Gaurav Prakash, Argha Saha, Astam Mandal, Animesh Ghosh, Jagrit Grover, Suman Maji, Tanay Pal, Suparna Dutta, Yogesh Bairagi, Adithyaraj and Aashi for their cooperation and help.

This journey would not have been possible without the support of my family, especially my brother Mr. Prasenjit Biswas, without whom I would never have reached this stage.

Outside of work zone I would like to thank my friends Dr. Aditya Borah, Dr. Hemen Gogoi and Krishna Puri, for standing by me all the time. I would also like to thank Dr. Arijit Singh Hazari, Dr. Rajesh Das, Dr. Salman Khan, Raktim Saikia and all my PhD batchmates for supporting me throughout. I would like to specially mention Dr. Geeti K. Dutta, Avilasha A. Sandilya, Dikshita Sharma, Uttam Pradhan and Suravi Saha for their mental support.

I would like to thank the Almighty for giving me strength to complete my Ph.D. Though I may have missed to mention some friends and colleagues by name, I greatly appreciate all their support and help throughout my time at IIT Bombay.

Jyoti Prasad Biswas

List of Abbreviations

°C	Degree Celsius
Atm	Atmosphere
Ar	Aryl
<i>i</i>Pr	Iso propyl
<i>t</i>Bu	Tertiary butyl
Cy	Cyclohexyl
cat.	Catalyst
acac	Acetylacetonate
calcd.	Calculated
dba	Dibenzylideneacetone
DCM	Dichloromethane
DMF	Dimethyl Formamide
DG	Directing group
DMSO	Dimethyl Sulfoxide
DCE	Dichloroethane
DTBP	Di-tertiary-butyl peroxide
equiv.	Equivalent
ESI	MS Electrospray Ionization Mass Spectrometry
Et₂O	Diethyl ether
EtOAc	Ethyl acetate
etc.	Et cetera
et al.	Etalii
EtOH	Ethanol
EWG	Electron-withdrawing group
EDG	Electron-donating group
GC	Gas chromatography
h	Hour

HRMS	High resolution mass spectrometry
HFIP	1,1,1,3,3,3-Hexafluoroisopropanol
IR	Infrared spectroscopy
KIE	Kinetic isotope effect
L	Ligand
MeOH	Methanol
mL	Milli liter
MS	Molecular sieves
mmol	Milli mole
M.P.	Melting point
NMR	Nuclear Magnetic Resonance
OAc	Acetate
OMe	Methoxy
Ph	Phenyl
rt	Room temperature
SET	Single electron transfer
t-BuOH	Tertiary butyl alcohol
TFA	Trifluoroacetic acid
t-Amy-OH	Tertiary amyl alcohol
DCE	Dichloroethane
TFT	Trifluorotoulene
THF	Tetrahydrofuran
TLC	Thin layer chromatography
TFE	Trifluoroethanol
XRD	X-Ray Diffraction
IR	Infrared Spectroscopy
HRMS	High resolution mass spectroscopy
KIE	Kinetic Isotope Effect

Table of Contents

Chapter 1

Introduction	1-17
1.1. General Introduction	1
1.2. Background	
1.2.1. Halogenation by non-heme iron-oxo	9
1.2.2. Non-covalent interaction mediate distal C–H functionalization of heterocycles	12
1.3. References	13

Chapter 2

Selective C–H Halogenation over Hydroxylation by Non-heme Iron(IV)-oxo and Iron(II)-halide Complexes	19-56
---	-------

Abstract	21
2.1. Introduction	23
2.2. Results and Discussion	25
2.3. Conclusions	36
2.4. Experimental details	36
2.4.1. Materials and Methods	36
2.4.2. Synthesis and characterization of complexes	37
2.4.3. General procedure for sp ³ C–H oxidation reactions	44
2.4.4. General procedure for 18-O labelling study for sp ³ C–H oxidation reactions	44
2.4.5. Kinetics study	44
2.4.6. General procedure for sp ³ C–H halogenations reactions	50
2.4.7. Representative GC-MS data of the products	51
2.5. References	53

Chapter 3

Regiocontrolled Remote C–H Olefination of Small Heterocycles	60-116
---	--------

Abstract	60
3.1. Introduction	62
3.2. Results and Discussion	63
3.3. Conclusions	68
3.4. Experimental details	68
3.4.1. Materials and Methods	68
3.4.2. Procedure for synthesis of tridentate template	69
3.4.3. Template regeneration	74
3.4.4. Mechanistic study	75
3.4.5. Compound Characterization Data	76
3.4.6. Representative NMR spectra	107
3.5. References	115

Chapter 4

Palladium catalyzed template directed C-5 selective olefination of thiazoles 120-155

Abstract	120
4.1. Introduction	122
4.2. Results and Discussion	125
4.3. Conclusions	130
4.4. Experimental details	131
4.4.1. Materials and Methods	131
4.4.2. General Procedure for synthesis of tridentate template	131
4.4.3. General Procedure for C-5 selective C–H olefination of thiazoles	132
4.4.4. Template regeneration	132
4.4.5. Characterization data	133
4.4.6. Representative NMR spectra	147
4.5. References	153

Chapter 5

Co-ordination assisted distal C–H alkylation of fused heterocycles 159-225

Abstract	159
5.1. Introduction	161
5.2. Results and Discussion	163
5.3. Conclusions	170
5.4. Experimental details	170
5.4.1. Materials and Methods	170
5.4.2. Procedure for synthesis of template	171
5.4.3. Template regeneration	175
5.4.4. Optimization	175
5.4.5. Characterization data	180
5.4.6. Representative NMR spectra	215
5.5. References	222

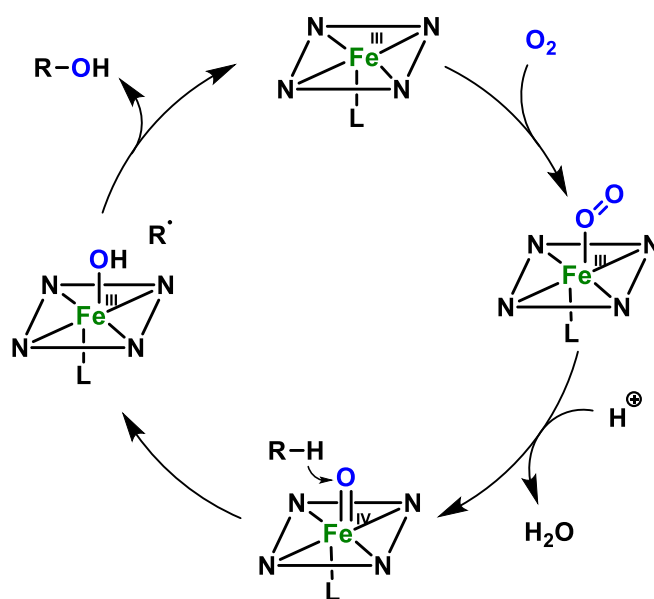
Chapter 1

Introduction

1.1.General Introduction:

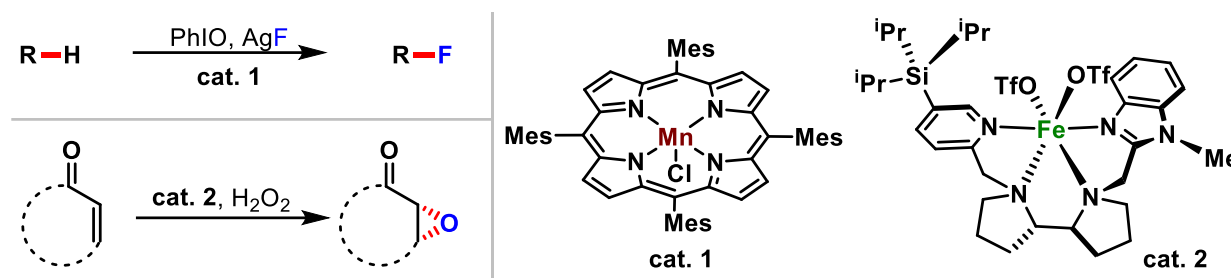
The development of innovative methodologies in order to achieve atom economic and cost effective manner is an ever evolving process in synthetic chemistry.¹ While some newly discovered pathways sharply reduced number of steps in total synthesis of vital molecules, others provide access to completely newer entities.² There are also reaction discoveries which help us solve mechanistic mysteries. However, the common goal behind all the advancements in laboratory is towards the application in the real world.³ The first major breakthrough in the evolution of synthetic chemistry is probably the use of a catalyst. Although catalysis originated way back in 16th century, the true role of catalyst was understood in 18-19th century.⁴ At present day, hardly any reaction is carried out without catalyst, be in industry or academic laboratory which is evident from the fact that production of 90% commercial goods involve use of catalysts.⁵ Besides, all the natural transformations are carried by the class of most efficient catalysts known as enzymes.⁶

Transition metals constitutes chief part of the catalyst community due to multiple advantages.⁵ Presence of partially filled d-orbitals allow them to access multiple co-ordination numbers as well as oxidation numbers.⁷ As a result, two or more reactant fragments can be accommodated by the metal, make them react and release the product. Another fascinating fact is the possibility of manipulating orbital energy (viz. HOMO and LUMO) through ligation to synergize with reactants.⁸ Owing to these incredible characteristics, transition metal catalysis has revolutionized synthetic and industrial chemistry in the past few decades. This can be comprehended from examples such as Zeigler-Natta catalysis, cross-coupling reactions etc. For instance, in current scenario, polymers are integral part of mankind, the growth of which began with the discovery of Zeigler-Natta catalysis and cross-coupling reactions has even greater impact due its vast use in fragrance to pharmaceutical industries.⁹⁻¹⁴



Scheme 1.1: Hydroxylation mechanism at active site of P450 type enzymes.

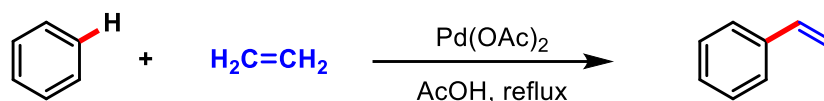
The most abundant bond found in organic realm is the C–H bond.¹⁵ For the obvious reason, the simplest and cheapest feedstock is also rich with these bonds. Therefore, the straightforward and cost-effective way to synthesize a functionalized molecule would be direct replacement of a C–H bond with the functional group.¹⁶ However, there are two fundamental challenges associated with this approach, firstly the high bond dissociation energy of C–H bond and similarity in electronegativity, and secondly the selective scissoring of one bond in their omnipresence. Nonetheless, this is a common natural approach towards enzyme catalyzed functionalization during biosynthesis.¹⁸ For instance, cytP450 enzymes are well known for installation of –OH group in a hydrocarbon.¹⁹ Such enzymes are usually equipped with a metal containing heme or non-heme active site embedded into a protein structure. These metal centers undergo oxidation to form highvalent metal-oxo species, which are capable of hydrogen atom abstraction (HAA) at biological temperature. The tertiary structure of the protein chain provides a specific substrate binding pocket so that only the particular bond to be functionalized is exposed to the active site. After the HAA, functional group incorporation takes place in a comparatively faster step resulting in site specific functionalization (**scheme 1.1**).



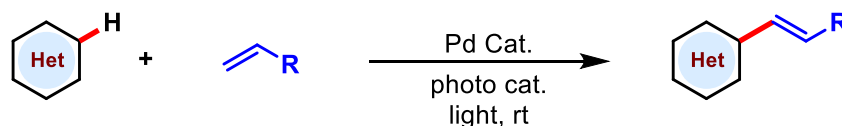
Scheme 1.2: Functional mimics of enzyme active sites.

C–H activation is a relatively newer concept in synthetic chemistry.²⁰ Although functionalization *via* metal mediated C–H activation might have started around the end of 19th century²¹, however its recognition started from 1970's.²² Due to step economy and non-requirement of pre-functionalized starting materials, C–H functionalization through activation gained immense attention and has seen exponential growth, yet far from reaching its full potential. At an early stage, more focus was concentrated on the biomimetic systems. Heme and non-heme based active site mimics of Fe, Mn, etc. have been studied over the years by forming high-valent metal-oxo complexes (**scheme 1.2**). Initially, uncontrolled product formations were observed due to their high reactivity and absence of protein chain. Gradual ligand modification and computational studies provided improved selectivities.²³⁻²⁸ Pioneering works of Que, Groves and others not only showed that the biomimetic complexes can be very efficient in C-H functionalization, but also provided insight into the mechanisms of biocatalysis.^{29,30} Enantioselective transformations are also found to be possible with proper ligand designing, although ee for C–H functionalization is still very poor.³¹ From sustainable point of view, this approach is highly valued as reactions occur at room temperature and water can be used as solvent, however these strategies yet to find their industrial application and further improvements are required.

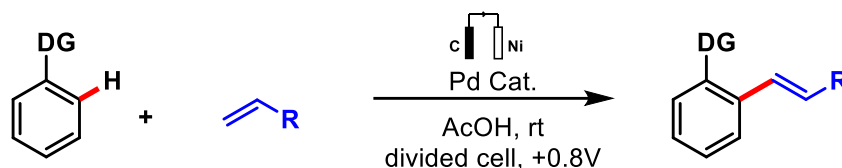
a) Fujiwara-Moritani reaction



b) Photocatalysed C–H activation



c) Electrocatalysed C–H activation



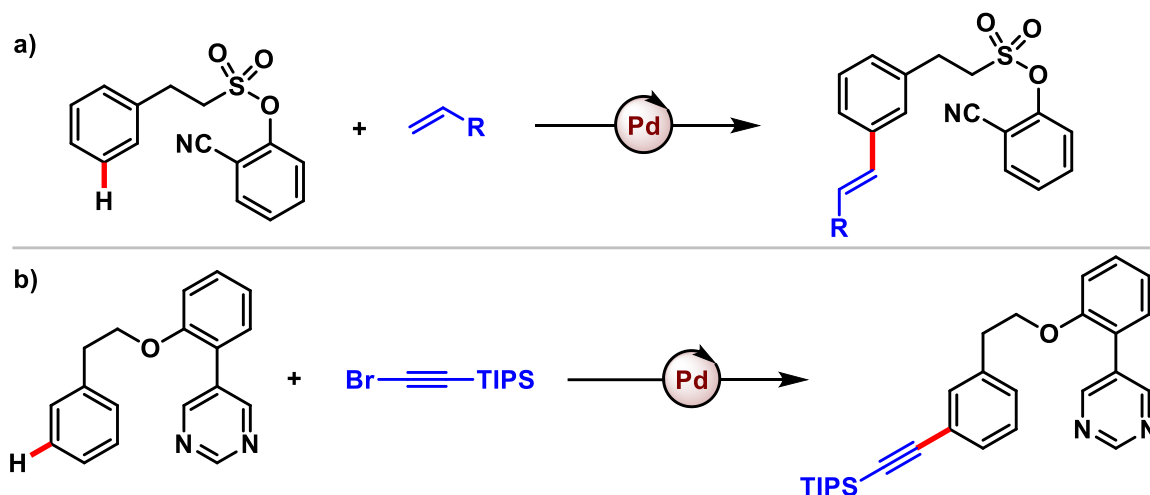
Scheme 1.3: Examples of C–H activation by different approaches.

Co-ordination and organometallic complexes of second and third transition series meanwhile became popular for C–H activation.²² With the discovery of agostic interaction and metal-alkyl complexes, the idea of weakening C–H bond for organic transformation became prominent.³² At the same time, cross-coupling reactions were being established.^{33,34} The obvious thought arised among the community that, if a metal-alkyl or metal-aryl complex can be synthesized *via* C–H activation instead from an alkyl halide, the following steps should be similar with that of cross-coupling for functionalization. With this motivation, Fujiwara and Moritani in year 1969 started the modern era of functionalization *via* C–H activation, by reporting olefination of benzene with alkene.³⁵ Numerous combination of hydrocarbons (aromatic as well as aliphatic), functional groups and catalysts has been studied since then.^{22,36,37} Although many metals are found to be capable of carrying out such functionalization, till now palladium has the highest success rate.^{38,39} Several mechanistic studies and general observation also made an impression that a salt of silver and HFIP as solvent are usually required for best performance,

however the stereotype is denied every now and then. In fact, electrocatalysis, photocatalysis etc. have also made their debut in the field (**scheme 1.3**).⁴⁰⁻⁴¹

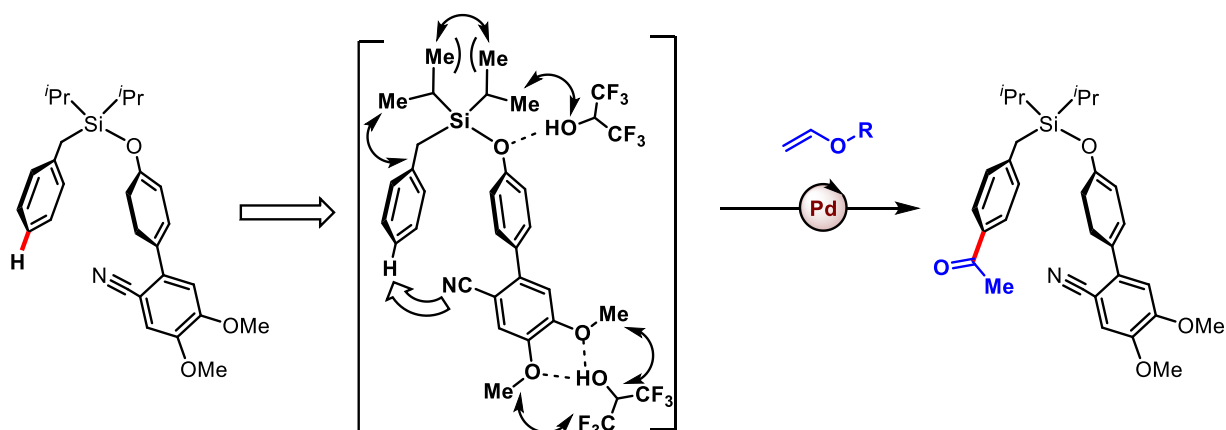
The more challenging part than the bond activation itself is the controlling the selectivity in multi-presence of energetically equivalent and non-equivalent C–H bonds within the system. Although inherent electronic properties of biased substrates can sometime allow site preferential functionalization, generalization has been inconvenient.⁴² Among various approaches to control selectivity, directing group approach became popular rapidly.⁴³ In this approach, a heteroatom present either in the native functional group or in a purposefully attached moiety, coordinates and directs the catalyst metal towards a specific C–H bond. At first, only selective *ortho*-C-H functionalizations of aromatic systems were seen compatible with the approach and soon extended to β -functionalizations in aliphatic systems.⁴⁴⁻⁴⁵ Keto, acid, amide etc. were proved to be extremely useful directing groups with the help of which numerous functionalized products were synthesized. The ease of *ortho* and β -C-H activation arises from the thermodynamic stability of the 5 or 6 membered metallacyclic intermediate formed upon activation. However, for the same reason selective activation of a distal C–H bond such as *meta* and *para*-C–H bonds in arenes were found difficult. Bypassing an *ortho*-C-H bond to form a 12-16 membered metallacycle is not only thermodynamically disparaging but also requires structural precision. Realizing that to achieve distal C–H activation, a structurally rigid yet reversibly coordinating group would be required, Yu and co-workers first introduced cyanophenyl directing group and successfully carried out palladium catalysed meta-olefination.⁴⁶ Gradually, modifications of directing group and diversifications have been made by various group.^{47,48} In that context, our group has contributed majorly in functionalization diversification using a relatively superior pyrimidine based directing group (**scheme 1.4**).⁴⁹ While the –CN group is chemically insecure under acidic or basic conditions and shows

competitive end-on and side on binding, pyrimidine can bear more extreme conditions and also provides better co-ordination with catalyst through back-bonding due to presence of an extra nitrogen in the ring.



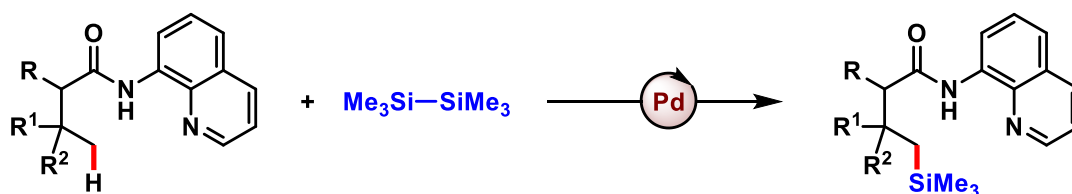
Scheme 1.4: *meta*-C-H activation with a) cyano DG and b) pyrimidine DG

Our group took DG assisted distal C-H activation to a further step by reporting first *para* functionalization of arenes. A biphenylcyano group, tethered to the arene substrate with a diisopropyl group was used as the DG.⁵⁰ The most challenging part was to keep the directing group in the vicinity of the substrate having a 13 atom distance between the C-H bond and directing atom. Experimental evidences suggest that there are two major factors that makes it a success, i) Thorpe-Ingold effect exerted by the two isopropyl groups and ii) π -interaction between substrate and DG arenes. It was later discovered that introducing two methoxy groups at *meta* and *para* to the cyano improves the reactivity. X-ray crystallographic studies showed hydrogen bonding of the methoxy groups with HFIP to further restrict DG's movement has a role to play in the enhancement (**scheme 1.5**).⁵¹

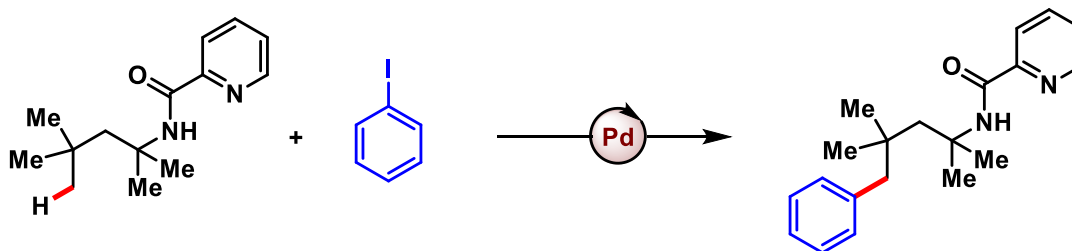


Scheme 1.5: DG assisted *para*-selective C-H functionalization.

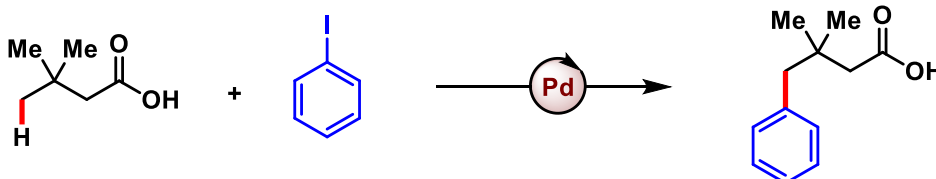
a) Aliphatic γ -C-H activation



b) Aliphatic δ -C-H activation



c) Inherent functional group directed aliphatic γ -C-H activation



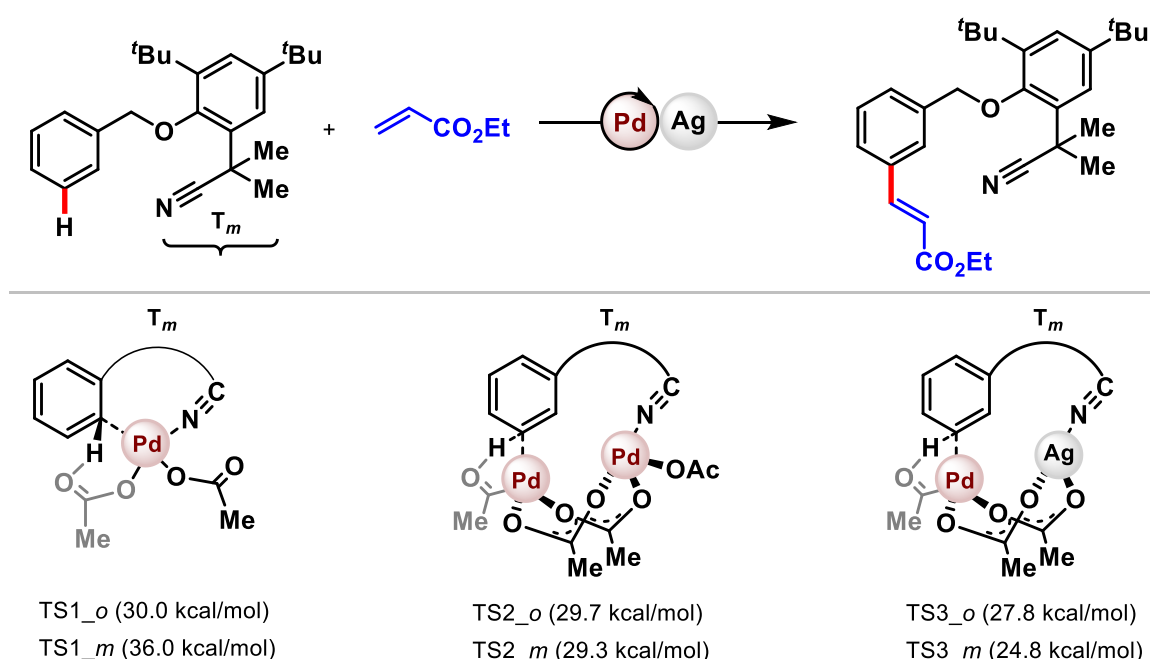
Scheme 1.6: Distal aliphatic C-H bond activation.

Simultaneously, functionalizations of aliphatic distal C-H bonds have also been discovered despite being more challenging comparatively.⁵² The aliphatic systems exert higher entropic barrier as well as the resultant organometallic intermediates are less stable. Mostly bidentate

and monodentate directing groups have been utilized for functionalization at different positions. To overcome the entropic barrier, usually specific substrate designs are required. Our group as well has discovered various methodologies for incorporating functionalities at γ - and δ -position (**scheme 1.6**).^{53,54} Recently, we along with others have developed directing group free distal C(sp³)-H functionalization with the help of inbuilt functional group such as carboxylic acid.⁵⁵

There have been number of mechanistic suggestions for the C–H activation.⁵⁶ Among which, concerted-metalation-deprotonation (CMD) is believed to be involved in most cases. CMD pathway initiates with interaction of the metal with sigma orbital of the C-H bond.⁵⁷ Gradually, the M-C bond starts to form while the hydrogen is being abstracted by a base simultaneously. In the transition state the four centers are loosely connected and depending on the metals position with respect to the C-H bond, the metalation can be oxidative, electrophilic or nucleophilic in nature. Once the metal-carbon intermediate is formed, various classical organometallic reaction steps lead to the functionalized product. To maximize the yields of such reactions, use of proper ligand and other additives are required along with the catalyst. It has been observed that, most of the palladium catalyzed methodologies utilize amino acid based ligands.⁴⁸ Computation and optimization studies revealed that amino acid co-ordination with palladium synergizes its concerned orbital with C–H bond. Moreover, inclusion of acetate or similar protecting group at the nitrogen center increases the deprotonation rate due to intramolecular action. It has also been observed that silver salts of carbonate or carboxylate play a crucial role in the transformations.⁵⁸ Although the straight forward explanation is its role in oxidation of the catalyst, also brings the question why other oxidizing agents tend to fail. Various studies prove that silver has multiple roles such as ligand exchange with catalyst, transmetalation and most importantly, it reduces the energy of C–H activation by forming a Pd-Ag bimetallic cluster (**scheme 1.7**).

Being highly effective, C–H activation has not only replaced many classical reactions, but also provided access to previously unknown molecules. Thus, C–H activation is proving to be a sustainable tool in the field of synthetic chemistry. However, we are far from reaching its full potential, and the scope for development is vast. For instance, these reactions are usually high energy demanding and functionalization of heterocycles *via* this method is scarce. In one part of the thesis, a biomimetic non-heme catalyst to mimic enzymatic halogenation, while in the other part, selective distal C–H functionalizations of heterocycles has been addressed.



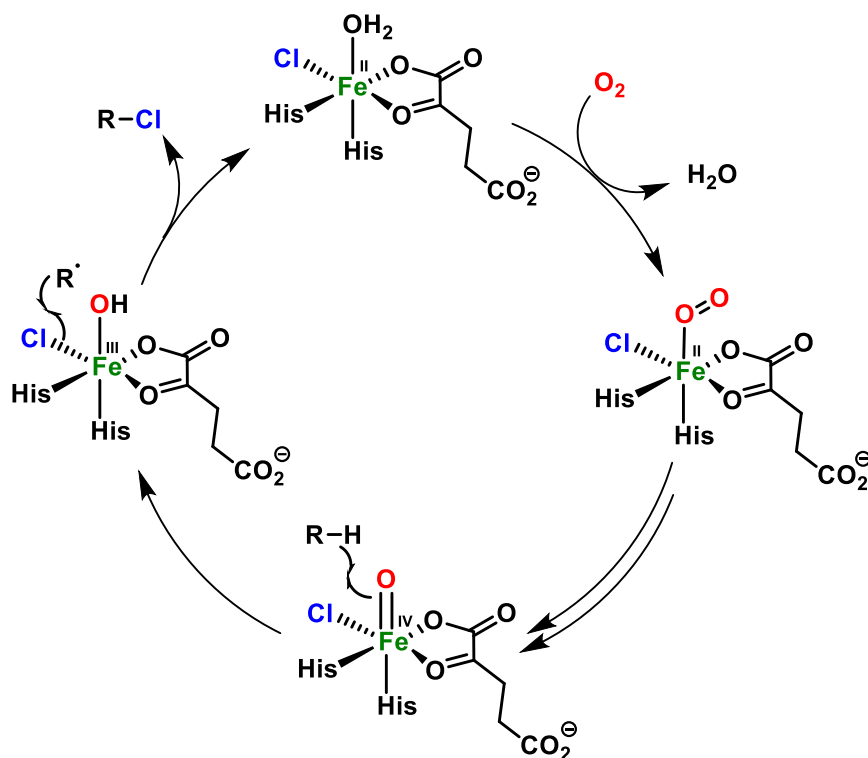
Scheme 1.7: Role of silver in achieving distal C–H activation.

1.2. Background:

1.2.1. Halogenation by non-heme iron-oxo:

In order to achieve catalytic effectiveness of enzymes, mimics of their active sites are being studied for decades. Among those, highvalent iron-oxo complexes are most widely considered.^{27,59} Although oxidation reactions with these complexes are well established, other

functionalizations such as halogenations are rare, particularly by non-heme iron-oxo complexes. Similar to any other iron-oxo enzymes, active-sites of such halogenases also abstracts hydrogen from hydrocarbon at the first step. Subsequently, the halide coordinated to the metal center rebounds with the radical to provide halogenated product.⁶⁰



Scheme 1.8: Mechanism for halogenation by α -KG dependent non-heme iron halogenase.

For instance, in α -ketoglutarate (α -KG) dependent SyrB2 halogenase has the iron center coordinated with two histidine residue, one aspartate residue, one halide and a water molecule *cis* to each other in its active site.⁶¹ An oxo ligand replaces the water molecule *via* oxidation to form the active species. Due to high affinity of iron-oxo to abstract hydrogen, it readily provides alkyl radical. The metal is now coordinated with both hydroxyl and halide ligand. Experimental evidences shows that the hydroxyl rebound and chloro rebound under the normal circumstances does not differ much energetically. Despite this, the protein cavity positions the

radical in such a way so that it can access only the halide to produce halogenated compound (scheme 1.8).

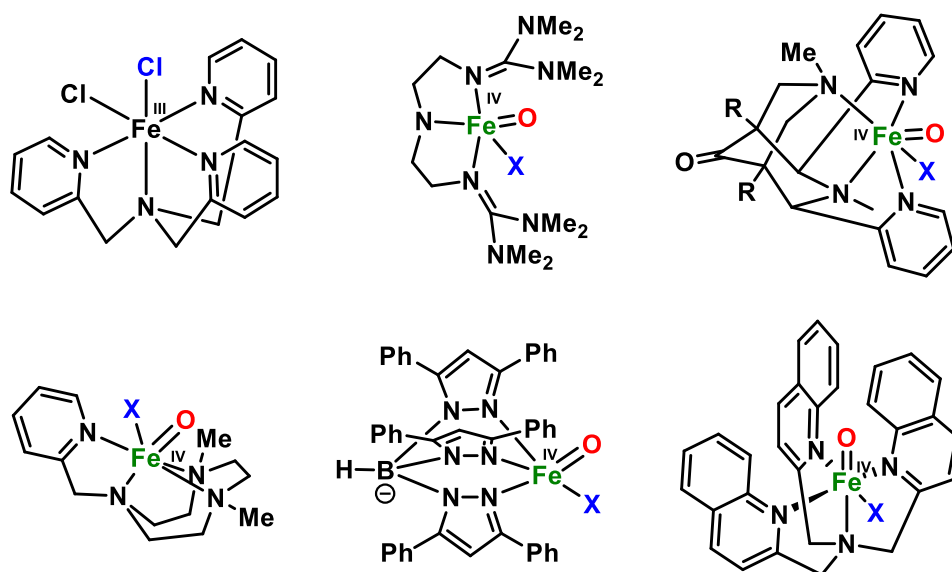


Figure 1.1: Non-heme iron-oxo complexes used for structural and functional mimic of halogenases.

In 2006, Que and co-workers synthesized first model non-heme halogenase with *N,N,N*-tris(2-pyridylmethyl)amine (TPA) ligand.⁶² The dichloride complex upon oxidation produces the active complex with *cis* configuration of oxo and chloride. However, when reactivity was tested, a mixture of both hydroxide and chloride was obtained. Similar energy demand and absence of protein chain are the obvious reasons attributed for this observation. Following this, several other tri- and tetradentate ligand systems were utilized to synthesize mimics of non-heme halogenases, though all those complexes produced similar result (figure 1.1).⁶³

Inspired from the fact that, at times two or more enzymes are involved in one transformation, we sought to carry out halogenation with two iron-complexes, one for carrying out HAA and another to deliver the halide to the hydrocarbon radical, which has been described in detail in chapter 2.

1.2.2. Non-covalent interaction mediate distal C–H functionalization of heterocycles:

The heterocycles are highly important class of compounds both biologically and industrially.^{64,65} Bioactive compounds are often built around various heterocyclic moieties. These decorated heterocycles are synthesized either by long retrosynthetic routes or by electronically guided functionalizations.⁶⁶ The electronically controlled functionalizations are not favorable at all positions as well as for all functional groups, though direct functionalization of readily available feedstock is highly desirable. The conventional directing group approach is not convenient due to lack of DG attaching sites, though there are a few examples known for indoles, where DG can be attached to the nitrogen center. Moreover, the heterocycles can coordinate with metals causing catalyst poisoning. Thus, site selective C-H functionalization at distal position of heterocycles is a formidable task.

Although covalently attached DG assisted approach solved the selectivity issue in distal C-H activation to a great extent, it is not free from shortcomings. The main drawbacks include additional steps required to install and remove the DG before and after the functionalization respectively, lack suitable functional group for DG attachment such as in heterocycles. Therefore, constant attempts are being made to achieve selectivity with non-covalently interacting DG. Kanai and co-workers first introduced H-bonding as non-covalent interaction in meta-borylation of aryl amides with iridium catalyst.⁶⁷ Subsequently, various other methodologies were developed for iridium catalyzed borylation using ion-pair, ion-dipole and H-bonding interactions (**Figure 1.2**).⁶⁸⁻⁷¹ Notably, these interactions are comparatively weak and does not exist at high temperatures. Since iridium catalyzed borylation is usually a room temperature reaction, the non-covalent interactions sustained well for directing the catalyst. However, palladium catalyzed functionalizations mostly require higher temperatures, thus complicates the use of this approach.

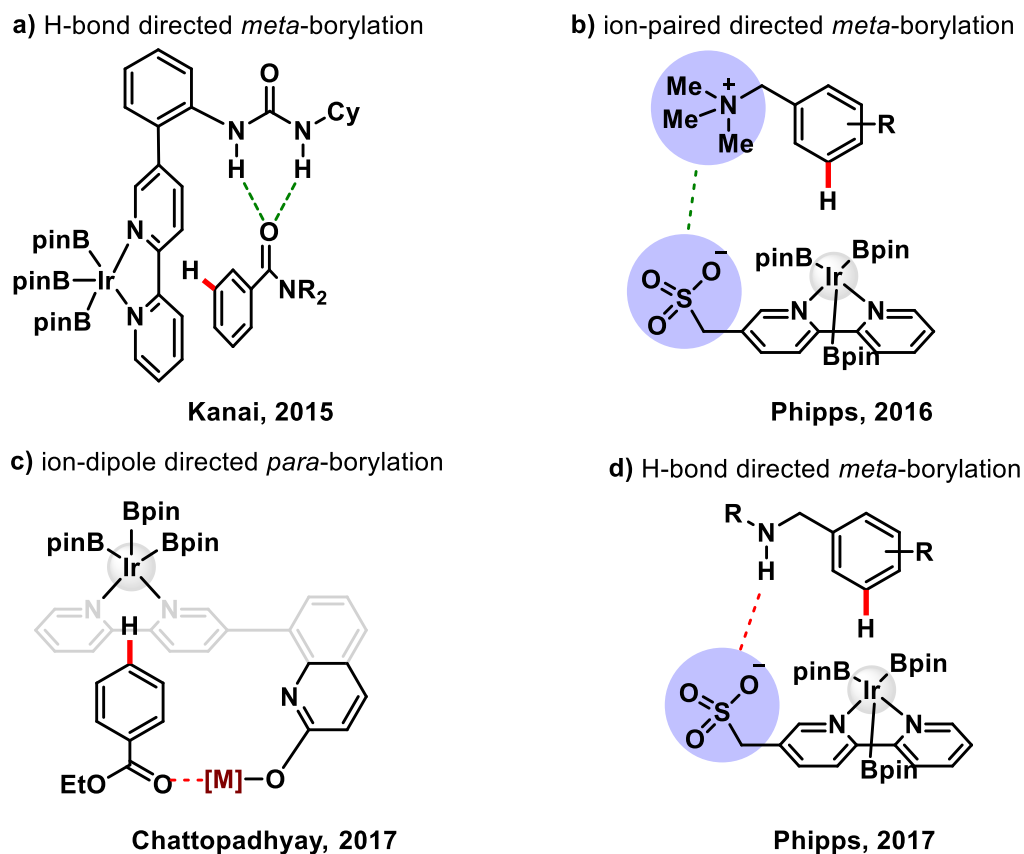


Figure 1.2: Non-covalent approaches for distal C-H activation.

To address the above issues, the unwanted coordination was utilized to anchor the heterocycle to a complex equipped with directing group, in a host-guest manner.⁷¹ By optimizing the hosting template structure, different functionalizations of various heterocycles were achieved, which have been described in chapter 3, chapter 4 and chapter 5.

1.3. References:

1. Trost, B. M. *Science* **1991**, *254*, 1471-1477
2. Nicolaou, K. C.; Hale, C. R. H.; Nilewski, C.; Ioannidou, H. A. *Chem. Soc. Rev.* **2012**, *41*, 5185-5238
3. Campos, K. R.; Coleman, P. J.; Alvarez, J. C.; Dreher, S. D.; Garbaccio, R. M.; Terrett, N. K.; Tillyer, R. D.; Truppo, M. D.; Parmee, E. R. *Science* **2019**, *363*, eaat0805
4. Wisniak, J. *Educ. quím.* **2010**, *21*, 60-69

5. Zhou, Q.-L. *Angew. Chem. Int. Ed.* **2016**, *55*, 5352 – 5353
6. Benkovic, S. J.; Hammes-Schiffer, S. *Science*, **2003**, *301*, 1196-1202
7. Masters, C. Homogeneous Transition-metal Catalysis: A Gentle Art. *Springer* -**1981**
8. Hashiguchi, B. G.; Bischof, S. M.; Konnick, M. M.; Periana, R. A. *Acc. Chem. Res.* **2012**, *45*, 885–898
9. Soga, K.; Shiono, T. *Prog. Polym. Sci.* **1997**, *22*, 1503-1546
10. Noël, T.; Buchwald, S. L. *Chem. Soc. Rev.* **2011**, *40*, 5010-5029
11. Seechurn, C. C. C. J.; Kitching, M. O.; Colacot, T. J.; Snieckus, V. *Angew. Chem. Int. Ed.* **2012**, *51*, 5062 – 5085
12. Devendar, P.; Qu, R.-Y.; Kang, W.-M.; He, B.; Yang, G.-F. *J. Agric. Food Chem.* **2018**, *66*, 8914–8934
13. Roy, D.; Uozumi, Y. *Adv. Synth. Catal.* **2018**, *360*, 602 –625
14. Buskes, M.J.; Blanco, M.-J. *Molecules* **2020**, *25*, 3493
15. Godula, K.; Sames, D. *Science* **2006**, *312*, 67-72
16. Kakiuchi, F.; Chatani, N. *Adv. Synth. Catal.* **2003**, *345*, 1077-1101
17. Hartwig, J. F.; Larsen, M. A. *ACS Cent. Sci.* **2016**, *2*, 281–292
18. Lewis, J. C.; Coelho, P. S.; Arnold, F. H. *Chem. Soc. Rev.* **2011**, *40*, 2003-2021
19. Guengerich, F. P. *J. Biochem. Mol. Toxicol.* **2007**, *21*, 163-168
20. Crabtree, B. *Chem. Rev.* **2017**, *117*, 8481–8482
21. Fenton, H. J. H. *J. Chem. Soc., Trans.* **1894**, *65*, 899-910
22. Shilov, A. E.; Shul'pin, G. B. *Chem. Rev.* **1997**, *97*, 2879-2932
23. Razzak, M.; De Brabander, J. K. *Nat. Chem. Biol.* **2011**, *7*, 865–875
24. Wang, V. C.-C.; Maji, S.; Chen, P. P.-Y.; Lee, H. K.; Yu, S. S.-F.; Chan, S. I. *Chem. Rev.* **2017**, *117*, 8574–8621
25. Breslow, R. *Chem. Record* **2001**, *1*, 3-11

26. Costas, M.; Chen, K.; Que Jr., L. *Coord. Chem. Rev.* **2000**, 200–202, 517 – 544
27. Nam, W. *Acc. Chem. Res.* **2007**, 40, 522–531
28. Bryliakov, K. P.; Talsi, E. P. *Coord. Chem. Rev.* **2014**, 276, 73-96
29. Oloo, W. N.; Que Jr.; L. *Acc. Chem. Res.* **2015**, 48, 2612–2621
30. Liu, W.; Groves, J. T. *Acc. Chem. Res.* **2015**, 48, 1727–1735
31. Chen, J.; Jiang, Z.; Fukuzumi, S.; Nam, W.; Wang, B. *Coord. Chem. Rev.* **2020**, 421, 213443
32. Brookhart, M.; Green, M. L. H.; Parkin, G. *Proc. Natl. Acad. Sci.* **2007**, 104, 6908-6914
33. Stanforth, S. P. *Tetrahedron* **1998**, 54, 263-303
34. Campeau, L.-C.; Hazari, N. *Organometallics* **2019**, 38, 3–35
35. Fujiwara, Y.; Moritani, I.; Danno, Asano, S. R.; Teranishi, S. *J. Am. Chem. Soc.* **1969**, 91 7166-7199
36. Labinger, J. A.; Bercaw, J. E. *Nature* **2002**, 417, 507-514
37. Gandeepan, P.; Müller, T.; Zell, D.; Cera, G.; Warratz, S.; Ackermann, L. *Chem. Rev.* **2019**, 119, 2192–2452
38. Yun, Y.-I.; Yang, J.; Miao, Y.; Sun, J.; Wang, X.-J. *J. Saudi Chem. Soc.* **2020**, 24, 151-185
39. He, J.; Wasa, M.; Chan, K. S. L.; Shao, Q.; Yu, J.-Q. *Chem. Rev.* **2017**, 117, 8754–8786
40. Saha, A.; Guin, S.; Ali, W.; Bhattacharya, T.; Sasmal, S.; Goswami, N.; Prakash, G.; Sinha, S. K.; Chandrashekar, H. B.; Panda, S.; Anjana, S. S.; Maiti, D. *J. Am. Chem. Soc.* **2022**, 144, 1929–1940
41. Sauermann, N.; Meyer, T. H.; Qiu, Y.; Ackermann, L. *ACS Catal.* **2018**, 8, 7086–7103
42. Kancherla, S.; Jørgensen, K. B.; Fernández-Ibáñez, M. A. *Synthesis* **2019**, 51, 643–663

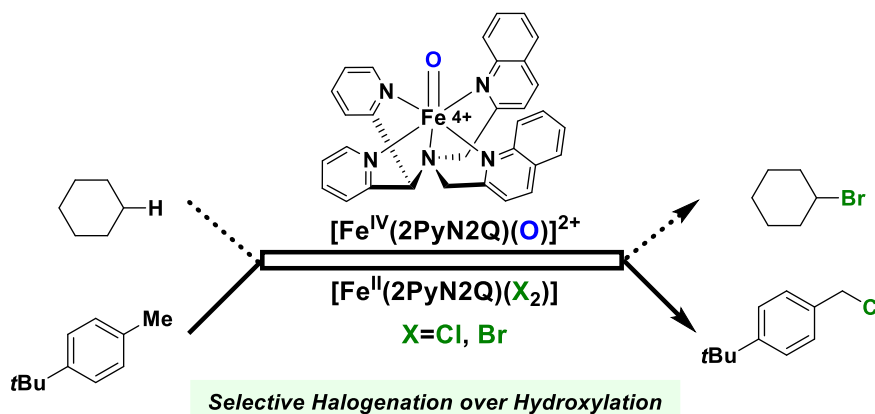
43. Sambigiagio, C.; Schönbauer, D.; Blicck, R.; Dao-Huy, T.; Pototschnig, G.; Schaaf, P.; Wiesinger, T.; Zia, M. F.; Wencel-Delord, J.; Besset, T.; Maes, B. U. W.; Schnürch, M. *Chem. Soc. Rev.* **2018**, *47*, 6603-6743
44. Davies, H. M. L.; Morton, D. *J. Org. Chem.* **2016**, *81*, 343–350
45. He, C.; Whitehurst, W. G.; Gaunt, M. J. *Chem* **2019**, *5*, 1031-1058
46. Leow, D.; Li, G.; Mei, T.-S.; Yu, J.-Q. *Nature*, **2012**, *486*, 518-522
47. Dutta, U.; Maiti, S.; Bhattacharya, T.; Maiti, D. *Science*, **2021**, *372*, 701
48. Sinha, S. K.; Guin, S.; Maiti, S.; Biswas, J. P.; Porey, S.; Maiti, D. *Chem. Rev.* **2022**, *122*, 5682–5841
49. Bag, S.; Jayarajan, R.; Mondal, R.; Maiti, D. *Angew. Chem. Int. Ed.* **2017**, *56*, 3182-3186
50. Bag, S.; Patra, T.; Modak, A.; Deb, A.; Maity, S.; Dutta, U.; Dey, A.; Kancherla, R.; Maji, A.; Hazra, A.; Bera, M.; Maiti, D. *J. Am. Chem. Soc.* **2015**, *137*, 11888–11891
51. Maji, A.; Guin, S.; Feng, S.; Dahiya, A.; Singh, V. K.; Liu, P.; Maiti, D. *Angew. Chem. Int. Ed.* **2017**, *56*, 14903-14907
52. Zhang, Q.; Shi, B.-F. *Chem. Sci.* **2021**, *12*, 841-852
53. Deb, A.; Singh, S.; Seth, A.; Pimparkar, S.; Bhaskararao, B.; Guin, S.; Sunoj, R. B.; Maiti, D. *ACS Catal.* **2017**, *7*, 8171-8175
54. Guin, S.; Dolui, P.; Zhang, X.; Paul, S.; Singh, V. K.; Pradhan, S.; Chandrashekar, H. B.; S. S. Anjana.; Paton, R. S.; Maiti, D. *Angew. Chem. Int. Ed.* **2019**, *58*, 5633-5638
55. Dolui, P.; Das, J.; Chandrashekar, H. B.; Anjana, S. S.; Maiti, D. *Angew. Chem. Int. Ed.* **2019**, *58*, 13773-13777
56. Gallego, D.; Baquero, E. A. *Open Chem.* **2018**, *16*, 1001–1058
57. Roudesly, F.; Oble, J.; Poli, G. *J. Mol. Catal. A Chem.* **2017**, *426*, 275-296
58. Bhattacharya, T.; Dutta, S.; Maiti, D. *ACS Catal.* **2021**, *11*, 9702–9714

59. Shaik, S.; Hirao, H.; Kumar, D. *Acc. Chem. Res.* **2007**, *40*, 532–542
60. Anderson, J. L. R.; Chapman, S. K. *Mol. BioSyst.*, **2006**, *2*, 350-357
61. Vaillancourt, F. H.; Yin, J.; Walsh, C. T. *Proc. Natl. Acad. Sci.* **2005**, *102*, 10111-10116
62. Rohde, J.-U.; Stubna, A.; Bominaar, E. L.; Münck, E.; Nam, W.; Que Jr., L. *Inorg. Chem.* **2006**, *45*, 6435–6445
63. Biswas, J. P.; Guin, S.; Maiti, D. *Coord. Chem. Rev.* **2020**, *408*, 213174
64. Al-Mulla, A. *Der Pharma Chemica* **2017**, *9*, 141-147
65. Arora, P.; Arora, V.; Lamba, H. S.; Wadhwa, D. *Int. J. Pharm. Sci. Res.* **2012**, *3*, 2947-2954
66. Li, J.-J.; Corey, E. J. *Name Reactions in Heterocyclic Chemistry*. Wiley, **2004**
67. Kuninobu, Y.; Ida, H.; Nishi, M.; Kanai, M. *Nat. Chem.* **2015**, *7*, 712-717
68. Davis, H. J.; Genov, G. R.; Phipps, R. J. *Angew. Chem. Int. Ed.* **2017**, *56*, 13351-13355
69. Bisht, R.; Chattopadhyay, B. *J. Am. Chem. Soc.* **2016**, *138*, 84-87
70. Hoque, M. E.; Bisht, R.; Haldar, C.; Chattopadhyay, B. *J. Am. Chem. Soc.* **2017**, *139*, 7745-7748
71. Zhang, Z.; Tanaka, K. Yu, J.-Q. *Nature* **2017**, *543*, 538-542

Chapter 2

Chapter 2

Selective C–H Halogenation over Hydroxylation by Non-heme Iron(IV)-oxo and Iron(II)-halide Complexes



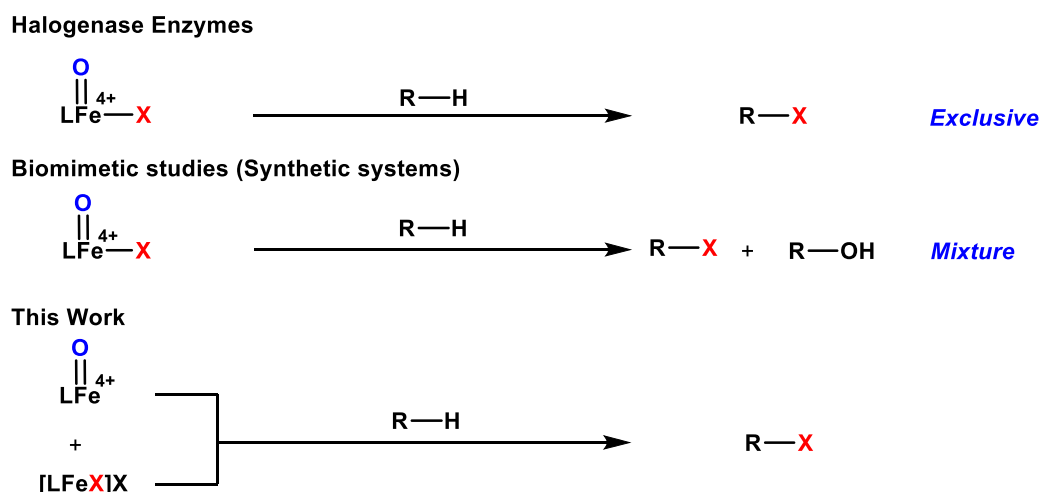
Abstract: Non-heme iron based halogenase enzymes promote selective halogenation of sp^3 -C–H bond through iron(IV)-oxo-halide active species. During halogenation, competitive hydroxylation can be prevented completely in enzymatic systems. However, *synthetic* iron(IV)-oxo-halide intermediates often result in a mixture of halogenation and hydroxylation products. In this report, we have developed a new synthetic strategy by employing non-heme iron based complexes for selective sp^3 -C–H halogenation by overriding hydroxylation. A room temperature stable, iron(IV)-oxo complex, $[\text{Fe}(2\text{PyN}2\text{Q})(\text{O})]^{2+}$ was directed for hydrogen atom abstraction (HAA) from aliphatic substrates and the iron(II)-halide $[\text{Fe}^{\text{II}}(2\text{PyN}2\text{Q})(\text{X})]^+$ (X , halogen) was exploited in conjunction to deliver the halogen atom to the ensuing carbon centered radical. Despite iron(IV)-oxo being an effective promoter of hydroxylation of aliphatic substrates, the perfect interplay of HAA and halogen atom transfer in this work leads to the halogenation product selectively by diverting the hydroxylation pathway.

2.1. Introduction:

High-valent iron-oxo species serve as the key intermediate for performing different natural transformation like halogenation, hydroxylation and olefin epoxidation.¹ Several oxygenases including Cyt P450, Rieske oxygenases, α -keto glutarate-dependent oxygenases and various halogenases exhibit their activity via formation of an iron-oxo intermediate.² Among these mononuclear iron based enzymes, α -KG-dependent halogenases carry out biosynthesis of several halogen based natural products by implementing selective halogenations of sp^3 C–H bonds by overriding hydroxylation.³ These enzymes contain α -KG as the key structural motif which is coordinated to an iron(II) cofactor in a facial triad fashion along with two histidine moieties. Other halogenases such as CytC3 and SyrB2 differ structurally compared to α -KG dependent halogenases,^{2a,4} in a sense wherein halide is coordinated to the iron centre instead of carboxylate from α -KG. Although these enzymes differ structurally, their mode of action towards C–H halogenation is very much similar. First, iron(II) cofactor performs O_2 activation resulting in a high-spin ($S=2$) cis-iron(IV)-oxo-halide species.^{1a,5} Subsequently, it performs the hydrogen atom abstraction (HAA) from C–H bond. The corresponding nascent radical and iron(III)-halide are placed in such a way that the radical selectively undergoes rebound with halide to generate halogenated products.

Biomimetic non-heme iron(III)-halide complex, $[Fe^{III}(TPA)Cl_2]^+$ was first synthesized and judiciously employed by Que and co-workers for sp^3 C–H halogenation.⁶ The iron(V)-oxo-halide, $[Fe^V(TPA)(O)(Cl)]^{2+}$ was proposed as the key intermediate for the halogenation reaction. Recent studies showed that substrate positioning between halide and hydroxide is a key factor to ensure selectivity for halogenation.⁷ Later on Comba reported C–H halogenations with $[Fe^{II}(\text{bispidine})(Cl_2)]$ where iron(IV)-oxo-halide, $[Fe^{IV}(\text{bispidine})(O)(Cl)]^{2+}$ was proposed as the key intermediate.⁹ Subsequently Costas synthesized *cis*-iron(IV)-oxo-halide,

$[\text{Fe}^{\text{IV}}(\text{O})(\text{X})(\text{Pytacn})]^+$ (X, Cl and Br) for pursuing sp^3 C–H halogenation.¹⁰ Later Paine and co-workers have reported halogenations of aliphatic and benzylic C–H bonds where similar iron(IV)-oxo-halide, $[\text{TP}^{\text{Ph}}\text{Fe}^{\text{IV}}(\text{O})(\text{Cl})]^{2+}$ was proposed as the key intermediate.¹¹



Scheme 2.1. sp^3 -C–H halogenation by non-heme complexes

Very recently Que and co-workers have employed high-spin ($S=2$) iron(IV)-oxo-halide complexes, $[\text{Fe}^{\text{IV}}(\text{TQA})(\text{O})(\text{X})]^{2+}$ (X= Cl and Br) for sp^3 C–H halogenations.¹² These elegant explorations demonstrated that despite having the potential for promoting selective halogenation chemistry, formation of hydroxylation product often remained as the bottleneck for the synthesis of selective halogenated compounds (scheme 2.1). A clear opportunity for synthetic chemists, therefore, resides on discovering a selective halogenation protocol by utilizing the potential of non-heme iron(IV)-oxo complex.

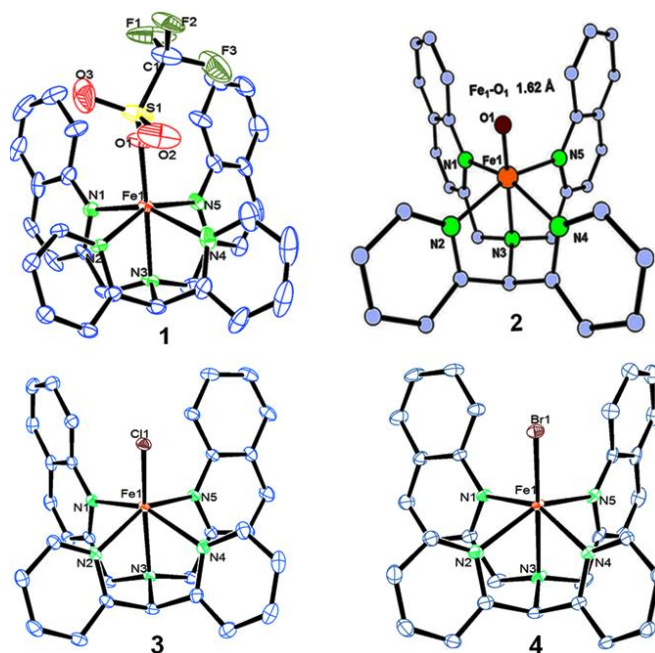


Figure 2.1. ORTEP diagram of triflate anion coordinated iron(II)-complex **1** (CCDC 1505984), and DFT optimized structure of iron(IV)-oxo **2**, $[\text{Fe}^{\text{IV}}(2\text{PyN}2\text{Q})(\text{O})]^{2+}$, ORTEP diagram of iron(II)-halide complexes **3** (1505989) and **4** (1505986)

2.2. Result and discussion:

We have explored a new strategy for the halogenation reaction involving a non-heme iron complex with the expectation to discover a selective $sp^3\text{-C-H}$ halogenation protocol by overriding hydroxylation chemistry, along with what is observed in α -KG-dependent halogenases. We planned to employ a room temperature stable pentacoordinated iron(IV)-oxo species $[\text{Fe}^{\text{IV}}(2\text{PyN}2\text{Q})(\text{O})]^{2+}$ (**2**) supported by 2PyN2Q ligand, (1,1-di(pyridin-2-yl)-*N,N*-bis(quinolin-2-ylmethyl)methanamine, Figure 2).¹³, The corresponding iron(II)-complex was synthesized by reacting $\text{Fe}(\text{OTf})_2(\text{CH}_3\text{CN})_2$ with the ligand, 2PyN2Q in acetonitrile. The synthesized complex $[\text{Fe}^{\text{II}}(2\text{PyN}2\text{Q})(\text{OTf})_2]$, **1**, showed UV-vis band at 368 nm ($\epsilon \sim 1954 \text{ M}^{-1}\text{L}^{-1}$) and 470 nm ($\epsilon \sim 887 \text{ M}^{-1}\text{L}^{-1}$). Complex **1** was also characterized by ESI-MS ($[\text{Fe}^{\text{II}}(2\text{PyN}2\text{Q})(\text{OTf})]^+$, $m/z =$ experimental 672.09; calculated = 672.09). Further, **1** showed paramagnetic shift in ^1H NMR spectroscopy (shift from -60 to 140 ppm). Complex **1** was also

characterized by X-ray crystallography (Figure 2.1). Synthesis of the reactive iron(IV)-oxo ($[\text{Fe}^{\text{IV}}(\text{2PyN2Q})(\text{O})]^{2+}$) complex **2** was performed by adding $\text{MesI}(\text{OAc})_2/m\text{CPBA}$ (1.5 equiv.) in acetonitrile and it showed characteristic UV-vis band at 770 nm ($\epsilon \sim 250\text{M}^{-1}\text{L}^{-1}$). The complex **2** was further characterized by FT-IR spectroscopy where $\text{Fe}^{\text{IV}}=\text{O}$ stretching appeared at 833 cm^{-1} .

Further, complex **2** was characterized by Mössbauer spectroscopy. Figure 2.2 presents the spectrum recorded at 80 K with a small field (60 mT) applied parallel to the γ rays. The center of the spectrum is dominated by two overlapping quadrupole doublets and a broad component can be discerned on both sides and positive velocities. Application of a high parallel magnetic field (7 T, Figure 2.2 bottom) turns the latter component into a sextet extending from -7.4 to 8 mms^{-1} . By contrast, the two central features are slightly broadened. These two spectra can be simulated simultaneously by considering the presence of three components.¹⁴ Component A (red line in the simulations), which amounts to 35% of total iron, is a spin $S=1$ species with an isomer shift $\delta = 0.043\text{ mms}^{-1}$, a quadrupole splitting $\Delta E_{\text{Q}} = 0.57\text{ mms}^{-1}$ and a D value ca 26 cm^{-1} . These parameters are consistent with a $\text{Fe}^{\text{IV}}=\text{O}$ species. Component B (blue line in the simulations, 12% of total iron) is a μ -oxodiferric $S=0$ species with $\delta = 0.5\text{ mm s}^{-1}$ and a quadrupole splitting $\Delta E_{\text{Q}} = 1.5\text{ mms}^{-1}$. The additional magnetic component (C, green line) can be accounted for by considering that it is a high spin Fe^{III} species (53%, $S = 5/2$, $\delta = 0.56\text{ mms}^{-1}$, $\Delta E_{\text{Q}} = 0.72\text{ mms}^{-1}$). These Mössbauer experiments thus show the formation of iron(IV)oxo, $\text{Fe}^{\text{IV}}=\text{O}$, species which is reactive at room temperature forming a μ -oxo diferric species together with another ferric species.

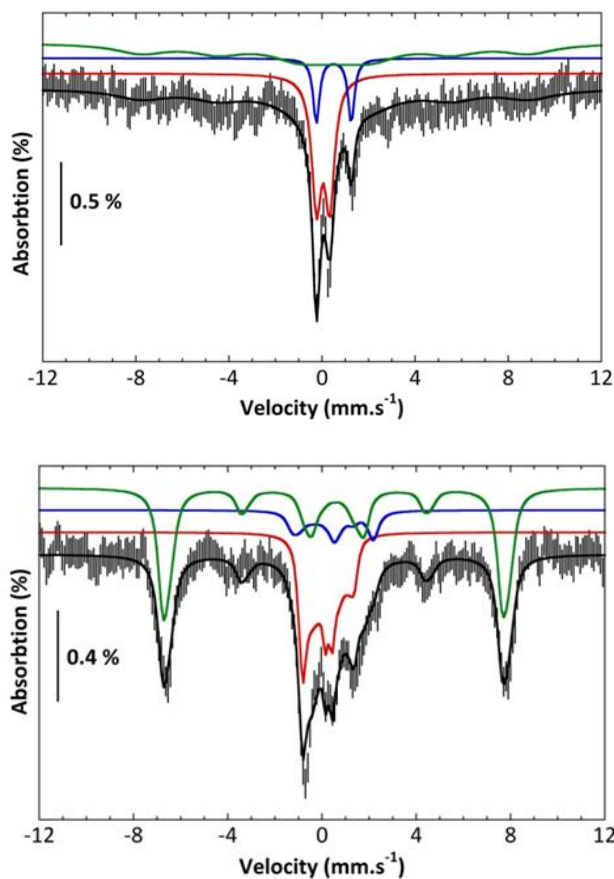


Figure 2.2. a) Mössbauer spectra recorded at 80 K and 60 mT top and b) at 5.5 K and 7 T (bottom). Experimental spectra: hatched bars; solid black line: simulation; colored lines: contributions of species A (red), B (blue) and C (green).

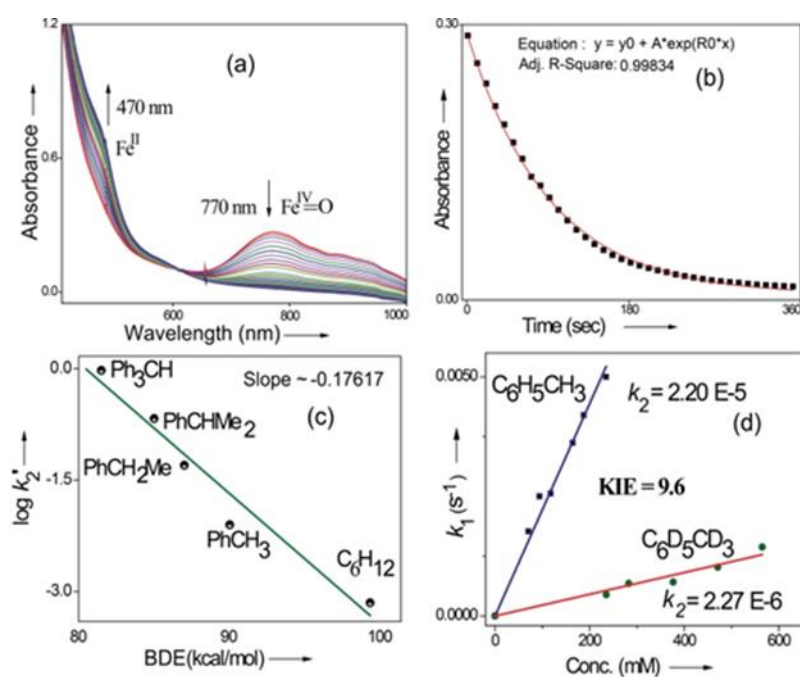
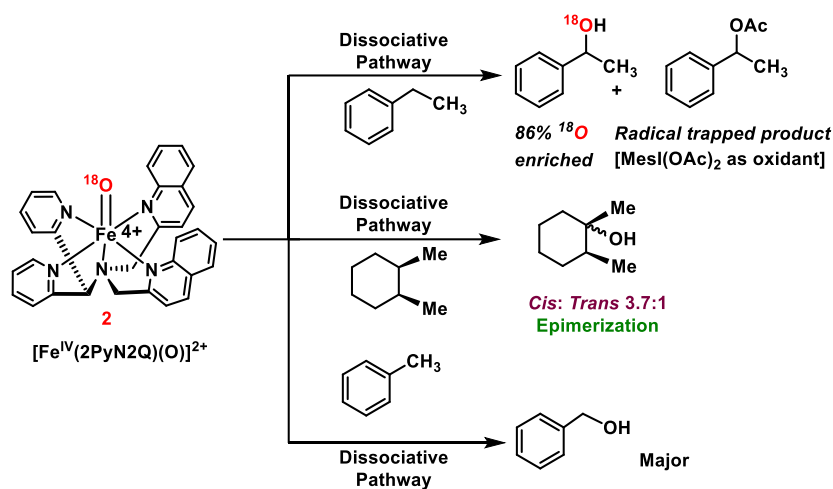


Figure 2.3. (a) UV-vis change during C–H oxidation of ethylbenzene (b) time trace of **2** at 770 nm (c) bond dissociation energy (BDE) correlation plot: Bell-Evans-Polyani plot during C–H oxidation by **2** (d) kinetic isotope effect study (kinetics studies were carried out under N₂ atmosphere at 25 °C)

Initially we opted for demonstrating the feasibility of HAA step by iron(IV)-oxo species, [Fe^{IV}(2PyN2Q)(O)]²⁺ (**2**) during C–H oxidation. Substrates like ethylbenzene, toluene and cyclohexane yielded the corresponding oxidation products when reacted with the room temperature stable iron(IV)-oxo species **2**.

Kinetic study of C–H oxidation reactions were performed (UV-vis, Figure 2.3a-b) under pseudo first order conditions. The second order rate constant (k_2) values were found to be 20 times higher when compared to the previously reported rates of C–H oxidation by *penta*-coordinated nitrogen containing iron(IV)-oxo species,^{15a,16} which could be due to the steric bulk originating from quinoline moiety.¹⁷

The Bell-Evans-Polayni (BEP) plot ($\log k_2$ vs BDE) showed linear correlation (Figure 2.3c). Further we studied the kinetic isotope effect (KIE, k_H/k_D) between C₆H₅CH₃/C₆D₅CD₃ and the value was found to be 9.6 (Figure 2.3d). The linearity in BEP plot and large KIE value suggested that initial HAA step is the rate-determining step (RDS) during C–H oxidation.¹⁸ The slope ($-0.176 \text{ (kcal/mol)}^{-1}$) of the BEP plot is related with Bronsted parameter (α) by $\alpha = [(\text{slope} \cdot RT)]$ and it results: $\alpha \sim -0.10$. *i.e.* the value is closer to 0. The value of Bronsted parameter suggest reactant like transition state is involved during C–H oxidation reactions *via* HAA step which is further supported by computational study described in the following.



Scheme 2.2. C–H oxidation by $[\text{Fe}^{\text{IV}}(2\text{PyN}2\text{Q})(\text{O})]^{2+}$, **2** (Reactions were carried out under N_2 atmosphere inside the Glove Box at 25 °C)

We moved towards product analysis during C–H oxidation to gain insights into the mechanistic pathway. When ethyl benzene was reacted with complex **2**, it provided 1-phenylethanol (34%), 1-phenylethylacetate (26%) and acetophenone (5%) under N_2 atmosphere. Control reactions were carried out between 1-phenylethanol and $\text{MesI}(\text{OAc})_2$ as well as between 1-phenylethanol and *in situ* generated complex **2**. None of these cases, 1-phenyl ethyl acetate was detected. Therefore, the formation of 1-phenylethylacetate during the reaction with ethyl benzene could occur *via* reaction between cage-escaped radical and acetoxy radical ($\cdot\text{OAc}$) generated from $\text{MesI}(\text{OAc})_2$ during the reaction (Scheme 2.2). This observation suggests that radical could dissociate from the solvent cage after HAA step. Toluene and cyclohexane (N_2 atmosphere) produced 48% of benzyl alcohol and 3% of benzaldehyde (Scheme 2.2), whereas cyclohexane provided cyclohexanol (54%) and cyclohexanone (3%). Further, experiments with O-18 labelled **2** and ethylbenzene provided 1-phenylethanol with 86% of O-18 labelling which supported **2** as the sole oxygen source during C–H oxidation.¹⁹

The C–H oxidation reactions with ethylbenzene, toluene and cyclohexane under air was found out to produce alcohol/ketone (A/K) products with a ratio of 1 or <1. Additionally, radical trap

experiments with CCl_3Br were carried out. Expectedly, cyclohexane and toluene provided exclusive radical trapped product bromocyclohexane and benzyl bromide, respectively. Similarly, ethylbenzene provided radical trapped products (1-chloroethyl)benzene (20%), (1-bromoethyl)benzene (10%) and 1-phenylethylacetate (25%). Such observations implied dissociation of the carbon radical from the solvent cage,²⁰ following which it undergoes a rebound with iron(III)-hydroxide to provide C–H oxidation product. Further the cage escape behaviour of the radical was confirmed by carrying out a reaction of pure stereoisomer of *cis*-1,2-dimethylcyclohexane with **2**. It provided a mixture of *cis/trans*-1,2-dimethylcyclohexanol (46% yield, 3.7:1 ratio). The high-degree of *epimerization* in the products arises from a long-lived radical, which could be generated due to the dissociation of the radical from solvent cage after HAA (Scheme 2.2).²¹

Although complex **2** was found to be suitable for HAA from $sp^3\text{-C-H}$ bond of cyclohexane, our attempts to promote halogenation of cyclohexane by a combination of complex **2** and 1 *equiv.* of halide source $\text{Bu}_4\text{N}^+\text{Cl}^-$ or $\text{Bu}_4\text{N}^+\text{Br}^-$ failed. Such an observation could be attributed to the inability of **2** to form reactive iron(IV)-oxo-halide intermediate with the pentacoordinated 2PyN2Q ligand. Additionally, complex **2** reacted with halide anion faster compared to abstracting hydrogen atom from $sp^3\text{-C-H}$ bond of cyclohexane.²² Further in order to get more insight we have carried out the kinetics study for the oxidation of chloride (Cl^-) and bromide (Br^-) by **2**. We found that second order rate constant, k_2 for Cl^- and Br^- oxidation are 221 and 938 $\text{M}^{-1}\text{s}^{-1}$ respectively. The complex **2** oxidizes Br^- faster than Cl^- and also halide oxidation phenomenon's is very much faster process compared to hydrogen atom abstraction process (for C–H oxidation of toluene and cyclohexane the second order rate constants are k_2 0.0242 and 0.011 $\text{M}^{-1}\text{s}^{-1}$ respectively).

With these unsuccessful attempts, our attention returned to the existing report for the formation of a mixture of halogenation and hydroxylation products. Notably, halide rebound of cage escaped radical with metal-halide was well documented with Mn-catalyzed fluorination reaction by Groves and co-workers.²³ We envisioned that if we can outcompete iron(III)-hydroxide (formed upon HAA of sp^3 -C-H bond by **2**) with iron(III)-halide, then the cage-escaping carbon centered radical will undergo rebound with iron(III)-halide. The iron(III) halide can potentially act as a suitable halide donor and can be generated *in situ via* one-electron oxidation (by oxidant *m*CPBA) of the corresponding iron(II)-halide complexes [Fe^{II}(2PyN2Q)(X)](X) [X = Cl (**3**) and Br (**4**)] (Figure 2). Reaction of **4** with **2** and cyclohexane led to the formation of bromocyclohexane (90%) product selectively (Table 2.1, entry 1, **4** as the limiting reagent under N₂ atmosphere). Use of excess amount of **4** was detrimental for the formation of bromocyclohexane. Furthermore, we focussed on the discovery and implementation of the new strategy for promoting selective halogenation reaction by overcoming the hydroxylation chemistry described above. The chlorination reactions with cyclohexane in presence of **2** and **3** gave 52% yield of chlorocyclohexane with 5:1 selectivity for halogenation over hydroxylation (Table 2.1, entry 2).

The appreciable levels of selectivity for the synthetic non-heme iron-oxo mediated halogenation chemistry clearly suggest that the carbon centered radical, generated upon HAA, escapes the solvent cage and combines with the free halide radical generated upon halide oxidation by **2**. Similar to non-heme halogenase enzymes, this carbon radical engages the halide radical from iron(III)-halide intermediate to yield halogenation product preferably over hydroxylation (Figure 2.4).

Table 2.1. Scope for C–H bromination and chlorination
$$\text{R-H} \xrightarrow[\text{MeCN, N}_2 \text{ atm.}]{\begin{array}{l} [\text{Fe}^{\text{IV}}(\text{N2QuPy})(\text{O})]^{2+} \text{ (2)} \\ [\text{Fe}^{\text{II}}(\text{N2QuPy})(\text{X})] \text{X (3/4)} \end{array}} \text{R-X} \quad \text{X=Cl, Br}$$

Entry	Substrate (s)	Product (s)	Entry	Substrate (s)	Product (s)
1		90% <i>Selective</i>	9		97% <i>Selective</i>
2		52%, 10% Cy-OH	10		60% <i>Selective</i>
3		52% ^a <i>Selective</i>	11		54% ^a
4		60% <i>Selective</i>	12		50% <i>Selective</i>
5		A : B 2.27 : 1 65% <i>Selective</i>	13		60% <i>Selective</i>
6		50% ^a <i>Selective</i>	14		46% <i>Selective</i>
7		50% <i>Selective</i> Cis : Trans : 2° C-Br 1: 1.18 : 1.2	15		56% <i>Selective</i>
8		60% <i>Selective</i> Cis : Trans : 2° C-Br multiple products	16		62% ^a

^aMinor hydroxylation (~5% w.r.t. 3 or 4)

Further in order to get mechanistic insight, we synthesized iron(II)-halide complexes with perchlorate as counter anion, $[\text{Fe}^{\text{II}}(\text{2PyN2Q})(\text{X})](\text{ClO}_4)$, X = Cl, **5** (1516453), Br, **6** (1516421), and characterized these complexes by X-ray crystallography. Interestingly, when **6** was used for bromination of cyclohexane, we selectively obtained bromocyclohexane (7:1). Similarly, employing complex **5** we obtained selective benzylic chlorinated product with 4-tertbutyltoluene. Moreover the solution of **4** (also **6**) with 0.5 (or 1 equiv.) *m*CPBA provided brominated product efficiently and therefore suggested the feasibility of one electron oxidation of these halide complexes to provide iron(III)-halide required for halide rebound step (Figure 2.4).²⁴ Additionally, we have tested the possibility of one electron oxidation of the halide complexes by recording EPR spectrum of **6** with 0.5 equiv. or 1 equiv. *m*CPBA (pre-oxidized

solution) in acetonitrile at 4 k. The EPR spectra showed rhombic signal ($g_1=1.99$, $g_2=4.38$, $g_3=6.24$) which is characteristic of a high spin ($S=5/2$) iron(III)-species (Figure 7).²⁵

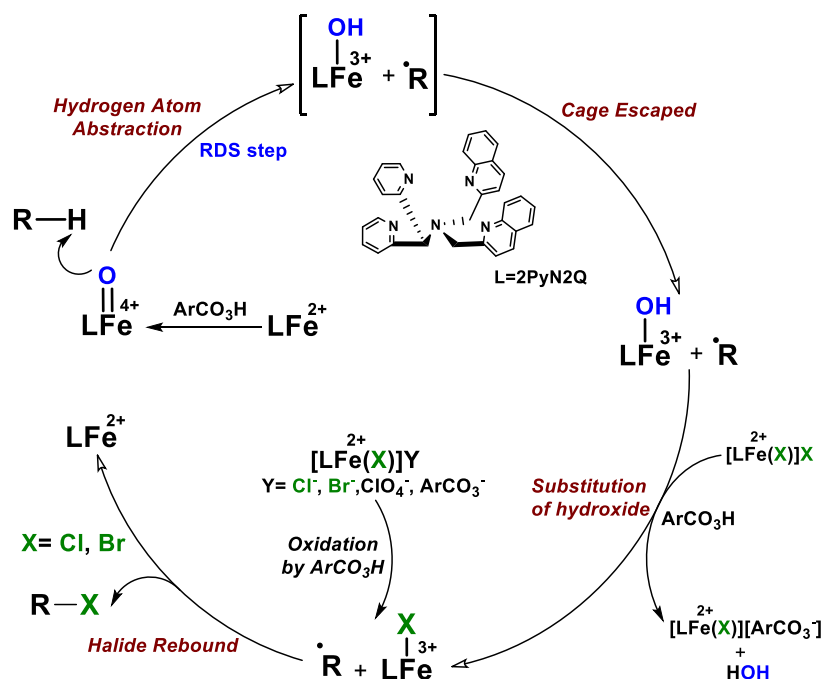


Figure 2.4. Plausible mechanism of C–H halogenation by iron(IV)-oxo, **2** in presence of iron(II)-halide complex **3** or **4**

These observations suggested that the halide complexes **5** and **6** (also **3** and **4**) possibly undergo one electron oxidation in presence of **2 equiv. mCPBA** used in halogenation to provide iron(III)-halide which would undergo halide rebound with the cage escaped radical (Figure 2.4). Moreover we have measured the one electron oxidation potential of halide complexes (**3-6**) by cyclic voltametry study. The halide complexes, **3-6** showed Fe^{II}/Fe^{III} oxidation potentials around ~0.9–1.0 V in acetonitrile vs SCE (saturated calomel electrode). Thus it can be oxidized by mCPBA as its oxidation potential is around, ~ 2 V. Notably as the iron(II)-halide complexes (**3-6**) undergo rapid one electron oxidation under the halogenation reaction condition and generate iron(III)-halide species, they do not participate in the known *comproportionation*

reaction with iron(IV)-oxo **2**. However, possibility of *comproportionation* reaction cannot be completely ruled out.

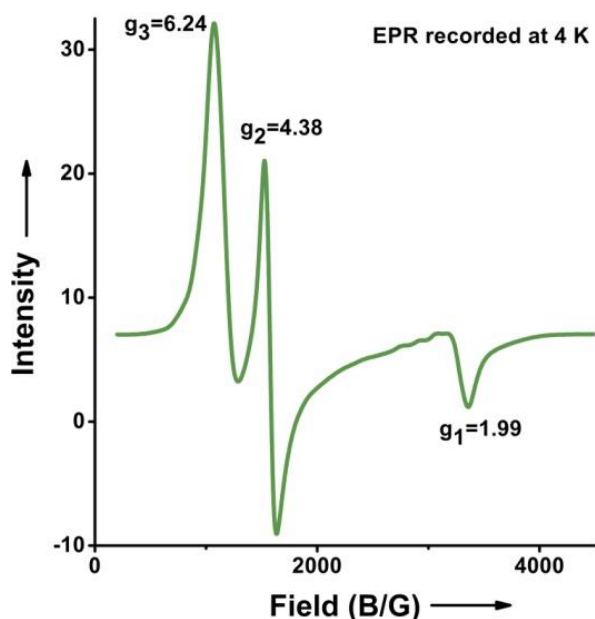


Figure 2.5. EPR spectrum showing one electron oxidation of **6** using 0.5 of *m*CPBA (Temperature 4 k, X-band frequency 9.376 GHz, Modulation Amplitude 4G, Modulation Frequency 100 KHz, Attenuation 22 dB).

The higher selectivity of bromination over chlorination can be rationalized by ease of halide rebound of the cage escaped radical with iron(III)-bromide compared to iron(III)-chloride (Figure 2.4). Additionally the ease of formation of Br^\bullet from Br^- ($E_{\text{Br}^-/\text{Br}^\bullet}^0$, 1.07 V vs SHE) compared to Cl^\bullet from Cl^- ($E_{\text{Cl}^-/\text{Cl}^\bullet}^0$, 1.36 V vs SHE) from complex **3,4** (which can combine with the cage escaped radical and can lead to the partial formation of halogenated products) can also be accounted for higher selectivity.⁹ The formation of iron(III)-halide complex could also occur *via substitution* by halide anion from iron(II)-halide complex (Figure 2.4). Furthermore, we observed that the use of *m*CPBA as an oxidant, instead of $\text{MesI}(\text{OAc})_2$, during bromination reaction with cyclohexane increases bromocyclohexane product yield from 18% to 90%. The ease of hydroxide substitution by halide ion in presence of H^+ from *m*CPBA can

be accounted for higher yield. Similar substitution of hydroxide bound to iron centre in presence of proton source was elegantly described by de Visser, Hillier and Paine groups (Figure 2.4).^{11,26}

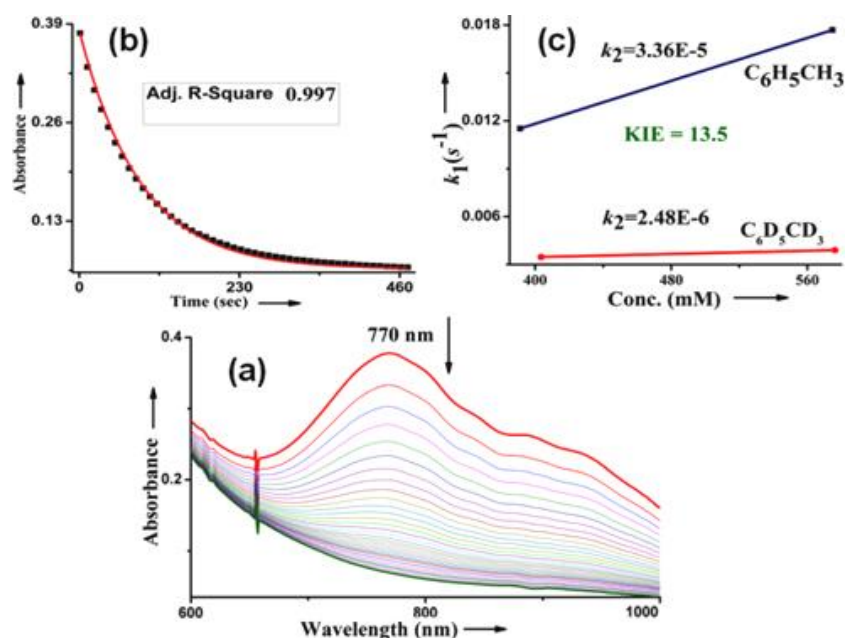


Figure 2.6. (a) UV-vis change during bromination of toluene, (b) inset 770 nm decay plot of **2** during bromination of toluene, (c) kinetic isotope effect study during bromination reaction (kinetics studies were carried out under N_2 atmosphere at $25\text{ }^\circ\text{C}$)

No halogenation products were obtained in presence of air; rather we obtained exclusive C–H oxidation products. This phenomenon suggested that cage escaped radical was intercepted by O_2 (air).²⁷ Further studies were carried out in order to get insights about these selective halogenation reactions. Addition of $[Fe^{II}(2PyN2Q)Br](Br)$ (**3**) to a solution of $[Fe^{IV}(2PyN2Q)O]^{2+}$ (**2**) showed the iron(IV)-oxo band at 770 nm (Figure 2.6a). This experiment suggests that iron(IV)-oxo exists in solution in presence of iron(II) halides. Iron(IV)-oxo is the key species for the initiation of the halogenation reactions. The kinetic isotope effect study between $C_6H_5CH_3$ and $C_6D_5CD_3$ under standard halogenation reaction

conditions gave a value of 13.5 (Figure 2.6c), which supported initial HAA step as the rate determining step.

Following this, cyclopentane, cycloheptane, cyclooctane, norbornane, *trans*-1,2-dimethylcyclohexane and *trans*-decaline were subjected to the same reaction conditions. Expectedly, selective formation of halogenation products was encountered in these cases (Table 2.1, entries 3-8). After successful halogenation of the sp^3 -C–H bond of aliphatic substrates, we decided to explore benzylic halogenation. Under the standard reaction protocol, toluene provided benzyl bromide in an excellent yield (97%, Table 2.1, entry 9). Differentially substituted benzylic substrates provided selective brominated products as well (Table 2.1, entries 10-14). Interestingly, 4-*tert*-butyltoluene showed excellent selectivity towards benzylic chlorination (Table 2.1, entry 15). Ethyl benzene demonstrated good selectivity as well towards chlorination over hydroxylation (Table 2.1, entry 16).

2.3. Conclusion:

In summary we have developed a new strategy for selective halogenation by using a room-temperature stable non-heme iron(IV)-oxo complex in presence iron(II)-halide complexes. The interplay of non-heme iron(IV)-oxo and iron(II)-halide complexes provided selective halogenation *via* HAA and subsequent halide rebound pathway or via radical recombination between halide radical and carbon centred radical. The present strategy is expected to have immense importance for further development of selective halogenations methods.

2.4. Experimental Details:

2.4.1. Materials and Methods. All ^1H NMR spectra were reported in units of parts per million (ppm) and measured relative to the signals for residual chloroform (7.26 ppm) in CDCl_3 / and for residual CH_3CN in CD_3CN at 1.96 ppm, unless otherwise stated. All ^{13}C NMR spectra were

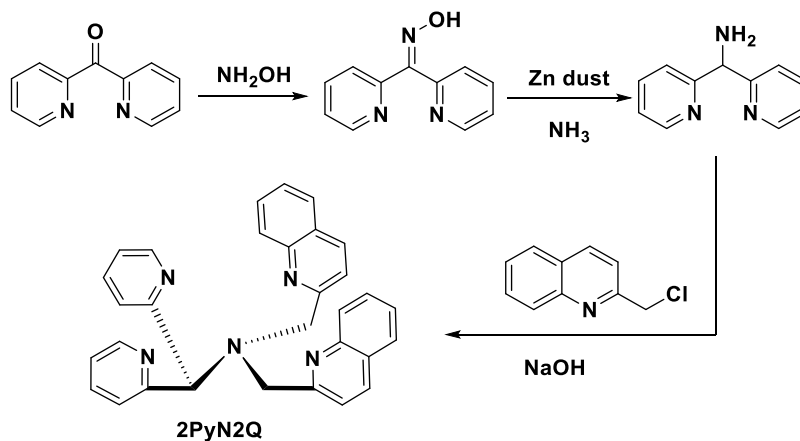
reported in ppm relative to CDCl_3 (77.23 ppm), unless otherwise stated and were obtained with ^1H decoupling. Acetonitrile, CD_3CN , $\text{Fe}^{\text{II}}\text{Cl}_2$, $\text{Fe}^{\text{II}}\text{Br}_2$, trimethylsilyltriflate (TMSOTf) were bought from Sigma Aldrich. Diethyl ether was bought from Spectrochem chemicals. Ethylbenzene was bought from TCI chemical company. H_2^{18}O was bought from Sigma Aldrich and ICON-isotope. 2-(chloromethyl)quinoline hydrochloride was purchased from TCI chemical company and di(2-pyridyl)ketone were bought from alfa aesar. All the products were analyzed by GC/GC-MS analysis. The product yields were calculated from the GC-trace obtained from the Thermo Scientific GC-MS instrument by comparing with the area percentage of standard product. Yields of the different products were calculated with respect to area% of the standard products. Unless otherwise stated all the yields mentioned in the main manuscript are $\pm 5\%$ range of error. Some of the benzyl bromide derivatives and benzyl chloride derivatives by reacting corresponding toluene derivatives with NBS/NCS in presence of benzoyl peroxide under reflux condition.

All the kinetics studies were carried out under N_2 atmosphere. The kinetics of the reactions does not vary from N_2 atmosphere to air atmosphere. First order rate constant (k_1) were calculated based on non-linear exponential fit in OriginPro8 software. All the kinetics were carried out in pseudo-first-order conditions (substrate > 10 equiv. were used). The rate constant (k_1) was calculated based on the decay pattern of iron(IV)-oxo complex at 770 nm by nonlinear curve fitting, [$y = y_0 + A \cdot \exp(-R_0 \cdot x)$], (where x is time, t and R_0 is rate constant, k_1 , y is absorbance) and showed good fit in rate constant value within 10% error. Resulting k_1 values corroborated linearly with substrate concentration to give second-order rate constant k_2

2.4.2. Synthesis and characterization of complexes.

Synthesis and characterization of 2PyN2Q ligand. Hydroxylamine hydrochloride (750.5 mg, 10.8 mmol) and sodium acetate (NaOAc) (886 mg, 10.8 mmol) were heated in 10 mL of

distilled water at 60 °C for one hour. After the heating the solution for one hour, a solution of di(2-pyridyl)ketone (1g, 5.43 mmol) in 5mL MeOH was added. The resulting mixture was stirred at 80 °C overnight. Consequently the pink color solidified oxime was obtained. The product oxime was washed with methanol (MeOH) and the solvent was dried over rotary evaporator. The crude oxime, a pink solid, was used in the next step without further purification. The above prepared oxime (1 g, 5 mmol), ammonium acetate (NH₄OAc, 655 mg, 8.5 mmol), ammonia (NH₃, 25% aqueous solution, 15 ml), ethanol (20 mL) were mixed along with 10 mL of water heated at 80 °C. Activated Zn dust (1.47 g, 22.5 mmol) was then added to the reaction mixture in small amounts for over a duration of 30 minutes. The resulting mixture was refluxed for 4 hours and then stirred at room temperature for overnight. The mixture was filtered and the residue was washed with methanol (MeOH) and water. The filtrate was concentrated and the resulting aqueous solution was made strongly alkaline with 10 (M) sodium hydroxide (NaOH) solution. The amine was then extracted with dichloromethane and the organic phase was then washed with brine, dried over Na₂SO₄ and concentrated in rotary evaporator and vacuum to afford brown oil. ¹H NMR (400 MHz, CDCl₃, δ): 8.48 (m, 2H, Py), 7.55 (m, 2H, Py), 7.31 (d, 2H), 7.04(m, 2H), 5.25 (s, 1H, CH), 2.43 (s, 2H, NH₂). 2-(chloromethyl)-quinoline hydrochloride (9.866 mmol, 2.2 g) was added to an aqueous solution of sodium hydroxide (NaOH) (5 mL, 5 M) at 0 °C. After stirring for 10 minutes, the solution was added to bis(2-pyrimidyl) methylamine (0.969 g; 5.23 mmol) and another portion of aqueous solution of NaOH (5 M, 5 mL). The solution was allowed to stir for 36 hours at room temperature and then concentrated perchloric acid (HClO₄) was added dropwise to get a sticky brownish precipitate, which was recrystallized from hot water. Treatment of this perchlorate salt with 2.5 (M) NaOH solutions and extraction with dichloromethane yielded yellowish solid N₂QuPy in 40% yield.



The synthesized ligand was thoroughly characterized by ^1H , ^{13}C NMR and ESI-MS analysis. The obtained NMR data for ligand, N2QuPy: ^1H NMR (500 MHz, CDCl_3 , δ): 4.21 (s, 4H), 5.452 (s, 1H), 7.11 (2H), 7.45 (2H), 7.60-7.68 (6H, m), 7.73 (2H), 7.80 (2H), 8.01 (4H), 8.58 (2H). ^{13}C NMR (125 MHz, CDCl_3): δ 58.40, 72.69, 121.51, 122.40, 124.51, 126.20, 127.36, 127.55, 129.06, 129.44, 136.33, 136.57, 147.60, 149.44, 160.54, 160.02. ESI-MS ($[\text{M}+\text{Na}]$: observed, 490.197 calculated for $\text{C}_{31}\text{H}_{25}\text{N}_5\text{Na}$: 490.20).

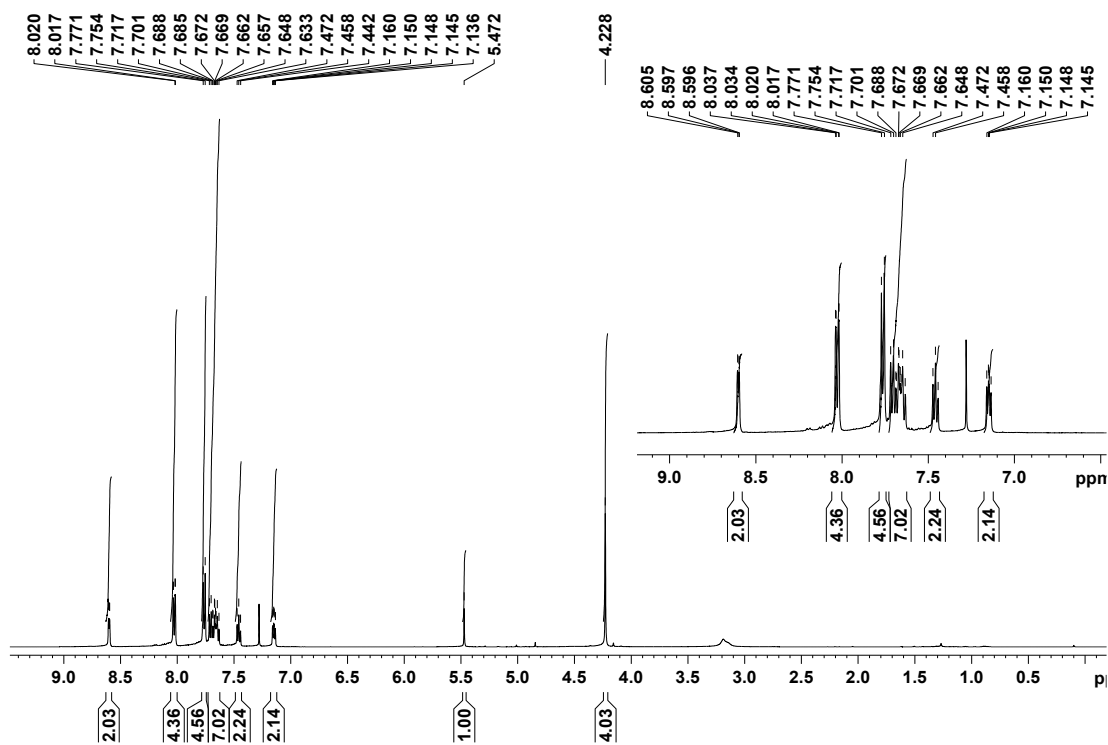


Figure 2.7: ^1H NMR of 2PyN2Q ligand.

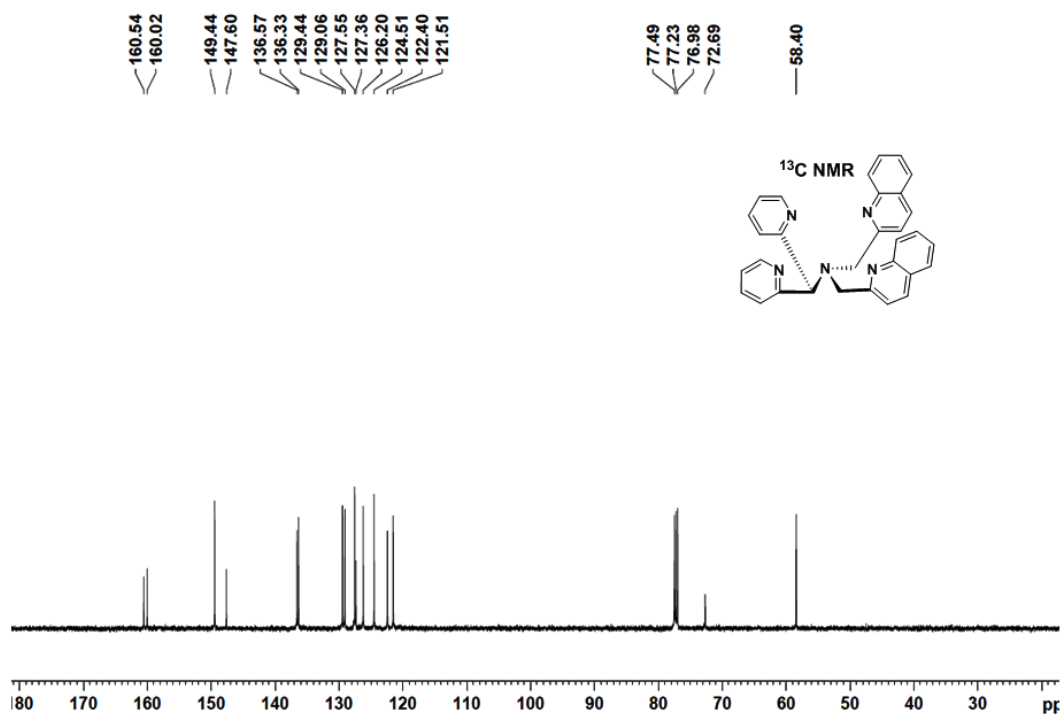
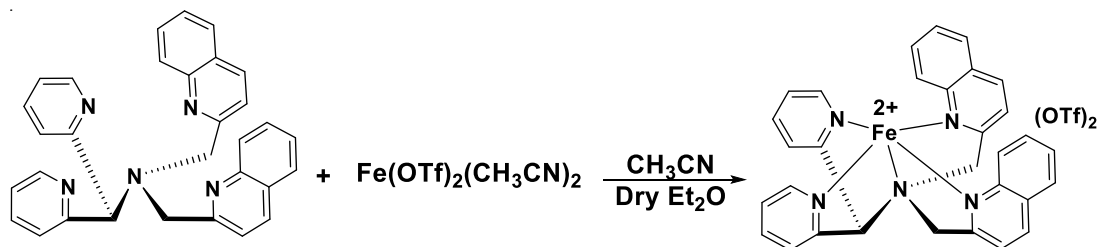


Figure 2.8: ¹³C NMR of 2PyN2Q ligand.

Synthesis and characterization of iron(II)-complex [Fe^{II}(2PyN2Q)](OTf)₂.



The ligand 2PyN2Q (1.2 mmol) and iron(II)-precursor complex Fe(OTf)₂·2CH₃CN (1.0 mmol) were reacted for overnight in excess amount of acetonitrile (40 mL) inside the glove box. The reaction mixture was concentrated by applying vacuum. Then excess dry diethyl ether was added to the reaction mixture and the schlenk was shaken vigorously to get precipitate of complex. The mixture was kept undisturbed to settle down the precipitate of complex at the bottom of the schlenk flask. The clear solution part above the precipitate was decanted off. Then the precipitate was dried properly by applying vacuum and kept under N₂ atmosphere of glove box. Resultant complex was crystallized from dichloromethane and diethyl ether solvent

mixture. The corresponding triflate anion coordinated single crystal was grown from acetonitrile-toluene or acetonitrile-diethylether solvent combination. The obtained complex was characterized spectroscopically. UV-vis (MeCN): 368 nm ($\epsilon \sim 1954 \text{ Lmol}^{-1}\text{cm}^{-1}$) and 470 nm ($\epsilon \sim 1954 \text{ Lmol}^{-1}\text{cm}^{-1}$). ESI-MS (observed, 688.090 calculated, 688.093), Elemental Anal. (Calculated for $\text{C}_{33}\text{H}_{25}\text{F}_6\text{FeN}_5\text{O}_6\text{S}_2$), C, 48.25; H, 3.07; N, 8.52; S, 7.80; found: C, 48.145, H, 3.30, N, 8.256, S, 7.65.

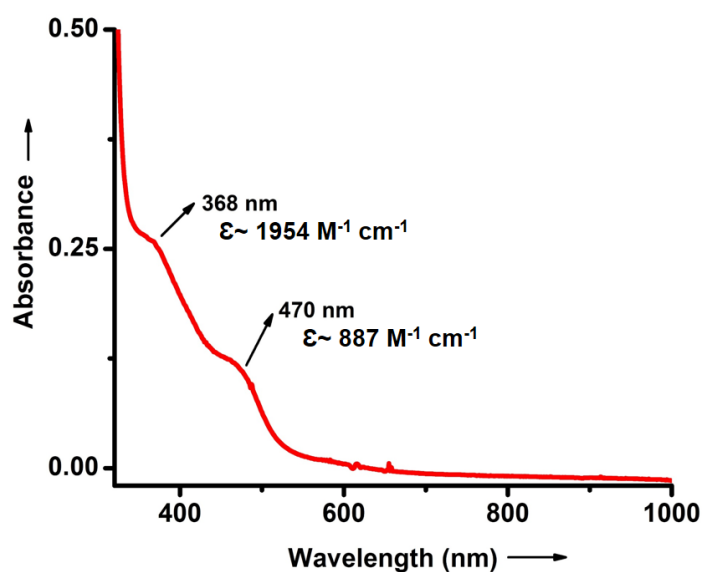
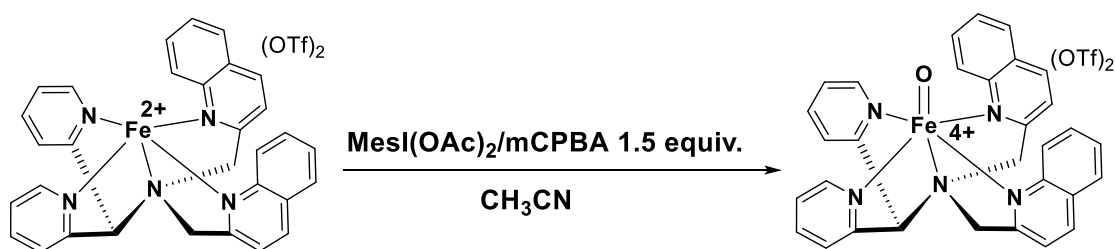


Figure 2.9: UV-vis of complex, $[\text{Fe}^{\text{II}}(2\text{PyN}2\text{Q})](\text{OTf})_2$

Synthesis and characterization of iron(IV)-oxo-complex, $[\text{Fe}^{\text{IV}}(2\text{PyN}2\text{Q})(\text{O})]^{2+}$.



The complex **1** (1.21 mM solution in acetonitrile) was reacted with 1.5-2 equiv. of $\text{MesI}(\text{OAc})_2$ or mCPBA in acetonitrile. The resulting solution forms iron(IV)-oxo complex **2**, within 1 minutes of addition of the oxidants. The corresponding iron(IV)-oxo complex showed UV-vis band at 770 nm (d-d transition) with a molar extinction coefficient, $\epsilon \sim 250 \text{ Lmol}^{-1}\text{cm}^{-1}$. The

formation of the iron(IV)-oxo complex **2** was monitored by UV-vis. The complex **2** showed the half-life around ~30 minutes. The iron(IV)-oxo species **2** was characterized by ESI-MS (Calculated for $[\text{Fe}^{\text{IV}}(\text{2PyN2Q})(\text{O})(\text{OTf})]^+$, m/z 688.093, obtained 688.090).

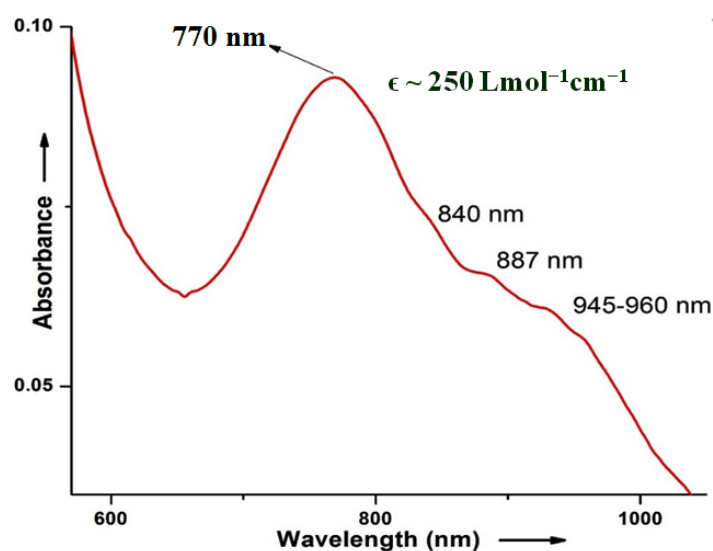


Figure 2.10: UV-vis of complex, $[\text{Fe}^{\text{II}}(\text{2PyN2Q})(\text{O})]^{2+}$

Synthesis and characterization of iron(II)-complex $[\text{Fe}^{\text{II}}(\text{2PyN2Q})(\text{Cl})]\text{Cl}$ The ligand N2QuPy (1 mmol) and iron(II)-chloride, FeCl_2 (1.2 mmol) were reacted for overnight in excess amount of tetrahydrofuran (THF) and acetonitrile (40 mL) inside the glove box. The reaction mixture was concentrated by applying vacuum. Then excess dry hexane was added to the reaction mixture and shaken to get precipitate of complex. Then the mixture was allowed to settle down the precipitate of complex get settled at the bottom of the schlenk flask. The clear solution part above the precipitate was decanted off. Then the precipitate was dried properly by applying vacuum and kept under N_2 atmosphere of glove box. The single crystal of the corresponding chloro complex was obtained from acetonitrile. The crystallized complex was characterized spectroscopically. UV-vis (MeCN): $\lambda_{\text{max}} = 358 \text{ nm}, 454 \text{ nm}$, ESI-MS (observed, 558.10 calculated, 558.11), Elemental Anal. (Calculated for $\text{C}_{31}\text{H}_{25}\text{Cl}_2\text{FeN}_5$) C, 62.65; H, 4.24; N, 11.78; found: C, 62.50, H, 4.20, N, 11.71.

Synthesis and characterization of iron(II)-complex [Fe^{II}(N2QuPy)(Br)]Br: The ligand 2PyN2Q (1.2 mmol) and iron(II)-bromide, FeBr₂ (1.0 mmol) were reacted for overnight in excess amount of tetrahydrofuran (40 mL) and acetonitrile inside the glove box. The reaction mixture was concentrated by applying vacuum. Then excess dry hexane was added to the reaction mixture and shaken to get precipitate of complex. The mixture was left undisturbed to settle down the precipitate of complex at the bottom of the schlenk flask. The clear solution part above the precipitate was decanted off. Then the precipitate was dried properly by applying vacuum and kept under N₂ atmosphere of glove box. UV-vis (MeCN): $\lambda_{\text{max}} = 352 \text{ nm}, 460 \text{ nm}$, ESI-MS (observed, m/z, 558.10 calculated, 558.11), Elemental Anal. (Calculated for C₃₁H₂₅Br₂FeN₅) C, 54.50; H, 3.69; N, 10.25; found: C, 54.41, H, 3.60, N, 10.10.

Synthesis and characterization of iron(II)-complex [Fe^{II}(2PyN2Q)(X)](ClO₄) (5 and 6).

The above-synthesized complexes **3** and **4** were reacted with 2.5 equiv. NaClO₄ of in MeOH-MeCN solvent and the resulting solution was stirred for 4 hours. This process was repeated for second time. The complex solution was dried to get orange powder complex. Then the residue was dissolved in dichloromethane (DCM) to get complex in the solution. The remaining white residue remained at the bottom of the round schlenk flask. The solution was kept unstirred for 1 hour to settle down the white precipitate. Then the clear red solution was decanted off and filtered through Whatman filter paper fitted in sintered funnel. The filtrate was dried to get orange powdered [Fe^{II}(2PyN2Q)(X)](ClO₄). The complexes were crystallized from chloroform/hexane and used for halogenations reactions. The anion exchange was carried out for both the complexes **3** and **4**. The obtained perchlorate anion containing complexes **5** and **6** showed the same UV-vis like complexes **3** and **4**. Further the complexes were characterized by X-ray crystallographic study. For complex **5**, UV-vis (MeCN): $\lambda_{\text{max}} = 355 \text{ nm}, 466 \text{ nm}$, ESI-MS (observed, m/z 558.103 calculated, 558.115), Elemental Anal. (Calculated for C₃₁H₂₅Cl₂FeN₅O₄) C, 56.56; H, 3.83; N, 10.64; found: C, 56.46, H, 3.70, N, 10.50. For complex

6, UV-vis (MeCN): $\lambda_{\text{max}} = 355 \text{ nm}, 445 \text{ nm}$, ESI-MS (observed, m/z 602.056 calculated, 602.064), Elemental Anal. (Calculated for $\text{C}_{31}\text{H}_{25}\text{BrClFeN}_5\text{O}_4$) C, 52.98; H, 3.59; N, 9.97; found: C, 52.75, H, 3.47, N, 9.73.

2.4.3. General procedure for sp^3 C–H oxidation reactions. From stock solution of complex 1, (2.43 mM solution acetonitrile solution), 1.5 mL of solution was taken in a 20 mL vial along with stir bar. 1.5 equiv. of $\text{MesI}(\text{OAc})_2$ was added under stirring condition. After 1 minutes excess amount (>100 equiv.) substrate was added to the reaction mixture and the reaction was stirred for 30 min. Finally, the reactions mixtures were analyzed by GC/GC-MS. Yield of the hydroxylation products were calculated based on calculated area of the standard products.

2.4.4. General procedure for 18-O labelling study for sp^3 C–H oxidation reactions. To solution of 2.43 mM of complex 2 equiv. of $\text{MesI}(\text{OAc})_2$ was added to generate the iron(IV)-oxo complex 2 inside glove box. 50 μL of H_2^{18}O was added to this solution. The resulting solution was kept at -35°C freeze inside the glove box for 30-40 minutes so that all the iron(IV)-oxo complex 2 gets labelled with 18-O. The solution was taken out from the freeze and ethylbenzene was added and the reaction was continued for 30 minutes. After completion of the reactions the reactions mixture were analyzed by GC-MS in order to detect the percentage of 18-O labeled in the products.

2.4.5. Kinetics study

A stock solution of complex 1 (1.21 mM) was prepared in dry acetonitrile inside the glove-box. The kinetics were carried out by taking 2 mL of stock solution of complex 1 and reacting with 1.5 equiv. $\text{MesI}(\text{OAc})_2$ or mCPBA. The 2 mL solution was taken in a 3 mL cuvette and subsequently $\text{MesI}(\text{OAc})_2$ was added. After addition of oxidant, $\text{MesI}(\text{OAc})_2$, within 1-2 minutes of reaction duration the formation of iron(IV)-oxo 2 species gets completed. The complex 2 showed the half-life around 30 min as monitored by UV-vis study. We carried out

the kinetics study under pseudo-first order reaction condition (substrates were used >10 equiv. compared to complex concentration). Every kinetics was finished within 10 minutes. The rate constant were determined by following the exponential decay pattern of 770 nm band iron(IV)-oxo.

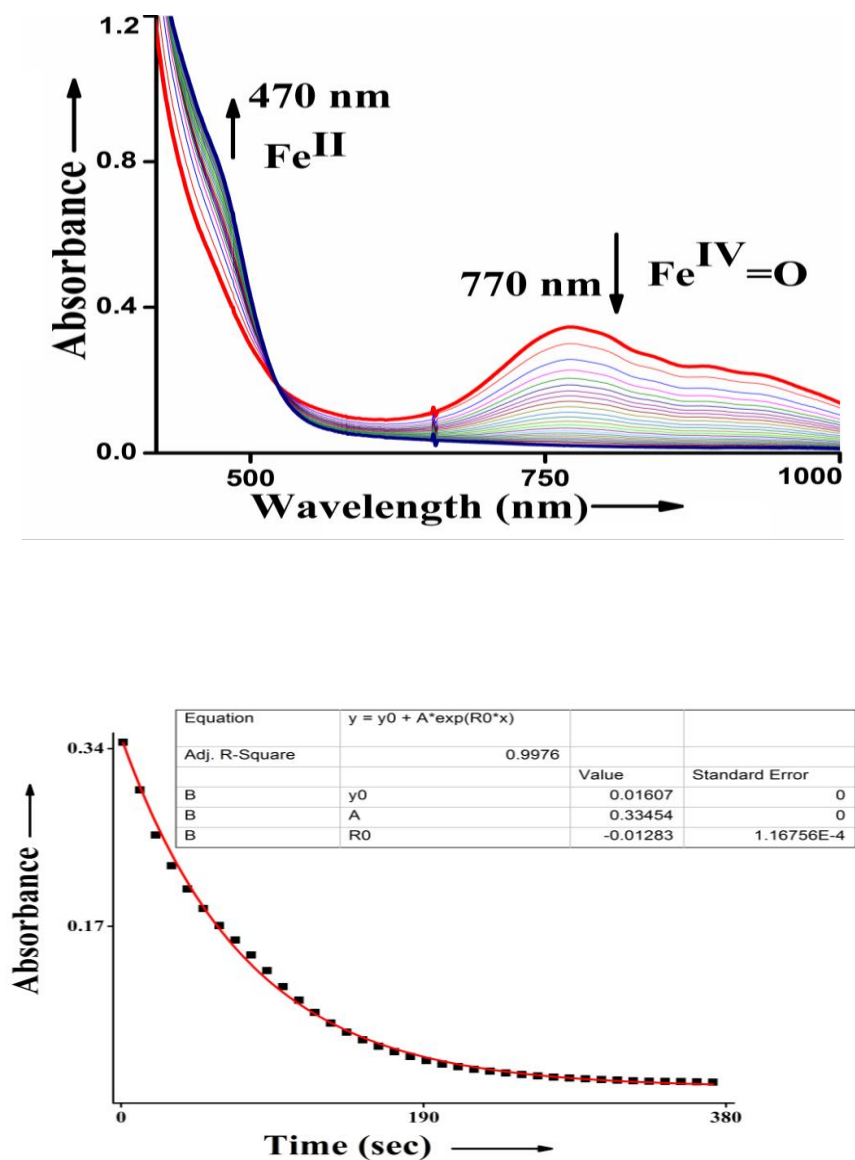


Figure 2.11: UV-vis change plot during C-H oxidation reaction with triphenylmethane and decay plot at 770 nm band fitted well with exponential curve fitting.

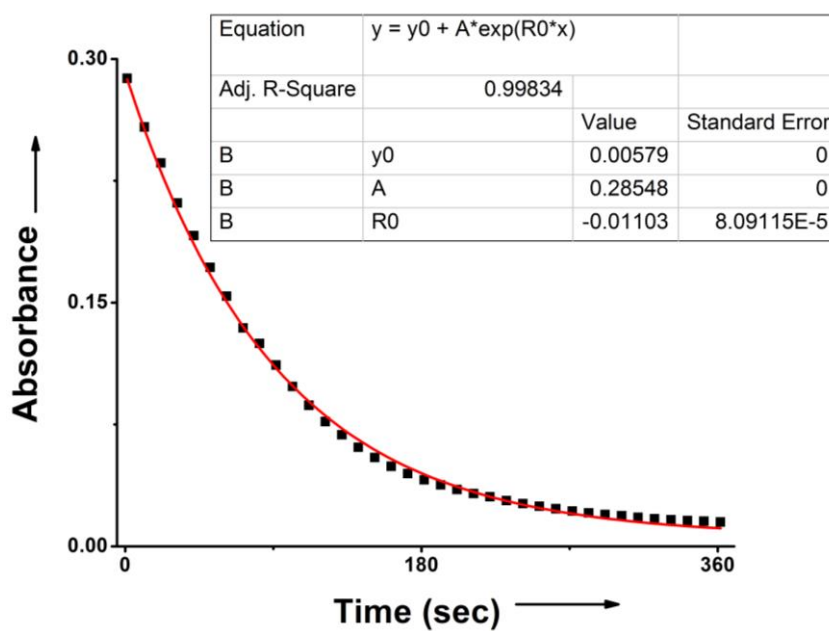
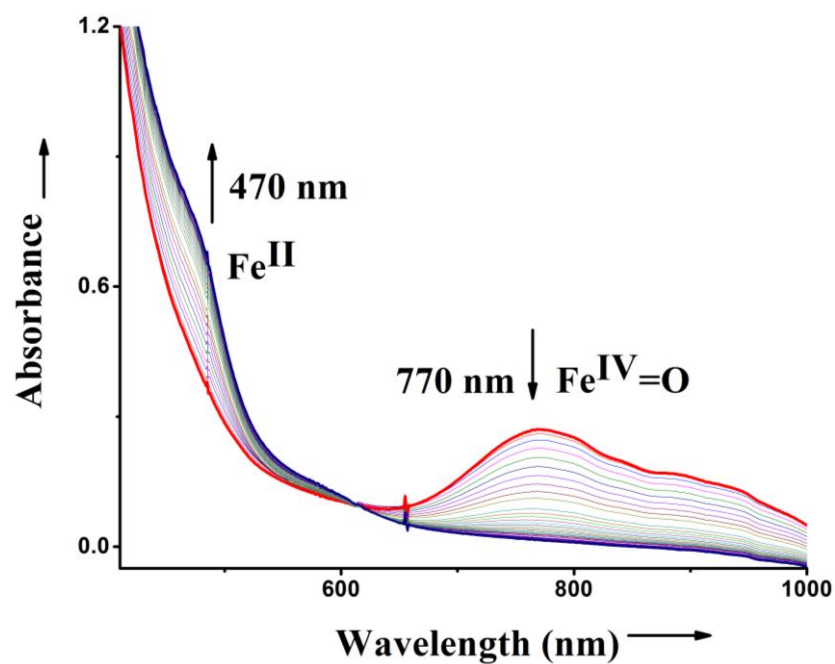
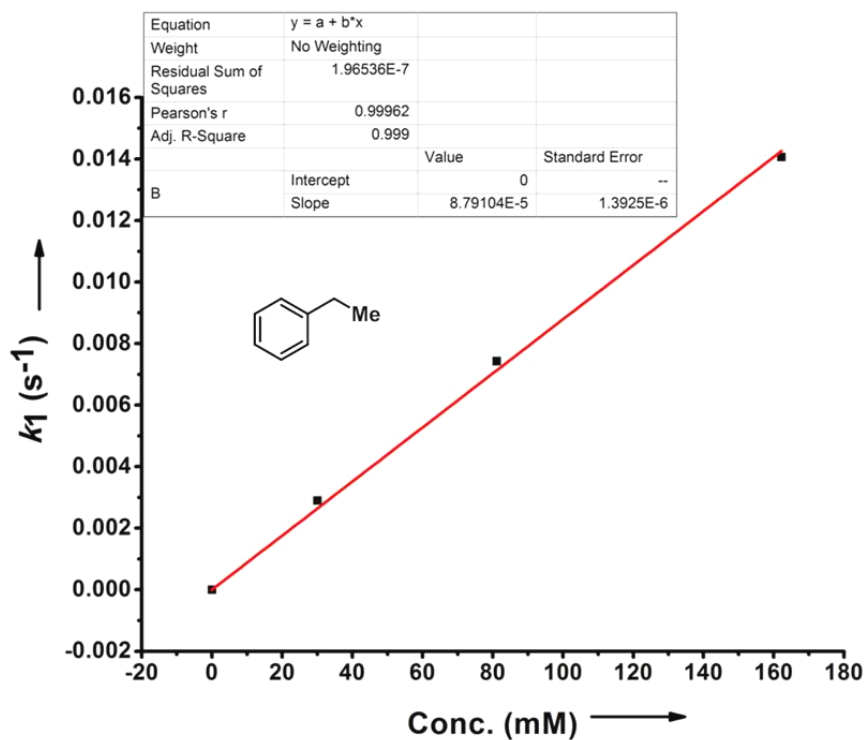


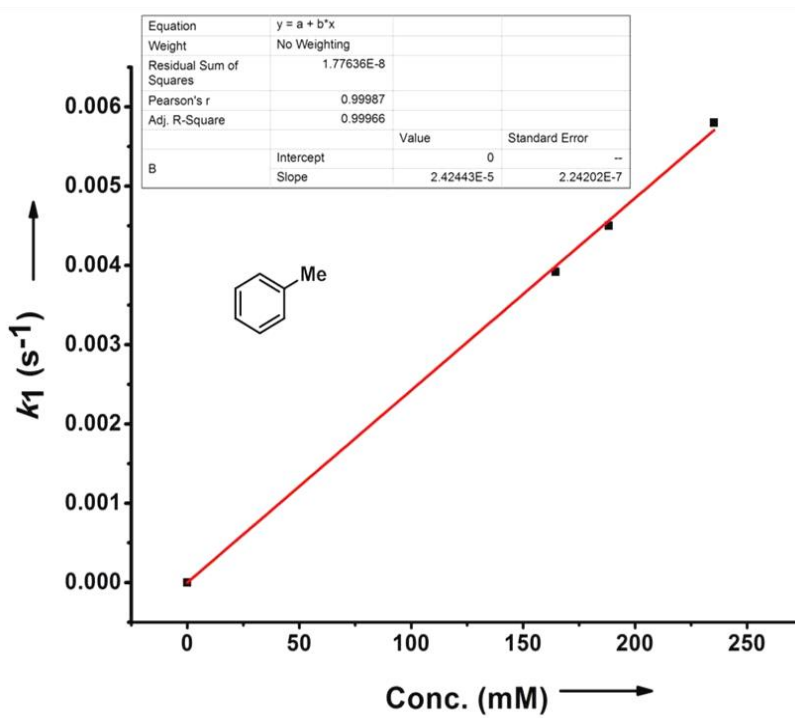
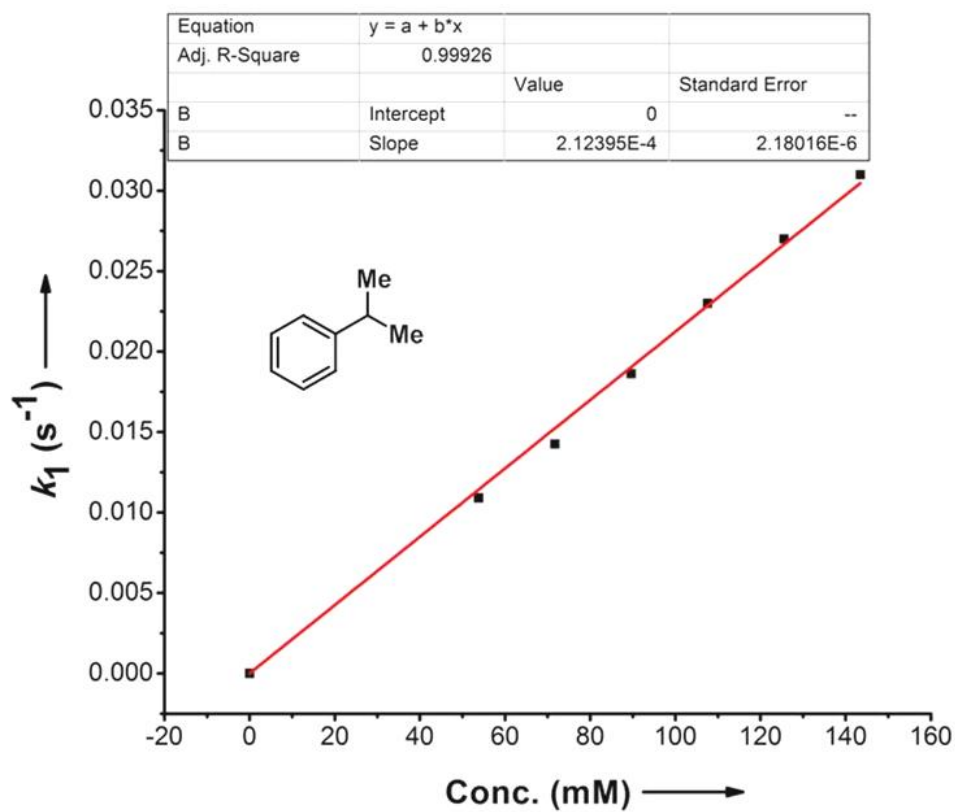
Figure 2.12: UV-vis change plot during C-H oxidation reaction with ethyl benzene and decay plot at 770 nm band fitted well with exponential curve fitting.

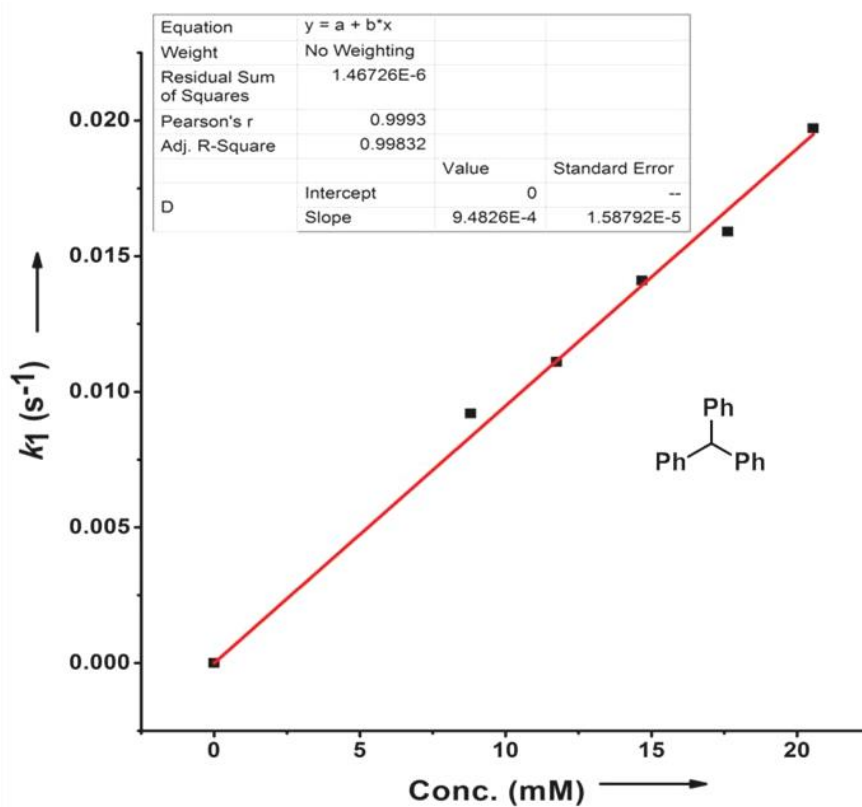
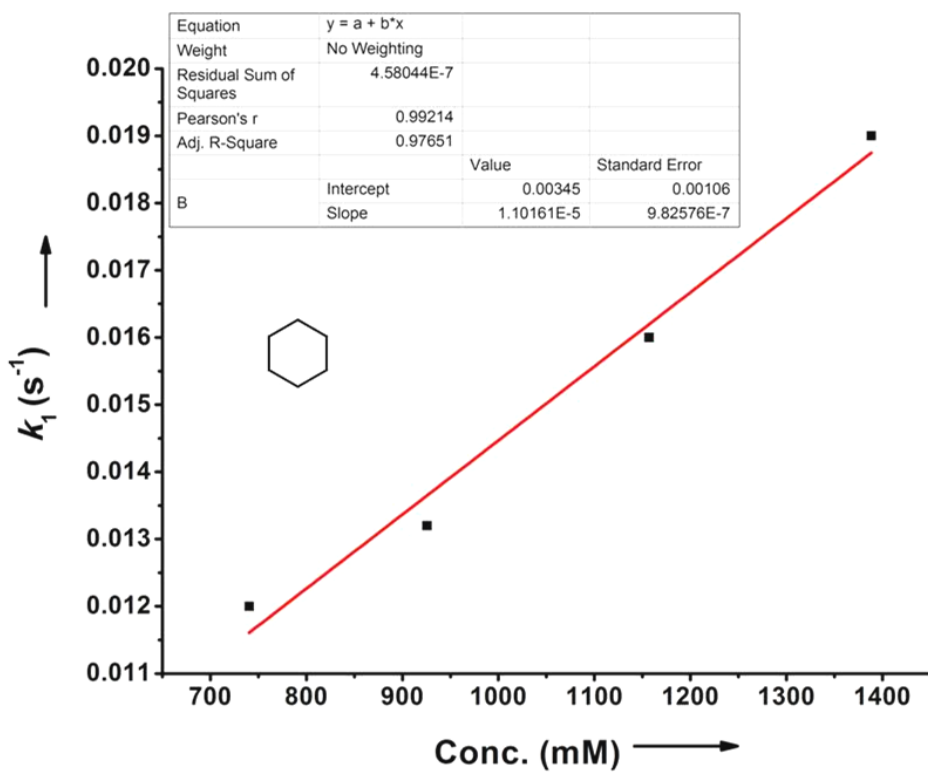
Correlation diagram: BDE vs $\log k'2$ (Bell-Evans-Polayni plot):

Table 2.2

BDE (kcal/mol)	k_2 ($M^{-1}s^{-1}$)	$\log k'2$	Substrate
81.5	0.948	-0.0232	TPM
85	0.212	-0.673	Cumene
87	0.088	-1.35	Ethylbenzene
90	0.0242	-2.1	Toluene
99.5	0.011	-3.03	Cyclohexane







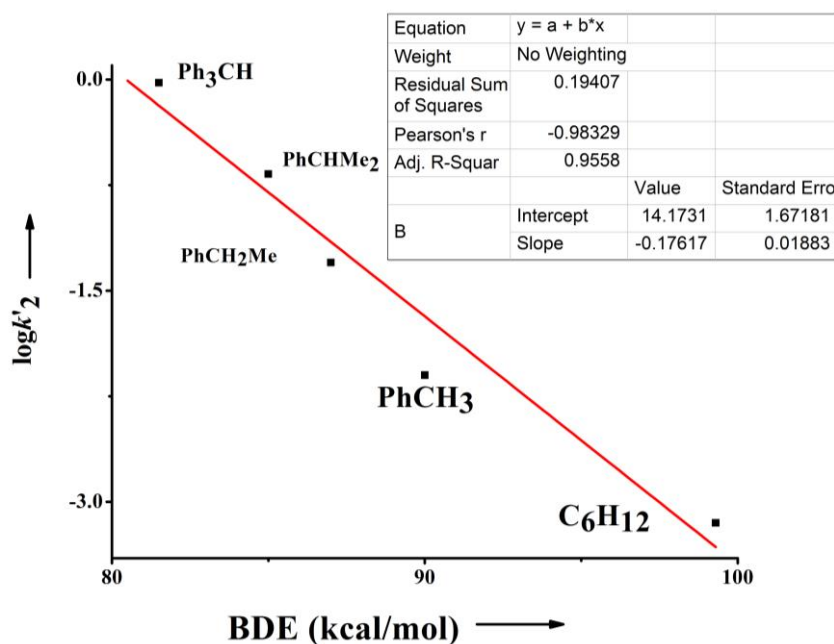
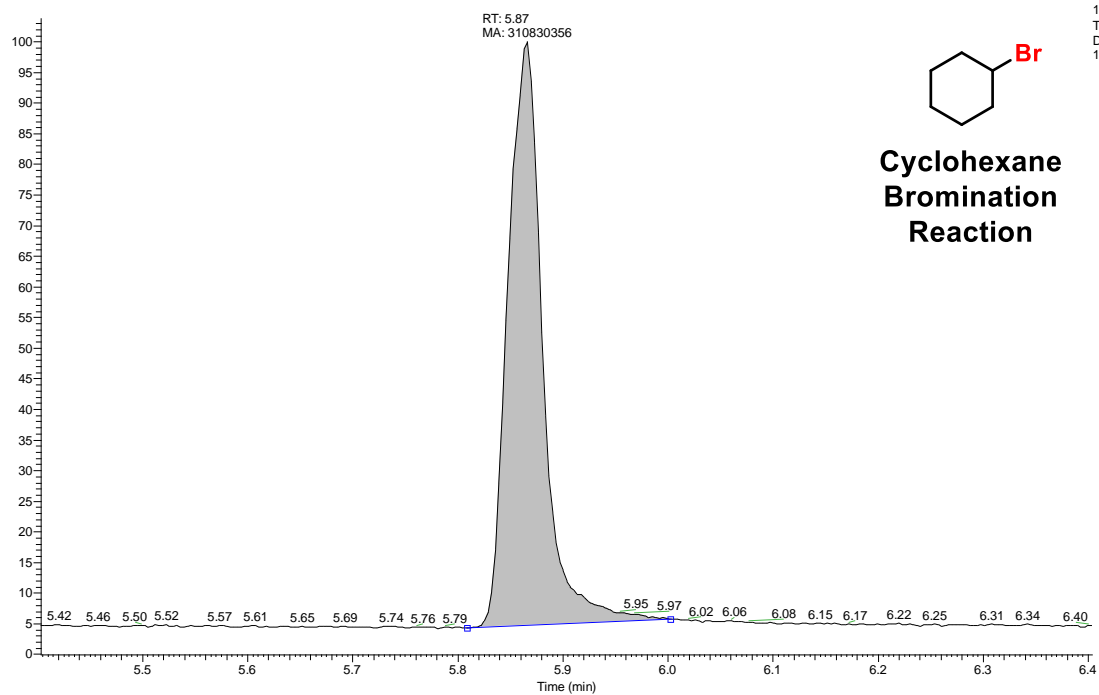


Figure 2.13: Second order kinetics plot of cumene, cyclohexane, ethylbenzene, triphenylmethane and toluene, for constructing Bells-Evans-Polayni plot

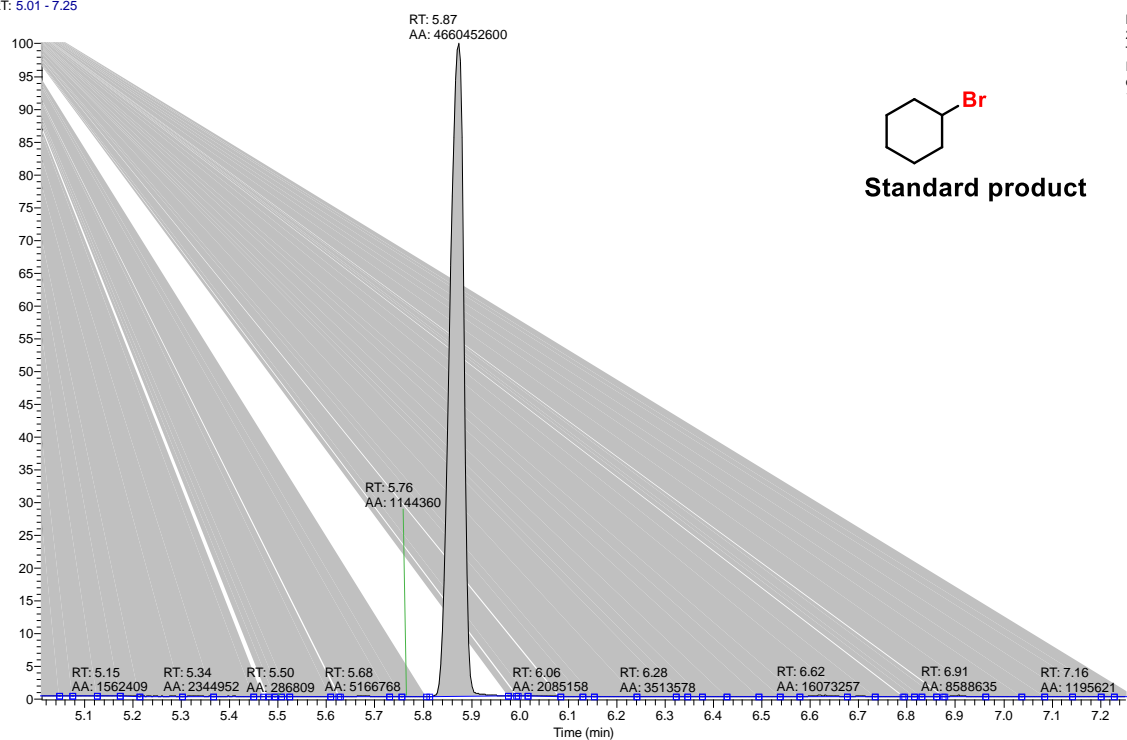
2.4.6. General procedure for sp^3 C–H halogenations reactions. From a stock solution of complex **1**, (4 mM solution in acetonitrile), 1 mL of solution was taken in a 20 mL vial with a stir bar. Subsequently 2 equiv. of mCPBA was added under stirring condition. Immediately a solution of halide complexes **3**, [Fe(2PyN2Q)(Cl)](Cl) or **4**, [Fe(2PyN2Q)(Br)](Br) was added to it (40 mol% w.r.t. complex **2** concentration). Then excess amount (>100 equiv.) substrate was added to the reaction mixture and the reaction was stirred for 30 minutes. Finally the reactions mixtures were analyzed by both GC/GC-MS.

2.4.7. Representative GC-MS data of the products:

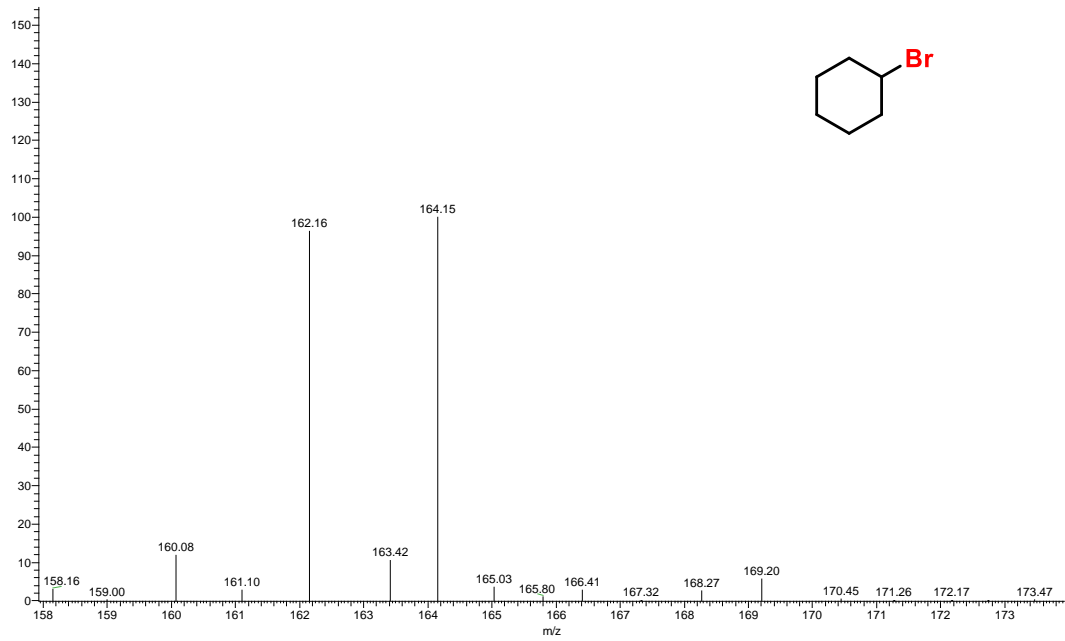
RT: 5.40 - 6.40



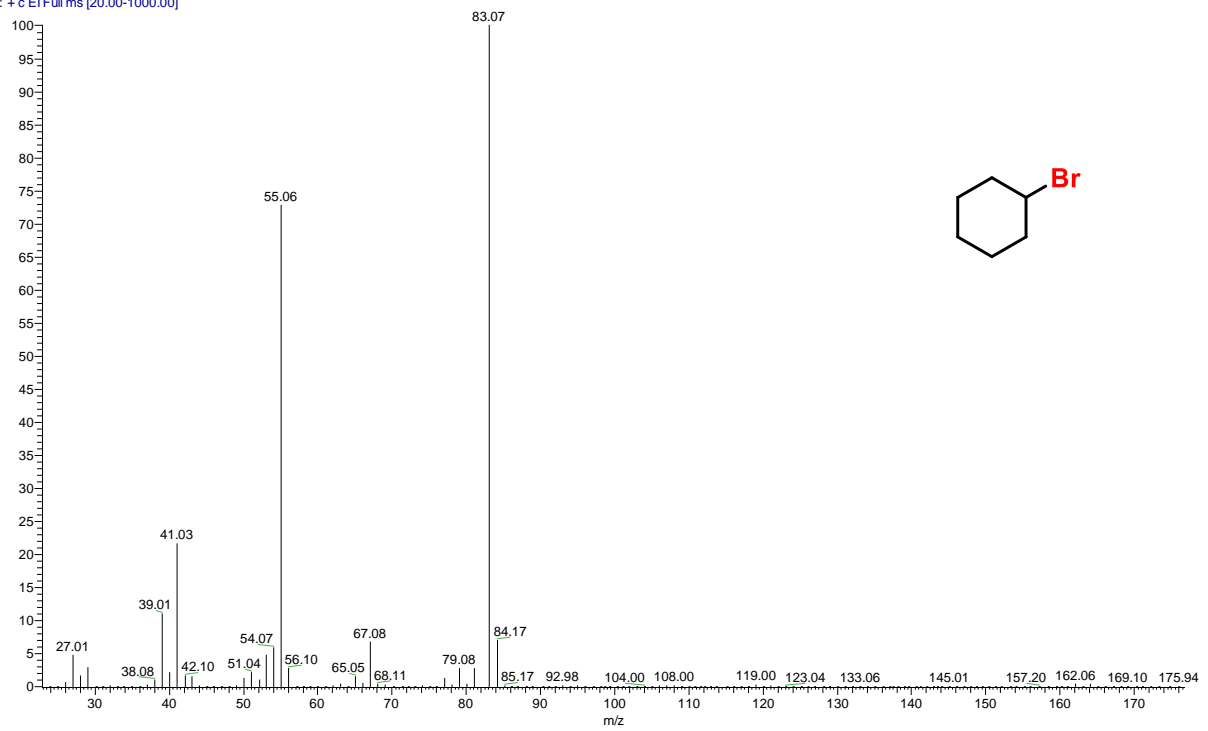
RT: 5.01 - 7.25



DM-SR5-144-2 #1019 RT: 5.86 AV: 1 NL: 9.66E4
T: + c EI Full ms [20.00-1000.00]



dm-sr5-137-1 #1021 RT: 5.87 AV: 1 NL: 8.48E8
T: + c EI Full ms [20.00-1000.00]



2.5. References:

1. (a) Vaillancourt, F. H.; Yeh, E.; Vosburg, D. A.; Garneau-Tsodikova, S.; Walsh, C. T. *Chem. Rev.* **2006**, *106*, 3364-3378; (b) Fujimori, D. G.; Walsh, C. T. *Curr. Opin. Chem. Biol.* **2007**, *11*, 553-560; (c) Rittle, J.; Green, M. T. *Science* **2010**, *330*, 933-937; (d) Krebs, C.; Galonić Fujimori, D.; Walsh, C. T.; Bollinger, J. M. *Acc. Chem. Res.* **2007**, *40*, 484-492; (e) Holm, R. H.; Kennepohl, P.; Solomon, E. I. *Chem. Rev.* **1996**, *96*, 2239-2314; (f) Sahu, S.; Goldberg, D. P. *J. Am. Chem. Soc.* **2016**, *138*, 11410-11428; (g) Sono, M.; Roach, M. P.; Coulter, E. D.; Dawson, J. H. *Chem. Rev.* **1996**, *96*, 2841-2888; (h) Cook, S. A.; Hill, E. A.; Borovik, A. S. *Biochemistry* **2015**, *54*, 4167-4180; (i) Que, L. Jr. *J. Biol. Inorg. Chem.* **2017**, *22*, 1-278
2. (a) Blasiak, L. C.; Vaillancourt, F. H.; Walsh, C. T.; Drennan, C. L. *Nature* **2006**, *440*, 368-371; (b) Vaillancourt, F. H.; Yin, J.; Walsh, C. T. *Proc. Natl. Acad. Sci. U.S.A.* **2005**, *102*, 10111-10116; (c) Solomon, E. I.; Wong, S. D.; Liu, L. V.; Decker, A.; Chow, M. S. *Curr. Opin. Chem. Biol.* **2009**, *13*, 99-113; (d) Barry, S. M.; Challis, G. L. *ACS Catal.* **2013**, *3*, 2362-2370; (e) Kovaleva, E. G.; Lipscomb, J. D. *Nat. Chem. Biol.* **2008**, *4*, 186-193; (f) Siitonen, V.; Selvaraj, B.; Niiranen, L.; Lindqvist, Y.; Schneider, G.; Metsä-Ketelä, M. *Proc. Natl. Acad. Sci. U.S.A.* **2016**, *113*, 5251-5256.
3. (a) Knauer, S. H.; Hartl-Spiegelhauer, O.; Schwarzinger, S.; Hänzelmann, P.; Dobbek, H. *FEBS J.* **2012**, *279*, 816-831; (b) Hausinger, R. P. *Crit. Rev. Biochem. Mol. Biol.* **2004**, *39*, 21-68; (c) Martinez, S.; Hausinger, R. P. *J. Biol. Chem.* **2015**, *1*.
4. (a) Galonić Fujimori, D.; Barr, E. W.; Matthews, M. L.; Koch, G. M.; Yonce, J. R.; Walsh, C. T.; Bollinger, J. M.; Krebs, C.; Riggs-Gelasco, P. J. *J. Am. Chem. Soc.* **2007**, *129*, 13408-13409; (b) Wong, C.; Fujimori, D. G.; Walsh, C. T.; Drennan, C. L. *J. Am. Chem. Soc.* **2009**, *131*, 4872-4879 (c) Borowski, T.; Noack, H.; Radoń, M.; Zych, K.;

- Siegbahn, P. E. M. *J. Am. Chem. Soc.* **2010**, *132*, 12887-12898; (d) Huang, J.; Li, C.; Wang, B.; Sharon, D. A.; Wu, W.; Shaik, S. *ACS Catal.* **2016**, *6*, 2694-2704.
5. Neumann, C. S.; Fujimori, D. G.; Walsh, C. T. *Chem. Biol.* **2008**, *15*, 99-109.
6. Kojima, T.; Leising, R. A.; Yan, S.; Que, L. Jr. *J. Am. Chem. Soc.* **1993**, *115*, 11328-11335.
7. (a) Wong, S. D.; Srnec, M.; Matthews, M. L.; Liu, L. V.; Kwak, Y.; Park, K.; Bell III, C. B.; Alp, E. E.; Zhao, J.; Yoda, Y.; Kitao, S.; Seto, M.; Krebs, C.; Bollinger, J. M.; Solomon, E. I. *Nature* **2013**, *499*, 320-323; (b) Matthews, M. L.; Neumann, C. S.; Miles, L. A.; Grove, T. L.; Booker, S. J.; Krebs, C.; Walsh, C. T.; Bollinger, J. M. *Proc. Natl. Acad. Sci. U.S.A.* **2009**, *106*, 17723-17728.
8. Srnec, M.; Solomon, E. I. *J. Am. Chem. Soc.* **2017**, *139*, 2396-2407.
9. Comba, P.; Wunderlich, S. *Chem. Eur. J.* **2010**, *16*, 7293-7299.
10. Planas, O.; Clemancey, M.; Latour, J.-M.; Company, A.; Costas, M. *Chem. Commun.* **2014**, *50*, 10887-10890.
11. Chatterjee, S.; Paine, T. K. *Angew. Chem. Int. Ed.* **2016**, *55*, 7717-7722.
12. Puri, M.; Biswas, A. N.; Fan, R.; Guo, Y.; Que, L. Jr. *J. Am. Chem. Soc.* **2016**, *138*, 2484-2487.
13. (a) Lo, W. K. C.; McAdam, C. J.; Blackman, A. G.; Crowley, J. D.; McMorran, D. A. *Inorg. Chim. Acta.* **2015**, *426*, 183-194; (b) Massie, A. A.; Denler, M. C.; Cardoso, L. T.; Walker, A. N.; Hossain, M. K.; Day, V. W.; Nordlander, E.; Jackson, T. A. *Angew. Chem. Int. Ed.* **2017**, *56*, 4178-4182.
14. See experimental section.
15. (a) Kaizer, J.; Klinker, E. J.; Oh, N. Y.; Rohde, J.-U.; Song, W. J.; Stubna, A.; Kim, J.; Münck, E.; Nam, W.; Que, L. Jr. *J. Am. Chem. Soc.* **2004**, *126*, 472-473; (b) Cho, K.-

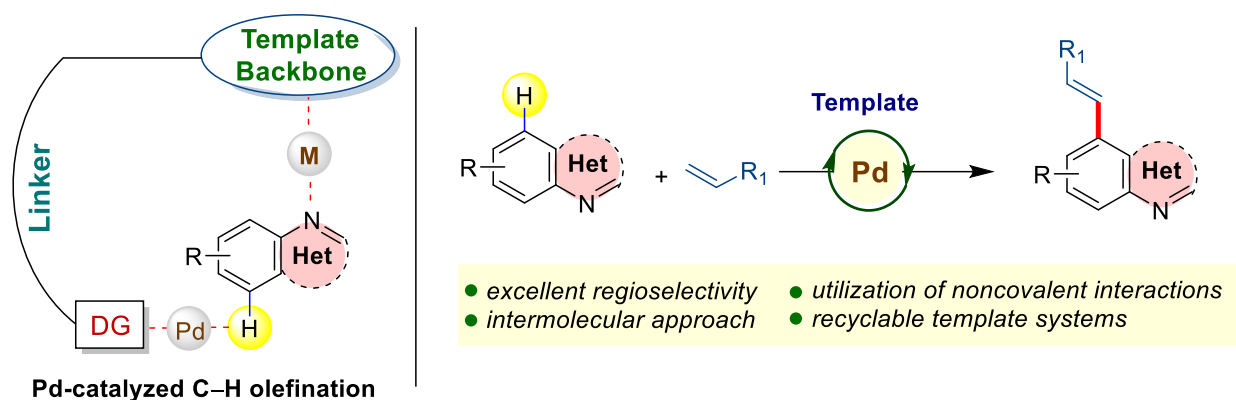
- B.; Wu, X.; Lee, Y.-M.; Kwon, Y. H.; Shaik, S.; Nam, W. *J. Am. Chem. Soc.* **2012**, *134*, 20222- 20225.
16. (a) Serrano-Plana, J.; Oloo, W. N.; Acosta-Rueda, L.; Meier, K. K.; Verdejo, B.; García-España, E.; Basallote, M. G.; Münck, E.; Que, L., Jr.; Company, A.; Costas, M. *J. Am. Chem. Soc.* **2015**, *137*, 15833-15842; (b) Paria, S.; Que, L., Jr.; Paine, T. K. *Angew. Chem. Int. Ed.* **2011**, *50*, 11129-11132; (c) Rana, S.; Dey, A.; Maiti, D. *Chem. Commun.* **2015**, *51*, 14469-14472; (d) Mitra, M.; Nimir, H.; Demeshko, S.; Bhat, S. S.; Malinkin, S. O.; Haukka, M.; Lloret-Fillol, J.; Lisensky, G. C.; Meyer, F.; Shteinman, A. A.; Browne, W. R.; Hrovat, D. A.; Richmond, M. G.; Costas, M.; Nordlander, E. *Inorg. Chem.* **2015**, *54*, 7152-7164.
17. (a) Puri, M.; Que, L., Jr. *Acc. Chem. Res.* **2015**, *48*, 2443-2452; (b) Engelmann, X.; Monte-Pérez, I.; Ray, K. *Angew. Chem. Int. Ed.* **2016**, *55*, 7632-7649; (c) Ray, K.; Pfaff, F. F.; Wang, B.; Nam, W. *J. Am. Chem. Soc.* **2014**, *136*, 13942-13958; (d) Sahu, S.; Widger, L. R.; Quesne, M. G.; de Visser, S. P.; Matsumura, H.; Moëgne-Loccoz, P.; Siegler, M. A.; Goldberg, D. P. *J. Am. Chem. Soc.* **2013**, *135*, 10590-10593; (e) Sahu, S.; Quesne, M. G.; Davies, C. G.; Dürr, M.; Ivanović-Burmazović, I.; Siegler, M. A.; Jameson, G. N. L.; de Visser, S. P.; Goldberg, D. P. *J. Am. Chem. Soc.* **2014**, *136*, 13542-13545.
18. (a) Bryant, J. R.; Mayer, J. M. *J. Am. Chem. Soc.* **2003**, *125*, 10351-10361; (b) Mayer, J. M. *Acc. Chem. Res.* **1998**, *31*, 441-450; (c) Ghosh, M.; Singh, K. K.; Panda, C.; Weitz, A.; Hendrich, M. P.; Collins, T. J.; Dhar, B. B.; Sen Gupta, S. *J. Am. Chem. Soc.* **2014**, *136*, 9524-9527; (d) Ghosh, M.; Nikhil, Y. L.; Dhar, B. B.; Sen Gupta, S. *Inorg. Chem.* **2015**, *54*, 11792-11798.
19. Kwon, E.; Cho, K. B.; Hong, S.; Nam, W. *Chem. Commun.* **2014**, *50*, 5572-5575.

20. (a) Cho, K.-B.; Hirao, H.; Shaik, S.; Nam, W. *Chem. Soc. Rev.* **2016**, *45*, 1197-1210; (b) Dhuri, S. N.; Cho, K.-B.; Lee, Y.-M.; Shin, S. Y.; Kim, J. H.; Mandal, D.; Shaik, S.; Nam, W. *J. Am. Chem. Soc.* **2015**, *137*, 8623-8632.
21. (a) Cho, K.-B.; Hirao, H.; Shaik, S.; Nam, W. *Chem. Soc. Rev.* **2016**, *45*, 1197-1210; (b) Lindhorst, A. C.; Haslinger, S.; Kuhn, F. E. *Chem. Commun.* **2015**, *51*, 17193-17212; (c) Bae, S. H.; Seo, M. S.; Lee, Y.-M.; Cho, K.-B.; Kim, W.-S.; Nam, W. *Angew. Chem. Int. Ed.* **2016**, *55*, 8027-8031.
22. (a) Vardhaman, A. K.; Sastri, C. V.; Kumar, D.; de Visser, S. P. *Chem. Commun.* **2011**, *47*, 11044-11046; (b) Vardhaman, A. K.; Barman, P.; Kumar, S.; Sastri, C. V.; Kumar, D.; de Visser, S. P. *Chem. Commun.* **2013**, *49*, 10926-10928; (c) Vardhaman, A. K.; Barman, P.; Kumar, S.; Sastri, C. V.; Kumar, D.; de Visser, S. P. *Angew. Chem. Int. Ed.* **2013**, *52*, 12288-12292.
23. (a) Liu, W.; Groves, J. T. *Angew. Chem. Int. Ed.* **2013**, *52*, 6024-6027; (b) Liu, W.; Huang, X.; Cheng, M.-J.; Nielsen, R. J.; Goddard, W. A.; Groves, J. T. *Science* **2012**, *337*, 1322-1325.
24. Ray, K.; Lee, S. M.; Que, L. J. *Inorg. Chim. Acta* **2008**, *361*, 1066-1069.
25. (a) Zang, Y.; Kim, J.; Dong, Y.; Wilkinson, E. C.; Appelman, E. H.; Que, L. Jr. *J. Am. Chem. Soc.* **1997**, *119*, 4197-4205; (b) Hubin, T. J.; McCormick, J. M.; Alcock, N. W.; Busch, D. H. *Inorg. Chem.* **2001**, *40*, 435-444; (c) Rana, S.; Bag, S.; Patra, T.; Maiti, D. *Adv. Synth. Catal.* **2014**, *356*, 2453-2458.
26. (a) de Visser, S. P.; Latifi, R. *J. Phys. Chem. B* **2009**, *113*, 12-14; (b) Pandian, S.; Vincent, M. A.; Hillier, I. H.; Burton, N. A. *Dalton Trans.* **2009**, 6201-6207.
27. Puri, M.; Biswas, A. N.; Fan, R.; Guo, Y.; Que, L., Jr. *J. Am. Chem. Soc.* **2016**, *138*, 2484-2487.

Chapter 3

Chapter 3

Regiocontrolled Remote C–H Olefination of Small Heterocycles



Abstract: Achieving site-selective C–H functionalization in arene is a fundamental challenge, as it is mainly controlled by electronic nature of the molecules. Chelation assisted C–H functionalization strategy overcomes the selectivity issues by utilizing distance and geometry of covalently attached directing groups (DGs). This strategy requires stoichiometric DG installation/removal and a suitable functional group on which to tether DG. Such strategies are ineffective for the small heterocycles without having attachable functional groups. Moreover, heterocycles are not the judicious choice as substrates owing to the possibilities of catalyst deactivation. Inspired by recent developments, herein we demonstrate utilization of chelating template backbone bearing covalently attached directing groups which enables site-selective remote C–H functionalization of heterocycles. Observed selectivity is the outcome of non-covalent interactions between the heterocycles and bifunctional template backbone.

3.1. Introduction:

Non-covalent interactions play a key activating and controlling role for enantioselectivity in asymmetric catalysis.¹⁻² Such interactions have been harnessed in relatively limited examples for controlling regioselectivity or site-selectivity in catalysis. Recently, utilization of these weak interactions for directed regiocontrolled C–H functionalization has drawn a significant interest in the synthetic community.³ Innate regioselectivity in arenes is mainly controlled by electronic nature of the molecules.

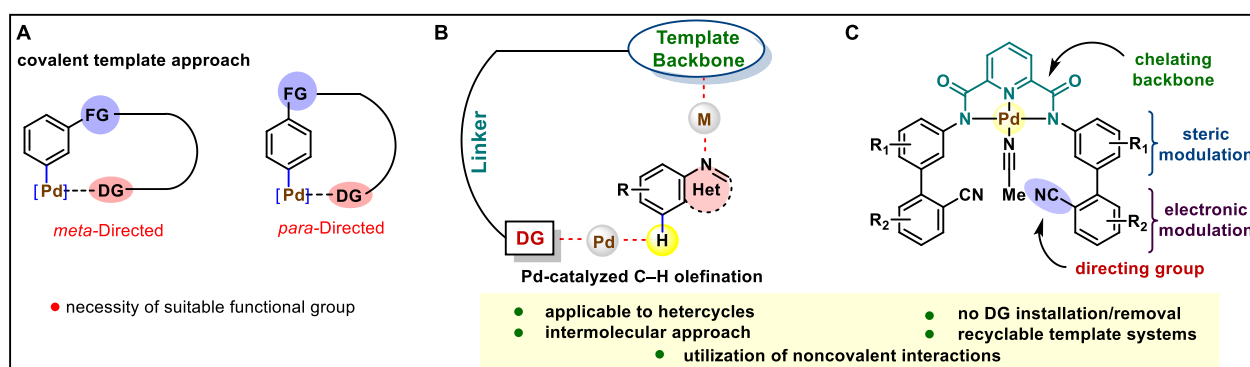


Figure 3.1. Remote site-selective C–H functionalization. **(A)** Covalent approach: necessity of a suitable functional group to tether the DG. **(B)** Strategy: utilization of coordination approach. **(C)** Bis-amide based tri-coordinating backbone. **(D)** Bidentate template

On contrary, achieving site selectivity is a fundamental challenge if the precursors contain several C–H bonds having comparable steric and electronic environment. Chelation assisted C–H functionalization overcomes the selectivity issues by employing covalently attached directing groups (DGs, Figure 1A).⁴⁻¹⁷ However, this strategy bears certain limitations of using a stoichiometric amount of DG and necessity of having a suitable functional group to tether the DG. Sometimes, the DGs are so bulky that their use limit the practicality and scalability of the methods. Additionally, such approach has not been feasible for small heterocycles, which do not have any suitable functional group to tether the DG. Moreover, heterocycles act as catalyst poison by coordinating with the transition metal catalyst.¹⁸ Thus, it would be highly intriguing

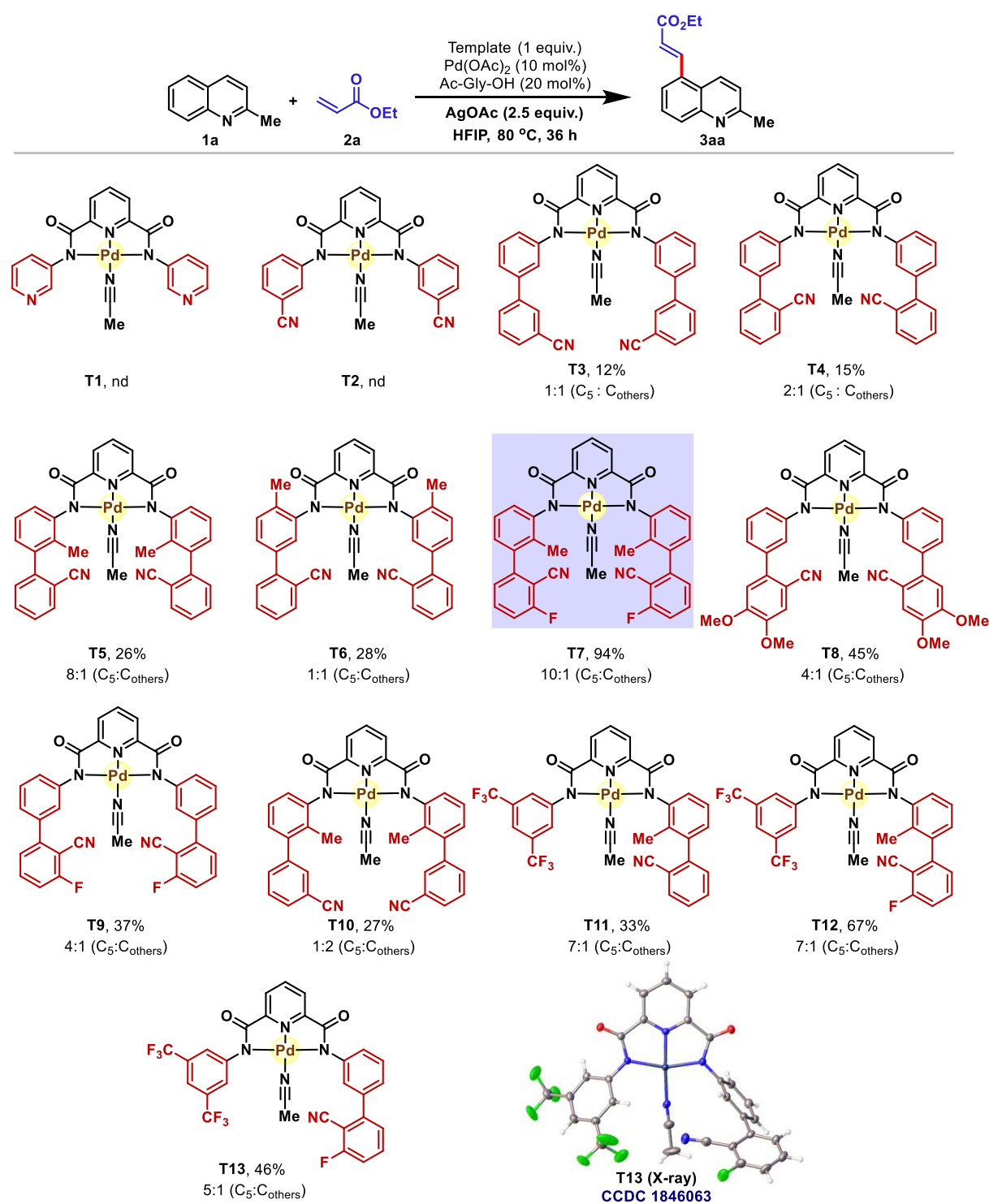
if a generalized strategy could overcome these inadequacies. In this context, we intend to utilize this non-productive coordination as a useful tool for remote C–H functionalization of pharmaceutically relevant heterocycles by synthesizing an appropriate template system which binds the heterocycles in a host-guest complexation manner.

Regioselective C–H activation of arenes by employing non-covalent interaction is one of the emerging research area.³ Several innovative attempts have been made to exercise remote C–H functionalization of arenes by employing H-bond, ion-paired, electrostatic, and ion-dipole interactions.¹⁰⁻¹³ Recently, Yu's group has pioneered an elegant approach for palladium catalyzed site-selective remote functionalization of heterocycles.²³ An appropriate proximity and geometry of the template plays a crucial role for selective manipulations of the heterocycles. Further development of methods to synthesize site-selective remote C–H functionalized heterocycles is still in high demand to streamline the overall synthesis. On the basis of weak-interaction promoted *para*-C–H activation²⁴ and recent report,²⁵ we thought to explore the non-covalent interaction to access the remote C–H bond of heterocycles.

3.2. Result and discussion:

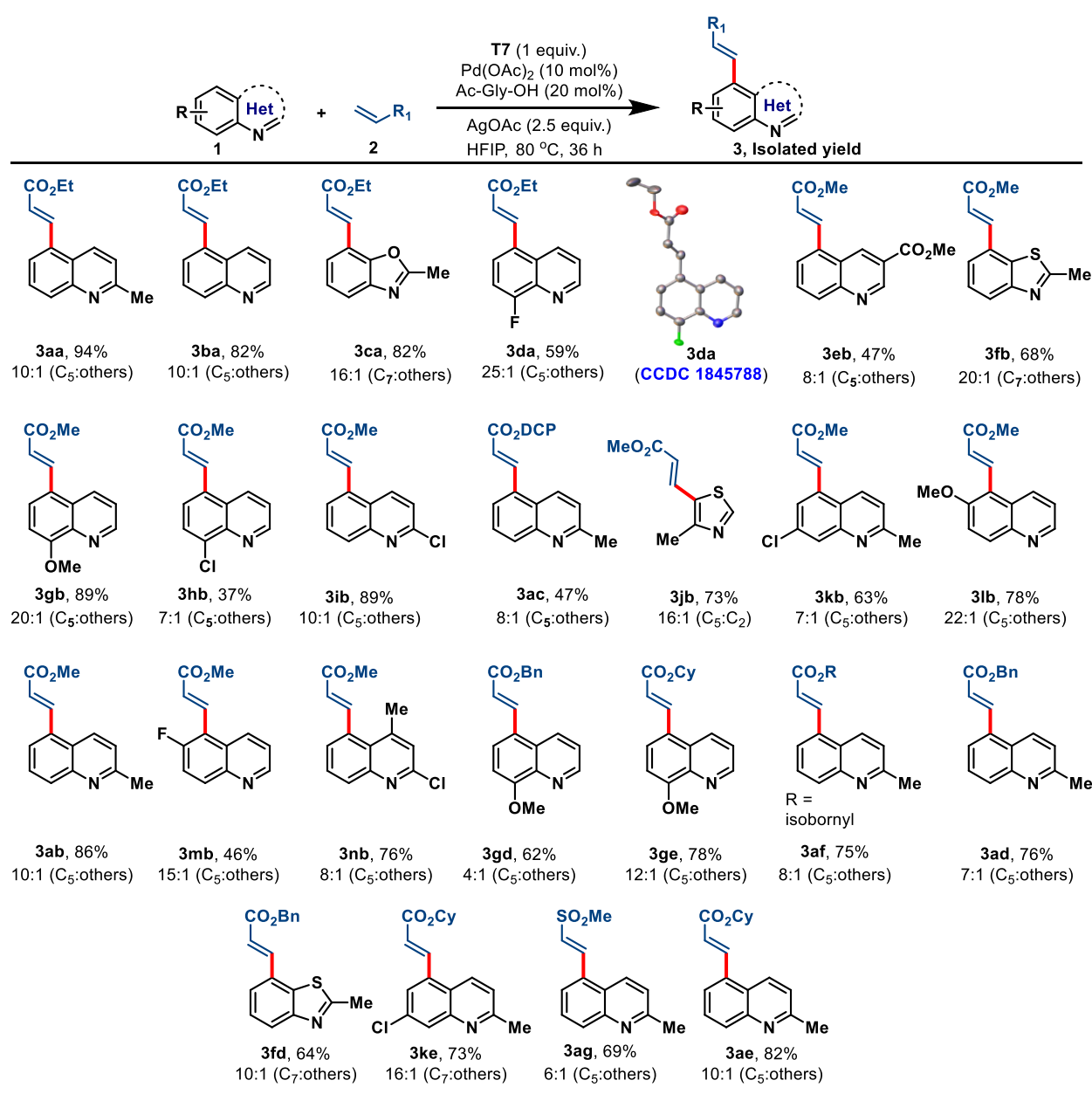
Considering challenges associated with heterocycles and to accomplish both the reactivity and the remote-selectivity, we have synthesized heterocycle-based chelating templates covalently attached with directing groups.^{12,23} The non-productive coordination of heterocycles with the metal center could be ironically useful to preorganize the heterocycles in such a way that the distal C–H bond would be exposed to the DG (Figure 3.1B). We synthesized bis-amide based tri-coordinating backbone which further tethered with DG (Figure 3.1C). These bifunctional template systems simultaneously bind with two metals: first metal which binds with tri-coordinating backbone helps to pendant the substrate and the covalently attached DG directs

the second metal catalyst to the specific remote C–H bond. Appropriate steric modulation at linker might be reinforced to achieve the virtuous selectivity.



Scheme 3.1. Evaluation of tri-coordinating templates for site-selective remote C–H functionalizations of heterocycles

Pincer ligand based on imines and amides are well studied and have been extensively utilized in diverse applications.²⁵⁻²⁷ In this context, a di-picolinamide as a tri-coordinating backbone which tethers symmetrically with biphenyl based directing group was tested. The distance and geometry of the template allowed quinoline based heterocycles for site-selective remote C–H functionalizations. Di-picolinamide based templates containing different directing groups with diverse steric and electronic factor were synthesized.



Scheme 3.2. Site-selective olefination of heterocycles with T7

We carried out olefination reaction of quinaldine (1a) as a model reaction in the presence of 10 mol% palladium(II) acetate, 20 mol% N-acetylglycine. With the template T1 and T2, attempts were in vain. Presumably, shorter distance of side arm DGs could not reach the specific position to deliver the metal catalyst. Interestingly, switching to template T4 produced the olefination compound (3aa) in 15% yield with the selectivity 2:1 (C5: others). Introduction of steric effect into the inner core dramatically increases the selectivity with T5. However, T6 bearing methyl substituents outer side of the core failed to promote selective olefination. These results clearly indicate the importance of the distance and geometrical constraint of the template. Modulating the electronic environment on DGs, T7 was found to be most effective and produced the olefination products in 94% yield with excellent C5 selectivity (10:1). Presence of fluorine atoms in T7 helps to make the reaction homogeneous which might be the key controlling factor for enhancing the reactivity and selectivity. Replacing T7 with electronically rich template T8 led to the loss of reactivity and selectivity. Comparison of unsymmetrical and symmetrical templates was informative (T5 vs T11, T7 vs T12, and T9 vs T13). Overall these observations further confirm the effect of directing group and geometrical constraint of the template.

In evaluation of the scope of the site-selective remote C–H olefination with the template **T7**, we found that functionally diverse quinoline derivatives were olefinated at C₅ positions (Scheme 3.2). Electron withdrawing groups are well tolerated and provided the desired olefination product with good yields and selectivity. Electron donating alkyl and alkoxy groups containing quinoline derivatives also underwent olefination successfully. Further, this protocol was extended to check the feasibility of distal C–H functionalization with other heterocycles. Benzothiaole and benzoxazole derivatives also provided olefination products with synthetically useful yields and selectivity.

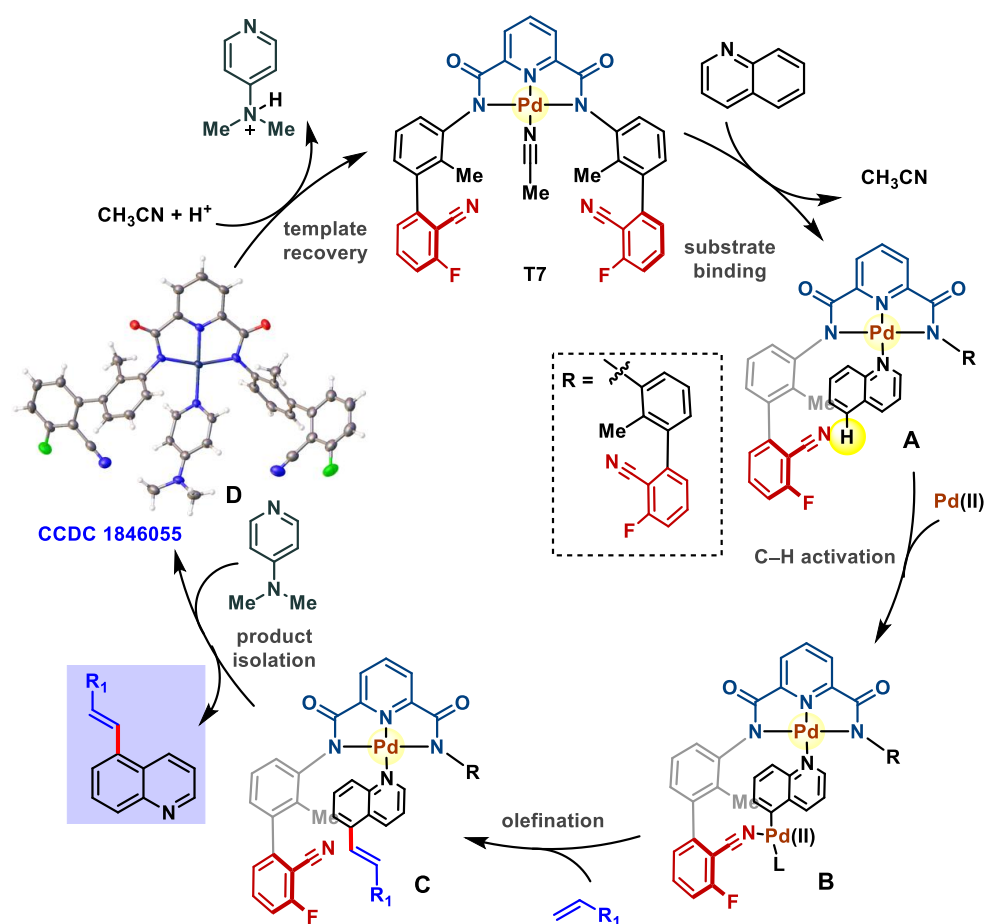


Figure 3.2. Template recovery cycle

To elucidate the mechanistic pathway, we carried out stepwise reactions for remote C–H functionalization of quinoline. Spectral characterization of **A** clearly reveals the role of template for site-selective C–H olefination. Desired C–H bond was selectively exposed to the DG upon anchoring the substrate through tridentate coordination. In the presence of a catalytic amount of palladium acetate and a mono-protected aminoacid ligand (*N*-acetylglycine), C₅–H of quinoline will be activated and subsequently will be functionalized with olefin. Following successful functionalization of quinoline, strong coordinating 4-dimethylaminopyridine (DMAP) was utilized to replace the desired product from the template backbone. Intermediate **A** and **D** were spectroscopically characterized. Finally, the template was recovered by treating **D** with methane sulfonic acid under reflux condition in acetonitrile. This simple protocol aided

to recover the template in 92% yield and therefore rendering **T7** as recyclable template for site-selective remote C–H activation of small heterocycles.

3.3. Conclusion:

In conclusion, we have synthesized prudent bifunctional templates, which can promote site-selective remote C–H bond functionalization of heterocycles. The recyclability of the template provides additional merit to the protocol. Present findings could broaden non-covalent approach for directed C–H activation methodology. We anticipate that such an approach will be useful in the synthesis of complex molecular scaffolds.

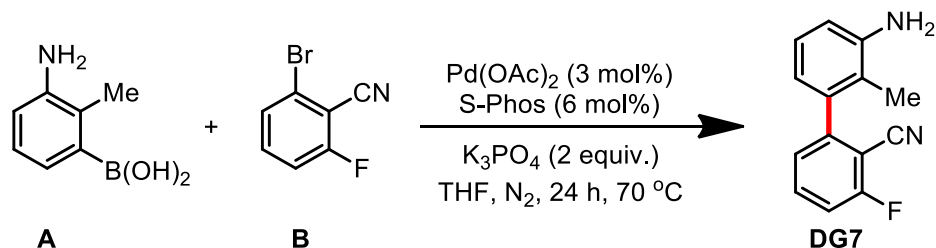
3.4. Experimental Details:

3.4.1. Materials and Methods. All reactions were carried out under aerobic condition in screw cap reaction tubes, unless otherwise stated. Solvents were bought from Aldrich in sure-seal bottle and were used as received. Olefins were purchased from TCI, India. All the other chemicals were bought from Aldrich, TCI-India, and Alfa Aesar. Compounds were purified by column chromatography using 100-200 mesh silica gel and Petroleum ether/Ethyl acetate solvent mixture as an eluent, unless stated otherwise. All isolated compounds were characterized by ^1H , ^{13}C spectroscopy, and HRMS. Unless otherwise stated, all Nuclear Magnetic Resonance spectra were recorded on a Bruker 400 MHz and 500 MHz instrument. NMR spectra are reported in parts per million (ppm), and were measured relative to the signals for residual solvent (7.26 ppm for ^1H and 77.16 ppm for ^{13}C NMR in CDCl_3 ; 2.5 ppm for ^1H and 39.51 ppm for ^{13}C NMR in DMSO-d_6 ; 1.94 ppm for ^1H and 1.32 ppm for ^{13}C in CD_3CN) in the deuterated solvent, unless otherwise stated. All ^{13}C NMR spectra were obtained with ^1H decoupling. High-resolution mass spectra (HRMS) were recorded on a micro-mass ESI TOF (time of flight) mass spectrometer.

3.4.2. Procedure for synthesis of tridentate template:

General Procedure A: Synthesis of directing group (DG)

Method 1.

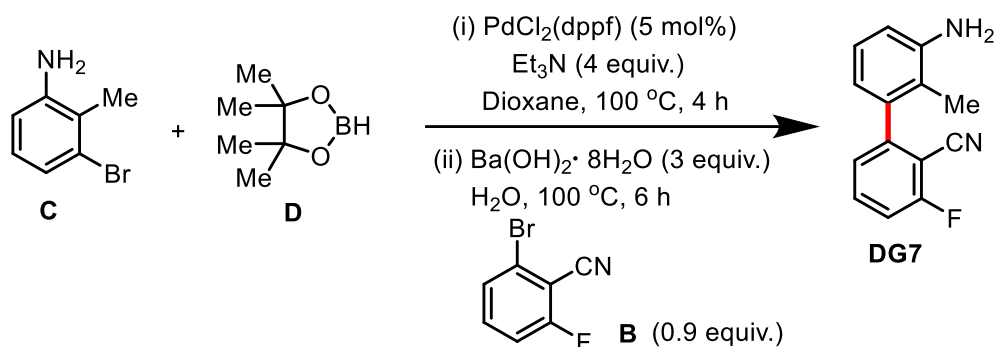


In a clean and oven dried reaction tube Pd(OAc)₂ (3 mol%), S-phos (6 mol%), 2-Bromo-6-fluorobenzonitrile (3 mmol), 3-Amino-2-methylphenyl boronic acid (3.5 mmol) and K₃PO₄ (2 eq.) were added. The reaction tubes were capped with Teflon cap and purged with N₂ gas (3 times) using Schlenk line set up. 6 mL THF was injected to the reaction tube and stirred for 24 h on a preheated oil bath at 70 °C. The reaction was diluted with ethyl acetate and excess base was quenched with saturated NH₄Cl solution. The organic part was washed 3 times with saturated NH₄Cl solution. Combined aqueous portion was again extracted with ethyl acetate, dried over anhydrous Na₂SO₄ and evaporated under reduced pressure. Pure directing group (**DG7**) was obtained from column chromatography using 7% ethyl acetate/pet ether solvent mixture as an eluent.

Yield:82%

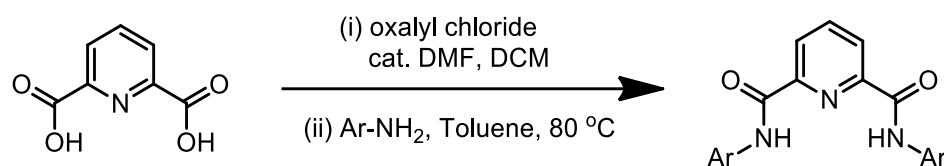
Appearance:white solid.

Method 2. (Ref. Kuninobu, Y.; Ida, H.; Nishi, M.; Kanai, M. *Nat. Chem.* **2015**, 7,712)



In an oven dried reaction tube 3-Bromo-2-methylaniline (1 g, 5.3 mmol) was taken and dissolved in dioxane (10 mL). To a solution of 3-Bromo-2-methylaniline, Et₃N (4.0 equiv.), PdCl₂(dppf) (5 mol%), and pinacolborane (3.0 equiv.) were added dropwise. The mixture was stirred at 100 °C for 4 h, then cooled to room temperature, and water (2.5 mL), Ba(OH)₂·8H₂O (3.0 equiv.), and 2-Bromo-6-fluorobenzonitrile (0.92 equiv) were successively added. Then the mixture was stirred at 100 °C for 6 h. Upon completion, the reaction mixture was cooled to room temperature and quenched with water (50 mL). The mixture was filtered through Celite. The filtrate was extracted with ethyl acetate and the organic layer was dried over Na₂SO₄. The solvent was removed and the residue was further purified by column chromatography using 7% ethyl acetate/pet ether as an eluent (69% yield).

Characterization data: ¹H NMR (400 MHz, CDCl₃) δ 7.60 (td, *J* = 8.1, 5.9 Hz, 1H), 7.24 – 7.14 (m, 2H), 7.10 (t, *J* = 7.8 Hz, 1H), 6.77 (d, *J* = 7.9 Hz, 1H), 6.64 (d, *J* = 7.5 Hz, 1H), 3.75 (s, 2H), 1.99 (s, 3H); ¹³C NMR (101 MHz, CDCl₃) δ 163.49 (d, ¹*J*_{FC} = 259.2 Hz), 148.40 (s), 145.34 (s), 137.88 (d, ⁴*J*_{FC} = 2.0 Hz), 134.03 (d, ³*J*_{FC} = 8.9 Hz), 126.62 (s), 126.40 (s), 126.36 (s), 120.13 (s), 119.93 (s), 115.77 (s), 114.51 (d, ²*J*_{FC} = 19.7 Hz), 14.27 (s).

General Procedure B: *Synthesis of symmetrical tridentate template*

In a clean, oven dried Schlenk tube with previously placed magnetic stirring bar, 2,6-pyridine carboxylic acid (500 mg, 3 mmol) was taken. Then the reaction tube was evacuated and back filled with nitrogen and this sequence was repeated two additional times. Then dry DCM (10 mL) followed by oxalyl chloride (2.5 equiv.) and 3-4 drops of DMF were added dropwise to the reaction tube and kept for 6 h stirring at room temperature. After completion, solvent was removed under reduced pressure. Next dissolved aromatic primary amine (2 equiv.) in dry toluene was added to the reaction tube and submerged into an oil bath pre-heated to 80 °C. The reaction mixture was allowed to stir overnight at 80 °C. Upon completion, the reaction mixture was cooled to room temperature. The residue was filtered through filter paper and subsequently washed with toluene and diethyl ether to afford the purified amide.

General Procedure C: *Synthesis of unsymmetrical tridentate template***Procedure for methyl 6-((3,5-bis(trifluoromethyl)phenyl)carbamoyl)picolinate:**

To a solution of 2,6-pyridinedicarboxylic acid (8.3 g, 50 mmol) in DCM (150 mL) was added oxalyl chloride (10.7 mL, 125 mmol, 2.5 equiv.) at 0 °C. Then DMF (0.2 mL) was added and the reaction mixture was stirred for 12 h at room temperature. Upon completion, the reaction mixture was concentrated under reduced pressure. Next, toluene (600 mL) and 3,5-bis(trifluoromethyl) aniline (11.7 mL, 75 mmol) were added and submerged into an oil bath preheated to 70 °C. Then, the oil bath was heated to 90 °C and the reaction mixture was allowed to stir 12 h. Upon completion, the reaction mixture was cooled down and added 200 mL of methanol. Then the reaction mixture was refluxed for 12 h. Upon completion, the reaction

mixture was cooled to room temperature and concentrated under reduced pressure. The white precipitate was collected by filtration and recrystallized from hot MeOH to give methyl 6-((3,5-bis(trifluoromethyl)phenyl)carbamoyl)-colinate (12.3 g, 62%) as a white solid.

Procedure for 6-((3,5-bis(trifluoromethyl)phenyl)carbamoyl)picolinic acid:

To a solution of methyl 6-((3,5-bis(trifluoromethyl)phenyl)carbamoyl)picolinate (9.8 g, 25 mmol) in MeOH (250 mL) was added LiOH monohydrate (3.14 g, 75 mmol) in three portions. After completion, the reaction mixture was concentrated under reduced pressure. The crude residue was dissolved in water and acidified by 6 M HCl, then extracted with EtOAc three times. The combined organic phase was dried with anhydrous Na_2SO_4 , and concentrated to yield 6-((3,5-bis(trifluoromethyl)phenyl)carbamoyl)picolinic acid (8.4 g, 89%) as a white solid.

Procedure for amide formation:

To a solution of 6-((3,5-bis(trifluoromethyl)phenyl)carbamoyl)picolinic acid (0.75 g, 2 mmol) in toluene was added thionyl chloride (0.36 mL, 5 mmol) dropwise at room temperature. Then DMF (3 drops) was added and the reaction mixture was stirred at 70 °C. Upon completion, the toluene was evaporated under reduced pressure, amine (2.1 mmol) and 10 mL toluene were added and submerged into an oil bath preheated to 70 °C. Then, the oil bath was heated to 90 °C and the reaction mixture was allowed to stir 12 h. After completion the solid was filtered and washed with toluene and diethyl ether to yield corresponding amide.

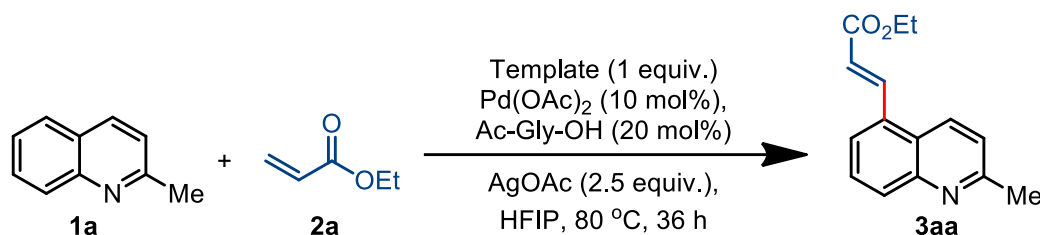
General Procedure D: Preparation of metal complex

Corresponding amide (1 mmol) and $\text{Pd}(\text{OAc})_2$ (1 mmol) were taken in 50 mL reaction flask equipped with a stir bar. 10 mL acetonitrile was added to the flask and the resulting mixture was stirred at 60 °C for 6 h. Upon completion, solvent was removed in vacuo. Next the residue

was purified by column chromatography on silica gel using DCM/MeOH as the eluent giving the pure template.

Note: Owing to the solubility problem template **T1** was prepared *in situ* and used for olefination reaction.

General Procedure E: Site-selective C-H olefination of heterocycles with tridentate template



A clean, oven dried reaction tube was charged with **1a** (0.1mmol), tridentate template (0.1 mmol), magnetic stirring bar and minimal amount of DCM to dissolve the substrate and template. After 20 min stirring at room temperature, the mixture was concentrated in vacuo. Then Pd(OAc)₂ (0.01 mmol), *N*-Ac-Gly-OH (0.02 mmol), AgOAc (0.25 mmol), HFIP (1.0 ml) and **2a** (0.3 mmol) were added in the reaction tube in aerobic condition. The reaction tube was sealed and allowed to stir at 80 °C for 36 h. Then the reaction mixture was cooled to room temperature and diluted with EtOAc and filtered through a short pad of celite with additional EtOAc. The filtrate was concentrated in vacuo. The residue was dissolved in toluene (2-3 mL) and 2-3 equiv. of DMAP was added to it. The solution was then stirred at 80 °C for 5-10 min. Upon completion, the reaction was cooled to room temperature and the mixture was passed through a short pad of silica using EtOAc/hexanes=1:1 as the eluent to give the product mixture. Finally the compound (**3aa**) was purified by column chromatography/on preparative TLC using EtOAc/pet ether solvent mixture as an eluent.

(The silica pad was then washed with DCM/MeOH=10:1 to get the crude template solution for the template regeneration.)

3.4.3. Template regeneration

The crude template solution was concentrated in vacuo and the residue was dissolved in acetonitrile. To this solution 2 equiv. of methanesulfonic acid was added and the resulting mixture was placed to a pre-heated oil bath at 60 °C for 2 h. Upon completion, the reaction mixture was cooled to room temperature and the solvent was removed under reduced pressure. Then the residue was dissolved in DCM and washed with water. The organic layer was dried over anhydrous Na₂SO₄ and concentrated in vacuo. Finally the template was purified by column chromatography (100-200 mesh silica gel) using 5% MeOH/DCM as a solvent eluent.

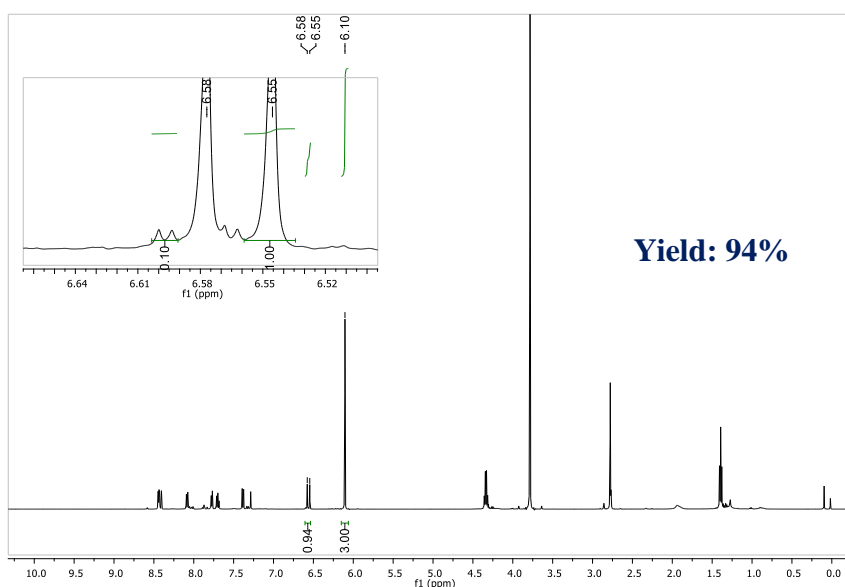


Figure 3.3. ¹H NMR of crude reaction mixture of **1a** with **2a** under standard reaction condition using template **T7**; 1,3,5-Trimethoxybenzene was used as internal standard.

3.4.4. Mechanistic study:

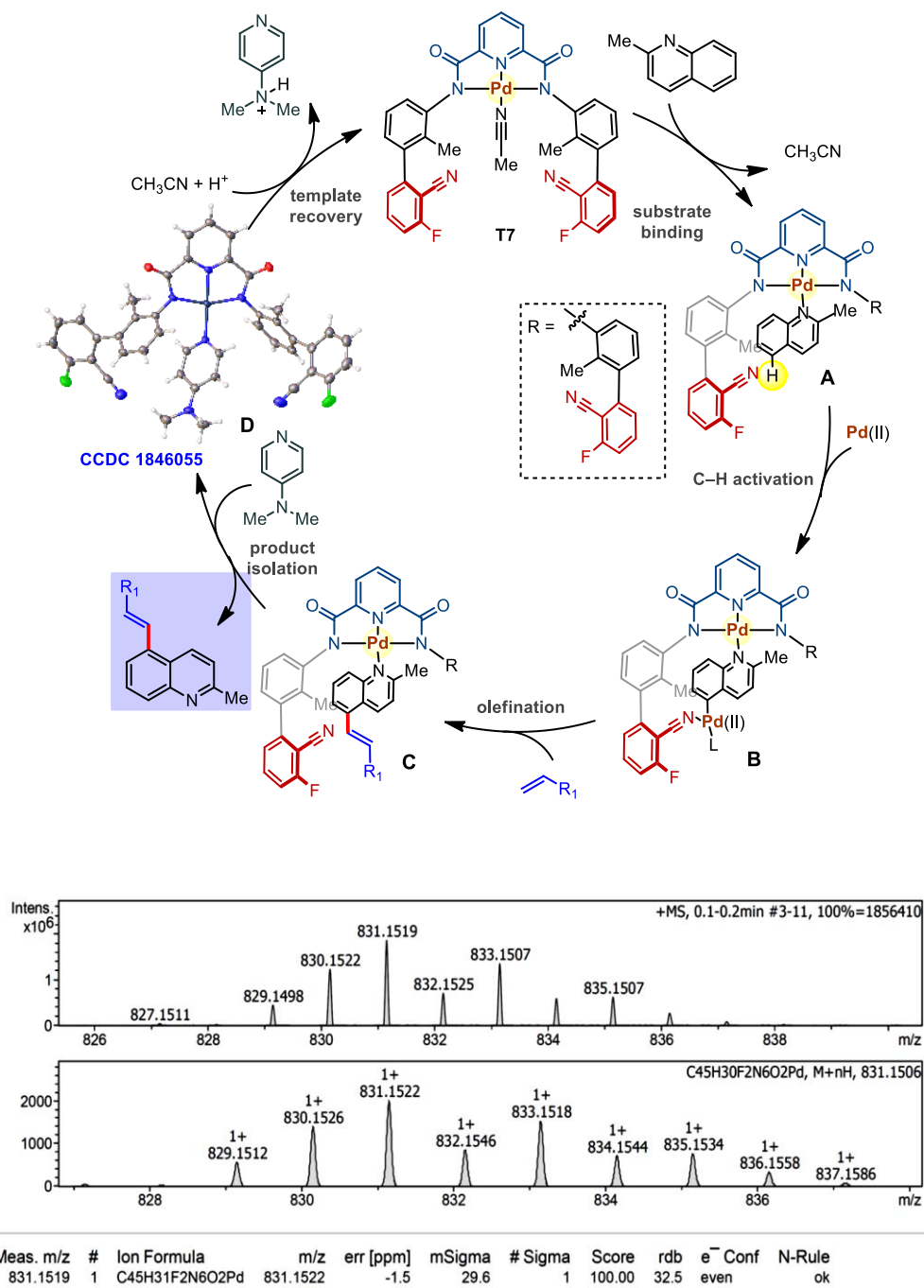


Figure 3.4. HRMS spectra of intermediate A

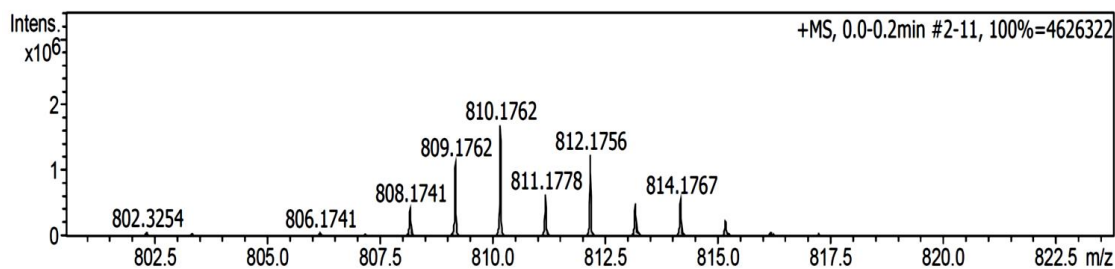


Figure 3.5. HRMS spectra of intermediate **D** (calcd for $[M+ H^+]$, 810.1620; found, 810.1762)

3.4.5. Compound Characterization Data:

Crystallographic Data:

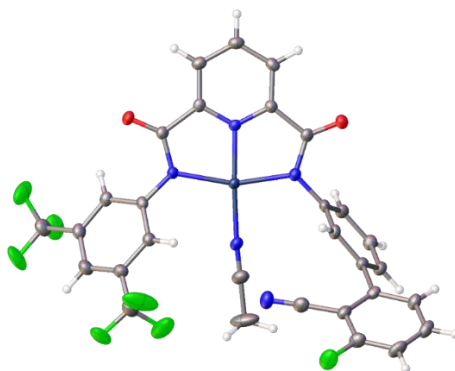


Figure 3.6: Crystal structure of **T13** (CCDC 1846063)

Cell: a=7.01867(18) b=14.1116(3) c=15.2062(4)
 alpha=111.032(2) beta=93.683(2) gamma=99.895(2)

Temperature: 150 K

Crystal size 0.18 x 0.16 x 0.06 mm³

Volume 1371.81(6)

Space group P -1

Moiety formula C₃₀ H₁₆ F₇ N₅ O₂ Pd

Data completeness= 0.993 Theta(max)= 24.999

R(reflections)= 0.0318(4427) wR2(reflections)= 0.0924(4799)

Figure 3.8: Crystal structure of **T2-DMAP** adduct (CCDC 1845634)

Cell: a=21.0115(5) b=14.9551(3) c=8.08336(17)

alpha=90 beta=96.259(2) gamma=90

Temperature: 150 K

Crystal size 0.27 x 0.13 x 0.12 mm³

Volume 2524.89(10)

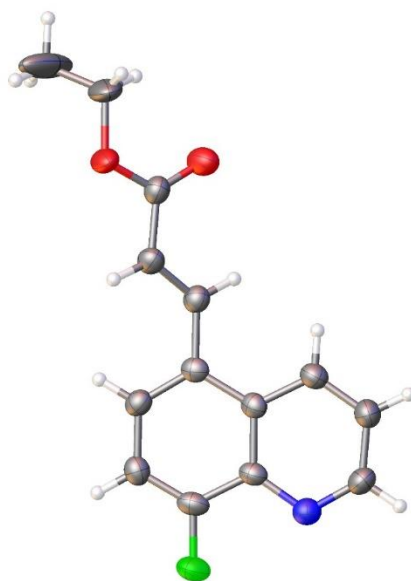
Space group P 1 21/c 1

Hall group -P 2ybc

Moiety formula C₂₈ H₂₁ N₇ O₂ Pd, H₂ O

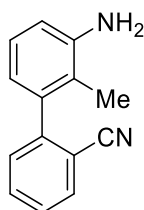
Data completeness= 0.997 Theta(max)= 25.000

R(reflections)= 0.0287(4102)wR2(reflections)= 0.0741(4432)

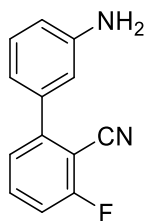
**Figure 3.9:** Crystal structure of **3da** (Figure 3) (CCDC 1845788)

Cell: a=7.4845(11) b=20.004(3) c=7.9353(13)

alpha=90	beta=93.957(14)	gamma=90
Temperature: 150 K		
Crystal size	0.14 x 0.11 x 0.07 mm ³	
Volume	1185.3(3)	
Space group	P 1 21/c 1	
Hall group	-P 2ybc	
Moiety formula	C ₁₄ H ₁₂ F N O ₂	
Data completeness= 0.974	Theta(max)= 25.000	
R(reflections)= 0.0728(1300)	wR2(reflections)= 0.2069(2037)	

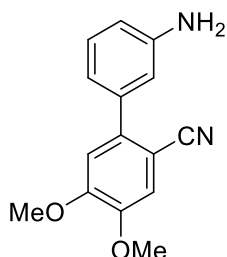
Compound NMR Data:**3'-Amino-2'-methyl-[1,1'-biphenyl]-2-carbonitrile:**

White solid; yield 73% (760 mg); ¹H NMR (500 MHz, CDCl₃) δ 7.73 (dd, *J* = 7.8, 0.7 Hz, 1H), 7.61 (td, *J* = 7.7, 1.2 Hz, 1H), 7.43 (td, *J* = 7.7, 1.1 Hz, 1H), 7.37 (d, *J* = 7.7 Hz, 1H), 7.10 (t, *J* = 7.7 Hz, 1H), 6.76 (d, *J* = 7.9 Hz, 1H), 6.66 (d, *J* = 7.5 Hz, 1H), 3.73 (s, 2H), 1.98 (s, 3H); ¹³C NMR (126 MHz, CDCl₃) δ 146.41, 145.22, 139.05, 132.78, 132.43, 130.71, 127.43, 126.48, 120.30, 120.17, 118.34, 115.47, 113.07, 14.26; HRMS (*m/z*): [M+H]⁺calcd for C₁₄H₁₃N₂, 209.1079; found, 209.1075.



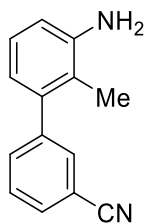
3'-Amino-3-fluoro-[1,1'-biphenyl]-2-carbonitrile:

White solid; yield 81% (859 mg); ^1H NMR (500 MHz, CDCl_3) δ 7.61 (td, $J = 8.1, 6.0$ Hz, 1H), 7.37 – 7.24 (m, 2H), 7.19 (t, $J = 8.5$ Hz, 1H), 6.94 (d, $J = 7.6$ Hz, 1H), 6.86 (s, 1H), 6.79 (dd, $J = 8.0, 1.6$ Hz, 1H), 3.74 (s, 2H); ^{13}C NMR (126 MHz, CDCl_3) δ 164.20 (d, $J_{\text{FC}} = 258.5$ Hz), 147.74 (s), 146.92 (s), 138.17 (d, $J_{\text{FC}} = 2.1$ Hz), 134.30 (d, $J_{\text{FC}} = 9.2$ Hz), 129.91 (s), 125.57 (d, $J_{\text{FC}} = 3.2$ Hz), 118.95 (s), 115.90 (s), 115.13 (s), 114.54 (d, $J_{\text{FC}} = 20.0$ Hz), 113.74 (s), 100.71 (d, $J_{\text{FC}} = 15.2$ Hz); HRMS (m/z): $[\text{M}+\text{H}]^+$ calcd for $\text{C}_{13}\text{H}_{10}\text{FN}_2$, 213.0828; found, 228.0824.



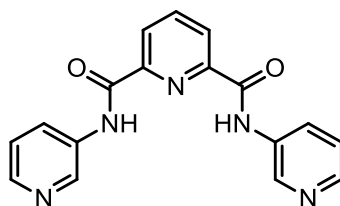
3'-Amino-4,5-dimethoxy-[1,1'-biphenyl]-2-carbonitrile:

White solid; yield 69% (877 mg); ^1H NMR (500 MHz, CDCl_3) δ 7.27 (dd, $J = 13.4, 5.6$ Hz, 6H), 7.15 (s, 5H), 6.92 (dd, $J = 11.9, 4.3$ Hz, 11H), 6.85 (s, 5H), 6.75 (dd, $J = 8.0, 2.2$ Hz, 5H), 3.96 (s, 15H), 3.95 (s, 15H), 3.81 (s, 9H); ^{13}C NMR (126 MHz, CDCl_3) δ 152.56, 148.28, 146.79, 140.54, 139.42, 129.77, 119.31, 119.03, 115.27, 115.09, 112.52, 102.32, 56.38, 56.26; HRMS (m/z): $[\text{M}+\text{H}]^+$ calcd for $\text{C}_{15}\text{H}_{15}\text{N}_2\text{O}_2$, 255.1134; found, 255.1126.

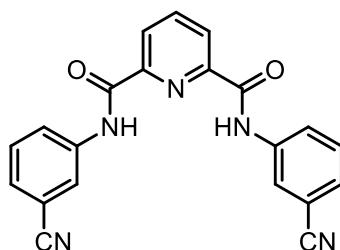


3'-Amino-2'-methyl-[1,1'-biphenyl]-3-carbonitrile:

White solid; yield 77% (801 mg); $^1\text{H NMR}$ (400 MHz, CDCl_3) δ 7.66 – 7.58 (m, 2H), 7.57 – 7.47 (m, 2H), 7.09 (t, $J = 7.8$ Hz, 1H), 6.78 – 6.71 (m, 1H), 6.63 (dd, $J = 7.6, 0.7$ Hz, 1H), 3.76 (s, 2H), 2.03 (s, 3H); $^{13}\text{C NMR}$ (101 MHz, CDCl_3) δ 145.36, 143.72, 140.68, 133.95, 132.91, 130.44, 128.96, 126.59, 120.22, 119.57, 119.04, 114.92, 112.24, 14.41; HRMS (m/z): $[\text{M}+\text{H}]^+$ calcd for $\text{C}_{14}\text{H}_{13}\text{N}_2$, 209.1079; found, 209.1028.



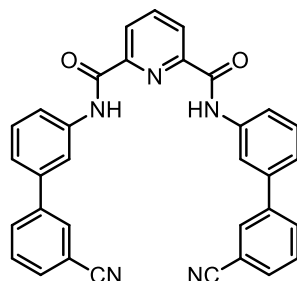
White solid; yield 81% (517 mg); $^1\text{H NMR}$ (400 MHz, DMSO) δ 11.32 (s, 2H), 9.16 (d, $J = 2.1$ Hz, 2H), 8.41 (dt, $J = 9.5, 5.5$ Hz, 5H), 7.50 (dd, $J = 8.2, 4.8$ Hz, 2H); $^{13}\text{C NMR}$ (126 MHz, DMSO) δ 162.68 (s), 148.35 (s), 141.22 (s), 140.13 (s), 138.57 (s), 136.52 (s), 132.09 (s), 126.18 (s), 125.23 (s).



N^2, N^6 -bis(3-cyanophenyl)pyridine-2,6-dicarboxamide:

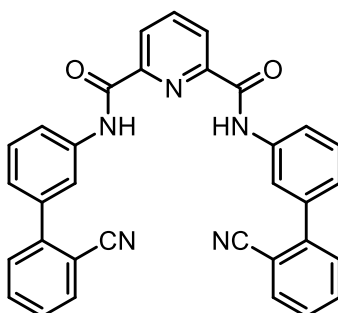
White solid; yield 82% (602 mg); $^1\text{H NMR}$ (400 MHz, DMSO) δ 11.24 (s, 2H), 8.44 (s, 2H), 8.43 – 8.37 (m, 2H), 8.35 – 8.27 (m, 1H), 8.23 (dd, $J = 6.9, 2.2$ Hz, 2H), 7.72 – 7.61 (m, 4H);

^{13}C NMR (101 MHz, DMSO) δ 162.02 (s), 148.30 (s), 140.18 (s), 138.91 (s), 130.26 (s), 127.85 (s), 125.80 (s), 125.61 (s), 123.59 (s), 118.69 (s), 111.61 (s).



***N*²,*N*⁶-bis(3'-cyano-[1,1'-biphenyl]-3-yl)pyridine-2,6-dicarboxamide:**

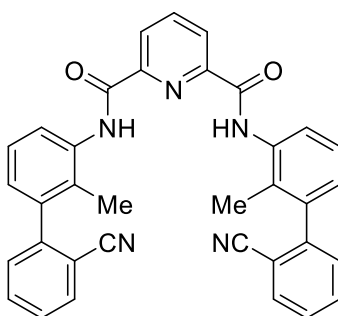
White solid; yield 76% (789 mg); ^1H NMR (500 MHz, DMSO) δ 11.15 (s, 2H), 8.43 (d, J = 7.6 Hz, 2H), 8.34 (s, 3H), 8.16 (s, 2H), 8.05 (d, J = 7.8 Hz, 2H), 7.96 (d, J = 3.4 Hz, 2H), 7.87 (d, J = 7.6 Hz, 2H), 7.70 (t, J = 7.7 Hz, 2H), 7.58 (s, 4H); ^{13}C NMR (126 MHz, DMSO) δ 161.82 (s), 148.76 (s), 141.07 (s), 140.07 (s), 138.73 (s), 138.57 (s), 131.44 (s), 131.26 (s), 130.24 (s), 129.59 (s), 128.18 (s), 125.44 (s), 123.01 (s), 121.20 (s), 119.69 (s), 118.72 (s), 112.19 (s).



***N*²,*N*⁶-bis(2'-cyano-[1,1'-biphenyl]-3-yl)pyridine-2,6-dicarboxamide:**

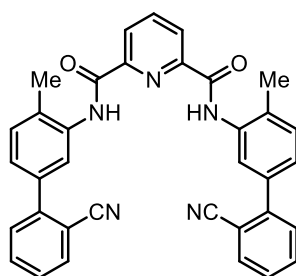
White solid; yield 78% (810 mg); ^1H NMR (500 MHz, DMSO) δ 11.21 (s, 2H), 8.45 – 8.40 (m, 2H), 8.33 (dd, J = 8.4, 7.1 Hz, 1H), 8.19 (t, J = 1.8 Hz, 2H), 8.04 – 7.96 (m, 4H), 7.82 (td, J = 7.7, 1.3 Hz, 2H), 7.69 – 7.58 (m, 6H), 7.40 (ddd, J = 7.7, 1.7, 1.0 Hz, 2H); ^{13}C NMR (126 MHz, DMSO) δ 161.93 (s), 148.76 (s), 144.39 (s), 140.18 (s), 138.51 (s), 133.91 (s), 133.66

(s), 130.12 (s), 129.29 (s), 128.47 (s), 125.56 (s), 124.72 (s), 121.22 (d, $J = 20.0$ Hz), 118.43 (s), 110.28 (s).



***N*²,*N*⁶-bis(2'-cyano-2-methyl-[1,1'-biphenyl]-3-yl)pyridine-2,6-dicarboxamide:**

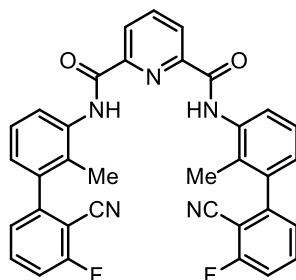
White solid; 845 mg. Yield: 77%; ¹H NMR (500 MHz, DMSO) δ 11.03 (s, 2H), 8.39 (d, $J = 7.6$ Hz, 2H), 8.31 (dd, $J = 8.3, 7.2$ Hz, 1H), 7.96 (d, $J = 7.5$ Hz, 2H), 7.80 (t, $J = 7.6$ Hz, 2H), 7.61 (t, $J = 7.5$ Hz, 2H), 7.56 (d, $J = 7.8$ Hz, 2H), 7.47 (d, $J = 7.6$ Hz, 2H), 7.41 (t, $J = 7.7$ Hz, 2H), 7.22 (d, $J = 7.4$ Hz, 2H), 2.06 (s, 6H); ¹³C NMR (101 MHz, DMSO) δ 161.98, 148.66, 144.56, 140.07, 139.12, 136.30, 133.25, 133.13, 132.20, 130.59, 128.39, 127.87, 127.74, 126.00, 125.15, 117.94, 111.77, 15.13; HRMS (m/z): $[M+H]^+$ calcd for C₃₅H₂₆N₅O₂, 548.2087; found, 548.2081.



***N*²,*N*⁶-bis(2'-cyano-4-methyl-[1,1'-biphenyl]-3-yl)pyridine-2,6-dicarboxamide:**

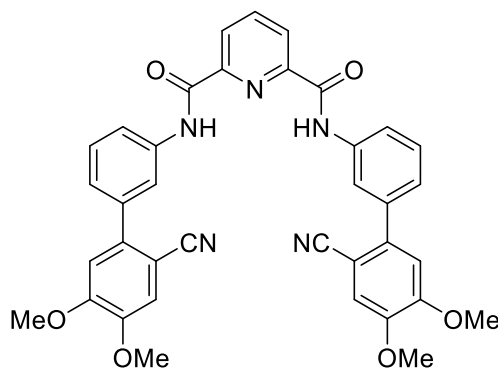
White solid; yield 88% (964 mg); ¹H NMR (400 MHz, DMSO) δ 10.80 (d, $J = 3.1$ Hz, 1H), 8.38 (dd, $J = 7.2, 1.4$ Hz, 1H), 8.32 (dd, $J = 12.0, 6.8$ Hz, 2H), 7.96 (d, $J = 7.7$ Hz, 1H), 7.90 (d, $J = 1.1$ Hz, 1H), 7.81 (t, $J = 7.6$ Hz, 1H), 7.64 (d, $J = 7.7$ Hz, 1H), 7.58 (d, $J = 7.6$ Hz, 1H),

7.49 (d, $J = 7.9$ Hz, 1H), 7.43 (dd, $J = 7.9, 1.4$ Hz, 1H), 2.39 (s, 3H); ^{13}C NMR (101 MHz, DMSO) δ 164.79 (s), 161.42 (s), 148.95 (s), 146.36 (s), 140.26 (s), 135.99 (s), 133.89 (s), 133.59 (s), 132.54 (s), 130.90 (s), 130.02 (s), 128.24 (s), 127.16 (s), 125.99 (s), 125.56 (s), 124.54 (s).



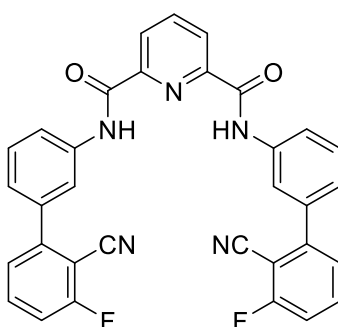
***N*²,*N*⁶-bis(2'-cyano-3'-fluoro-2-methyl-[1,1'-biphenyl]-3-yl)pyridine-2,6-dicarboxamide:**

White solid; yield 84% (980 mg); ^1H NMR (400 MHz, DMSO) δ 11.01 (s, 2H), 8.39 (d, $J = 7.2$ Hz, 2H), 8.31 (dd, $J = 8.5, 6.8$ Hz, 1H), 7.86 (dd, $J = 14.2, 8.1$ Hz, 2H), 7.63 – 7.54 (m, 4H), 7.43 (t, $J = 7.8$ Hz, 2H), 7.35 (d, $J = 7.7$ Hz, 2H), 7.27 (d, $J = 7.2$ Hz, 2H), 2.09 (s, 6H); ^{13}C NMR (101 MHz, DMSO) δ 162.8 (d, $J_{\text{FC}} = 255$ Hz), 161.97 (s), 148.61 (s), 146.38 (s), 140.10 (s), 137.88 (s), 136.38 (s), 135.53 (d, $J_{\text{FC}} = 9.1$ Hz), 132.19 (s), 128.08 (s), 127.81 (s), 126.84 (d, $J_{\text{FC}} = 2.5$ Hz), 126.12 (s), 125.18 (s), 115.3 (d, $J_{\text{FC}} = 19.5$ Hz), 113.16 (s), 101.0 (d, $J_{\text{FC}} = 14.7$ Hz), 15.10 (s).

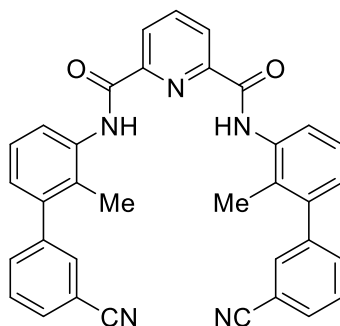


***N*²,*N*⁶-bis(2'-cyano-4',5'-dimethoxy-[1,1'-biphenyl]-3-yl)pyridine-2,6-dicarboxamide:**

White solid; 756 mg. Yield: 59%; ¹H NMR (500 MHz, DMSO) δ 11.14 (s, 2H), 8.49 – 8.26 (m, 3H), 8.14 (s, 2H), 8.01 (s, 2H), 7.66 – 7.31 (m, 6H), 7.15 (s, 2H), 3.88 (s, 12H); ¹³C NMR (126 MHz, DMSO) δ 161.78, 152.49, 148.71, 148.30, 140.07, 138.93, 138.64, 138.25, 129.03, 125.48, 124.81, 121.30, 120.98, 118.89, 115.40, 112.81, 101.17, 56.09, 55.93; HRMS (*m/z*): [M+H⁺] calcd for C₃₇H₃₀N₅O₆, 640.2196; found, 640.2183.

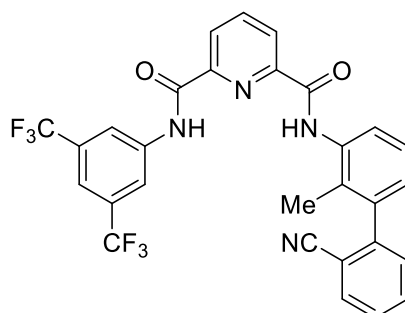
***N*²,*N*⁶-bis(2'-cyano-3'-fluoro-[1,1'-biphenyl]-3-yl)pyridine-2,6-dicarboxamide:**

White solid; 915 mg. Yield: 82%; ¹H NMR (400 MHz, DMSO) δ 11.20 (s, 2H), 8.43 (d, *J* = 7.9 Hz, 2H), 8.23 (s, 2H), 8.03 (d, *J* = 8.0 Hz, 2H), 7.87 (d, *J* = 6.1 Hz, 2H), 7.60 (dd, *J* = 10.1, 4.8 Hz, 3H), 7.53 (d, *J* = 7.7 Hz, 1H), 7.44 (d, *J* = 7.4 Hz, 2H), 7.20 (dd, *J* = 26.9, 7.6 Hz, 3H); ¹³C NMR (101 MHz, DMSO) δ 163.40 (d, *J*_{FC} = 255.7 Hz), 161.88, 147.43 (d, *J*_{FC} = 250.9 Hz), 140.06, 138.52, 137.26, 135.70 (d, *J*_{FC} = 9.7 Hz), 129.31, 128.51 (d, *J*_{FC} = 70.5 Hz), 126.08, 125.40 (d, *J*_{FC} = 24.2 Hz), 124.61, 121.72, 120.99, 115.29 (d, *J*_{FC} = 19.8 Hz), 113.45, 99.52 (d, *J*_{FC} = 15.4 Hz), 21.01; HRMS (*m/z*): [M+H]⁺ calcd for C₃₃H₂₀F₂N₅O₂, 556.1585; found, 556.1581.



***N*²,*N*⁶-bis(3'-cyano-2-methyl-[1,1'-biphenyl]-3-yl)pyridine-2,6-dicarboxamide:**

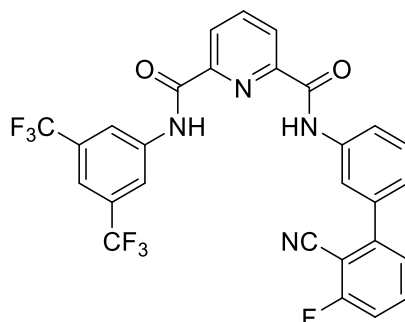
White solid; 835 mg. Yield: 76%; ¹H NMR (500 MHz, DMSO) δ 10.95 (s, 2H), 8.39 (d, *J* = 7.8 Hz, 2H), 8.32 (d, *J* = 7.1 Hz, 1H), 7.91 – 7.86 (m, 2H), 7.80 (s, 2H), 7.68 (d, *J* = 5.0 Hz, 4H), 7.52 (d, *J* = 7.7 Hz, 2H), 7.39 (t, *J* = 7.8 Hz, 2H), 7.23 (d, *J* = 7.4 Hz, 2H), 2.16 (s, 6H); ¹³C NMR (126 MHz, DMSO) δ 161.90, 148.63, 142.20, 140.50, 140.05, 136.38, 134.09, 132.39, 131.74, 131.06, 129.58, 127.99, 127.16, 126.10, 125.09, 118.69, 111.61, 15.44; HRMS (*m/z*): [M+Na]⁺calcd for C₃₅H₂₅N₅NaO₂, 570.1906; found, 570.1898.



***N*²-(3,5-bis(trifluoromethyl)phenyl)-*N*⁶-(2'-cyano-2-methyl-[1,1'-biphenyl]-3-yl)pyridine-2,6-dicarboxamide:**

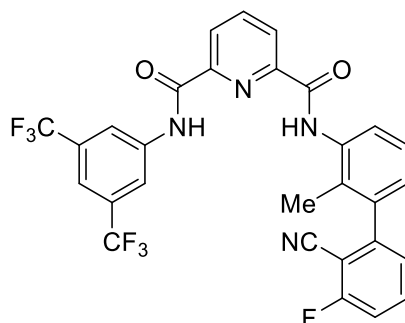
White solid; 978 mg. Yield: 86%; ¹H NMR (400 MHz, DMSO) δ 11.41 (s, 1H), 10.96 (s, 1H), 8.57 (s, 2H), 8.51 – 8.40 (m, 2H), 8.34 (t, *J* = 7.7 Hz, 1H), 7.99 (dd, *J* = 7.8, 0.8 Hz, 1H), 7.88 (s, 1H), 7.82 (td, *J* = 7.7, 1.3 Hz, 1H), 7.72 (d, *J* = 7.5 Hz, 1H), 7.63 (td, *J* = 7.7, 1.1 Hz, 1H), 7.50 (d, *J* = 7.7 Hz, 1H), 7.45 (t, *J* = 7.8 Hz, 1H), 7.24 (d, *J* = 7.6 Hz, 1H), 2.12 (s, 3H); ¹³C NMR (126 MHz, DMSO) δ 162.55, 161.58, 148.30 (d, *J* = 104.8 Hz), 144.56, 140.31, 140.02, 139.25, 136.09, 133.27, 133.06, 131.60, 130.91, 130.65, 130.56, 128.41, 127.68, 126.97,

126.06, 124.30, 122.13, 120.79, 117.90, 117.26, 111.81, 14.98; HRMS (m/z): $[M+H]^+$ calcd for $C_{29}H_{19}F_6N_4O_2$, 569.1412; found, 569.1412.



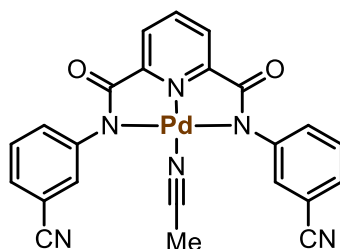
***N*²-(3,5-bis(trifluoromethyl)phenyl)-*N*⁶-(2'-cyano-3'-fluoro-[1,1'-biphenyl]-3-yl)pyridine-2,6-dicarboxamide:**

White solid; 901 mg. Yield: 78%; ¹H NMR (500 MHz, DMSO) δ 11.49 (s, 1H), 11.10 (s, 1H), 8.67 (s, 2H), 8.44 (t, *J* = 7.7 Hz, 2H), 8.35 (d, *J* = 7.7 Hz, 1H), 8.27 (s, 1H), 8.04 (d, *J* = 8.1 Hz, 1H), 7.89 (d, *J* = 5.8 Hz, 2H), 7.65 (t, *J* = 7.9 Hz, 1H), 7.60 (s, 1H), 7.55 (d, *J* = 7.7 Hz, 1H), 7.46 (d, *J* = 7.7 Hz, 1H); ¹³C NMR (126 MHz, DMSO) δ 164.49, 162.44, 161.56, 148.62, 147.88, 146.13, 140.11, 138.46, 137.23, 135.61 (d, *J* = 9.5 Hz), 130.75 (q, *J* = 32.8 Hz), 129.37, 126.50, 126.00, 125.70 (d, *J* = 22.4 Hz), 124.53, 124.33, 122.16, 121.43, 120.93, 120.39, 116.94, 115.29 (d, *J* = 19.8 Hz), 113.41, 99.50 (d, *J* = 15.4 Hz); HRMS (m/z): $[M+Na]^+$ calcd for $C_{28}H_{15}F_7N_4NaO_2$, 595.0981; found, 595.0972.

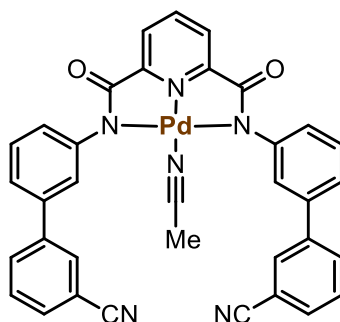


***N*²-(3,5-bis(trifluoromethyl)phenyl)-*N*⁶-(2'-cyano-3'-fluoro-2-methyl-[1,1'-biphenyl]-3-yl)pyridine-2,6-dicarboxamide:**

White solid; 976 mg. Yield: 83%; ^1H NMR (500 MHz, DMSO) δ 11.42 (s, 1H), 10.97 (s, 1H), 8.58 (s, 2H), 8.53 – 8.40 (m, 2H), 8.35 (t, $J = 7.7$ Hz, 1H), 7.88 (dd, $J = 13.8, 7.3$ Hz, 2H), 7.74 (d, $J = 7.9$ Hz, 1H), 7.60 (t, $J = 8.9$ Hz, 1H), 7.47 (t, $J = 7.8$ Hz, 1H), 7.37 (d, $J = 7.7$ Hz, 1H), 7.29 (d, $J = 7.5$ Hz, 1H), 2.14 (s, 3H); ^{13}C NMR (126 MHz, DMSO) δ 162.51, 161.59, 148.67, 147.87, 146.41, 140.25, 140.04, 138.01, 136.23, 135.53 (d, $J = 9.3$ Hz), 131.62, 130.79 (d, $J = 32.9$ Hz), 127.58, 127.32, 126.80, 126.17, 125.67 (d, $J = 22.3$ Hz), 124.29, 122.13, 120.70, 117.15, 115.36 (d, $J = 19.3$ Hz), 113.09, 101.10 (d, $J = 14.7$ Hz), 14.96; HRMS (m/z): $[\text{M}+\text{H}]^+$ calcd for $\text{C}_{29}\text{H}_{18}\text{F}_7\text{N}_4\text{O}_2$, 587.1318; found, 587.1314.

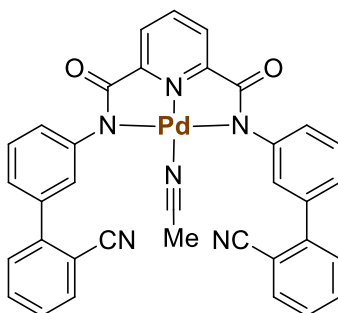


Yellow solid; yield 83% (425 mg); ^1H NMR (400 MHz, DMSO) δ 8.34 (br, 1H), 7.86 (s, 2H), 7.67 – 7.52 (m, 8H), 2.07 (s, 3H); ^{13}C NMR (101 MHz, DMSO) δ 168.14 (s), 151.52 (s), 146.55 (s), 142.28 (s), 131.97 (s), 130.09 (s), 129.42 (s), 127.68 (s), 126.13 (s), 118.79 (s), 110.89 (s), 1.15 (s).

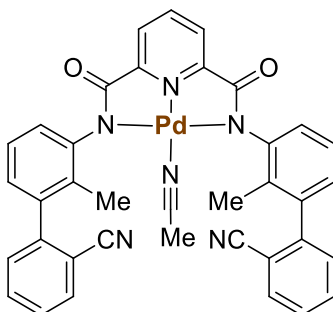


Yellow solid; yield 71% (472 mg); ^1H NMR (500 MHz, DMSO) δ 8.33 (t, $J = 7.5$ Hz, 1H), 8.09 (s, 2H), 7.97 (d, $J = 6.5$ Hz, 2H), 7.83 (d, $J = 7.8$ Hz, 4H), 7.62 (d, $J = 31.8$ Hz, 4H), 7.47 (s, 2H), 7.41 (t, $J = 7.4$ Hz, 2H), 7.28 (d, $J = 4.8$ Hz, 2H); ^{13}C NMR (126 MHz, DMSO) δ

167.99 (s), 152.04 (s), 146.82 (s), 141.98 (s), 141.11 (s), 137.89 (s), 131.37 (s), 131.00 (s), 130.12 (s), 130.05 (s), 128.86 (s), 126.98 (s), 125.66 (s), 125.32 (s), 122.70 (s), 118.80 (s), 112.09 (s); HRMS (m/z): [(M-CH₃CN)+H]⁺calcd for C₃₃H₂₀N₅O₂Pd, 624.0652; found,624.0480.

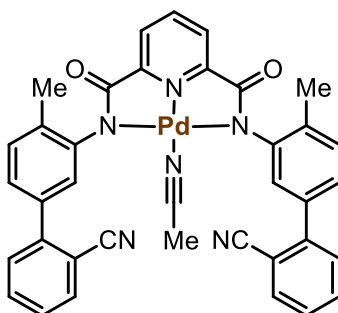


Yellow solid; 394 mg. Yield: 59%; ¹H NMR (400 MHz, CD₃CN+DMSO-*d*₆) δ 8.20 (s, 1H), 7.77 (d, *J* = 8.1 Hz, 4H), 7.66 (d, *J* = 6.8 Hz, 2H), 7.56 – 7.18 (m, 12H); ¹³C NMR (101 MHz, CD₃CN+DMSO-*d*₆) δ 168.62, 152.25, 147.36, 144.93, 142.18, 138.41, 133.77, 133.28, 130.19, 128.47, 127.98, 127.16, 126.85, 125.92, 124.87, 118.71, 110.79; HRMS (m/z): [(M-CH₃CN)+H]⁺calcd for C₃₃H₂₀N₅O₂Pd, 624.0652; found, 625.0659.

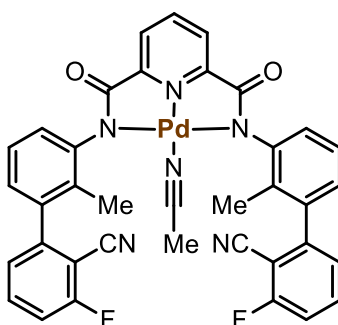


Yellow solid; 564 mg. Yield: 81%; ¹H NMR (400 MHz, DMSO-*d*₆) δ 8.32 (s, 1H), 7.94 (d, *J* = 6.5 Hz, 2H), 7.87 – 7.69 (m, 4H), 7.67 – 7.52 (m, 2H), 7.50 – 7.17 (m, 6H), 7.07 (s, 2H),

2.08 (s, 6H); ^{13}C NMR (101 MHz, DMSO- d_6) δ 167.11, 151.83, 145.92, 145.07, 141.97, 138.48, 133.12, 132.10, 130.75, 128.11, 127.89, 127.80, 126.16, 125.47, 118.29, 111.46, 15.45; HRMS (m/z): [(M-CH₃CN)+H]⁺calcd for C₃₅H₂₄N₅O₂Pd, 652.0965; found,652.0927.

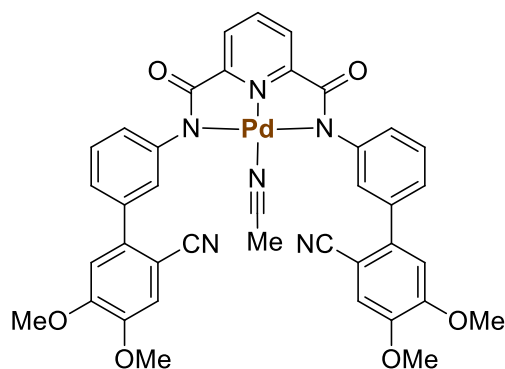


Yellow solid; yield 76% (526 mg); ^1H NMR (400 MHz, CD₃CN) δ 8.25 (s, 1H), 7.83 – 7.76 (m, 5H), 7.71 (t, J = 7.7 Hz, 2H), 7.57 (d, J = 7.7 Hz, 2H), 7.51 (t, J = 7.6 Hz, 2H), 7.40 – 7.34 (m, 5H), 2.39 (s, 6H); ^{13}C NMR (101 MHz, CD₃CN) δ 171.31 (s), 169.28 (s), 151.89 (s), 146.77 (s), 143.34 (s), 137.67 (s), 136.52 (s), 134.67 (s), 134.21 (s), 131.46 (s), 131.12 (s), 128.82 (s), 128.48 (s), 128.11 (s), 127.63 (s), 127.26 (s), 119.76 (s), 111.87 (s), 18.40 (s); HRMS (m/z): [(M-CH₃CN)+H]⁺calcd for C₃₅H₂₄N₅O₂Pd, 652.0965; found,652.0820.

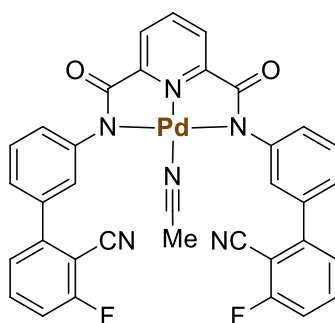


Yellow solid; yield 83% (605 mg); ^1H NMR (400 MHz, CD₃CN) δ 8.24 (t, J = 7.8 Hz, 1H), 7.84 – 7.67 (m, 4H), 7.36 – 7.24 (m, 7H), 7.21 – 7.12 (m, 1H), 7.05 (dd, J = 5.3, 2.9 Hz, 2H), 2.23 (s, 3H), 2.15 (s, 3H); ^{13}C NMR (101 MHz, CD₃CN) δ 169.03 (s), 164.29 (d, J_{FC} = 257 Hz), 153.04 (s), 148.68 (d, J_{FC} = 2.9 Hz), 148.09 (d, J_{FC} = 6.7 Hz), 143.14 (s), 138.93 (s),

135.97 (d, $J_{FC} = 9.0$ Hz), 133.03 (d, $J_{FC} = 3.7$ Hz), 128.89 (d, $J_{FC} = 6.9$ Hz), 127.87 (d, $J_{FC} = 12.9$ Hz), 127.60 (d, $J_{FC} = 24.4$ Hz), 127.25 (s), 126.85 (d, $J_{FC} = 6$ Hz), 115.71 (d, $J_{FC} = 19.5$ Hz), 114.37 (s), 102.76 (d, $J_{FC} = 15.3$ Hz), 15.76 (s); HRMS (m/z): $[M+H]^+$ calcd for $C_{37}H_{24}F_2N_6NaO_2Pd$, 751.0869; found, 751.0863.

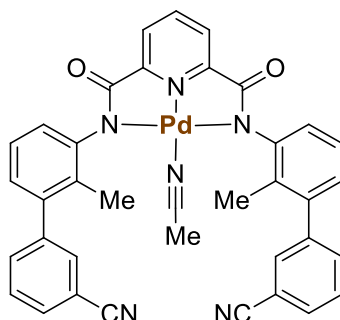


Yellow solid; 371 mg. Yield: 47%; 1H NMR (400 MHz, CD_3CN) δ 8.22 (s, 1H), 7.78 (s, 2H), 7.49 – 7.22 (m, 10H), 7.03 (s, 2H), 3.88 (s, 6H), 3.86 (s, 6H); ^{13}C NMR (126 MHz, CD_3CN) δ 168.67, 152.88, 152.36, 148.54, 142.10, 139.61, 138.57, 129.78, 128.34, 126.82, 126.71, 125.74, 124.90, 119.08, 117.28, 115.34, 112.89, 101.70, 55.89, 55.83; HRMS (m/z): $[(M-CH_3CN)+H]^+$ calcd for $C_{37}H_{28}N_5O_6Pd$, 744.1074; found, 744.1083.

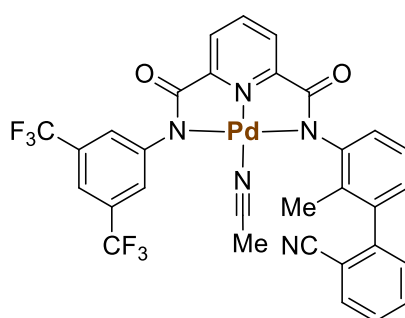


Yellow solid; 554 mg. Yield: 79%; 1H NMR (500 MHz, $DMSO-d_6$) δ 8.32 (s, 1H), 7.83 (d, $J = 7.7$ Hz, 4H), 7.54 (t, $J = 8.8$ Hz, 2H), 7.50 – 7.24 (m, 10H), 2.07 (s, 3H); ^{13}C NMR (126 MHz, $DMSO-d_6$) δ 167.98, 163.41 (d, $J_{FC} = 255.5$ Hz), 151.93, 146.49, 146.25, 142.06, 136.56,

135.68 (d, $J_{FC} = 9.5$ Hz), 128.51, 127.77, 126.86, 126.06, 126.04, 125.75, 124.49, 118.06, 115.07 (d, $J_{FC} = 19.8$ Hz), 113.63, 99.39 (d, $J_{FC} = 15.4$ Hz), 1.14; HRMS (m/z): [(M-CH₃CN)+H]⁺calcd for C₃₃H₁₈F₂N₅O₂Pd, 660.0463; found, 660.0468.

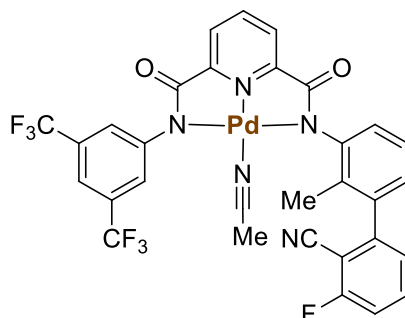


Yellow solid; 582 mg. Yield: 84%; ¹H NMR (500 MHz, CD₃CN) δ 8.27 (t, $J = 7.8$ Hz, 1H), 7.81 (d, $J = 7.8$ Hz, 2H), 7.73 (s, 4H), 7.67 – 7.58 (m, 4H), 7.24 (t, $J = 6.2$ Hz, 4H), 7.06 (d, $J = 5.3$ Hz, 2H), 2.22 (s, 6H); ¹³C NMR (126 MHz, CD₃CN) δ 167.92, 152.17, 147.02, 143.17, 142.14, 140.50, 134.08, 132.76, 131.40, 131.38, 130.69, 129.19, 127.02, 126.98, 126.51, 125.84, 125.51, 118.76, 112.00, 15.30; HRMS (m/z): [M+H]⁺calcd for C₃₇H₂₇N₆O₂Pd, 693.1230; found, 690.1236.

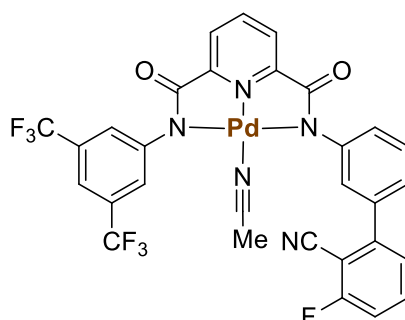


Yellow solid; 630 mg. Yield: 88%; ¹H NMR (400 MHz, CD₃CN) δ 8.27 (t, $J = 7.8$ Hz, 1H), 7.90 – 7.78 (m, 5H), 7.72 (q, $J = 8.0$ Hz, 1H), 7.65 (s, 1H), 7.60 – 7.44 (m, 2H), 7.34 – 7.26 (m, 2H), 7.11 (d, $J = 7.0$ Hz, 1H), 2.16 (s, 3H); ¹³C NMR (101 MHz, CD₃CN) δ 169.01, 167.96, 151.83, 148.89, 146.62, 145.67, 142.41, 139.20, 132.95, 132.73, 132.53, 130.79, 130.53,

130.47, 127.94, 127.75, 126.82, 126.47, 126.19, 126.04, 125.82, 125.02, 122.32, 118.28, 112.49, 14.74; HRMS (m/z): $[M+Na]^+$ calcd for $C_{31}H_{19}F_6N_5NaO_2Pd$, 736.0375; found, 754.0384.

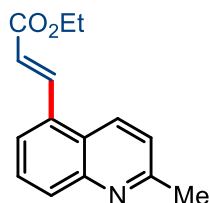


Yellow solid; 544 mg. Yield: 74%; 1H NMR (400 MHz, $DMSO-d_6$) δ 8.36 (t, $J = 7.8$ Hz, 1H), 7.95 – 7.77 (m, 6H), 7.72 (s, 1H), 7.56 (t, $J = 8.9$ Hz, 1H), 7.34 (dd, $J = 7.6, 4.3$ Hz, 2H), 7.18 (d, $J = 6.5$ Hz, 1H), 2.11 (s, 3H); ^{13}C NMR (101 MHz, $DMSO-d_6$) δ 168.52, 167.28, 162.91 (d, $J_{FC} = 256.2$ Hz), 151.39, 147.80, 146.75, 145.64, 142.24, 137.39, 135.44 (d, $J_{FC} = 9.2$ Hz), 133.01, 129.75 (q, $J_{FC} = 32.4$ Hz), 128.42, 127.49, 126.94, 126.69, 126.04 (d, $J_{FC} = 8.3$ Hz), 125.91, 124.78, 122.07, 119.36, 116.50, 115.10 (d, $J_{FC} = 19.4$ Hz), 113.61, 100.80 (d, $J_{FC} = 14.4$ Hz), 15.37, 0.06; HRMS (m/z): $[M+Na]^+$ calcd for $C_{31}H_{18}F_7N_5NaO_2Pd$, 754.0821; found, 754.0290.



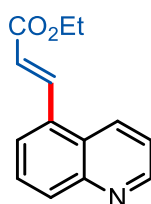
Yellow solid; 467 mg. Yield: 65%; 1H NMR (400 MHz, $DMSO-d_6$) δ 8.35 (td, $J = 7.8, 2.4$ Hz, 1H), 7.90 (d, $J = 7.6$ Hz, 1H), 7.88 – 7.78 (m, 4H), 7.73 (s, 1H), 7.60 – 7.29 (m, 6H), 2.07 (s, 3H); ^{13}C NMR (101 MHz, $DMSO-d_6$) δ 169.01, 168.52, 163.91 (d, $J_{FC} = 255.5$ Hz), 152.21,

151.76, 148.29, 146.69, 146.60, 142.73, 137.20, 136.17 (d, $J_{FC} = 9.5$ Hz), 131.02 – 129.56 (m), 128.82 (d, $J_{FC} = 83.6$ Hz), 127.58, 126.64, 126.54, 126.52, 125.29 (d, $J_{FC} = 14.8$ Hz), 122.50, 119.79, 117.17, 115.71, 115.52, 114.13, 99.88 (d, $J_{FC} = 15.4$ Hz); HRMS (m/z): [(M-CH₃CN)+H]⁺calcd for C₂₈H₁₄F₇N₄O₂Pd, 677.0040; found,677.0046.



(E)-ethyl 3-(2-methylquinolin-5-yl)acrylate (3aa):

White solid; yield 94% (22.6 mg); ¹H NMR (400 MHz, CDCl₃) δ 8.41 (dd, $J = 12.2, 8.2$ Hz, 2H), 8.06 (d, $J = 8.3$ Hz, 1H), 7.76 (d, $J = 7.1$ Hz, 1H), 7.72 – 7.65 (m, 1H), 7.37 (d, $J = 8.7$ Hz, 1H), 6.54 (d, $J = 15.8$ Hz, 1H), 4.31 (q, $J = 7.1$ Hz, 2H), 2.76 (s, 3H), 1.37 (t, $J = 7.1$ Hz, 3H); ¹³C NMR (101 MHz, CDCl₃) δ 166.85 (s), 159.51 (s), 148.19 (s), 140.29 (s), 131.97 (s), 131.09 (s), 129.15 (s), 125.01 (s), 124.56 (s), 122.71 (s), 121.77 (s), 77.48 (s), 77.16 (s), 76.84 (s), 60.89 (s), 25.36 (s), 14.49 (s); HRMS (m/z): [M+H]⁺calcd for C₁₅H₁₆NO₂, 242.1181; found, 242.1167.

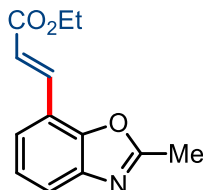


Ethyl (E)-3-(quinolin-5-yl)acrylate (3ba):

White solid; yield 82% (18.6 mg); ¹H NMR (500 MHz, CDCl₃) δ 8.97 (d, $J = 3.8$ Hz, 1H), 8.54 (d, $J = 8.6$ Hz, 1H), 8.42 (d, $J = 15.8$ Hz, 1H), 8.16 (d, $J = 8.4$ Hz, 1H), 7.82 (d, $J = 7.2$ Hz, 1H), 7.73 (t, $J = 7.8$ Hz, 1H), 7.49 (dd, $J = 8.6, 4.1$ Hz, 1H), 6.56 (d, $J = 15.8$ Hz, 1H), 4.32 (q, $J = 7.1$ Hz, 2H), 1.38 (t, $J = 7.1$ Hz, 3H); ¹³C NMR (126 MHz, CDCl₃) δ 166.74, 150.84,

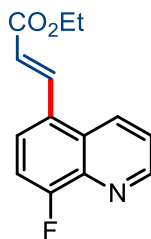
148.54, 140.05, 132.26, 131.90, 131.88, 129.18, 126.75, 125.42, 122.08, 121.74, 60.93, 14.49;

HRMS (m/z): $[M+H]^+$ calcd for $C_{14}H_{14}NO_2$, 228.1025; found, 228.0934.



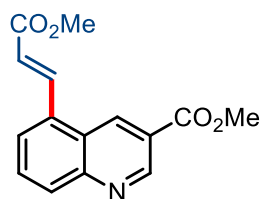
(E)-ethyl 3-(2-methylbenzo[d]oxazol-7-yl)acrylate (3ca):

White solid; yield 82% (18.9 mg); 1H NMR (500 MHz, $CDCl_3$) δ 7.79 (d, $J = 16.1$ Hz, 1H), 7.66 (d, $J = 7.7$ Hz, 1H), 7.38 (d, $J = 7.5$ Hz, 1H), 7.31 (t, $J = 7.7$ Hz, 1H), 6.89 (d, $J = 16.1$ Hz, 1H), 4.31 (q, $J = 7.1$ Hz, 2H), 2.71 (s, 3H), 1.37 (t, $J = 7.1$ Hz, 3H); ^{13}C NMR (126 MHz, $CDCl_3$) δ 167.15 (s), 164.35 (s), 149.28 (s), 142.23 (s), 138.97 (s), 126.41 (s), 124.64 (s), 122.19 (s), 121.32 (s), 119.17 (s), 77.41 (s), 77.16 (s), 76.91 (s), 60.84 (s), 14.76 (s), 14.49 (s).



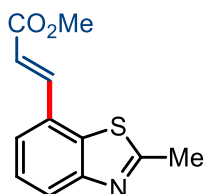
(E)-ethyl 3-(8-fluoroquinolin-5-yl)acrylate (3da):

White solid; yield 59% (14.5 mg); 1H NMR (500 MHz, $CDCl_3$) δ 9.08 – 8.98 (m, 1H), 8.56 (d, $J = 8.7$ Hz, 1H), 8.35 (d, $J = 15.7$ Hz, 1H), 7.79 (dd, $J = 8.1, 4.9$ Hz, 1H), 7.58 (dd, $J = 8.7, 4.1$ Hz, 1H), 7.44 (dd, $J = 9.9, 8.2$ Hz, 1H), 6.51 (d, $J = 15.7$ Hz, 1H), 4.32 (q, $J = 7.1$ Hz, 2H), 1.37 (t, $J = 7.1$ Hz, 3H); ^{13}C NMR (126 MHz, $CDCl_3$) δ 166.62 (s), 159.04 (d, $J_{FC} = 261$ Hz), (150.85 (s), 139.13 (d, $J_{FC} = 9.6$ Hz), 132.42 (s), 132.10 (s), 128.33 (d, $J_{FC} = 7.3$ Hz), 125.69 (d, $J_{FC} = 8.3$ Hz), 122.74 (s), 121.91 (d, $J_{FC} = 18.4$ Hz), 113.85 (d, $J_{FC} = 19.4$ Hz), 61.00 (s), 14.48 (s).



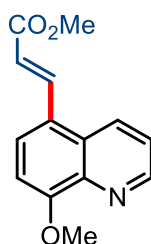
(E)-methyl 5-(3-methoxy-3-oxoprop-1-en-1-yl)quinoline-3-carboxylate (3eb):

White solid; yield 47% (12.7 mg); ^1H NMR (500 MHz, CDCl_3) δ 9.49 (d, $J = 1.6$ Hz, 1H), 9.19 (s, 1H), 8.47 (d, $J = 15.7$ Hz, 1H), 8.22 (d, $J = 8.2$ Hz, 1H), 7.90 – 7.83 (m, 2H), 6.59 (d, $J = 15.7$ Hz, 1H), 4.05 (s, 3H), 3.89 (s, 3H); ^{13}C NMR (126 MHz, CDCl_3) δ 166.93 (s), 150.39 (s), 139.59 (s), 134.66 (s), 131.62 (s), 131.58 (s), 126.24 (s), 122.64 (s), 52.83 (s), 52.18 (s); HRMS (m/z): $[\text{M}+\text{H}]^+$ calcd for $\text{C}_{15}\text{H}_{14}\text{NO}_4$, 272.0917; found, 272.0915.



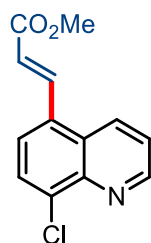
(E)-methyl 3-(2-methylbenzo[d]thiazol-7-yl)acrylate (3fb):

White solid; yield 68% (15.8 mg); ^1H NMR (400 MHz, CDCl_3) δ 7.99 (dd, $J = 7.8, 1.1$ Hz, 1H), 7.88 (d, $J = 16.1$ Hz, 1H), 7.58 – 7.46 (m, 2H), 6.56 (d, $J = 16.1$ Hz, 1H), 3.85 (s, 3H), 2.88 (s, 3H); ^{13}C NMR (101 MHz, CDCl_3) δ 167.35 (s), 167.30 (s), 154.61 (s), 143.02 (s), 134.75 (s), 129.00 (s), 126.46 (s), 126.39 (s), 124.41 (s), 120.23 (s), 52.08 (s), 20.24 (s).



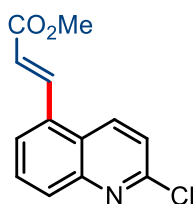
(E)-methyl 3-(8-methoxyquinolin-5-yl)acrylate (3gb):

White solid; yield 89% (21.6 mg); ^1H NMR (500 MHz, CDCl_3) δ 8.95 (d, $J = 3.1$ Hz, 1H), 8.50 (d, $J = 8.5$ Hz, 1H), 8.33 (d, $J = 15.7$ Hz, 1H), 7.79 (d, $J = 8.2$ Hz, 1H), 7.50 (dd, $J = 8.6, 4.1$ Hz, 1H), 7.05 (d, $J = 8.2$ Hz, 1H), 6.45 (d, $J = 15.7$ Hz, 1H), 4.10 (s, 3H), 3.82 (s, 3H); ^{13}C NMR (126 MHz, CDCl_3) δ 167.47 (s), 157.24 (s), 149.54 (s), 140.08 (d, $J = 9.6$ Hz), 131.77 (s), 127.75 (s), 126.26 (s), 123.69 (s), 122.37 (s), 118.80 (s), 107.52 (s), 77.41 (s), 77.16 (s), 76.91 (s), 56.31 (s), 51.87 (s); HRMS (m/z): $[\text{M}+\text{H}]^+$ calcd for $\text{C}_{14}\text{H}_{14}\text{NO}_3$, 244.0968; found, 244.0968.



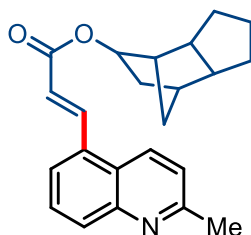
Methyl (E)-3-(8-chloroquinolin-5-yl)acrylate (3hb):

Colourless semi solid; yield 37% (9.2 mg); ^1H NMR (500 MHz, CDCl_3) δ 9.09 (dd, $J = 4.1, 1.5$ Hz, 1H), 8.55 (dd, $J = 8.6, 1.5$ Hz, 1H), 8.37 (d, $J = 15.8$ Hz, 1H), 7.86 (d, $J = 7.9$ Hz, 1H), 7.73 (d, $J = 7.9$ Hz, 1H), 7.57 (dd, $J = 8.6, 4.1$ Hz, 1H), 6.54 (d, $J = 15.7$ Hz, 1H), 3.86 (s, 3H); ^{13}C NMR (126 MHz, CDCl_3) δ 166.95, 151.30, 144.62, 139.44, 135.98, 132.50, 131.40, 129.47, 127.91, 125.25, 122.53, 122.05, 52.14; HRMS (m/z): $[\text{M} + \text{H}]^+$ calcd for $\text{C}_{13}\text{H}_{11}\text{ClNO}_2$, 248.0478; found, 248.0473.



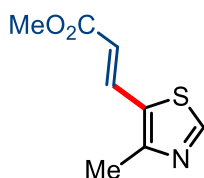
Methyl (*E*)-3-(2-chloroquinolin-5-yl)acrylate (3ib):

White solid; yield: 89% (22 mg); ^1H NMR (500 MHz, CDCl_3) δ 8.49 (d, $J = 8.9$ Hz, 1H), 8.38 (d, $J = 15.8$ Hz, 1H), 8.09 (d, $J = 8.3$ Hz, 1H), 7.91 – 7.72 (m, 2H), 7.49 (d, $J = 8.9$ Hz, 1H), 6.57 (d, $J = 15.8$ Hz, 1H), 3.88 (s, 3H); ^{13}C NMR (126 MHz, CDCl_3) δ 166.96, 151.34, 148.31, 139.83, 134.84, 132.30, 130.88, 130.39, 125.70, 125.35, 123.05, 122.22, 52.13; HRMS (m/z): $[\text{M}+\text{H}]^+$ calcd for $\text{C}_{13}\text{H}_{11}\text{ClNO}_2$, 248.0478; found, 248.0473.



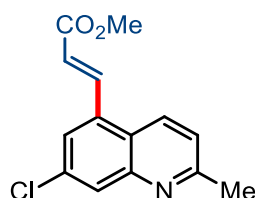
Octahydro-1*H*-4,7-methanoinden-5-yl (*E*)-3-(2-methylquinolin-5-yl)acrylate (3ac):

White solid; yield: 47% (16 mg); ^1H NMR (500 MHz, CDCl_3) δ 8.39 (dd, $J = 20.1, 12.2$ Hz, 2H), 8.06 (d, $J = 8.4$ Hz, 1H), 7.75 (d, $J = 7.2$ Hz, 1H), 7.71 – 7.64 (m, 1H), 7.36 (d, $J = 8.7$ Hz, 1H), 6.52 (d, $J = 15.7$ Hz, 1H), 4.75 (dd, $J = 7.0, 2.3$ Hz, 1H), 2.76 (s, 3H), 2.19 (s, 1H), 2.09 (d, $J = 4.3$ Hz, 1H), 2.00 – 1.61 (m, 7H), 1.54 (ddd, $J = 13.5, 4.2, 2.5$ Hz, 1H), 1.33 – 1.17 (m, 2H), 1.05 – 0.92 (m, 2H); ^{13}C NMR (126 MHz, CDCl_3) δ 166.62, 159.40, 148.11, 139.85, 131.97, 131.90, 130.94, 129.08, 124.93, 124.47, 122.62, 122.22, 77.63, 47.40, 46.34, 43.13, 39.74, 39.28, 32.13, 31.79, 29.60, 27.84, 25.30; HRMS (m/z): $[\text{M}+\text{H}]^+$ calcd for $\text{C}_{23}\text{H}_{26}\text{NO}_2$, 348.1964; found, 348.1946.



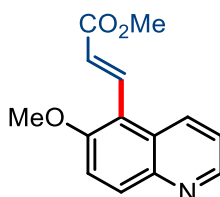
(E)-methyl 3-(4-methylthiazol-5-yl)acrylate (3jb):

White solid; yield 73% (13.4 mg); ^1H NMR (400 MHz, CDCl_3) δ 8.68 (s, 1H), 7.81 (d, $J = 15.6$ Hz, 1H), 6.15 (d, $J = 15.6$ Hz, 1H), 3.79 (s, 3H), 2.56 (s, 3H); ^{13}C NMR (101 MHz, CDCl_3) δ 166.91 (s), 155.99 (s), 152.84 (s), 134.03 (s), 128.36 (s), 119.50 (s), 77.48 (s), 77.16 (s), 76.84 (s), 51.96 (s), 15.76 (s).



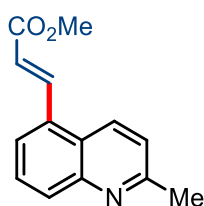
(E)-methyl 3-(7-chloro-2-methylquinolin-5-yl)acrylate (3kb):

White solid; yield 63% (16.5 mg); ^1H NMR (400 MHz, CDCl_3) δ 8.19 (d, $J = 16.0$ Hz, 1H), 8.08 (s, 1H), 8.04 (d, $J = 8.8$ Hz, 2H), 7.31 (d, $J = 8.5$ Hz, 1H), 6.55 (d, $J = 16.0$ Hz, 1H), 3.85 (s, 3H), 2.74 (s, 3H); ^{13}C NMR (101 MHz, CDCl_3) δ 166.90 (s), 161.55 (s), 148.60 (s), 140.70 (s), 136.37 (s), 135.42 (s), 131.00 (s), 129.36 (s), 127.01 (s), 125.19 (s), 123.11 (s), 121.30 (s), 77.48 (s), 77.16 (s), 76.84 (s), 52.09 (s), 25.65 (s); HRMS (m/z): $[\text{M}+\text{H}]^+$ calcd for $\text{C}_{14}\text{H}_{13}\text{ClNO}_2$, 262.0629; found, 262.0633.



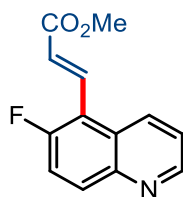
(E)-methyl 3-(6-methoxyquinolin-5-yl)acrylate (3lb):

White solid; yield 78% (18.9 mg); ^1H NMR (500 MHz, CDCl_3) δ 8.82 (d, $J = 3.2$ Hz, 1H), 8.54 (d, $J = 8.6$ Hz, 1H), 8.27 (d, $J = 16.2$ Hz, 1H), 8.15 (d, $J = 9.3$ Hz, 1H), 7.53 (d, $J = 9.4$ Hz, 1H), 7.43 (dd, $J = 8.7, 4.1$ Hz, 1H), 6.76 (d, $J = 16.2$ Hz, 1H), 4.05 (s, 3H), 3.86 (s, 3H); ^{13}C NMR (126 MHz, CDCl_3) δ 156.83 (s), 148.50 (s), 144.00 (s), 136.82 (s), 132.92 (s), 131.77 (s), 127.98 (s), 123.70 (s), 122.09 (s), 116.55 (s), 116.11 (s), 77.41 (s), 77.16 (s), 76.91 (s), 56.47 (s), 51.92 (s); HRMS (m/z): $[\text{M}+\text{H}]^+$ calcd for $\text{C}_{14}\text{H}_{14}\text{NO}_3$, 244.0968; found, 244.0967.



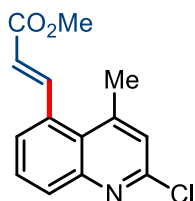
Methyl (*E*)-3-(2-methylquinolin-5-yl)acrylate (3ab):

White solid, yield 86% (19.5 mg); ^1H NMR (500 MHz, CDCl_3) δ 8.43 (s, 1H), 8.40 (d, $J = 4.8$ Hz, 1H), 8.07 (d, $J = 8.4$ Hz, 1H), 7.76 (d, $J = 7.2$ Hz, 1H), 7.68 (t, $J = 7.8$ Hz, 1H), 7.37 (d, $J = 8.7$ Hz, 1H), 6.55 (d, $J = 15.8$ Hz, 1H), 3.86 (s, 3H), 2.76 (s, 3H); ^{13}C NMR (101 MHz, CDCl_3) δ 167.26, 159.54, 148.19, 140.57, 131.91, 131.87, 131.20, 129.14, 125.01, 124.57, 122.74, 121.26, 52.02, 25.38; HRMS (m/z): $[\text{M}+\text{H}]^+$ calcd for $\text{C}_{14}\text{H}_{14}\text{NO}_2$, 228.1025; found, 228.1018.



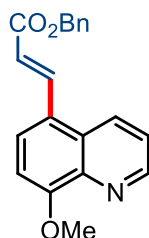
(*E*)-methyl 3-(6-fluoroquinolin-5-yl)acrylate (3mb):

White solid; yield 46% (10.6 mg); ^1H NMR (400 MHz, CDCl_3) δ 8.97 – 8.90 (m, 1H), 8.54 (d, $J = 8.6$ Hz, 1H), 8.17 (d, $J = 16.2$ Hz, 1H), 8.15 – 8.12 (m, 1H), 7.58 – 7.49 (m, 2H), 6.74 (d, $J = 16.2$ Hz, 1H), 3.87 (s, 3H); ^{13}C NMR (126 MHz, CDCl_3) δ 167.40 (s), 159.39 (d, $J_{\text{FC}} = 255.7$ Hz), 149.95 (d, $J_{\text{FC}} = 2.6$ Hz), 145.63 (s), 133.91 (s), 133.55 (d, $J_{\text{FC}} = 10.3$ Hz), 132.06 (d, $J_{\text{FC}} = 6.3$ Hz), 127.61 (d, $J_{\text{FC}} = 5.1$ Hz), 125.65 (d, $J_{\text{FC}} = 12.4$ Hz), 122.34 (s), 119.98 (d, $J_{\text{FC}} = 26.4$ Hz), 116.52 (d, $J_{\text{FC}} = 12.2$ Hz), 52.14 (s); HRMS (m/z): $[\text{M}+\text{H}]^+$ calcd for $\text{C}_{13}\text{H}_{11}\text{FNO}_2$, 232.0768; found, 232.0766.



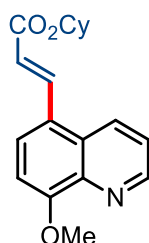
Methyl (E)-3-(2-chloro-4-methylquinolin-5-yl)acrylate (3nb):

White solid; Yield: 76% (19.9 mg); ^1H NMR (500 MHz, CDCl_3) δ 8.06 – 7.97 (m, 2H), 7.90 (dd, $J = 8.8, 1.6$ Hz, 1H), 7.86 (d, $J = 16.0$ Hz, 1H), 7.28 (s, 1H), 6.57 (d, $J = 16.0$ Hz, 1H), 3.84 (s, 3H), 2.70 (s, 3H); ^{13}C NMR (126 MHz, CDCl_3) δ 167.27, 151.79, 148.60, 148.21, 143.98, 132.83, 130.02, 128.15, 127.14, 125.50, 123.48, 119.46, 52.03, 18.70; HRMS (m/z): $[\text{M}+\text{H}]^+$ calcd for $\text{C}_{14}\text{H}_{13}\text{ClNO}_2$, 262.0635; found, 262.0630.



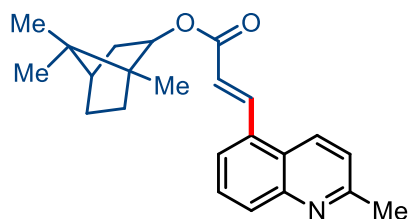
(E)-benzyl 3-(8-methoxyquinolin-5-yl)acrylate (3gd):

White solid; yield 62% (19.7 mg); ^1H NMR (400 MHz, CDCl_3) δ 9.02 – 8.96 (m, 1H), 8.54 (dd, $J = 8.6, 1.2$ Hz, 1H), 8.40 (d, $J = 15.7$ Hz, 1H), 7.83 (d, $J = 8.3$ Hz, 1H), 7.54 (dd, $J = 8.6, 4.1$ Hz, 1H), 7.39 (ddd, $J = 12.7, 8.0, 6.6$ Hz, 5H), 7.09 (d, $J = 8.3$ Hz, 1H), 6.53 (d, $J = 15.7$ Hz, 1H), 5.29 (s, 2H), 4.13 (s, 3H); ^{13}C NMR (126 MHz, CDCl_3) δ 166.91 (s), 157.19 (s), 149.47 (s), 140.63 (s), 140.36 (s), 136.17 (s), 132.16 (s), 128.77 (s), 128.59 (s), 128.48 (s), 128.46 (s), 126.52 (s), 123.75 (s), 122.45 (s), 119.01 (s), 107.73 (s), 66.62 (s), 56.40 (s); HRMS (m/z): $[\text{M}+\text{H}]^+$ calcd for $\text{C}_{20}\text{H}_{18}\text{NO}_3$, 320.1281; found, 320.1281.



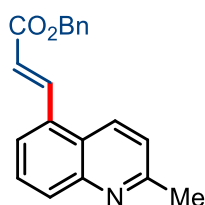
(E)-cyclohexyl 3-(8-methoxyquinolin-5-yl)acrylate (3ge):

White solid; yield 78% (24.3 mg); ^1H NMR (400 MHz, CDCl_3) δ 8.97 (dd, $J = 4.1, 1.5$ Hz, 1H), 8.54 (dd, $J = 8.6, 1.4$ Hz, 1H), 8.33 (d, $J = 15.7$ Hz, 1H), 7.82 (d, $J = 8.2$ Hz, 1H), 7.53 (dd, $J = 8.6, 4.1$ Hz, 1H), 7.08 (d, $J = 8.3$ Hz, 1H), 6.47 (d, $J = 15.7$ Hz, 1H), 4.98 – 4.87 (m, 1H), 4.12 (s, 3H), 1.98 – 1.90 (m, 2H), 1.78 (dd, $J = 8.8, 3.9$ Hz, 2H), 1.62 – 1.36 (m, 6H); ^{13}C NMR (101 MHz, CDCl_3) δ 166.57 (s), 157.14 (s), 149.53 (s), 140.15 (s), 139.55 (s), 131.97 (s), 127.81 (s), 126.26 (s), 123.98 (s), 122.37 (s), 120.04 (s), 107.59 (s), 73.03 (s), 56.33 (s), 31.92 (s), 25.57 (s), 23.98 (s); HRMS (m/z): $[\text{M}+\text{H}]^+$ calcd for $\text{C}_{19}\text{H}_{22}\text{NO}_3$, 312.1594; found, 312.1595.

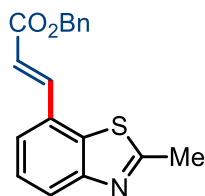


1,7,7-trimethylbicyclo[2.2.1]heptan-2-yl (*E*)-3-(2-methylquinolin-5-yl)acrylate (3af):

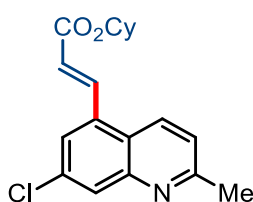
Colourless semi solid; yield 74% (26.1 mg); ^1H NMR (400 MHz, CDCl_3) δ 8.38 (dd, $J = 12.1$, 5.2 Hz, 2H), 8.06 (d, $J = 8.4$ Hz, 1H), 7.78 (d, $J = 7.2$ Hz, 1H), 7.71 – 7.64 (m, 1H), 7.37 (d, $J = 8.7$ Hz, 1H), 6.52 (d, $J = 15.7$ Hz, 1H), 4.85 (dd, $J = 7.2$, 4.4 Hz, 1H), 2.76 (s, 3H), 1.89 (t, $J = 6.4$ Hz, 2H), 1.84 – 1.64 (m, 4H), 1.09 (s, 3H), 0.93 (s, 3H), 0.88 (s, 3H); ^{13}C NMR (101 MHz, CDCl_3) δ 166.35, 159.47, 148.16, 139.89, 131.96, 131.86, 131.01, 129.14, 124.99, 124.53, 122.73, 122.26, 81.52, 49.08, 47.18, 45.24, 39.04, 33.89, 27.21, 25.34, 20.29, 20.17, 11.71; HRMS (m/z): $[\text{M}+\text{H}]^+$ calcd for $\text{C}_{23}\text{H}_{28}\text{NO}_2$, 350.2120; found, 350.2112.

**Benzyl (*E*)-3-(2-methylquinolin-5-yl)acrylate (3ad):**

Colourless Semi Solid; yield 76% (23mg); ^1H NMR (400 MHz, CDCl_3) δ 8.44 (d, $J = 15.8$ Hz, 1H), 8.40 (d, $J = 8.7$ Hz, 1H), 8.06 (d, $J = 8.3$ Hz, 1H), 7.75 (d, $J = 7.1$ Hz, 1H), 7.70 – 7.63 (m, 1H), 7.46 – 7.34 (m, 6H), 6.59 (d, $J = 15.8$ Hz, 1H), 5.30 (s, 2H), 2.75 (s, 3H). ^{13}C NMR (101 MHz, CDCl_3) δ 166.62, 159.50, 148.13, 144.53, 140.83, 136.05, 131.88, 131.77, 131.19, 129.11, 128.76, 128.47, 127.40, 124.97, 124.60, 122.72, 121.26, 66.70, 25.32; HRMS (m/z): $[\text{M}+\text{H}]^+$ calcd for $\text{C}_{20}\text{H}_{18}\text{NO}_2$, 304.1338; found, 304.1333.

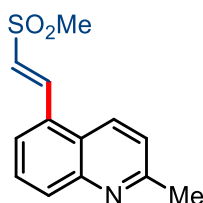
**(*E*)-benzyl 3-(2-methylbenzo[*d*]thiazol-7-yl)acrylate (3fd):**

White solid; yield 64% (19.8 mg); ^1H NMR (500 MHz, CDCl_3) δ 7.99 (d, $J = 7.8$ Hz, 1H), 7.91 (d, $J = 16.1$ Hz, 1H), 7.54 (d, $J = 7.2$ Hz, 1H), 7.49 (t, $J = 7.7$ Hz, 1H), 7.40 (ddd, $J = 23.5$, 11.5, 4.9 Hz, 5H), 6.60 (d, $J = 16.1$ Hz, 1H), 5.29 (s, 2H), 2.88 (s, 3H); ^{13}C NMR (126 MHz, CDCl_3) δ 167.38 (s), 166.71 (s), 154.59 (s), 143.34 (s), 136.04 (s), 128.97 (s), 128.79 (s), 128.53 (s), 128.51 (s), 126.53 (s), 126.46 (s), 66.79 (s), 20.22 (s); HRMS (m/z): $[\text{M}+\text{H}]^+$ calcd for $\text{C}_{19}\text{H}_{17}\text{NNaO}_3\text{S}$, 362.0821; found, 362.0821.



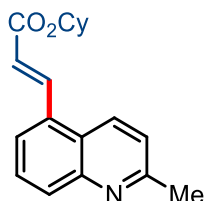
(E)-cyclohexyl 3-(7-chloro-2-methylquinolin-5-yl)acrylate (3ke):

White solid; yield 73% (24 mg); ^1H NMR (500 MHz, CDCl_3) δ 8.17 (d, $J = 15.9$ Hz, 2H), 8.08 (s, 2H), 8.02 (d, $J = 8.8$ Hz, 4H), 7.30 (d, $J = 8.4$ Hz, 2H), 6.54 (d, $J = 15.9$ Hz, 2H), 4.93 (ddd, $J = 12.8$, 8.7, 3.7 Hz, 2H), 2.74 (s, 6H), 1.99 – 1.72 (m, 9H), 1.57 – 1.28 (m, 12H); ^{13}C NMR (126 MHz, CDCl_3) δ 165.91 (s), 161.43 (s), 148.53 (s), 140.08 (s), 136.33 (s), 135.43 (s), 131.19 (s), 129.30 (s), 126.94 (s), 125.20 (s), 123.07 (s), 122.40 (s), 77.41 (s), 77.16 (s), 76.91 (s), 73.22 (s), 31.85 (s), 25.64 (s), 25.57 (s), 23.92 (s); HRMS (m/z): $[\text{M}+\text{H}]^+$ calcd for $\text{C}_{19}\text{H}_{21}\text{ClNO}_2$, 330.1255; found, 330.1251.



(E)-2-methyl-5-(2-(methylsulfonyl)vinyl)quinoline (3ag):

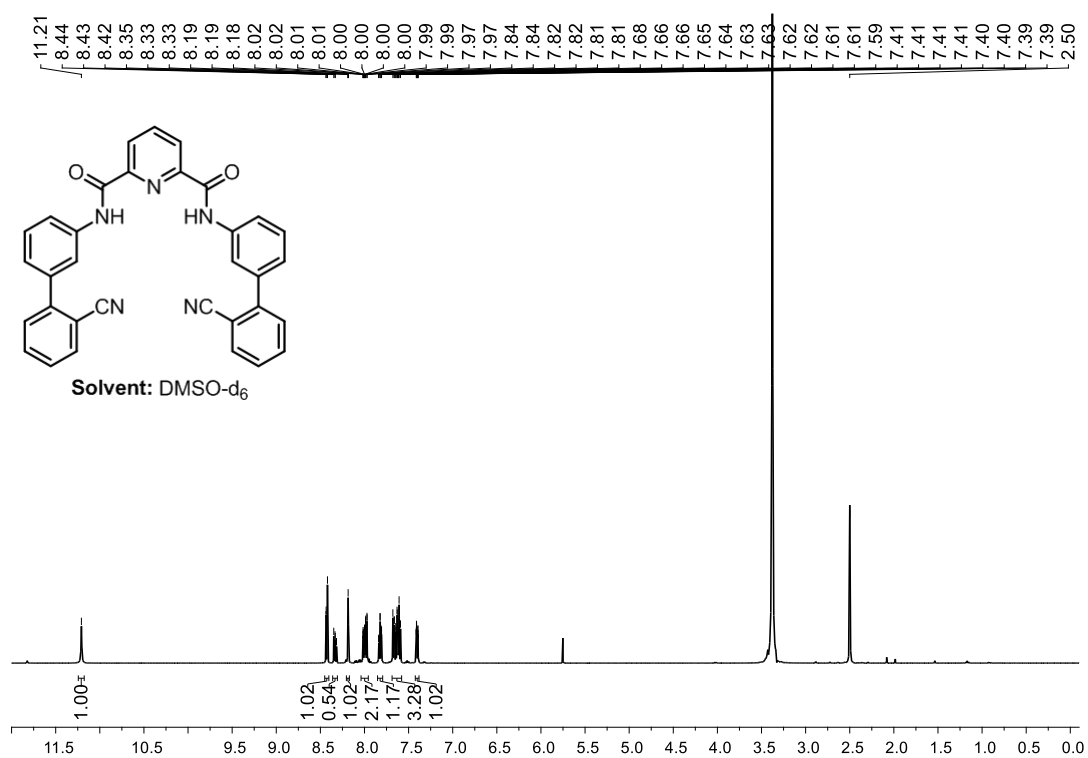
White Solid; yield 69% (17 mg); ^1H NMR (400 MHz, CDCl_3) δ 8.37 (d, $J = 2.6$ Hz, 1H), 8.34 (d, $J = 9.2$ Hz, 1H), 8.12 (d, $J = 8.0$ Hz, 1H), 7.72 (dt, $J = 15.4, 6.7$ Hz, 2H), 7.40 (d, $J = 8.7$ Hz, 1H), 7.04 (d, $J = 15.2$ Hz, 1H), 3.10 (s, 3H), 2.77 (s, 3H); ^{13}C NMR (101 MHz, CDCl_3) δ 159.98, 148.15, 139.75, 132.37, 131.46, 129.32, 129.04, 125.25, 125.00, 123.17, 43.35, 25.38; HRMS (m/z): $[\text{M}+\text{H}]^+$ calcd for $\text{C}_{13}\text{H}_{14}\text{NO}_2\text{S}$, 248.0745; found, 248.0739.

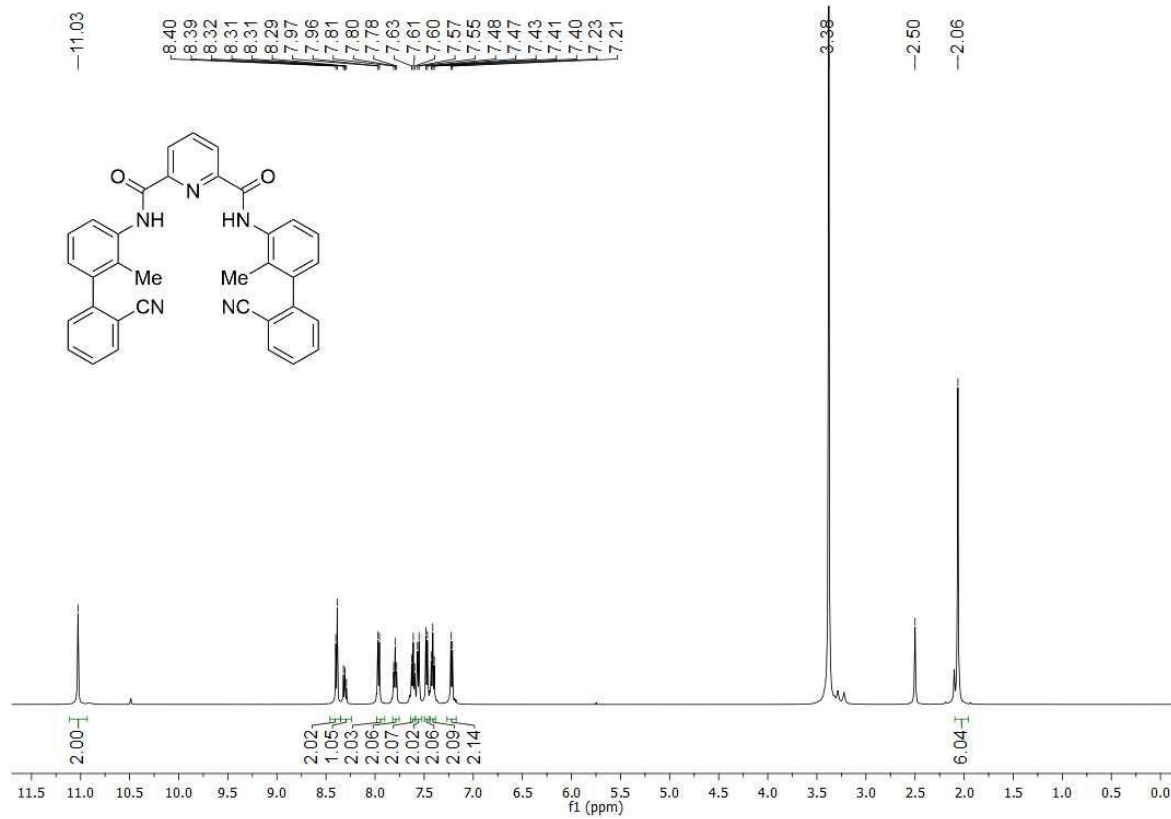
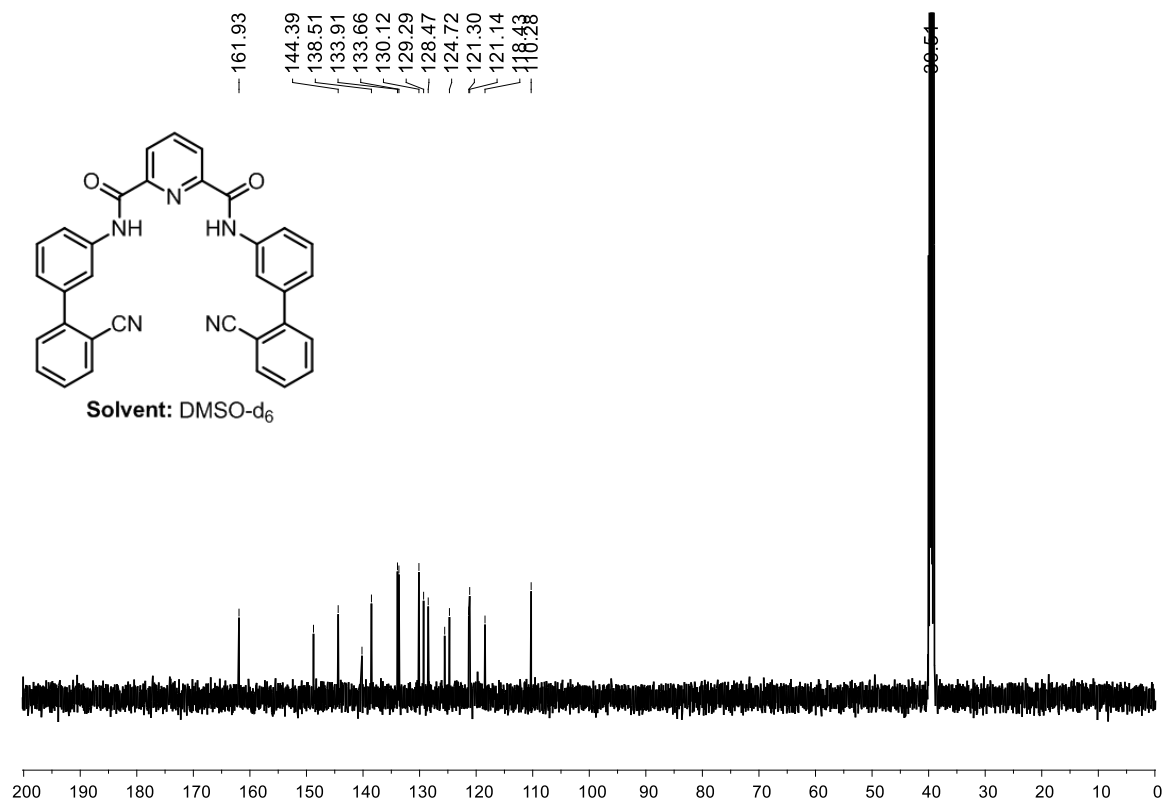


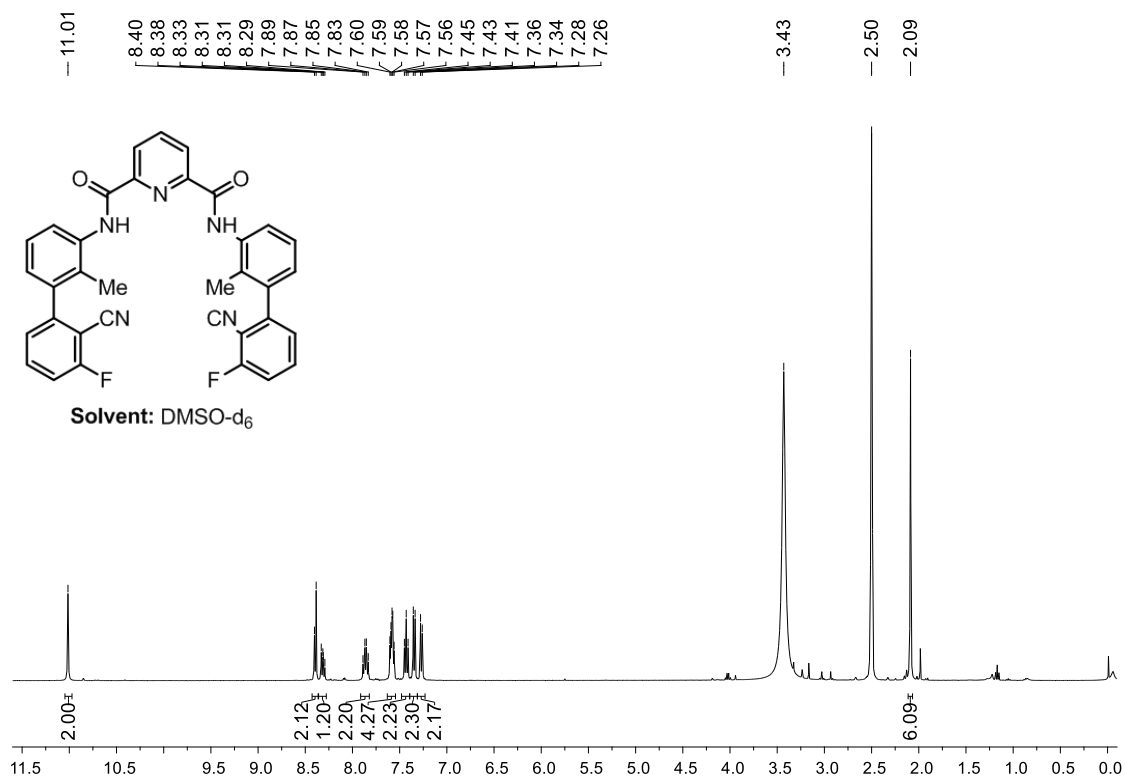
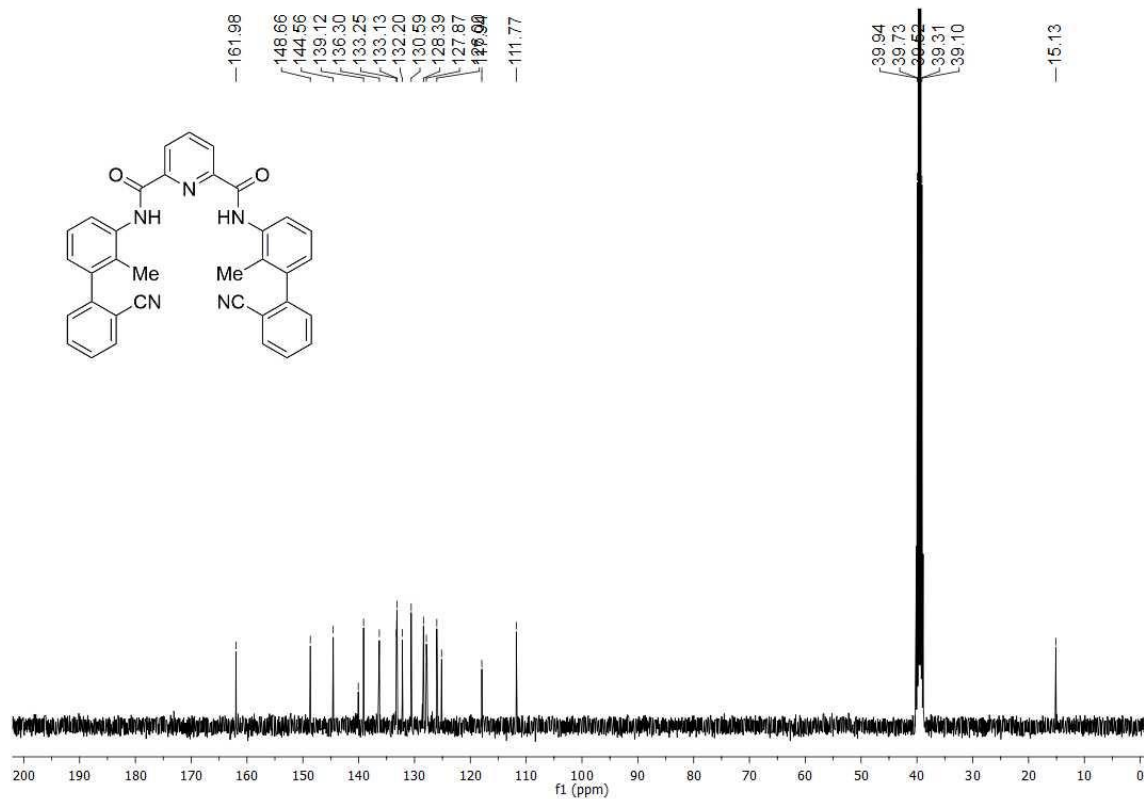
Cyclohexyl (*E*)-3-(2-methylquinolin-5-yl)acrylate (3ae):

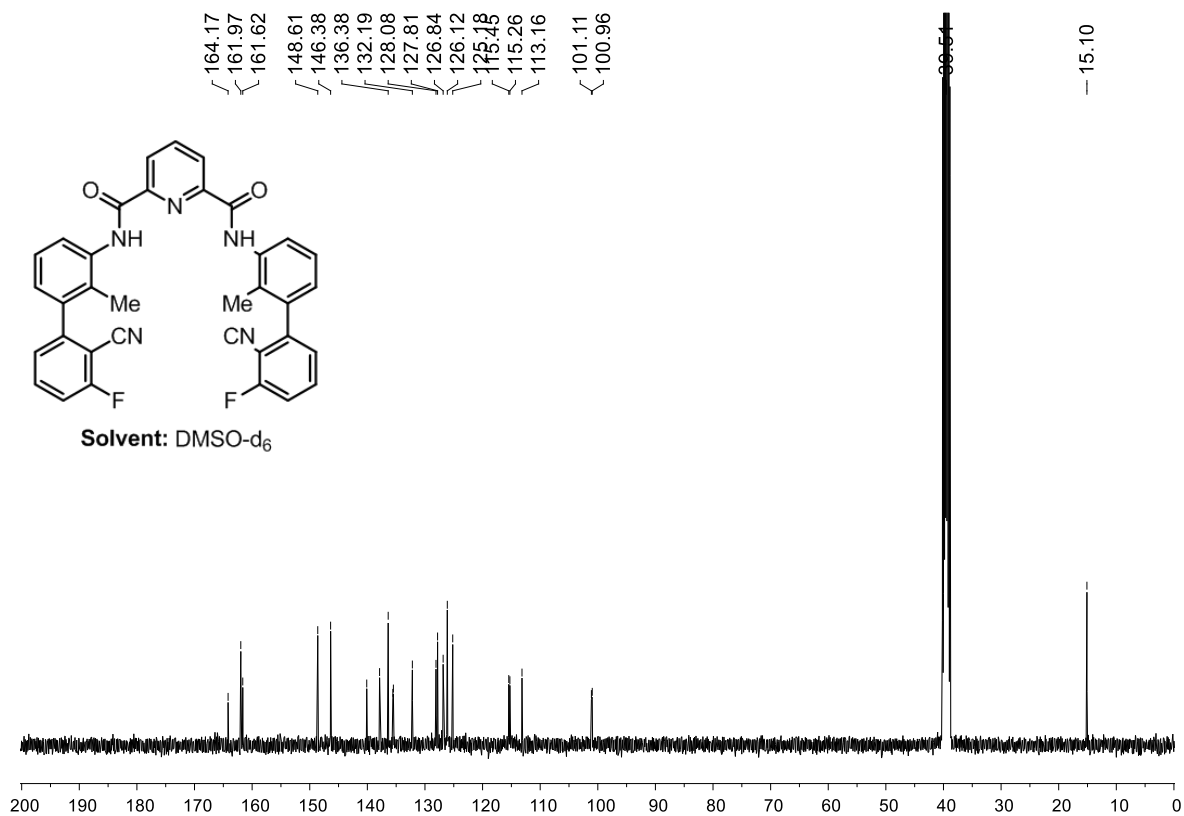
White solid; yield: 81% (24.2 mg), ^1H NMR (500 MHz, CDCl_3) δ 8.39 (dd, $J = 17.7, 12.2$ Hz, 2H), 8.05 (d, $J = 8.4$ Hz, 1H), 7.75 (d, $J = 7.2$ Hz, 1H), 7.71 – 7.62 (m, 1H), 7.35 (d, $J = 8.7$ Hz, 1H), 6.53 (d, $J = 15.7$ Hz, 1H), 5.07 – 4.73 (m, 1H), 2.75 (s, 3H), 1.98 – 1.93 (m, 2H), 1.82 – 1.73 (m, 2H), 1.60 – 1.49 (m, 3H), 1.47 – 1.39 (m, 2H), 1.30 (dd, $J = 13.8, 3.4$ Hz, 1H); ^{13}C NMR (101 MHz, CDCl_3) δ 166.25, 159.41, 148.13, 139.91, 132.01, 131.94, 130.94, 129.10, 124.95, 124.49, 122.62, 122.32, 73.15, 31.86, 25.53, 25.32, 23.93; HRMS (m/z): $[\text{M}+\text{H}]^+$ calcd for $\text{C}_{19}\text{H}_{22}\text{NO}_2$, 296.1651; found, 296.1649.

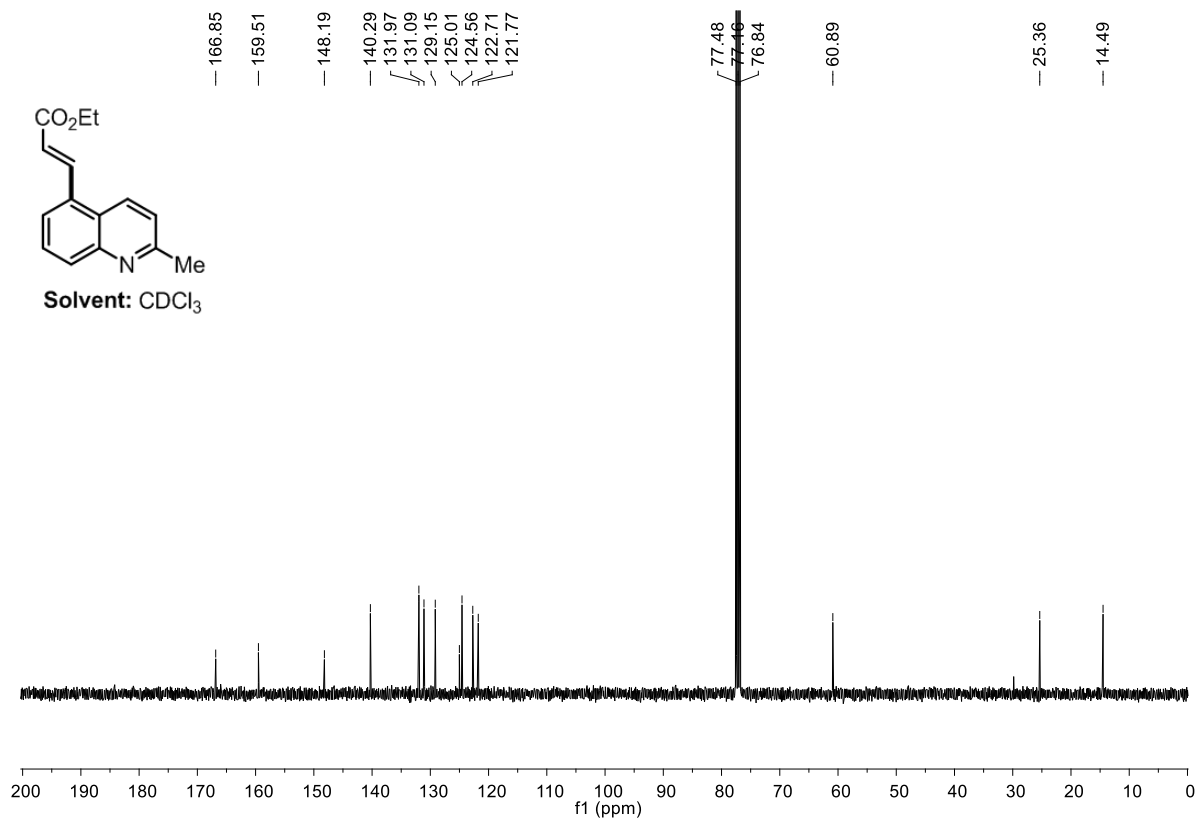
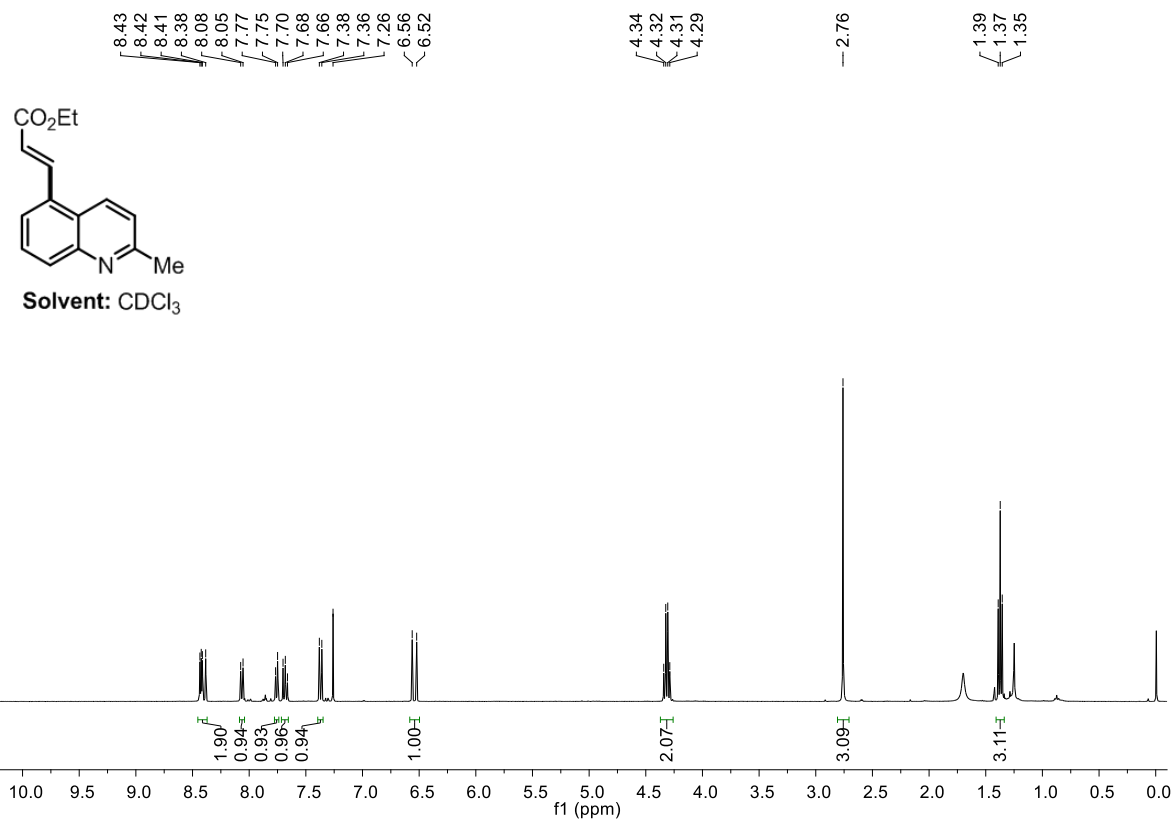
3.4.6. Representative NMR spectra:

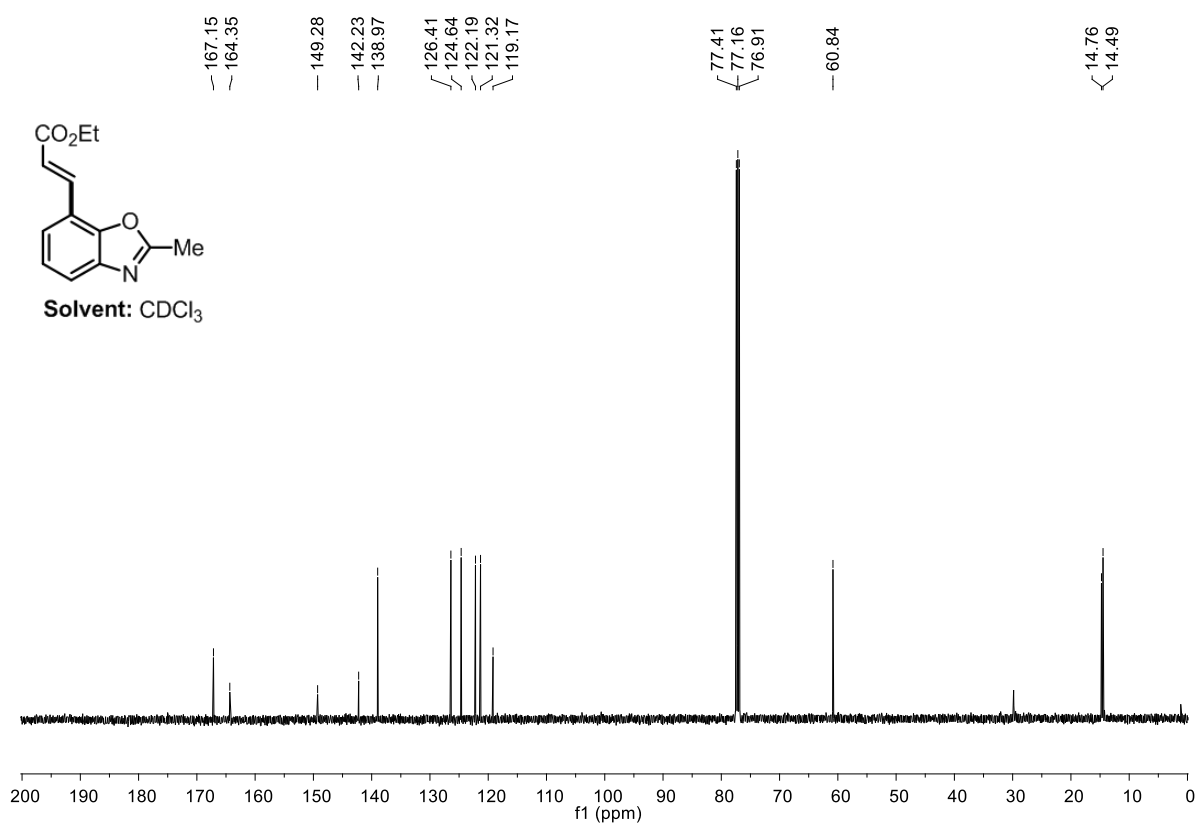
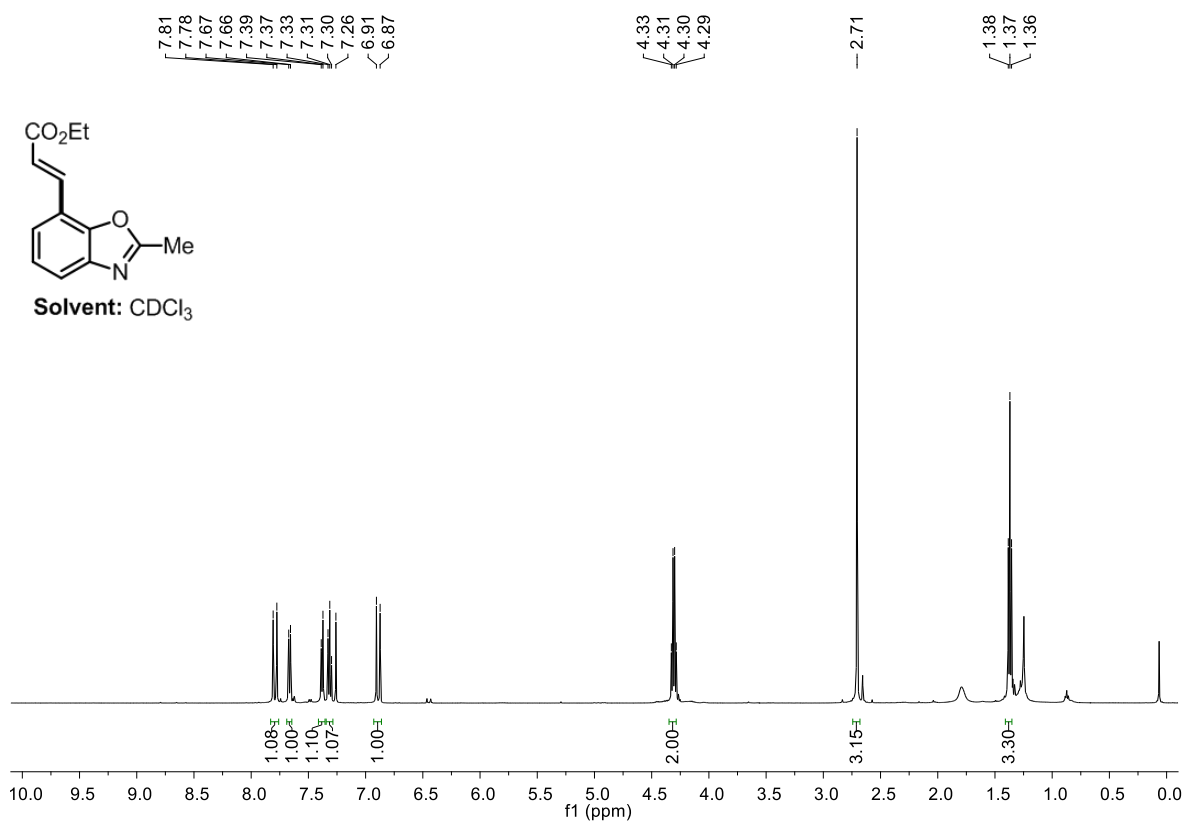


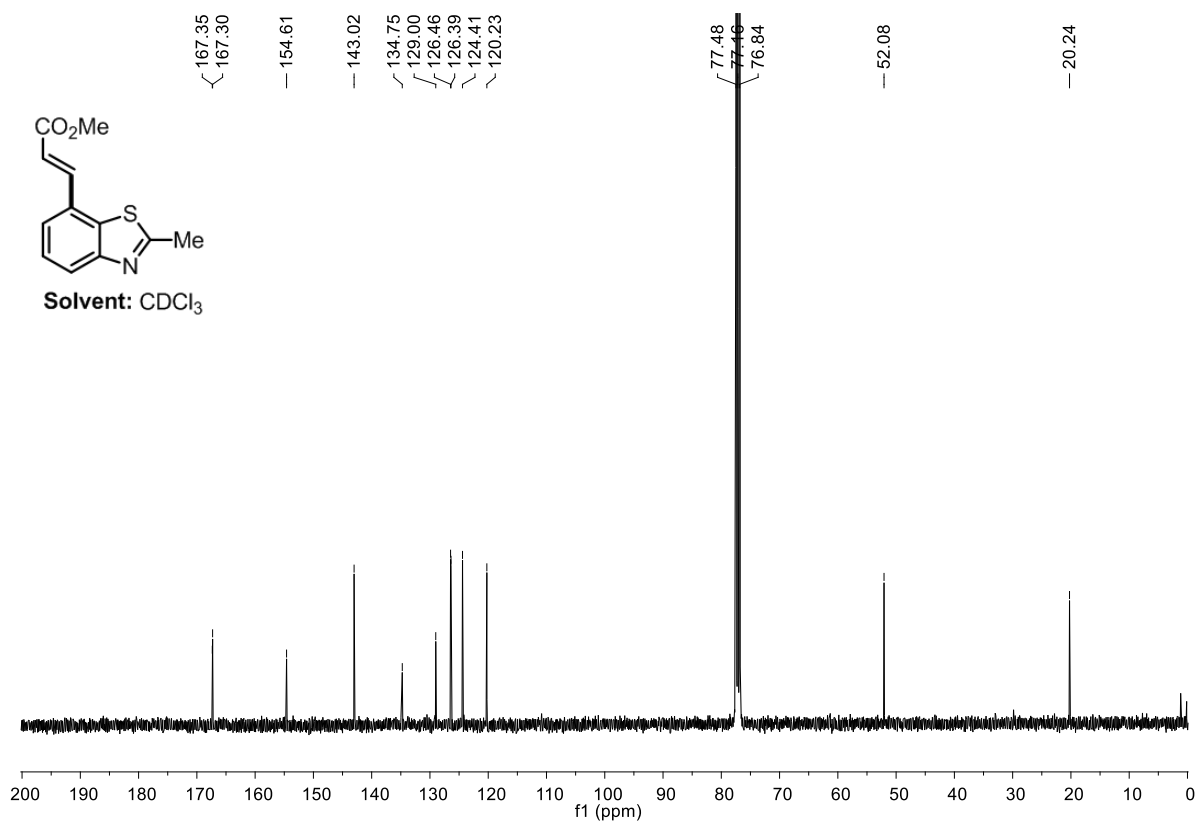
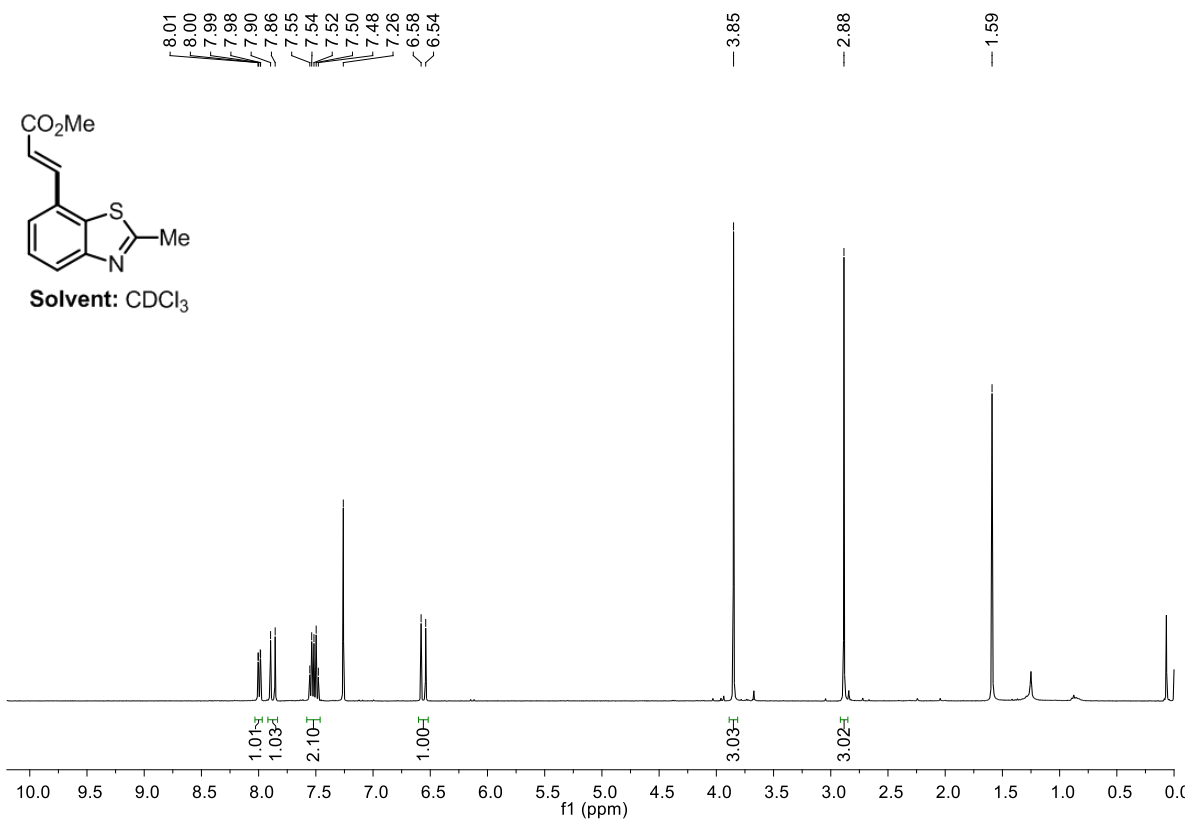


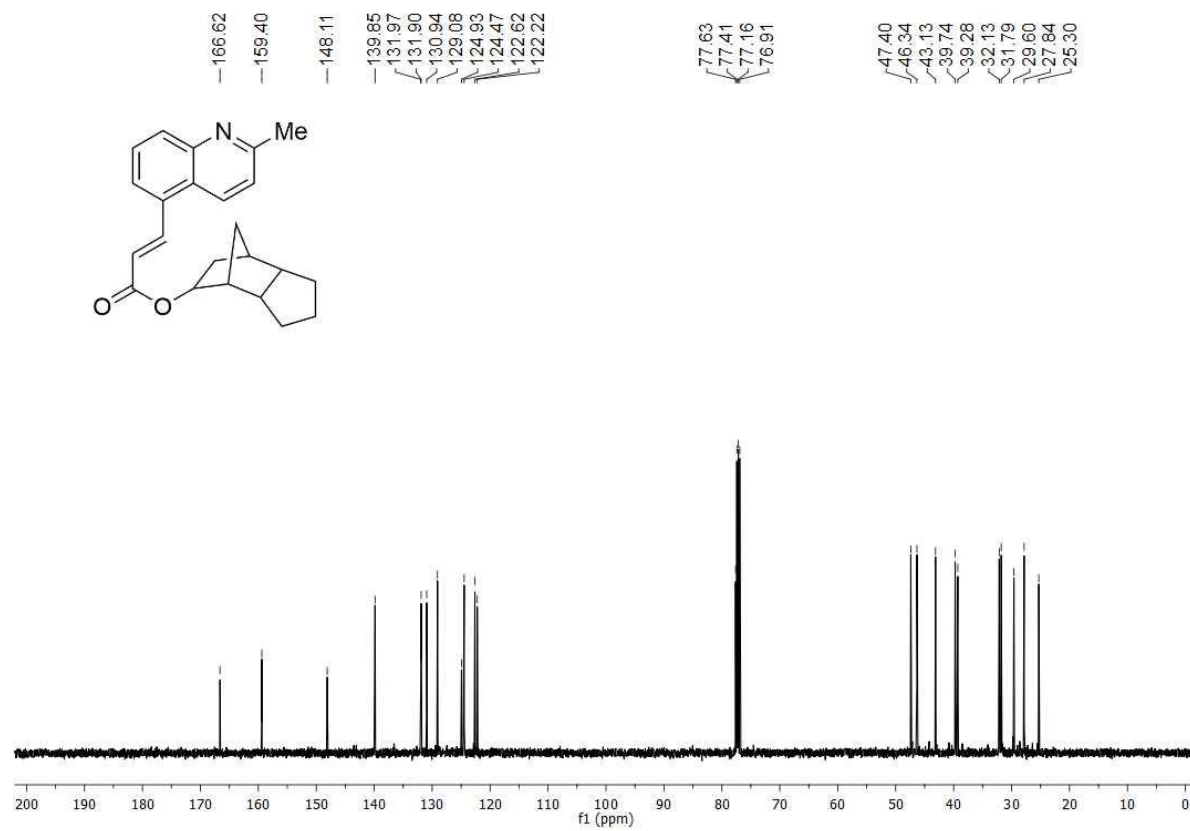
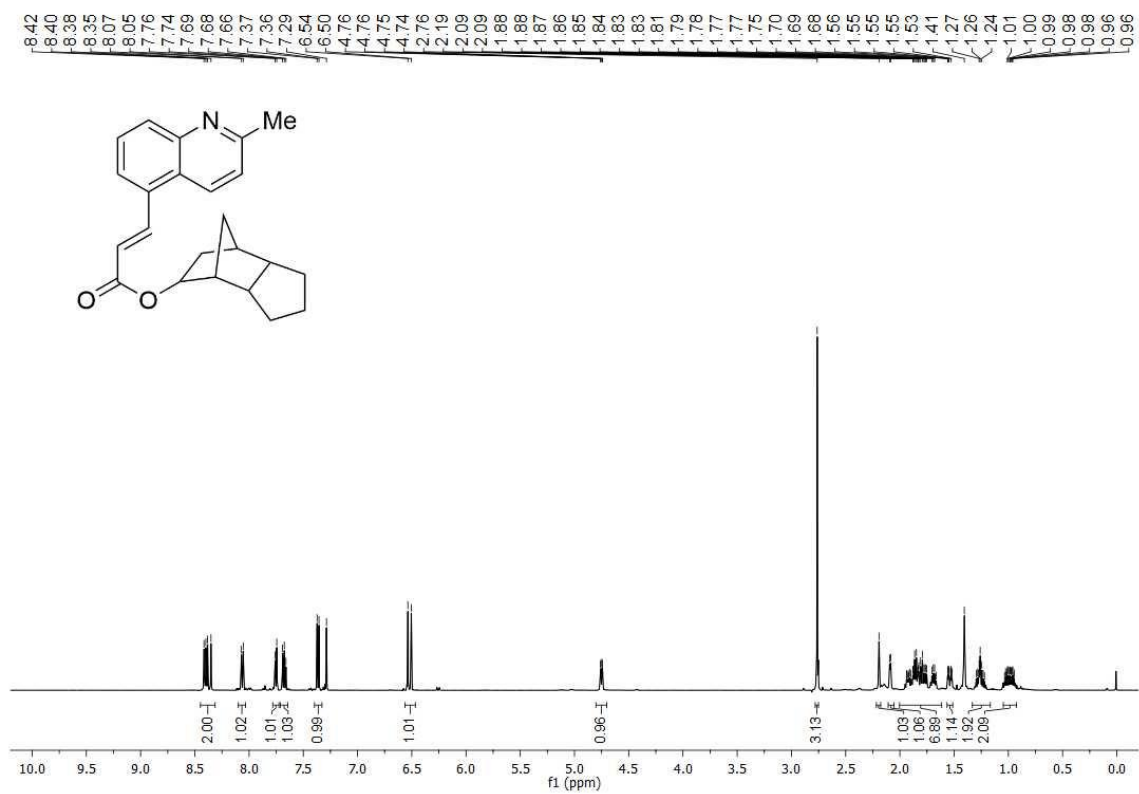












3.5. References:

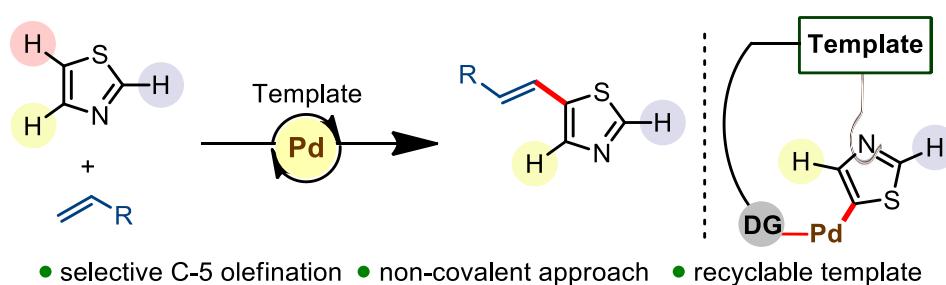
1. Tsuji, N.; Kennemur, J. L.; Buyck, T.; Lee, S.; Prévost, S.; Kaib, P. S. J.; Bykov, D.; Farès, C.; List, B. *Science* **2018**, *359*, 1501-1505.
2. Monaco, M. R.; Fazzi, D.; Tsuji, N.; Leutzsch, M.; Liao, S.; Thiel, W.; List, B. *J. Am. Chem. Soc.* **2016**, *138*, 14740-14749.
3. Doyle, A. G.; Jacobsen, E. N. *Chem. Rev.* **2007**, *107*, 5713-5743.
4. Davis, H. J.; Phipps, R. J. *Chem. Sci.* **2017**, *8*, 864-877.
5. Saidi, O.; Marafie, J.; Ledger, A. E. W.; Liu, P. M.; Mahon, M. F.; Kociok-Köhn, G.; Whittlesey, M. K.; Frost, C. G. *J. Am. Chem. Soc.* **2011**, *133*, 19298-19301.
6. Leow, D.; Li, G.; Mei, T.-S.; Yu, J.-Q. *Nature* **2012**, *486*, 518.
7. Hofmann, N.; Ackermann, L. *J. Am. Chem. Soc.* **2013**, *135*, 5877-5884.
8. Li, J.; Korvorapun, K.; De Sarkar, S.; Rogge, T.; Burns, D. J.; Warratz, S.; Ackermann, L. *Nat. Commun.* **2017**, *8*, 15430.
9. Yu, D.-G.; Gensch, T.; de Azambuja, F.; Vásquez-Céspedes, S.; Glorius, F. *J. Am. Chem. Soc.* **2014**, *136*, 17722-17725.
10. Li, J.; Warratz, S.; Zell, D.; De Sarkar, S.; Ishikawa, E. E.; Ackermann, L. *J. Am. Chem. Soc.* **2015**, *137*, 13894-13901.
11. Wang, H.; Schröder, N.; Glorius, F. *Angew. Chem. Int. Ed.* **2013**, *52*, 5386-5389.
12. Bera, M.; Maji, A.; Sahoo, S. K.; Maiti, D. *Angew. Chem. Int. Ed.* **2015**, *54*, 8515-8519.
13. Bag, S.; Patra, T.; Modak, A.; Deb, A.; Maity, S.; Dutta, U.; Dey, A.; Kancherla, R.; Maji, A.; Hazra, A.; Bera, M.; Maiti, D. *J. Am. Chem. Soc.* **2015**, *137*, 11888-11891.
14. Dong, Z.; Wang, J.; Dong, G. *J. Am. Chem. Soc.* **2015**, *137*, 5887-5890.
15. Murai, S.; Kakiuchi, F.; Sekine, S.; Tanaka, Y.; Kamatani, A.; Sonoda, M.; Chatani, N. *Nature* **1993**, *366*, 529.

16. Gemoets, H. P. L.;Laudadio, G.;Verstraete, K.;Hessel, V.;Noël, T. *Angew. Chem. Int. Ed.* **2017**, *56*, 7161-7165.
17. Arockiam, P. B.;Bruneau, C.;Dixneuf, P. H. *Chem. Rev.* **2012**, *112*, 5879-5918.
18. Reding, A.;Jones, P. G.;Werz, D. B. *Angew. Chem. Int. Ed.*, **2018**, doi:10.1002/anie.201805399.
19. Crabtree, R. H. *Chem. Rev.* **2015**, *115*, 127-150.
20. Davis, H. J.;Mihai, M. T.;Phipps, R. J. *J. Am. Chem. Soc.* **2016**, *138*, 12759-12762.
21. Davis, H. J.;Genov, G. R.;Phipps, R. J. *Angew. Chem. Int. Ed.* **2017**, *56*, 13351-13355.
22. Chattopadhyay, B.;Dannatt, J. E.;Andujar-De Sanctis, I. L.;Gore, K. A.;Maleczka, R. E.;Singleton, D. A.;Smith, M. R. *J. Am. Chem. Soc.* **2017**, *139*, 7864-7871.
23. Kuninobu, Y.;Ida, H.;Nishi, M.;Kanai, M. *Nat. Chem.* **2015**, *7*, 712.
24. Zhang, Z.;Tanaka, K.;Yu, J.-Q. *Nature* **2017**, *543*, 538.
25. Maji, A.;Guin, S.;Feng, S.;Dahiya, A.;Singh, V. K.;Liu, P.;Maiti, D. *Angew. Chem. Int. Ed.* **2017**, *56*, 14903-14907.
26. Gunanathan, C.;Milstein, D. *Chem. Rev.* **2014**, *114*, 12024-12087.
27. Atienza, C. C. H.;Diao, T.;Weller, K. J.;Nye, S. A.;Lewis, K. M.;Delis, J. G. P.;Boyer, J. L.;Roy, A. K.;Chirik, P. J. *J. Am. Chem. Soc.* **2014**, *136*, 12108-12118.
28. Wang, Q.-Q.;Begum, R. A.;Day, V. W.;Bowman-James, K. *J. Am. Chem. Soc.* **2013**, *135*, 17193-17199.

Chapter 4

Chapter 4

Palladium catalyzed template directed C-5 selective olefination of thiazoles



Abstract: An efficient method has been developed to afford highly C-5 selective olefination of thiazole derivatives utilizing bifunctional template in an intermolecular fashion. Coordinative interaction between substrates and metal chelated template backbone plays crucial role for high C-5 selectivity. Excellent selectivity for C-5 position was observed while mono substituted (2- or 4-) or even more challenging unsubstituted thiazoles were employed.

4.1. Introduction:

Over the two decades, transition metal-catalyzed C–H activation strategy has been emerged as an useful tool in organic synthesis owing to its versatile usefulness including late-stage functionalizations of pharmaceuticals, agrochemicals etc.¹⁻⁴ In this context, C–H olefination reaction has turned out as an important method as it allows to afford an array of pharmaceutical precursors and complex organic molecules synthesis in a step and atom economic way. Precisely, the palladium-catalyzed C–H olefination is one of the attractive reaction for accessing the olefinated products.^{5,6} Since the discovery of Fujiwara-Moritani and Mizoroki-Heck reaction, remarkable progress has been made to improve the efficacy and practicality of the oxidative olefination reaction.⁷⁻¹² However, presence of several C–H bonds in an organic molecule impose a challenge to achieve desired C–H bond functionalization selectively. Generally, regioselective C–H functionalizations are governed through the inherent electronic and steric factors of the aromatic compounds. Over the past few years, either directed or non-directed approaches have been utilized to resolve the selectivity issues.¹³⁻¹⁷ The directing group (DG) strategy often can have advantages over other strategies. However the directing groups (DGs) are not useful in certain molecules which lack the suitable functional group to tether the DG. Also the removal of the DG is usually essential, thus certainly limiting the practicality and scalability of the methods. Alternatively, utilization of electronically triggered substrates (non-directed) to enable innately distinguished C–H bond activation is desirable, especially for the (hetero)arenes though the selectivity remained major issues.^{18,19}

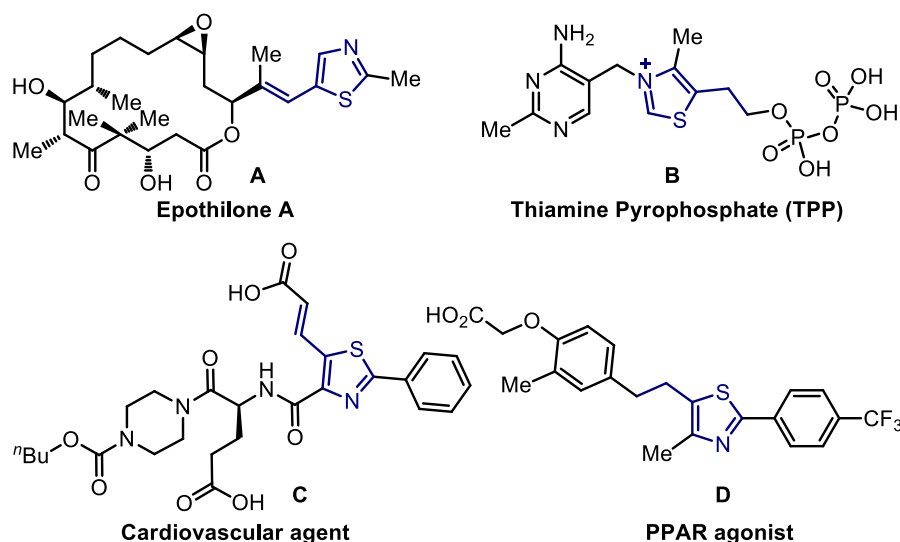
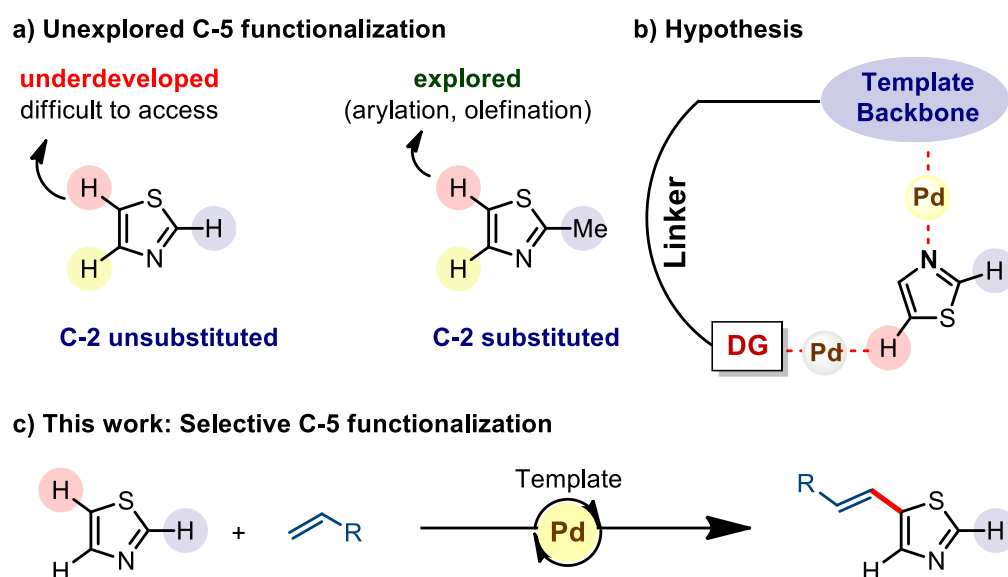


Figure 4.1. Representative examples of 5-olefinated/alkyl thiazole containing molecules.

Thiazole ring represents a privileged class of heterocyclic compounds, repeatedly found in many natural products, pharmaceutically active substrates and organic materials.²⁰⁻²² Recently, significant developments have been made to utilize thiazole ring as masked formyl group, derivatization of thiazole for better usability.^{23,24} Many 5-olefinated thiazole derivatives are found to be strong potential bioactive molecules. Epothilone A is a potential cancer drug, while 5-olefinated thiazole derivative, **C** is a cardiovascular agent (Figure 4.1).^{25,26} Hydrogenated congener of 5-olefinated thiazole, **D** is an agonist of peroxisome proliferator activated receptors (PPARs).²⁷ Consequently, development of C-5 selective functionalization of thiazoles are of immense medicinal value. With our continuous interest in developing template directed regioselective distal C–H bond functionalization of heterocycles, we intended to utilize bifunctional template for selective C5–H bond olefination of thiazole.²⁸ It is quite challenging to achieve C–H functionalization of thiazole because of their higher tendency to dimerize under oxidative conditions.^{29,30} Besides, selectivity inversion between C-2 and C-5 positions of thiazole is another intimidating challenge. Especially, when 2,5-unsubstituted thiazole derivatives were utilized as substrates under transition metal catalyzed oxidative conditions, 2-olefinated products were generally observed though the C-5 position possesses high electron

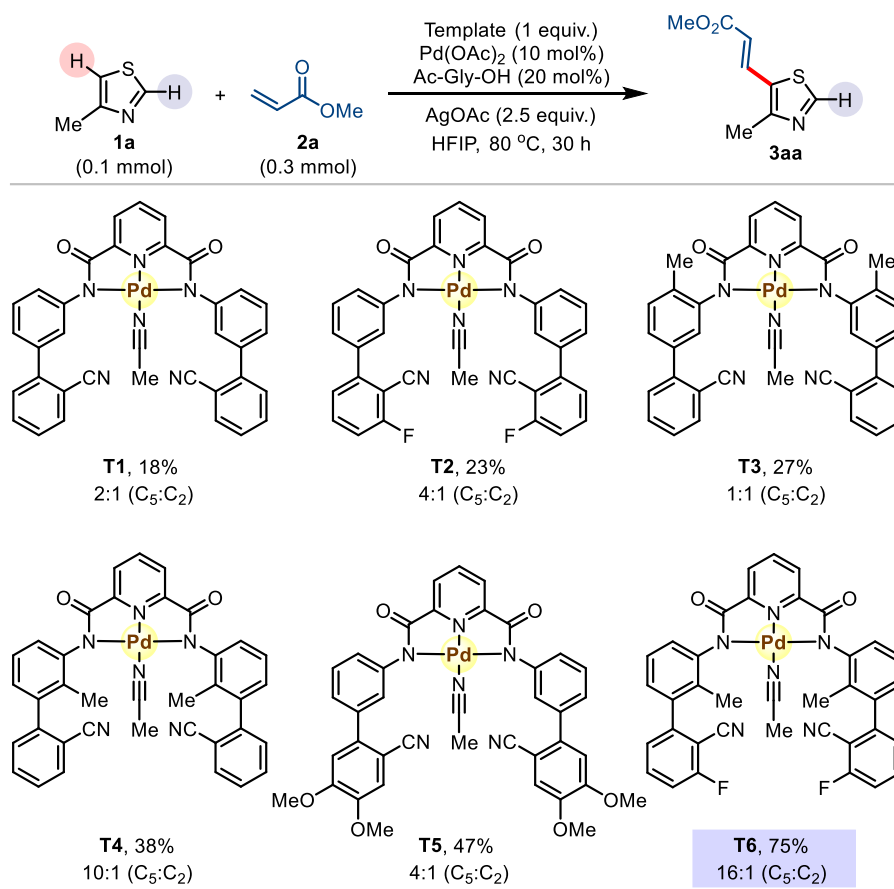
density.³¹ In general C2- substituted thiazole derivatives were used to afford C5-functionalized thiazoles (Scheme 4.1a).³²⁻³⁵ Development of C₅-H selective functionalization of unbiased thiazole are extremely challenging and remained very little explored.^{36,37} In this regard, utilization of non-covalent interactions could be useful to achieve site-selective C-H bond functionalized products.³⁸⁻⁴² Herein, we present our development of selective C₅-H bond olefination of thiazole utilizing bifunctional template (Scheme 4.1b). Template was designed in such a way that backbone helps to pendant the thiazole through coordination of *N*-center to chelated metal. On the other hand template containing side arm DG directs the metal catalyst to the desired C-H bond selectively.



Scheme 4.1. Site-selective C-5 olefination of thiazole. (a) Previous strategies and existing challenges in site-selective C-H functionalization. (b) Our hypothesis: Coordinative interactions promoted selective C-5 activations. (c) This work: Template directed C-5 selective olefination of thiazoles.

4.2. Result and discussion:

The tri-coordinating templates have been prepared by amidation reaction from di-picolinic acid and nitrile containing biphenyl amine.^{28,42} An appropriate distance and geometry of the template play the crucial role to host the substrate through coordinative interaction in a host-guest complexation manner. Geometry of di-picolinamide based templates might allow site-selective C–H bond functionalization of thiazole derivatives.

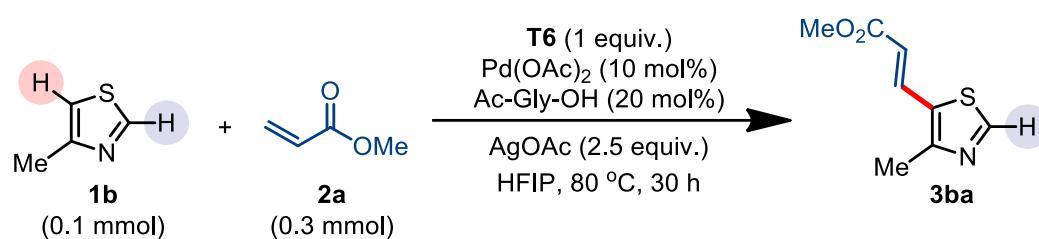


Scheme 4.2. Evaluation of templates for site-selective C₅–H functionalizations of thiazole.

To check the feasibility of this hypothesis, we initially carried out palladium catalyzed olefination reaction employing 4-methylthiazole **1a** as a model substrate with methyl acrylate **2a** in presence of mono protected amino acid (MPAA) ligand, Ac-Gly-OH (Scheme 4.2). To our delight, the desired C₅-olefinated thiazole moiety was achieved in 18% yield with template

T1. Slightly better yield and selectivity was obtained with template **T2** and **T5**. Introducing the steric effect into the inner core of the template (**T4**) enhances the selectivity significantly. The necessity of steric and geometrical constraint of the inner core was further supported by template **T3**. Presence of methyl substituents outer side of the core failed to endorse the higher selectivity. Presence of fluorine atom in the DGs of template **T6**, enhanced the homogeneity of the reaction mixture and also apparently modulated the electronic environment around the DGs. As a result, template **T6** was found to be an effective template for C₅-olefination of thiazole derivatives.

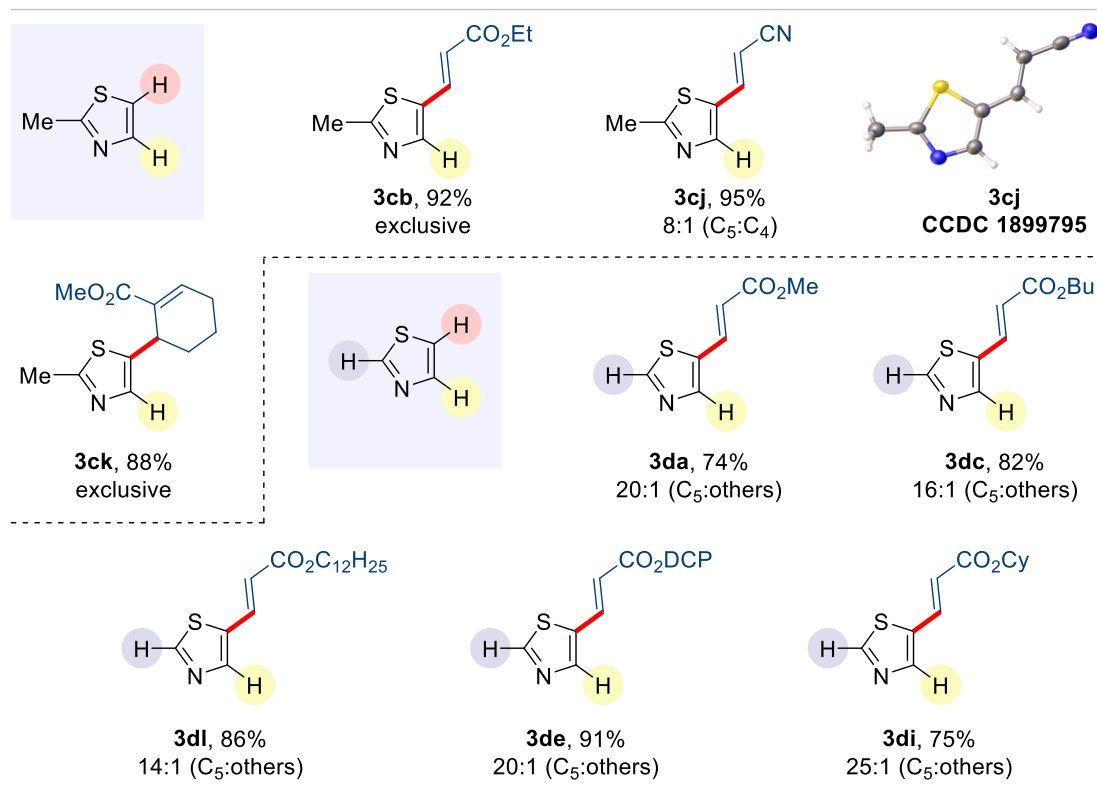
Table 4.1. Screening of the reaction parameters.^a



entry	condition	Yield (%), ^b selectivity (C5:C2)
1	Standard condition	75 (16:1)
2	In absence of Template (T6)	Complex mixture
3	In absence of Pd(OAc) ₂	0
4	Ag ₂ CO ₃ instead of AgOAc	65 (15:1)
5	AgOAc (3 equiv)	73 (16:1)
6	AgOAc (2 equiv)	52 (16:1)
7	36 h	73 (16:1)
8	Pd(OAc) ₂ (8 mol%), Ac-Gly-OH (16 mol%)	68 (16:1)
9	Pd(OAc) ₂ (12 mol%), Ac-Gly-OH (24 mol%)	75 (16:1)

^aAll the reactions were carried out with 4-methylthiazole (**1a**, 0.1 mmol), methyl acrylate (**2a**, 0.3 mmol) in 1 mL solvent under aerobic condition. ^bIsolated yield.

oxidant to Ag_2CO_3 . Variation in the reaction time and catalyst loading could not effect much in yield of the desired product (entries 7–9). The optimal reaction conditions were obtained while 10 mol% of $\text{Pd}(\text{OAc})_2$ was used along with 20 mol% acetylglycine and AgOAc (2.5 equiv) at $80\text{ }^\circ\text{C}$ in HFIP for 30 h.



Scheme 4.3b. Substrates scope for C-5 selective olefination of thiazole derivatives.

With the optimized condition, we further evaluated the scope of thiazole derivatives and olefin coupling partners for C_5 -selective olefination reactions. As shown in Scheme 3, 4-methylthiazole and 4-chlorothiazole reacted smoothly with varieties of olefins to afford 5-olefinated products in excellent yields and selectivity. In spite of having unsubstituted C-2 position, the observed excellent selectivity further emphasized the importance of suitable bifunctional template for this particular reaction system. Bulky olefins such as dicyclopentanyl acrylate (**2e**), benzyl acrylate (**2g**), methyl cyclopentene-1-carboxylate (**2h**), cyclohexyl acrylate (**2i**) and electron deficient vinyl arene (**2f**) were found to be well tolerated and provided

the desired products with excellent yields and selectivity. Methyl cyclopentene-1-carboxylate (**2h**) proceeded to provide exclusive C₅-selective allylated thiazole derivatives in excellent yield under the reaction conditions. Formation of allylated derivatives could be attributed by the sterically feasible β -H elimination rather than sterically encumbered one.

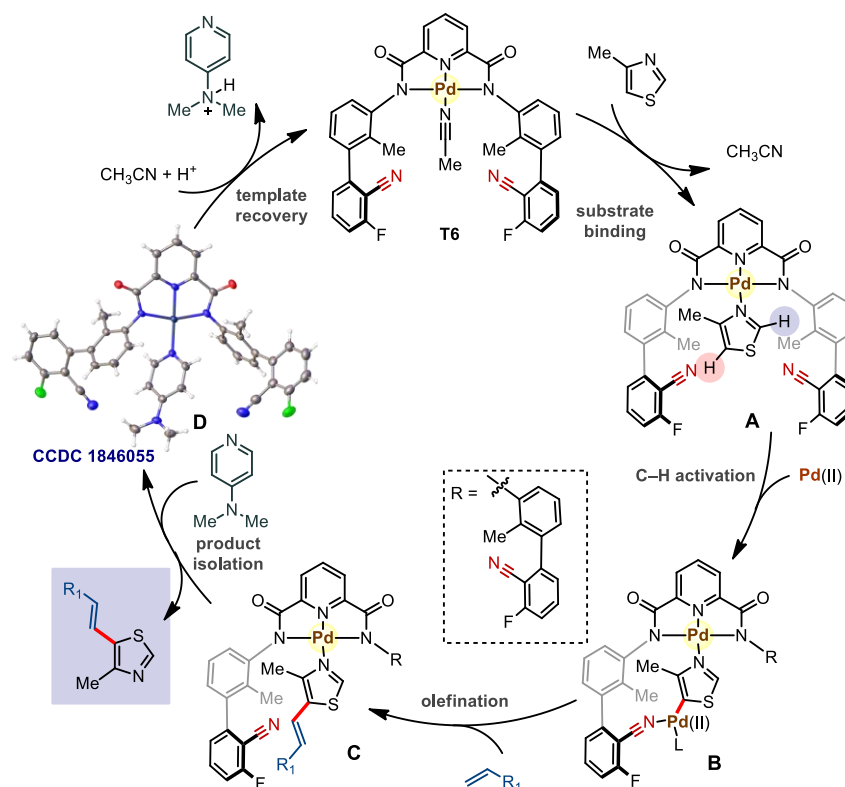


Figure 4.2. Stepwise reaction pathway for recyclable template.

Based on our investigations, a plausible reaction pathway is depicted in Figure 4.2. To elucidate the role of template, we performed stepwise reaction for C-5 selective olefination of 4-methylthiazole (**1a**). Spectral characterization of **A** clearly establishes the complexation of substrate and template system. As a proof-of-concept, we were successfully able to characterize the quinaldine appended **T6** by X-ray crystallography (Figure 4.3). In the presence of catalytic palladium(II) acetate and MPAA ligand, the exposed C₅-H bond of **1a** was activated selectively and subsequently reacted with olefin. The functionalized product was isolated from template backbone by treating the reaction mixture with strong coordinating 4-dimethylamino

pyridine (DMAP). DMAP bound **T6**, the intermediate **D** was characterized spectroscopically (X-ray, CCDC 1846055). Acidic treatment of **D** in acetonitrile under reflux condition helps to regenerate the template in 87% yield. The straightforward synthetic protocol represents **T6** as recyclable template.

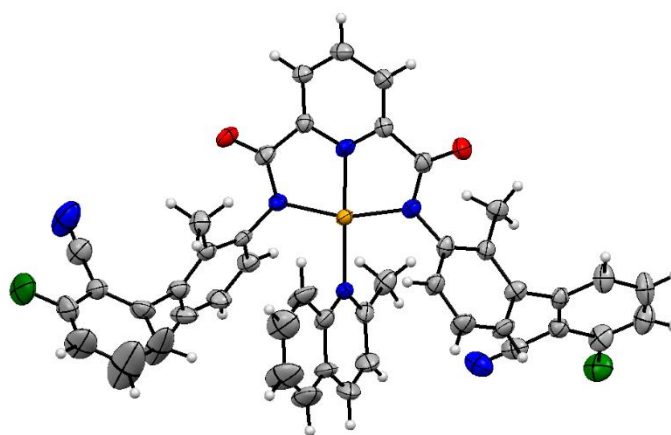


Figure 4.3. X-ray crystal structure of quinaldine appended **T6** (CCDC 1899987). Ellipsoids are drawn at 50% probability level.

4.3. Conclusion:

In conclusion, we have developed an efficient and straightforward synthetic protocol for the synthesis of C-5 selective olefination of thiazole derivatives by employing non-covalent interaction. These findings will be useful to the synthetic community for utilization of non-covalent interactions towards regioselective functionalization of small heterocycles and also eventually will be helpful to access diverse array of 5-olefinated bioactive thiazole derivatives. Further exploration of this strategy and application in the synthesis of thiazole containing fluorescent materials are underway in our laboratory.

4.4. Experimental Details:

4.4.1. Materials and Methods. All reactions were carried out in screw cap reaction tubes under aerobic condition, unless stated otherwise. All the chemicals and solvents were bought from Aldrich, TCI-India, and Alfa-aesar and were used as received. The compounds were purified through column chromatography using 100-200 mesh silica gel and Petroleum ether/Ethyl acetate solvent mixture as an eluent, unless otherwise stated. Isolated compounds were characterized by ^1H , ^{13}C NMR spectroscopy, HRMS, EI-MS and FT-IR spectroscopy. Unless otherwise stated, all Nuclear Magnetic Resonance spectra were recorded on Bruker 400 MHz or 500 MHz instrument. NMR spectra are reported in parts per million (ppm), and were measured relative to the signals for residual solvent (7.26 ppm for ^1H NMR and 77.16 ppm for ^{13}C NMR in CDCl_3 ; 1.94 ppm for ^1H NMR and 1.32 ppm for ^{13}C NMR in CD_3CN) in the deuterated solvents used, unless otherwise stated. All ^{13}C NMR spectra were obtained as ^1H decoupled. Multiplicities were indicated as follows: s (singlet), d (doublet), t (triplet), q (quartet), m (multiplet). Coupling constants were reported in hertz (Hz). All the HRMS were recorded on a micro-mass ESI TOF (time of flight) mass spectrometer and EI-MS spectra were recorded on Agilent instruments. Melting points were determined in digital melting point apparatus (Buchi) and reported as uncorrected.

4.4.2. General Procedure for synthesis of tridentate template. Standard synthetic procedure was followed for the synthesis of tridentate template from our previously reported method.²⁸ Templates **T1-6** were used from our previous stock of the templates. For identification of the scope of the methodology template **T6** was prepared in large scale following the previous report.

T6:²⁸ Yellow solid; yield 82% (2.98 g); ^1H NMR (500 MHz, CD_3CN): δ 8.24 (s, 1H), 7.77 (ddd, $J = 23.1, 16.2, 7.3$ Hz, 4H), 7.30 (ddd, $J = 23.5, 14.8, 6.0$ Hz, 7H), 7.16 (d, $J = 7.4$ Hz,

1H), 7.06 (s, 2H), 2.20 (s, 3H), 2.15 (s, 3H); $^{13}\text{C}\{^1\text{H}\}$ NMR (126 MHz, CD_3CN): δ 169.0, 164.3 (d, $J = 256.5$ Hz), 153.0, 148.6 (d, $J = 30.8$ Hz), 148.1 (d, $J = 7.8$ Hz), 143.1, 138.9, 135.9 (d, $J = 9.8$ Hz), 133.0 (d, $J = 4.7$ Hz), 128.9 (d, $J = 8.7$ Hz), 127.4 (d, $J = 29.6$ Hz), 126.8 (d, $J = 8.4$ Hz), 126.6, 126.5, 115.7 (d, $J = 19.8$ Hz), 114.4, 102.7 (d, $J = 15.2$ Hz), 15.7.

4.4.3. General Procedure for C-5 selective C–H olefination of thiazoles with tridentate template. An oven dried reaction tube was charged with magnetic stirring bar, **1** (0.1 mmol), template (0.1 mmol), and 1 mL of DCM to dissolve the substrate and template. After stirring for 20 min at room temperature, the mixture was dried under reduced pressure. $\text{Pd}(\text{OAc})_2$ (0.01 mmol), *N*-Ac-Gly-OH (0.02 mmol), AgOAc (0.25 mmol), HFIP (1.0 ml) and **2** (0.3 mmol) were then added in the reaction tube under atmospheric condition. The reaction tube was sealed and kept under stirring condition in a pre-heated oil bath at 80 °C for 30 h. After cooling to room temperature, the reaction mixture was diluted with EtOAc and filtered through celite. The filtrate was concentrated and the residue was dissolved in toluene (2-3 mL). 2-3 equiv. of DMAP was added to the solution and stirred at 80 °C (pre-heated oil bath) for 5-10 min. The reaction was then cooled to room temperature and the mixture was passed through a short pad of silica using EtOAc/hexane (1:1) as the eluent to obtain the product mixture. Finally the compound (**3**) was purified by column chromatography using EtOAc/pet ether solvent mixture as an eluent.

After removing the product mixture, the silica pad was washed with DCM/MeOH (10:1) to get the crude template solution which is used for regeneration of the template.

4.4.4. Template regeneration. The crude template solution was concentrated in vacuo and the residue was dissolved in acetonitrile. 2 equiv. of methanesulfonic acid was added the solution and kept in a pre-heated oil bath at 60 °C for 2 h. Upon completion, the reaction mixture was allowed to cool and the solvent was then removed under reduced pressure. Then the residue

was dissolved in DCM and washed with water. The organic layer was dried over anhydrous Na_2SO_4 and concentrated under reduced pressure. Finally the template was purified by column chromatography (100-200 mesh silica gel) using 5% MeOH/DCM as the eluent.

Large scale synthesis. An oven dried 100 mL schlenk flask was charged with magnetic stirring bar, **1a** (182 μL , 2 mmol), template (1.45 g, 2 mmol), and 15 mL of DCM to dissolve the substrate and template. After stirring for 30 min at room temperature, the mixture was dried under reduced pressure. $\text{Pd}(\text{OAc})_2$ (45 mg, 0.2 mmol), *N*-Ac-Gly-OH (46.8 mg, 0.4 mmol), AgOAc (835 mg, 5 mmol), HFIP (20 ml) and methyl acrylate **2a** (543 μL , 6 mmol) were then added in the reaction flask under atmospheric condition. Then the flask was sealed and kept under stirring condition in a pre-heated oil bath at 80 °C for 30 h. After cooling to room temperature, the reaction mixture was diluted with EtOAc and filtered through celite. The filtrate was concentrated and the residue was dissolved in toluene (20-25 mL). 3 equiv. of DMAP was added to the solution and stirred at 80 °C (pre-heated oil bath) for 20 min. The reaction was then cooled to room temperature and the mixture was passed through a short pad of silica using EtOAc/hexane (1:1) as the eluent to obtain the product mixture. Finally the compound (**3aa**, 249 mg, 68%) was purified by column chromatography using EtOAc/pet ether solvent mixture as an eluent.

4.4.5. Characterization Data.

(E)-Methyl 3-(4-methylthiazol-5-yl)acrylate (**3aa**).³⁷ White solid; yield 75% (13.7 mg); R_f = 0.38 (ethyl acetate/hexane = 1:4); mp = 79–80 °C; ^1H NMR (400 MHz, CDCl_3): δ 8.68 (s, 1H), 7.81 (d, J = 15.6 Hz, 1H), 6.15 (d, J = 15.6 Hz, 1H), 3.79 (s, 3H), 2.56 (s, 3H); $^{13}\text{C}\{^1\text{H}\}$ NMR (101 MHz, CDCl_3): δ 166.9, 155.9, 152.8, 134.0, 128.4, 119.5, 51.9, 15.8; IR (KBr) $\tilde{\nu}$ 2987.0 (m), 2952.5 (m), 1737.8 (s), 1625.7 (s), 1435.0 (m), 1374.1 (m), 1309.7 (m), 1243.2 (s), 1169.6 (m), 1045.9 (m), 965.4 (m), 910.8 (m) cm^{-1} ; EI-MS calcd for $\text{C}_8\text{H}_9\text{NO}_2\text{S}$ 183.0, found 183.1.

(*E*)-Ethyl 3-(4-methylthiazol-5-yl)acrylate (**3ab**).³⁷ Yellow solid; yield 92% (18.1 mg); $R_f = 0.3$ (ethyl acetate/hexane = 1:4); mp = 75–77 °C; ^1H NMR (500 MHz, CDCl_3): δ 8.69 (s, 1H), 7.81 (d, $J = 15.6$ Hz, 1H), 6.16 (d, $J = 15.6$ Hz, 1H), 4.26 (q, $J = 7.1$ Hz, 2H), 2.57 (s, 3H), 1.33 (t, $J = 7.1$ Hz, 3H); $^{13}\text{C}\{^1\text{H}\}$ NMR (126 MHz, CDCl_3): δ 166.5, 155.9, 152.8, 133.8, 128.5, 120.1, 60.9, 15.8, 14.5; IR (KBr) $\tilde{\nu}$ 3021.1 (s), 1708.0 (s), 1627.7 (m), 1522.2 (m), 1214.7 (s), 929.8 (m) cm^{-1} ; HRMS (ESI-TOF) calcd for $\text{C}_9\text{H}_{12}\text{NO}_2\text{S}$ ($\text{M} + \text{H}^+$) 198.0583, found 198.0582.

(*E*)-Butyl 3-(4-methylthiazol-5-yl)acrylate (**3ac**).³⁷ Yellowish oil; yield 94% (21.1 mg); $R_f = 0.4$ (ethyl acetate/hexane = 1:4); ^1H NMR (500 MHz, CDCl_3): δ 8.68 (s, 1H), 7.80 (d, $J = 15.6$ Hz, 1H), 6.15 (d, $J = 15.6$ Hz, 1H), 4.20 (t, $J = 6.7$ Hz, 2H), 2.56 (s, 3H), 1.72 – 1.62 (m, 2H), 1.47 – 1.37 (m, 2H), 0.95 (t, $J = 7.4$ Hz, 3H); $^{13}\text{C}\{^1\text{H}\}$ NMR (126 MHz, CDCl_3): δ 166.6, 155.8, 152.7, 133.7, 128.5, 120.0, 64.8, 30.9, 19.3, 15.7, 13.8; IR (KBr) $\tilde{\nu}$ 2925.0 (s), 2854.8 (s), 1733.1 (s), 1461.1 (m), 1378.3 (m), 1018.2 (m) cm^{-1} ; HRMS (ESI-TOF) calcd for $\text{C}_{11}\text{H}_{16}\text{NO}_2\text{S}$ ($\text{M} + \text{H}^+$) 226.0896, found 226.0896.

(*E*)-2,2,2-Trifluoroethyl 3-(4-methylthiazol-5-yl)acrylate (**3ad**). White solid; yield 87% (21.8 mg); $R_f = 0.5$ (ethyl acetate/hexane = 1:4); mp = 84–85 °C; ^1H NMR (500 MHz, CDCl_3): δ 8.75 (s, 1H), 7.91 (d, $J = 15.5$ Hz, 1H), 6.20 (d, $J = 15.5$ Hz, 1H), 4.59 (q, $J = 8.4$ Hz, 2H), 2.59 (s, 3H); ^{19}F NMR (471 MHz, CDCl_3): δ -73.70 (t, $J = 8.4$ Hz); $^{13}\text{C}\{^1\text{H}\}$ NMR (126 MHz, CDCl_3): δ 164.8, 153.6, 136.2, 126.5 (q, $J = 254.5$ Hz), 117.4, 60.4 (q, $J = 14.5$ Hz), 15.9; IR (KBr) $\tilde{\nu}$ 2927.4 (m), 2856.0 (m), 1734.1 (s), 1625.5 (s), 1290.5 (s), 1149.6 (s), 966.1 (m) cm^{-1} ; EI-MS calcd for $\text{C}_9\text{H}_8\text{F}_3\text{NO}_2\text{S}$ 251.0, found 251.1; HRMS (ESI-TOF) calcd for $\text{C}_9\text{H}_9\text{F}_3\text{NO}_2\text{S}$ ($\text{M} + \text{H}^+$) 252.0300, found 252.0281.

(*E*)-(3a,4,7R,7a)-Octahydro-1H-4,7-methanoinden-5-yl 3-(4-methylthiazol-5-yl)acrylate (**3ae**). Yellowish oil; yield 91% (29.5 mg); $R_f = 0.28$ (ethyl acetate/hexane = 1:4); ^1H NMR (400 MHz, CDCl_3): δ 8.67 (s, 1H), 7.76 (d, $J = 15.5$ Hz, 1H), 6.12 (d, $J = 15.5$ Hz, 1H), 4.67

(d, $J = 6.5$ Hz, 1H), 2.55 (s, 3H), 2.12 (s, 1H), 2.05 (d, $J = 3.9$ Hz, 1H), 1.89 – 1.78 (m, 3H), 1.77 – 1.61 (m, 3H), 1.46 (ddd, $J = 13.5, 4.0, 2.4$ Hz, 1H), 1.35 (q, $J = 10.5$ Hz, 2H), 1.26 – 1.19 (m, 1H), 0.95 (ddd, $J = 23.5, 12.0, 5.4$ Hz, 2H); $^{13}\text{C}\{^1\text{H}\}$ NMR (101 MHz, CDCl_3): δ 166.3, 155.7, 152.7, 133.4, 128.5, 120.5, 77.6, 47.4, 46.3, 43.1, 39.7, 39.3, 32.1, 31.8, 29.6, 27.8, 15.7; IR (KBr) $\tilde{\nu}$ 2951.1 (s), 2863.9 (m), 1701.9 (s), 1626.0 (s), 1517.2 (m), 1170.8 (s), 964.2 (s) cm^{-1} ; HRMS (ESI-TOF) calcd for $\text{C}_{17}\text{H}_{21}\text{NNaO}_2\text{S}$ ($\text{M} + \text{Na}^+$) 326.1185, found 326.1186.

(*E*)-4-Methyl-5-(2-(perfluorophenyl)vinyl)thiazole (**3af**). White solid; yield 86% (28.8 mg); $R_f = 0.6$ (ethyl acetate/hexane = 1:4); mp = 107–108 °C; ^1H NMR (500 MHz, CDCl_3): δ 8.66 (s, 1H), 7.53 (d, $J = 16.4$ Hz, 1H), 6.67 (d, $J = 16.4$ Hz, 1H), 2.54 (s, 3H); ^{19}F NMR (471 MHz, CDCl_3): δ -142.61 (dd, $J = 21.4, 7.6$ Hz, 2F), -155.68 (t, $J = 20.7$ Hz, 1F), -162.54 (dt, $J = 21.4, 7.7$ Hz, 2F); $^{13}\text{C}\{^1\text{H}\}$ NMR (126 MHz, CDCl_3): δ 152.9, 151.3, 146.2 – 145.6 (m), 143.9 – 143.6 (m), 141.1 (dd, $J = 11.9, 6.8$ Hz), 139.2 – 138.6 (m), 137.3 – 136.6 (m), 130.5, 127.1 – 126.6 (m), 114.7, 114.7, 112.3 – 111.8 (m), 15.6; IR (KBr) $\tilde{\nu}$ 3091.9 (s), 2925.7 (s), 1786.2 (s), 1630.9 (s), 1491.1 (s), 1378.8 (s), 992.0 (s) cm^{-1} ; HRMS (ESI-TOF) calcd for $\text{C}_{12}\text{H}_7\text{F}_5\text{NS}$ ($\text{M} + \text{H}^+$) 292.0214, found 292.0213.

(*E*)-Benzyl 3-(4-methylthiazol-5-yl)acrylate (**3ag**).³⁷ Off-white solid; yield 77% (19.9 mg); $R_f = 0.33$ (ethyl acetate/hexane = 1:4); mp = 71–72 °C; ^1H NMR (500 MHz, CDCl_3): δ 8.68 (s, 1H), 7.85 (d, $J = 15.5$ Hz, 1H), 7.41 – 7.35 (m, 5H), 6.20 (d, $J = 15.5$ Hz, 1H), 5.24 (s, 2H), 2.56 (s, 3H); $^{13}\text{C}\{^1\text{H}\}$ NMR (126 MHz, CDCl_3): δ 166.3, 156.1, 152.9, 135.9, 134.3, 128.8, 128.5, 128.46, 128.4, 119.6, 66.7, 15.8; IR (KBr) $\tilde{\nu}$ 3021.2 (s), 1706.2 (s), 1627.0 (s), 1522.0 (m), 1214.8 (s), 1166.7 (s), 929.9 (m) cm^{-1} ; EI-MS calcd for $\text{C}_{14}\text{H}_{13}\text{NO}_2\text{S}$ 259.06, found 259.1.

Methyl 5-(4-methylthiazol-5-yl)cyclopent-1-enecarboxylate (**3ah**). White solid; yield 96% (21.4 mg); $R_f = 0.18$ (ethyl acetate/hexane = 1:4); mp = 56–57 °C; ^1H NMR (500 MHz, CDCl_3):

δ 8.51 (s, 1H), 6.93 (s, 1H), 4.48 – 4.40 (m, 1H), 3.63 (dd, $J = 6.4, 1.6$ Hz, 3H), 2.78 – 2.69 (m, 1H), 2.59 – 2.49 (m, 2H), 2.47 (s, 3H), 1.95 – 1.89 (m, 1H); $^{13}\text{C}\{^1\text{H}\}$ NMR (126 MHz, CDCl_3): δ 164.7, 149.1, 148.3, 145.1, 139.3, 136.0, 51.7, 41.9, 33.8, 31.9, 15.2; IR (KBr) $\tilde{\nu}$ 3021.3 (m), 2952.8 (m), 1718.4 (s), 1633.6 (m), 1437.7 (m), 1214.9 (s), 748.2 (s) cm^{-1} ; HRMS (ESI-TOF) calcd for $\text{C}_{11}\text{H}_{14}\text{NO}_2\text{S}$ ($\text{M} + \text{H}^+$) 224.0740, found 224.0737.

(*E*)-Ethyl 3-(4-chlorothiazol-5-yl)acrylate (**3bb**). Yellow solid; yield 98% (21.3 mg); $R_f = 0.55$ (ethyl acetate/hexane = 1:4); mp = 89–90 °C; ^1H NMR (500 MHz, CDCl_3): δ 8.70 (s, 1H), 7.79 (d, $J = 15.8$ Hz, 1H), 6.25 (d, $J = 15.8$ Hz, 1H), 4.26 (q, $J = 7.1$ Hz, 2H), 1.33 (t, $J = 7.1$ Hz, 3H); $^{13}\text{C}\{^1\text{H}\}$ NMR (126 MHz, CDCl_3): δ 165.8, 152.9, 142.8, 131.9, 127.5, 122.2, 61.1, 14.4; IR (KBr) $\tilde{\nu}$ 3089.5 (m), 2984.5 (m), 1707.6 (s), 1630.2 (s), 1269.5 (s), 1176.8 (s), 913.3 (s) cm^{-1} ; EI-MS calcd for $\text{C}_8\text{H}_8\text{ClNO}_2\text{S}$ 216.99, found 217.0; HRMS (ESI-TOF) calcd for $\text{C}_8\text{H}_9\text{ClNO}_2\text{S}$ ($\text{M} + \text{H}^+$) 218.0037, found 218.0018.

(*E*)-2,2,2-Trifluoroethyl 3-(4-chlorothiazol-5-yl)acrylate (**3bd**). Yellow solid; yield 89% (24.1 mg); $R_f = 0.6$ (ethyl acetate/hexane = 1:4); mp = 92–93 °C; ^1H NMR (500 MHz, CDCl_3): δ 8.76 (s, 1H), 7.92 (d, $J = 15.8$ Hz, 1H), 6.31 (d, $J = 15.8$ Hz, 1H), 4.60 (q, $J = 8.4$ Hz, 2H); ^{19}F NMR (471 MHz, CDCl_3): δ -73.68 (t, $J = 8.4$ Hz); $^{13}\text{C}\{^1\text{H}\}$ NMR (126 MHz, CDCl_3): δ 164.2, 153.7, 143.9, 134.4, 127.1, 123.0 (q, $J = 277.2$ Hz), 119.6, 60.8 (q, $J = 74.3$ Hz); IR (KBr) $\tilde{\nu}$ 3021.1 (m), 1735.9 (s), 1629.8 (s), 1482.4 (m), 1214.9 (s), 1152.0 (s), 969.7 (m) cm^{-1} ; EI-MS calcd for $\text{C}_8\text{H}_5\text{ClF}_3\text{NO}_2\text{S}$ 270.96, found 271.0.

(*E*)-Cyclohexyl 3-(4-chlorothiazol-5-yl)acrylate (**3bi**). Yellow solid; yield 92% (24.9 mg); $R_f = 0.4$ (ethyl acetate/hexane = 1:4); mp = 50–51 °C; ^1H NMR (400 MHz, CDCl_3): δ 8.69 (s, 1H), 7.77 (d, $J = 15.8$ Hz, 1H), 6.24 (d, $J = 15.8$ Hz, 1H), 4.91 – 4.83 (m, 1H), 1.89 (dd, $J = 9.3, 3.9$ Hz, 2H), 1.75 (dd, $J = 8.8, 3.5$ Hz, 2H), 1.56 – 1.35 (m, 5H), 1.31 – 1.23 (m, 1H); $^{13}\text{C}\{^1\text{H}\}$ NMR (101 MHz, CDCl_3): δ 165.3, 152.8, 142.6, 131.6, 127.6, 122.8, 73.5, 31.7, 25.5,

23.9, IR (KBr) $\tilde{\nu}$ 3020.9 (s), 1706.0 (s), 1520.8 (m), 1273.8 (m), 1214.7 (s), 928.5 (m) (s) cm^{-1} ; EI-MS calcd for $\text{C}_{12}\text{H}_{14}\text{ClNO}_2\text{S}$ 271.0, found 271.1; HRMS (ESI-TOF) calcd for $\text{C}_{12}\text{H}_{15}\text{ClNO}_2\text{S}$ ($\text{M} + \text{H}^+$) 272.0506, found 272.0491.

(*E*)-Ethyl 3-(2-methylthiazol-5-yl)acrylate (**3cb**). Yellowish oil; yield 92% (18.1 mg); $R_f = 0.6$ (ethyl acetate/hexane = 1:4); ^1H NMR (500 MHz, CDCl_3): δ 7.72 (d, $J = 5.1$ Hz, 1H), 7.71 (d, $J = 10.4$ Hz, 1H), 6.10 (d, $J = 15.7$ Hz, 1H), 4.23 (q, $J = 7.1$ Hz, 2H), 2.71 (s, 3H), 1.31 (td, $J = 7.1, 0.5$ Hz, 3H); $^{13}\text{C}\{^1\text{H}\}$ NMR (126 MHz, CDCl_3): δ 166.4, 145.6, 134.1, 119.9, 60.8, 19.8, 14.4; IR (KBr) $\tilde{\nu}$ 3020.9 (s), 2401.6 (m), 1707.3 (s), 1631.7 (s), 1516.9 (m), 1214.8 (s), 1166.8 (s), 968.9 (m) cm^{-1} ; EI-MS calcd for $\text{C}_9\text{H}_{11}\text{NO}_2\text{S}$ 197.05, found 197.1; HRMS (ESI-TOF) calcd for $\text{C}_9\text{H}_{12}\text{NO}_2\text{S}$ ($\text{M} + \text{H}^+$) 198.0583, found 198.0572.

(*E*)-3-(2-Methylthiazol-5-yl)acrylonitrile (**3cj**). Colorless solid; yield 95% (14.2 mg); $R_f = 0.32$ (ethyl acetate/hexane = 1:4); mp = 128–129 °C; ^1H NMR (400 MHz, CDCl_3): δ 7.73 (s, 1H), 7.44 (d, $J = 16.2$ Hz, 1H), 5.54 (d, $J = 16.2$ Hz, 1H), 2.74 (s, 3H); $^{13}\text{C}\{^1\text{H}\}$ NMR (101 MHz, CDCl_3): δ 169.5, 146.1, 140.0, 133.9, 117.5, 97.2, 19.9; IR (KBr) $\tilde{\nu}$ 2995.9 (m), 2922.1 (m), 2207.9 (s), 1611.3 (s), 1511.4 (m), 1169.1 (s), 903.6 (s) cm^{-1} ; EI-MS calcd for $\text{C}_7\text{H}_6\text{N}_2\text{S}$ 150.0, found 150.0.

Methyl 6-(2-methylthiazol-5-yl)cyclohex-1-enecarboxylate (**3ck**). Yellow oil; yield 88% (20.8 mg); $R_f = 0.2$ (ethyl acetate/hexane = 1:4); ^1H NMR (500 MHz, CDCl_3): δ 7.20 (s, 1H), 7.17 – 7.15 (m, 1H), 4.16 (s, 1H), 3.67 (s, 3H), 2.63 (s, 3H), 2.37 – 2.29 (m, 1H), 2.26 – 2.17 (m, 1H), 1.86 (dd, $J = 7.9, 3.9$ Hz, 2H), 1.66 – 1.57 (m, 2H); $^{13}\text{C}\{^1\text{H}\}$ NMR (126 MHz, CDCl_3): δ 167.1, 141.8, 139.2, 131.4, 51.9, 32.2, 30.8, 25.7, 19.3, 16.9; IR (KBr) $\tilde{\nu}$ 2927.5 (m), 2855.8 (m), 1717.4 (s), 1646.5 (m), 1436.2 (m), 1242.2 (s), 1059.7 (m) cm^{-1} ; HRMS (ESI-TOF) calcd for $\text{C}_{12}\text{H}_{16}\text{NO}_2\text{S}$ ($\text{M} + \text{H}^+$) 238.0896, found 238.0895.

(*E*)-Methyl 3-(thiazol-5-yl)acrylate (**3da**). White solid; yield 74% (12.5 mg); $R_f = 0.3$ (ethyl acetate/hexane = 1:4); mp = 65–67 °C; ^1H NMR (500 MHz, CDCl_3): δ 8.80 (s, 1H), 8.01 (s, 1H), 7.83 (d, $J = 15.7$ Hz, 1H), 6.27 (d, $J = 15.7$ Hz, 1H), 3.81 (s, 3H); $^{13}\text{C}\{^1\text{H}\}$ NMR (126 MHz, CDCl_3): δ 166.6, 154.7, 146.3, 133.9, 120.7, 52.1; IR (KBr) $\tilde{\nu}$ 3066.1 (m), 2925.7 (s), 2854.6 (m), 1714.8 (s), 1636.2 (s), 1388.4 (s), 1274.4 (s), 1174.6 (s), 992.7 (m) cm^{-1} ; EI-MS calcd for $\text{C}_7\text{H}_7\text{NO}_2\text{S}$ 169.0, found 169.0; HRMS (ESI-TOF) calcd for $\text{C}_7\text{H}_8\text{NO}_2\text{S}$ ($\text{M} + \text{H}^+$) 170.0270, found 170.0257.

(*E*)-Butyl 3-(thiazol-5-yl)acrylate (**3dc**).³⁷ Pale yellow oil; yield 82% (17.3 mg); $R_f = 0.4$ (ethyl acetate/hexane = 1:4); ^1H NMR (400 MHz, CDCl_3): δ 8.83 (s, 1H), 8.03 (s, 1H), 7.82 (d, $J = 15.7$ Hz, 1H), 6.27 (d, $J = 15.7$ Hz, 1H), 4.21 (t, $J = 6.7$ Hz, 2H), 1.71 – 1.65 (m, 2H), 1.43 (dd, $J = 15.0, 7.4$ Hz, 2H), 0.96 (t, $J = 7.4$ Hz, 3H); $^{13}\text{C}\{^1\text{H}\}$ NMR (126 MHz, CDCl_3): δ 166.3, 154.8, 146.3, 133.6, 121.3, 64.9, 30.9, 19.3, 13.9; IR (KBr) $\tilde{\nu}$ 2960.6 (m), 2930.4 (m), 2254.9 (m), 1712.5 (s), 1633.8 (m), 1171.7 (s), 906.5 (s) cm^{-1} ; EI-MS calcd for $\text{C}_{10}\text{H}_{13}\text{NO}_2\text{S}$ 211.06, found 211.1; HRMS (ESI-TOF) calcd for $\text{C}_{10}\text{H}_{14}\text{NO}_2\text{S}$ ($\text{M} + \text{H}^+$) 212.0739, found 212.0747.

(*E*)-Dodecyl 3-(thiazol-5-yl)acrylate (**3dl**). Yellow solid; yield 86% (27.8 mg); $R_f = 0.55$ (ethyl acetate/hexane = 1:4); mp = 58–59 °C; ^1H NMR (500 MHz, CDCl_3): δ 8.80 (s, 1H), 8.01 (s, 1H), 7.81 (d, $J = 15.7$ Hz, 1H), 6.26 (d, $J = 15.7$ Hz, 1H), 4.19 (t, $J = 6.7$ Hz, 2H), 1.71 – 1.66 (m, 2H), 1.40 – 1.26 (m, 17H), 0.88 (t, $J = 6.9$ Hz, 3H); $^{13}\text{C}\{^1\text{H}\}$ NMR (126 MHz, CDCl_3): δ 166.3, 154.6, 146.2, 133.5, 121.3, 65.2, 32.1, 29.79, 29.77, 29.7, 29.6, 29.5, 29.4, 28.8, 26.1, 22.8, 14.3; IR (KBr) $\tilde{\nu}$ 2926.2 (s), 2855.6 (s), 2254.3 (m), 1711.6 (s), 1634.2 (s), 1467.0 (m), 1267.7 (s), 905.4 (s) cm^{-1} ; HRMS (ESI-TOF) calcd for $\text{C}_{18}\text{H}_{30}\text{NO}_2\text{S}$ ($\text{M} + \text{H}^+$) 324.1992, found 324.1997.

(*E*)-(3a,4,7,7a)-Octahydro-1H-4,7-methanoinden-5-yl 3-(thiazol-5-yl)acrylate (**3de**). Yellowish solid; yield 91% (26.3 mg); $R_f = 0.38$ (ethyl acetate/hexane = 1:4); mp = 75–77 °C;

^1H NMR (500 MHz, CDCl_3): δ 8.78 (s, 1H), 8.00 (s, 1H), 7.77 (d, $J = 15.7$ Hz, 1H), 6.23 (d, $J = 15.7$ Hz, 1H), 4.69 (d, $J = 6.7$ Hz, 1H), 2.13 (s, 1H), 2.06 (d, $J = 4.1$ Hz, 1H), 1.90 – 1.75 (m, 4H), 1.70 (ddd, $J = 20.8, 9.2, 5.1$ Hz, 2H), 1.50 – 1.45 (m, 1H), 1.36 (dd, $J = 21.5, 10.7$ Hz, 2H), 1.21 (dd, $J = 10.4, 4.2$ Hz, 1H), 1.03 – 0.92 (m, 2H); $^{13}\text{C}\{^1\text{H}\}$ NMR (126 MHz, CDCl_3): δ 165.9, 154.6, 146.1, 135.1, 133.2, 121.8, 77.8, 47.4, 46.4, 43.1, 39.7, 39.3, 32.2, 31.8, 29.6, 27.9; IR (KBr) $\tilde{\nu}$ 3024.5 (m), 2986.3 (m), 2256.7 (m), 1732.6 (s), 1446.7 (m), 1374.4 (s), 1244.4 (s), 1045.5 (s) cm^{-1} ; EI-MS calcd for $\text{C}_{16}\text{H}_{19}\text{NO}_2\text{S}$ 289.1, found 289.1; HRMS (ESI-TOF) calcd for $\text{C}_{16}\text{H}_{20}\text{NO}_2\text{S}$ ($\text{M} + \text{H}^+$) 290.1209, found 290.1189.

(*E*)-Cyclohexyl 3-(thiazol-5-yl)acrylate (**3di**). Colorless liquid; yield 75% (17.7 mg); $R_f = 0.4$ (ethyl acetate/hexane = 1:4); ^1H NMR (500 MHz, CDCl_3): δ 8.79 (s, 1H), 8.01 (s, 1H), 7.80 (d, $J = 15.7$ Hz, 1H), 6.26 (d, $J = 15.7$ Hz, 1H), 4.88 (ddd, $J = 13.1, 9.0, 3.9$ Hz, 1H), 1.94 – 1.87 (m, 2H), 1.76 (dd, $J = 8.9, 3.9$ Hz, 2H), 1.43 (dddd, $J = 16.9, 13.9, 9.7, 3.4$ Hz, 6H); $^{13}\text{C}\{^1\text{H}\}$ NMR (126 MHz, CDCl_3): δ 154.6, 146.1, 133.3, 121.9, 73.3, 31.8, 29.8, 25.5, 23.9; IR (KBr) $\tilde{\nu}$ 2928.9 (s), 2857.8 (m), 2254.5 (m), 1707.5 (s), 1634.3 (m), 1174.7 (s), 907.0 (s) cm^{-1} ; EI-MS calcd for $\text{C}_{12}\text{H}_{15}\text{NO}_2\text{S}$ 237.08, found 237.1; HRMS (ESI-TOF) calcd for $\text{C}_{12}\text{H}_{16}\text{NO}_2\text{S}$ ($\text{M} + \text{H}^+$) 238.0896, found 238.0881.

Crystallographic data:

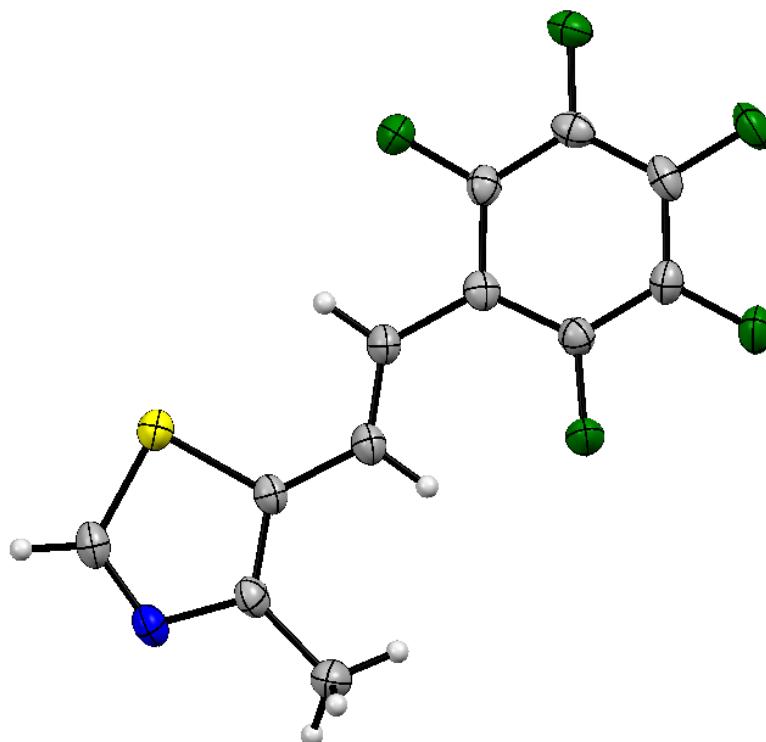


Figure 4.4. X-ray structure of **3af** (CCDC 1899792). Ellipsoids are drawn at 50% probability level.

Cell:	a = 7.4999(2)	b = 10.9169(6)	c = 14.4193(7)
	Alpha = 78.395(4)	beta = 81.878(3)	gamma = 82.656(3)
Temperature:	150 K		
	Calculated	Reported	
Volume	1138.83(9)	1138.82(9)	
Space group	P -1	P -1	
Hall group	-P 1	-P 1	
Data completeness = 0.999	Theta (max) = 24.999		
R (reflections) = 0.0544 (3418)	wR2 (reflections) = 0.1755 (3997)		

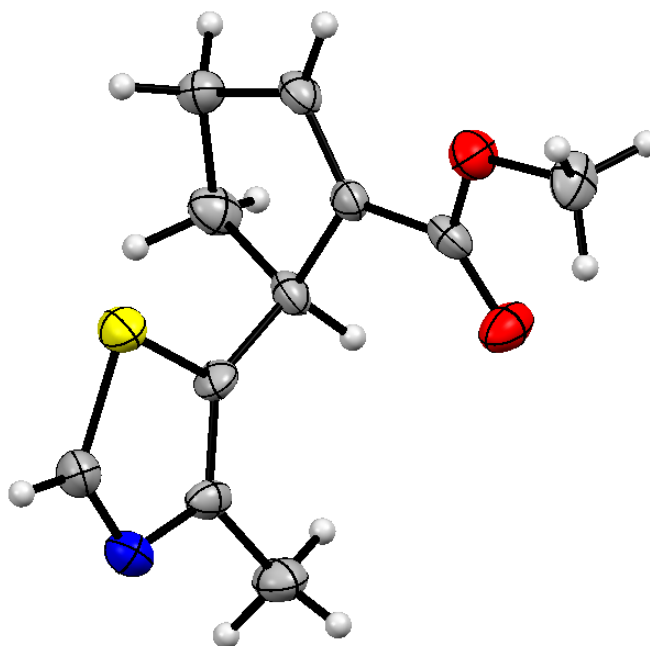


Figure 4.5. X-ray structure of **3ah** (CCDC 1899793). Ellipsoids are drawn at 50% probability level.

Cell: a = 11.2985(15) b = 6.4748(9) c = 15.103(2)
 alpha = 90 beta = 104.709(15) gamma = 90

Temperature: 150 K

	Calculated	Reported
Volume	1068.7(3)	1068.6(3)
Space group	P 21/n	P 1 21/n 1
Hall group	-P 2yn	-P 2yn
Data completeness = 0.998		Theta (max) = 24.999
R (reflections) = 0.0705 (1123)		wR2 (reflections) = 0.1860 (1881)

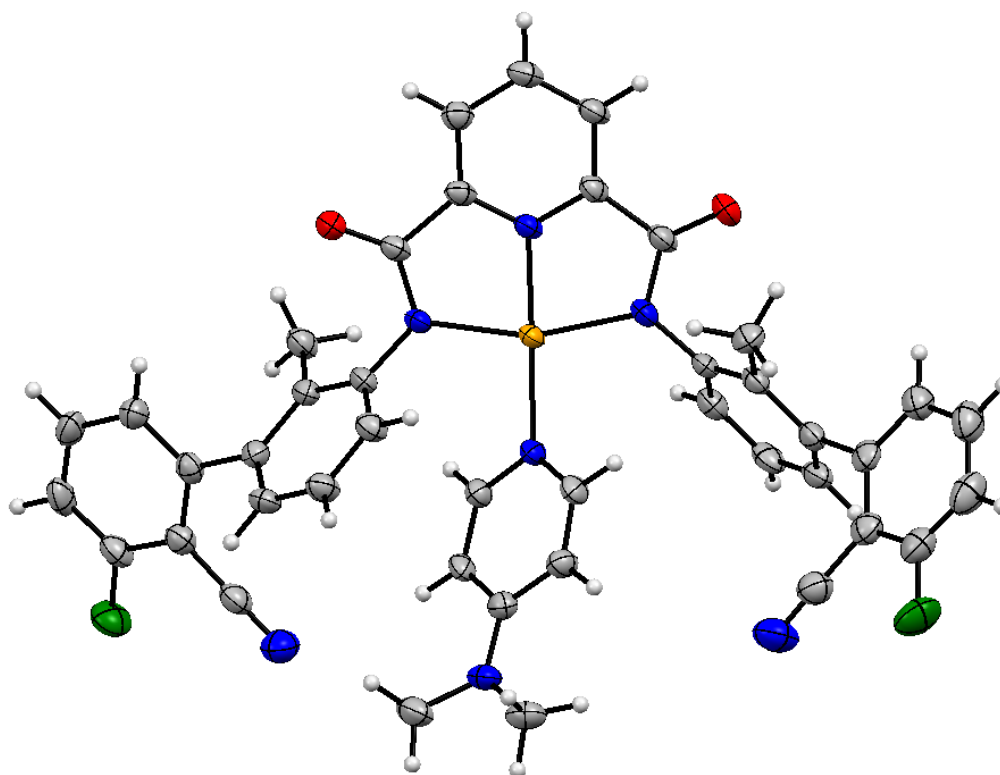


Figure 4.8. X-ray structure of **DMAP appended T6 (D)** (CCDC 1846055). Ellipsoids are drawn at 50% probability level.

Cell: a = 8.7124(4) b = 28.1168(10) c = 15.7854(5)
 alpha = 90 beta = 94.165(4) gamma = 90

Temperature: 150 K

	Calculated	Reported
Volume	3856.7(3)	3856.7(3)
Space group	P 21/c	P 1 21/c 1
Hall group	-P 2ybc	-P 2ybc

Data completeness = 0.998

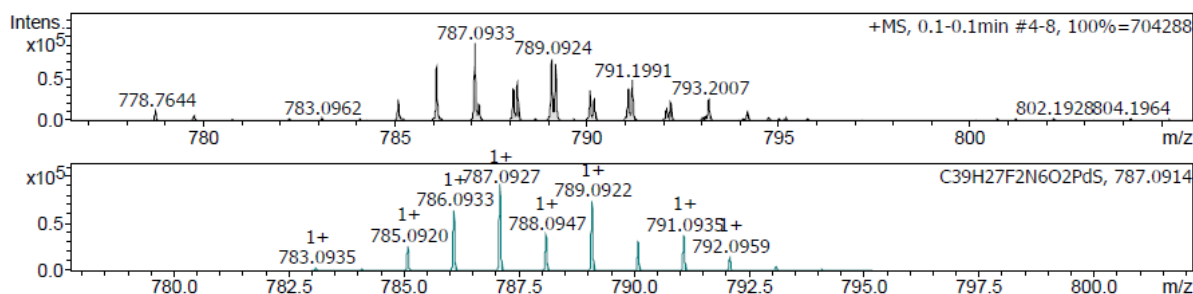
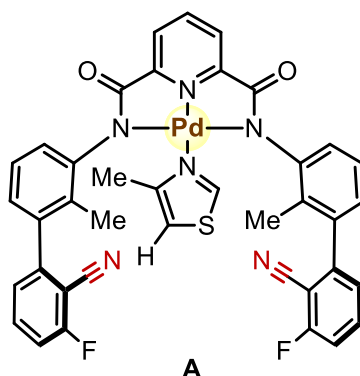
Theta (max) = 24.997

R (reflections) = 0.0471 (5394)

wR2 (reflections) = 0.1102 (6791)

ESI-MS study

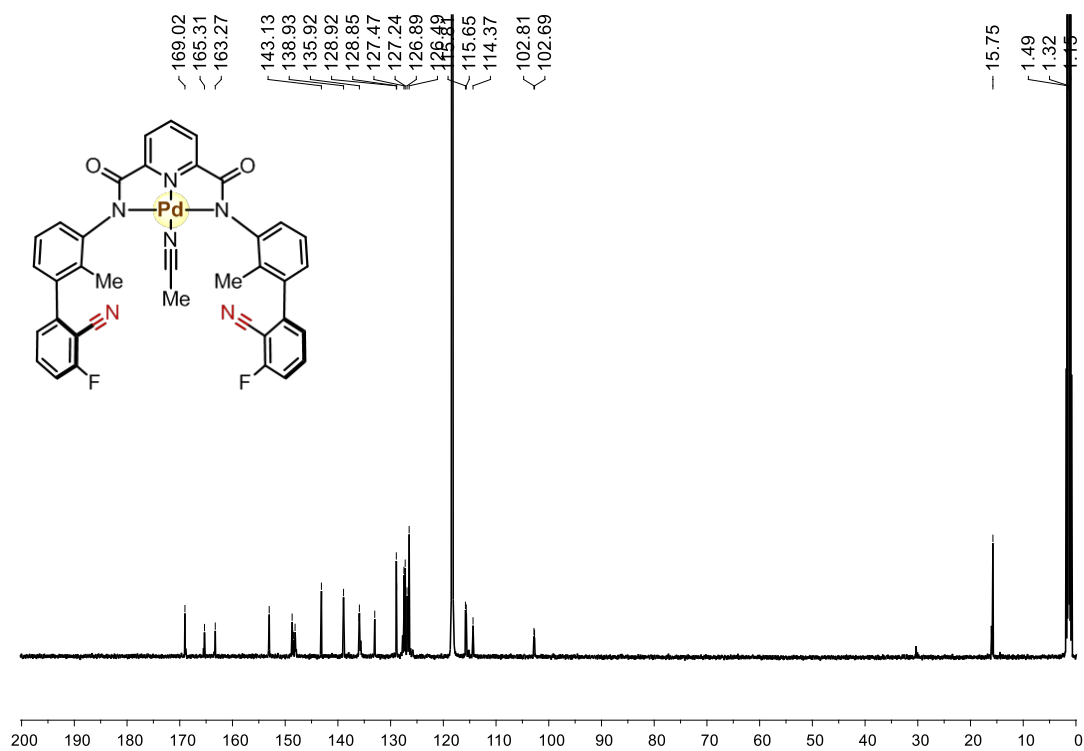
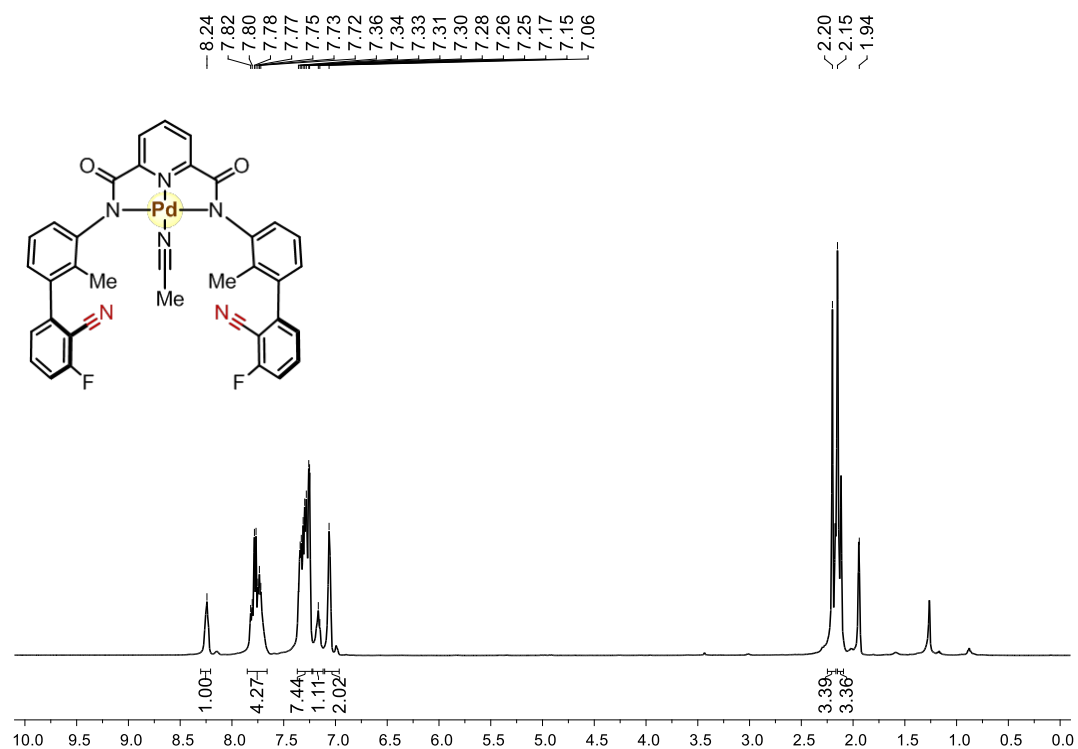
0.05 mmol of each T6 and thiazole were transferred to a clean reaction tube containing magnetic stirring bar. Then 1 mL DCM was added to it and kept stirring for 30 min at room temperature. After that DCM was removed under vacuo and dissolved in CH₃CN followed by ESI-MS was recorded.

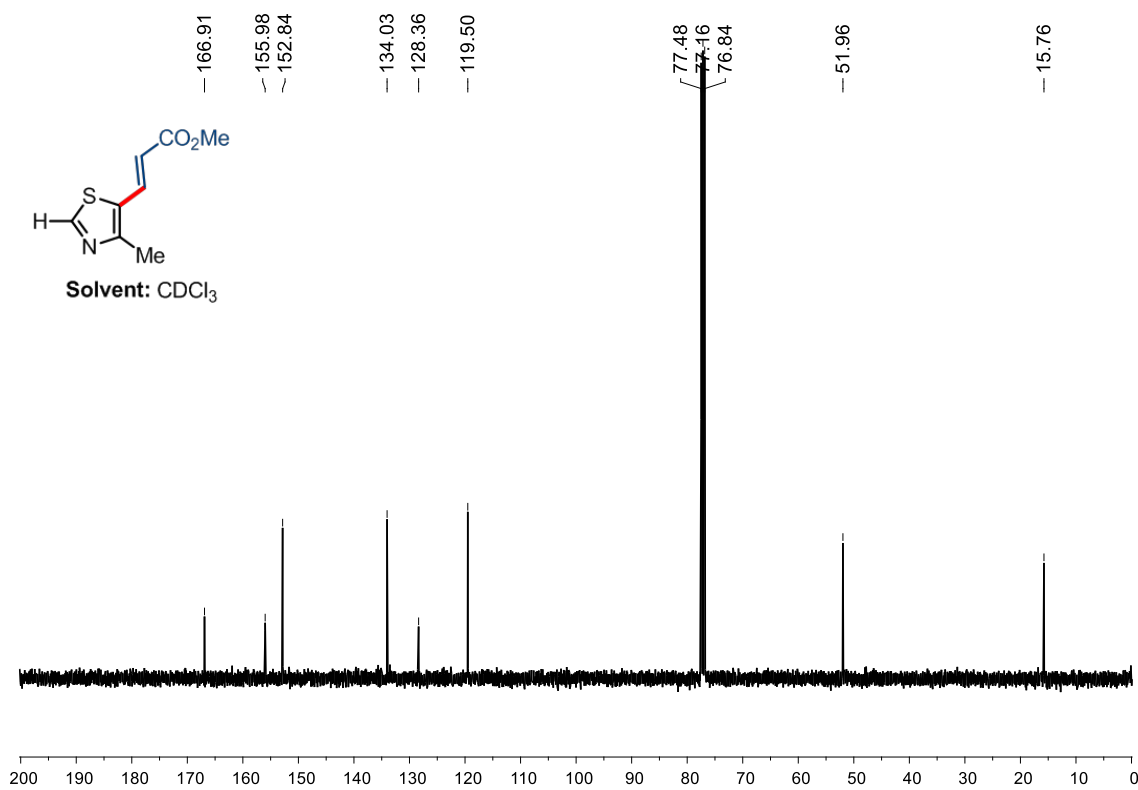
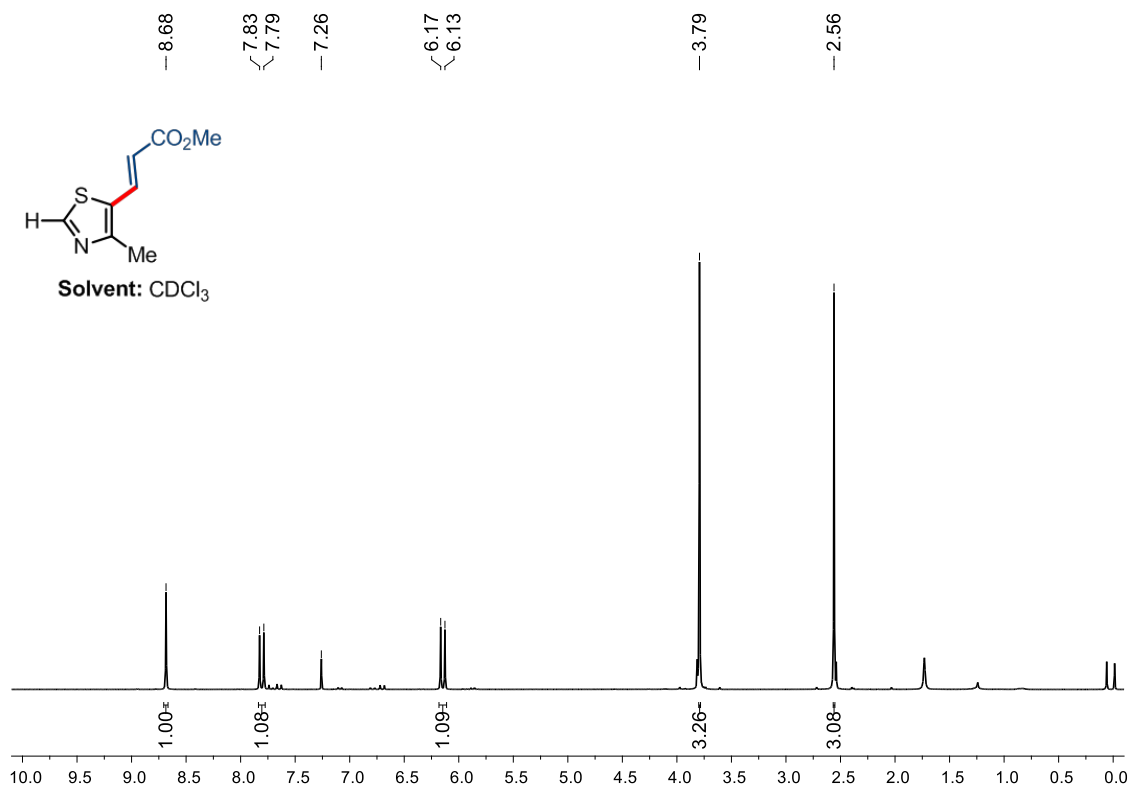


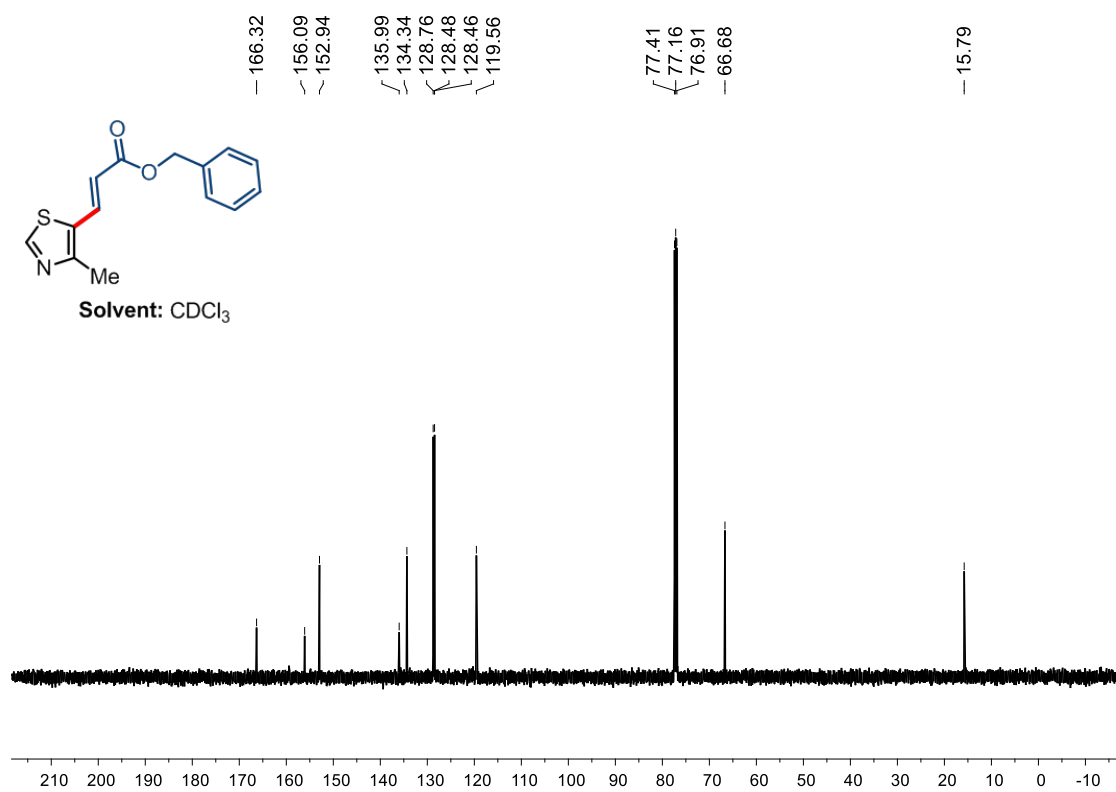
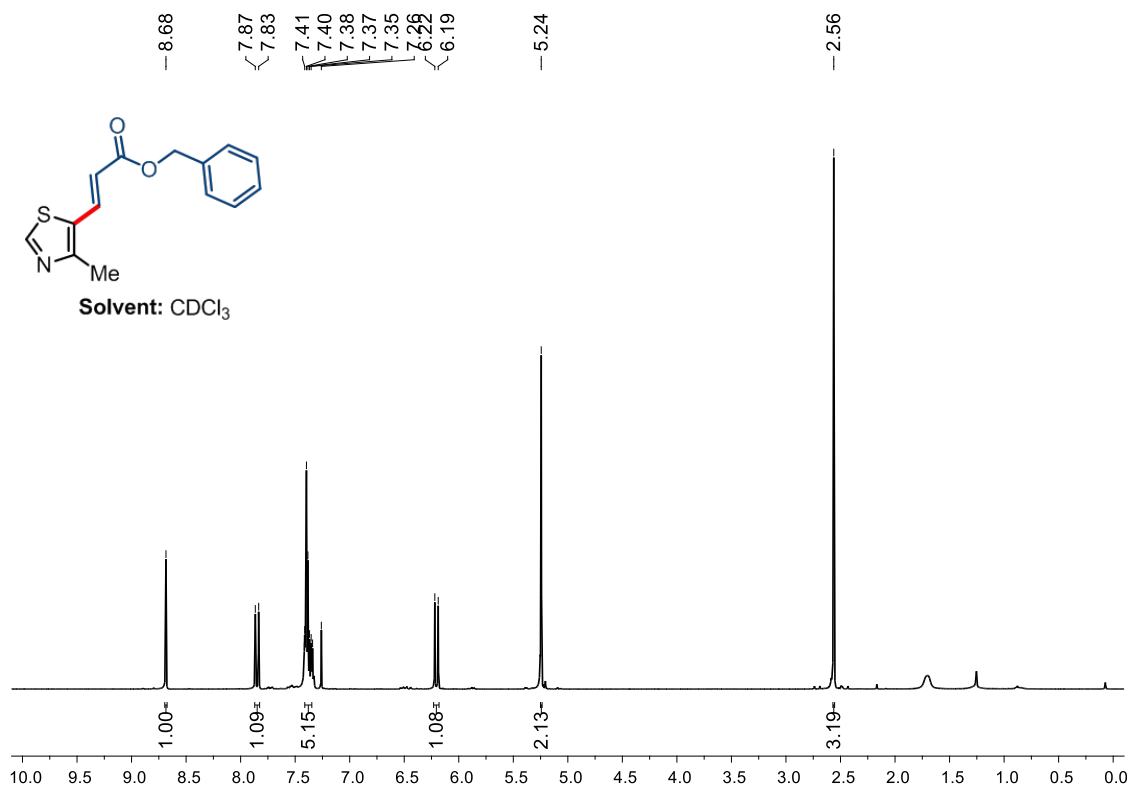
Meas. m/z	#	Ion Formula	m/z	err [ppm]	mSigma	# Sigma	Score	rdb	e ⁻ Conf	N-Rule
787.0933	1	C ₃₉ H ₂₇ F ₂ N ₆ O ₂ PdS	787.0927	-2.4	15.2	1	100.00	28.5	even	ok
	1	C ₃₇ H ₂₆ F ₂ N ₆ NaO ₂ PdS	788.0767	-24.4	363.6	1	100.00	26.5	even	ok

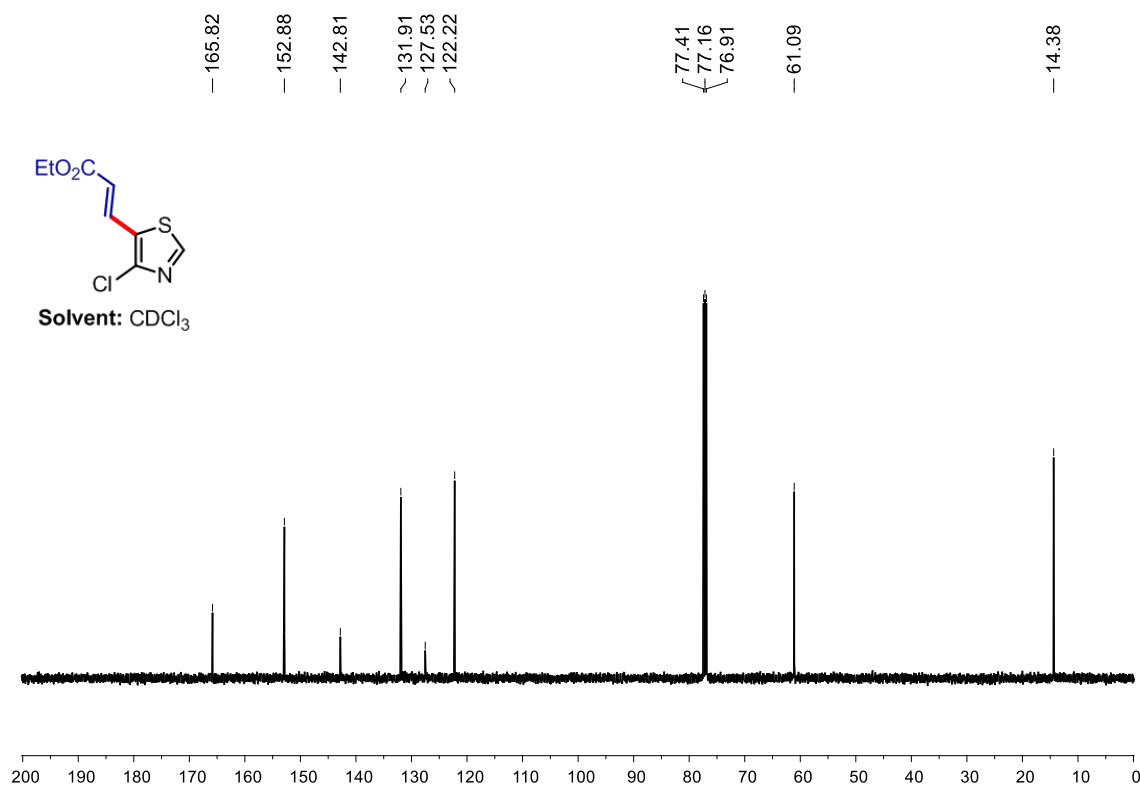
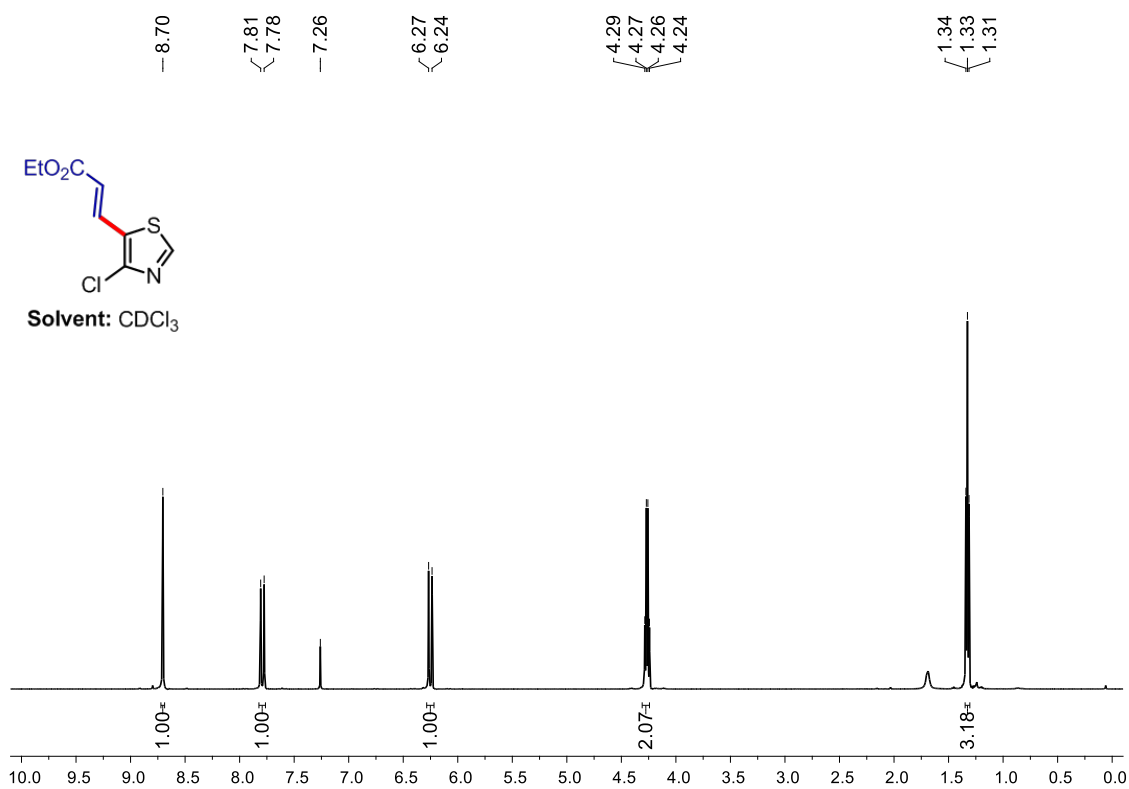
Figure 4.10. ESI-MS spectra of A (manuscript, Figure 2), **thiazole appended T6**.

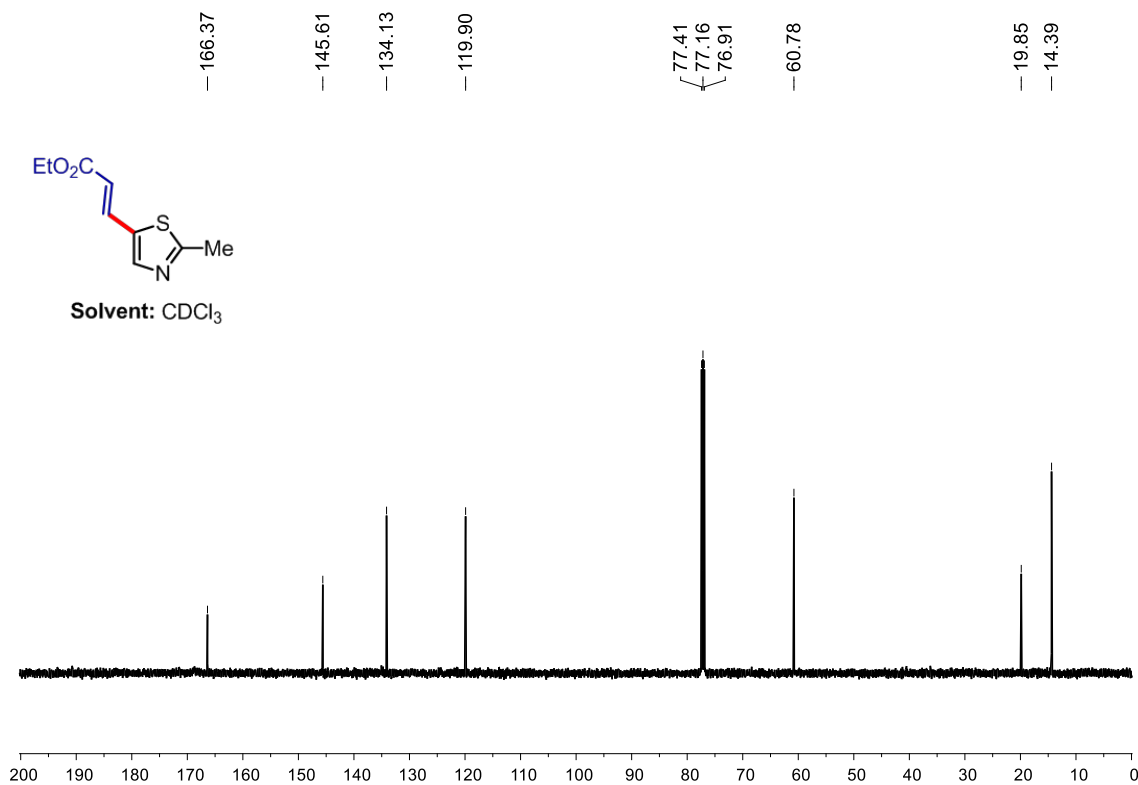
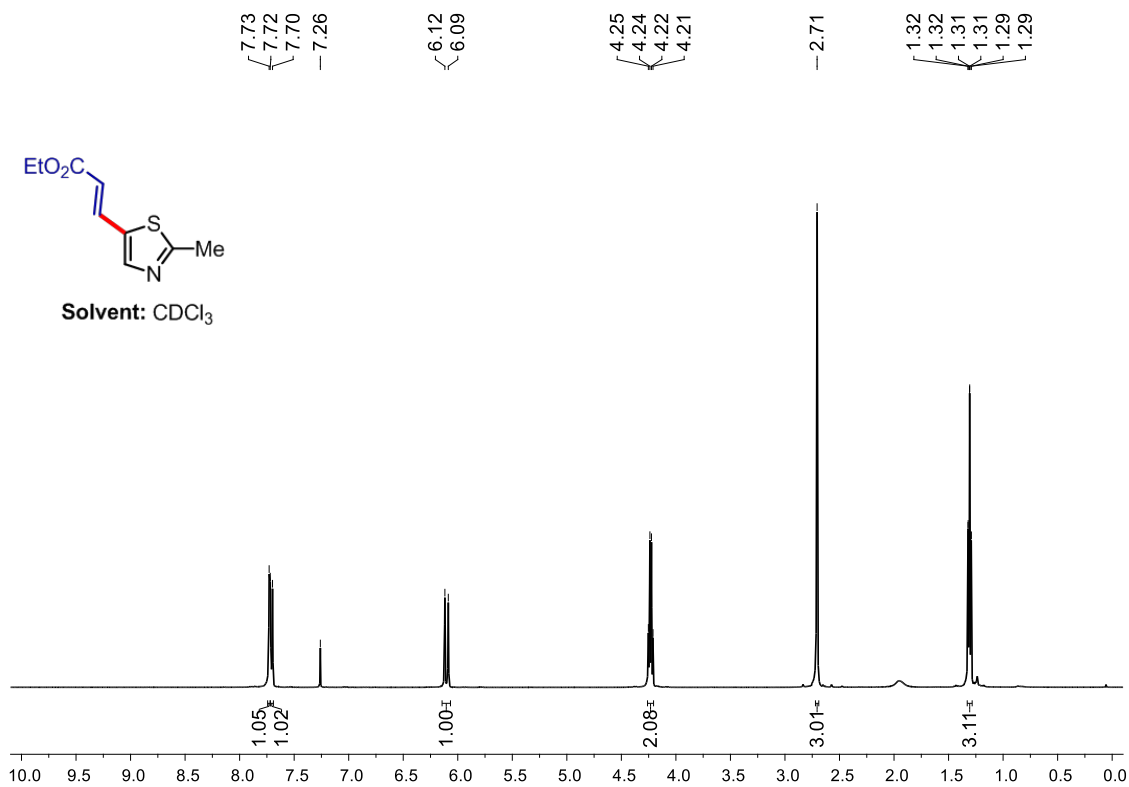
4.4.6. Representative NMR spectra:

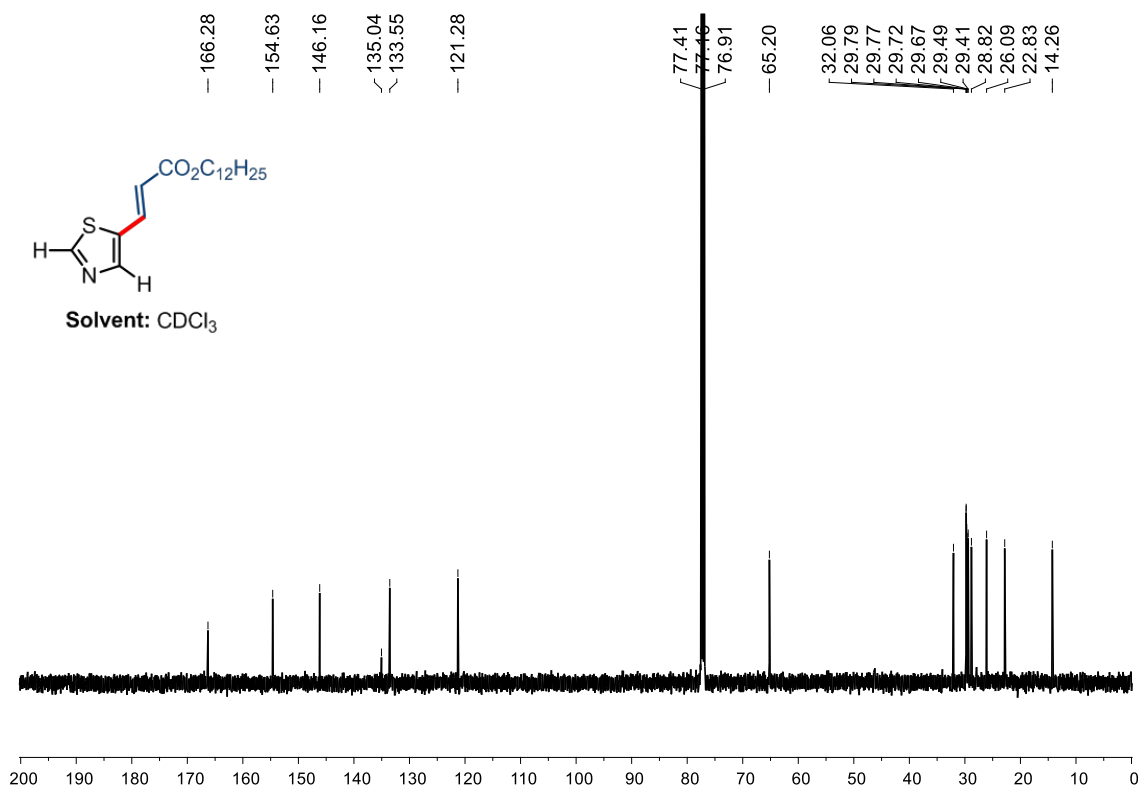
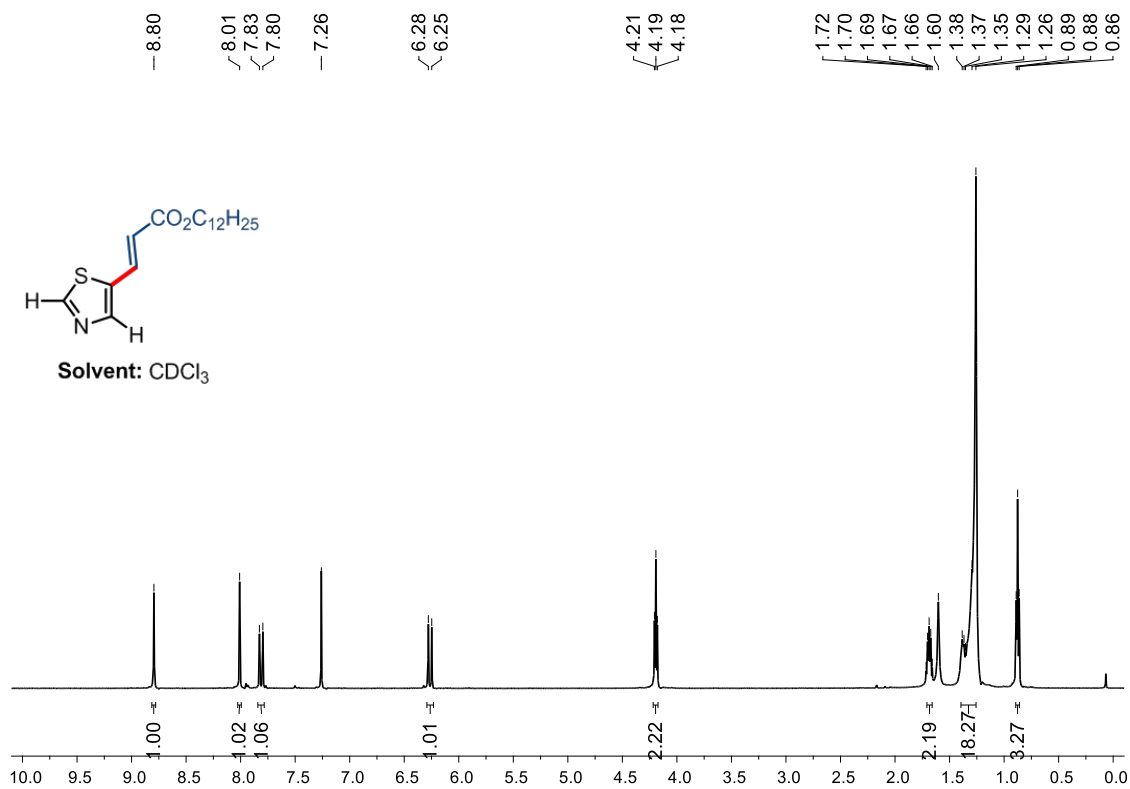












4.5. References:

1. Roughley, S. D.; Jordan, A. M. *J. Med. Chem.* **2011**, *54*, 3451.
2. Newhouse, T.; Baran, P. S. *Angew. Chem. Int. Ed.* **2011**, *50*, 3362.
3. Yamaguchi, J.; Yamaguchi, A. D.; Itami, K. *Angew. Chem. Int. Ed.* **2012**, *51*, 8960.
4. Wencel-Delord, J.; Glorius, F. *Nat. Chem.* **2013**, *5*, 369.
5. Moritani, I.; Fujiwara, Y. *Synthesis* **1973**, *1973*, 524.
6. Jia, C.; Kitamura, T.; Fujiwara, Y. *Acc. Chem. Res.* **2001**, *34*, 633.
7. Le Bras, J.; Muzart, J. *Chem. Rev.* **2011**, *111*, 1170.
8. Satoh, T.; Miura, M. *Chem. Eur. J.* **2010**, *16*, 11212.
9. Dyker, G. *Angew. Chem. Int. Ed.* **1999**, *38*, 1698.
10. Ritleng, V.; Sirlin, C.; Pfeffer, M. *Chem. Rev.* **2002**, *102*, 1731.
11. Bera, M.; Maji, A.; Sahoo, S. K.; Maiti, D. *Angew. Chem. Int. Ed.* **2015**, *54*, 8515.
12. Bag, S.; Patra, T.; Modak, A.; Deb, A.; Maity, S.; Dutta, U.; Dey, A.; Kancherla, R.; Maji, A.; Hazra, A.; Bera, M.; Maiti, D. *J. Am. Chem. Soc.* **2015**, *137*, 11888.
13. Chen, Z.; Wang, B.; Zhang, J.; Yu, W.; Liu, Z.; Zhang, Y. *Org. Chem. Front.* **2015**, *2*, 1107.
14. Dey, A.; Sinha, S. K.; Achar, T. K.; Maiti, D. *Angew. Chem. Int. Ed.*, *0*.
15. Wedi, P.; van Gemmeren, M. *Angew. Chem. Int. Ed.* **2018**, *57*, 13016.
16. Kuhl, N.; Hopkinson, M. N.; Wencel-Delord, J.; Glorius, F. *Angew. Chem. Int. Ed.* **2012**, *51*, 10236.
17. Gemoets, H. P. L.; Kalvet, I.; Nyuchev, A. V.; Erdmann, N.; Hessel, V.; Schoenebeck, F.; Noel, T. *Chem. Sci.* **2017**, *8*, 1046.
18. Wong, S.-M.; Kwong, F.-Y. In *Strategies for Palladium-Catalyzed Non-Directed and Directed C-H Bond Functionalization*; Kapdi, A. R., Maiti, D., Eds.; Elsevier: **2017**, p 49.

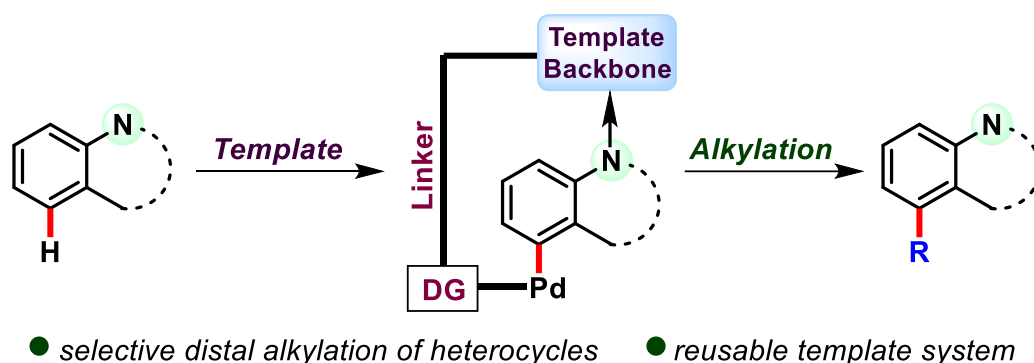
19. Naksomboon, K.; Valderas, C.; Gómez-Martínez, M.; Álvarez-Casao, Y.; Fernández-Ibáñez, M. Á. *ACS Catal.* **2017**, *7*, 6342.
20. Clarke, M. O.; Byun, D.; Chen, X.; Doerffler, E.; Leavitt, S. A.; Sheng, X. C.; Yang, C. Y.; Kim, C. U. *Bioorg. Med. Chem. Lett.* **2012**, *22*, 1095.
21. Ciufolini, M. A.; Lefranc, D. *Nat. Prod. Rep.* **2010**, *27*, 330.
22. Ando, S.; Murakami, R.; Nishida, J.-i.; Tada, H.; Inoue, Y.; Tokito, S.; Yamashita, Y. *J. Am. Chem. Soc.* **2005**, *127*, 14996.
23. Dondoni, A. *Org. Biomol. Chem.* **2010**, *8*, 3366.
24. Wu, Q.-F.; Zhao, B.; Fan, Z.-J.; Zhao, J.-B.; Guo, X.-F.; Yang, D.-Y.; Zhang, N.-L.; Yu, B.; Kalinina, T.; Glukhareva, T. *RSC Adv.* **2018**, *8*, 39593.
25. I. Ojima, G. D. V. a.; K. H. Altmann. *Anticancer Agents: Frontiers in Cancer Chemotherapy*, American Chemical Society, Washington, D. C. **2001**.
26. Nicolaou, K. C.; Roschangar, F.; Vourloumis, D. *Angew. Chem. Int. Ed.* **1998**, *37*, 2014.
27. Sierra, M. L.; Beneton, V.; Boullay, A.-B.; Boyer, T.; Brewster, A. G.; Donche, F.; Forest, M.-C.; Fouchet, M.-H.; Gellibert, F. J.; Grillot, D. A.; Lambert, M. H.; Laroze, A.; Le Grumelec, C.; Linget, J. M.; Montana, V. G.; Nguyen, V.-L.; Nicodème, E.; Patel, V.; Penfornis, A.; Pineau, O.; Pohin, D.; Potvain, F.; Poulain, G.; Ruault, C. B.; Saunders, M.; Toum, J.; Xu, H. E.; Xu, R. X.; Pianetti, P. M. *J. Med. Chem.* **2007**, *50*, 685.
28. Achar, T. K.; Ramakrishna, K.; Pal, T.; Porey, S.; Dolui, P.; Biswas, J. P.; Maiti, D. *Chem. Eur. J.* **2018**, *24*, 17906.
29. Truong, T.; Alvarado, J.; Tran, L. D.; Daugulis, O. *Org. Lett.* **2010**, *12*, 1200.
30. Li, Z.; Wang, Y.; Huang, Y.; Tang, C.; Xu, J.; Wu, X.; Yao, H. *Tetrahedron* **2011**, *67*, 5550.
31. Liu, W.; Yu, X.; Kuang, C. *Org. Lett.* **2014**, *16*, 1798.
32. Li, Z.; Ma, L.; Xu, J.; Kong, L.; Wu, X.; Yao, H. *Chem. Commun.* **2012**, *48*, 3763.

33. Li, Z.; Ma, L.; Tang, C.; Xu, J.; Wu, X.; Yao, H. *Tetrahedron Lett.* **2011**, *52*, 5643.
34. Miyasaka, M.; Hirano, K.; Satoh, T.; Miura, M. *J. Org. Chem.* **2010**, *75*, 5421.
35. Turner, G. L.; Morris, J. A.; Greaney, M. F. *Angew. Chem. Int. Ed.* **2007**, *46*, 7996.
36. Liu, X.-W.; Shi, J.-L.; Yan, J.-X.; Wei, J.-B.; Peng, K.; Dai, L.; Li, C.-G.; Wang, B.-Q.; Shi, Z.-J. *Org. Lett.* **2013**, *15*, 5774.
37. Liu, X.-W.; Shi, J.-L.; Wei, J.-B.; Yang, C.; Yan, J.-X.; Peng, K.; Dai, L.; Li, C.-G.; Wang, B.-Q.; Shi, Z.-J. *Chem. Commun.* **2015**, *51*, 4599.
38. Davis, H. J.; Phipps, R. J. *Chem. Sci.* **2017**, *8*, 864.
39. Kuninobu, Y.; Ida, H.; Nishi, M.; Kanai, M. *Nat. Chem.* **2015**, *7*, 712.
40. Davis, H. J.; Genov, G. R.; Phipps, R. J. *Angew. Chem. Int. Ed.* **2017**, *56*, 13351.
41. Maji, A.; Guin, S.; Feng, S.; Dahiya, A.; Singh, V. K.; Liu, P.; Maiti, D. *Angew. Chem. Int. Ed.* **2017**, *56*, 14903.
42. Zhang, Z.; Tanaka, K.; Yu, J.-Q. *Remote site-selective C–H activation directed by a catalytic bifunctional template. Nature* **2017**, *543*, 538.

Chapter 5

Chapter 5

Co-ordination assisted distal C–H alkylation of fused heterocycles



Abstract: Distal C-H bond functionalization of heterocycles remained extremely challenging with covalently attached directing groups (DG). Lack of proper site for DG attachment and inherent catalyst poisoning by heterocycles demand alternate routes for site selective functionalization of their distal C-H bonds. Utilizing non-productive co-ordinating property to hold the heterocycle into the cavity of a template system in a host-guest manner, we report distal C-H alkylation (*e.g.* C-5 of quinoline and thiazole, C-7 of benzothiazole and benzoxazole) of heterocycles. Upon complexation with heterocyclic substrate, nitrile DG in template directs the metal catalyst towards close vicinity of the specific distal C-H bond of heterocycles. Our hypothesized pathway has been supported by various X-ray crystallographically characterized intermediates.

5.1. Introduction:

Carbon-hydrogen bond activation has emerged as a highly valued tool for chemical transformations.¹ Reduced synthetic steps and potential of varied functional group installation can ease synthesis of complex molecules.² However, basic challenge lies in regioselectivity arising from the presence of multiple C-H bonds in organic molecules. Selective functionalization at a definite position is invariably guided by electronic factors if not controlled through external influence. In this context the directing group (DG) approach has become prevalent among chemists in order to achieve selective C-H functionalization at both aromatic as well as aliphatic systems.³⁻⁶

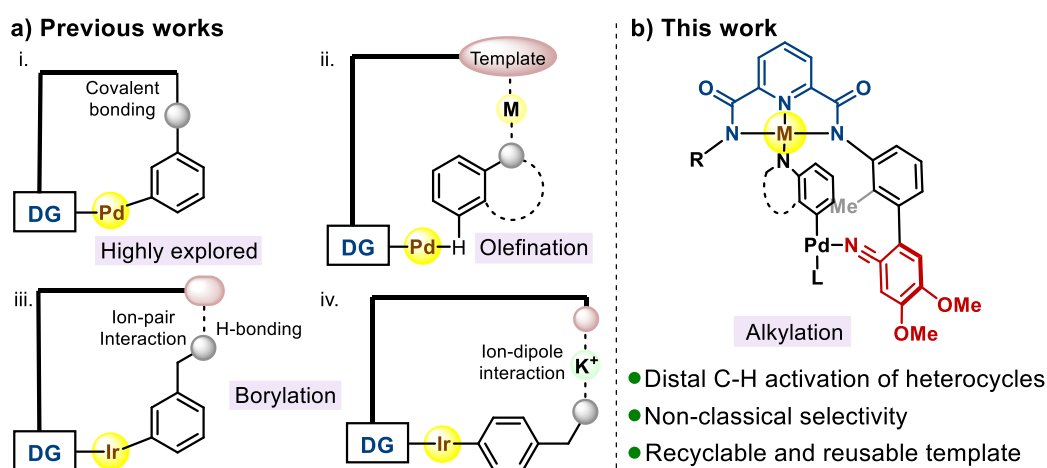


Figure 5.1. Strategies for distal $C(sp^2)$ -H activation

Over the time, evolution of directing groups led to selective activation at distal position of arene and aliphatic systems.⁷⁻¹¹ However, this approach consistently demands installation and removal of directing group pre- and post-functionalization, respectively. Moreover, heteroarene systems are not compatible with directing group support due to lack of site required for DG installation. Their intrinsic co-ordinative properties to the metal center that eventually lead to catalyst poisoning, inhibits the performance of metal catalyzed reactions. Therefore, development of newer and straightforward methodology is highly desirable.

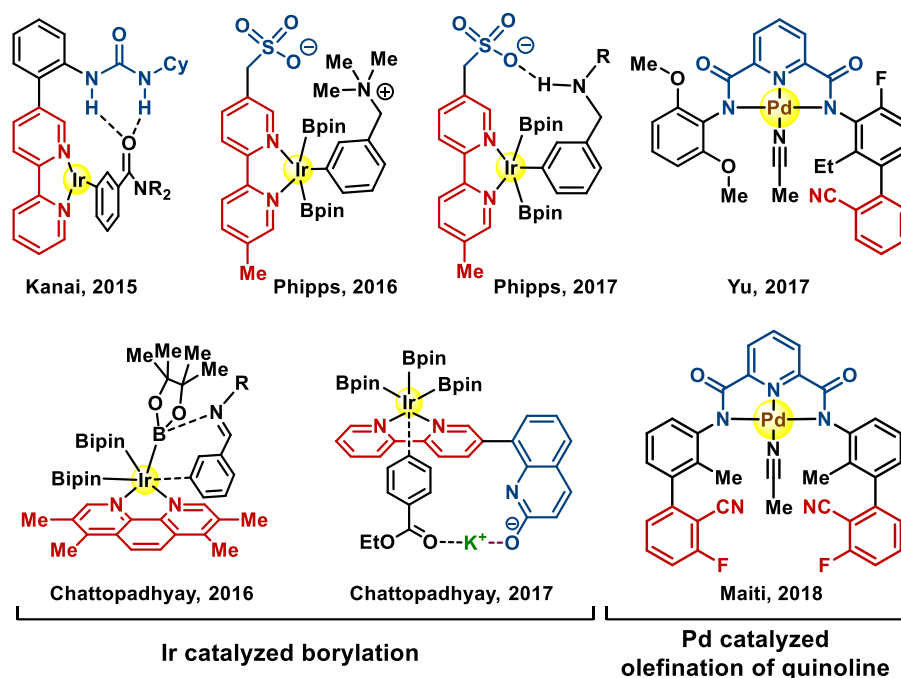


Figure 5.2. Bifunctional templates for distal $C(sp^2)$ -H activation

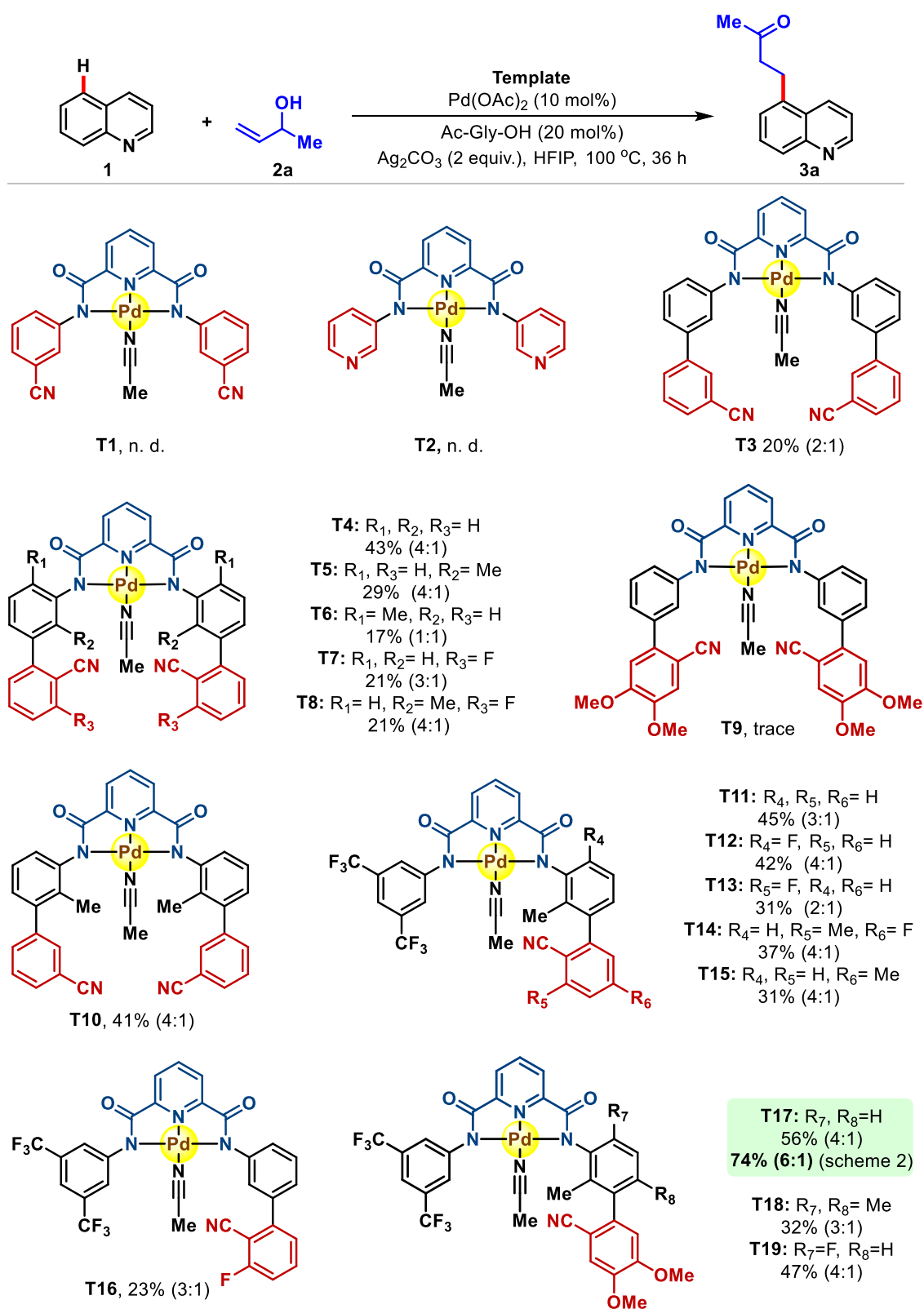
Recently, non-covalent interaction between substrate and DG has emerged as one of the most promising solution to replace DG approach.¹² Use of ion-ion, ion-dipole interaction, hydrogen bonding and bifunctional catalysis have been utilized to reach distal positions of arene rings.^{13,14} Mild condition required for borylation by iridium allows soft interaction to sustain in the reaction medium.¹³ Palladium catalyzed reaction has been efficient for olefination reaction using non-covalent interaction.¹⁴ Yu and co-workers pioneered bifunctional ligand for palladium catalyzed selective olefination at distal C-H bond of heterocycles.^{14a} In an excellent strategy, they have exploited complexation between substrate and bifunctional ligand through a metal center in order to reach distal position of heterocycles (Figure 5.2).^{14a} Palladium catalyzed olefination at C-5 position of quinoline derivatives and C-7 position of benzoxazole and benzothiazole derivatives were reported. Recently, we have reported synthetically facile template systems to achieve regioselective distal C-H olefination of quinolone, benzoxazole, benzothiazole, and thiazole.^{14b,c} However, beyond Ir-catalyzed borylation and Pd-catalyzed

olefination, non-covalent interaction promoted distal C-H functionalization of heterocycles remained extremely challenging.

5.2. Result and discussion:

A 2,6-di-substituted pyridine bis-amide ligand attached with suitable DG has been utilized to coordinate the heterocycle through metal-ligand backbone in a host-guest complexation manner (Figure 5.2). In accordance with previous reports, the directing group was expected to deliver the metal catalyst in the vicinity of concerned C-H bond.¹⁴ In the present work further optimization of the template has allowed for distal alkylation of fused nitrogen heterocycles with allylic alcohols as a new type of coupling partner. A different set of products is obtained than for the previously reported oxidative olefinations, specifically, saturated ketones with variable -R groups as well as α - and β -substituted saturated aldehydes. The approach is amenable to different types of fused nitrogen heterocycles including for a variety of substitution patterns.

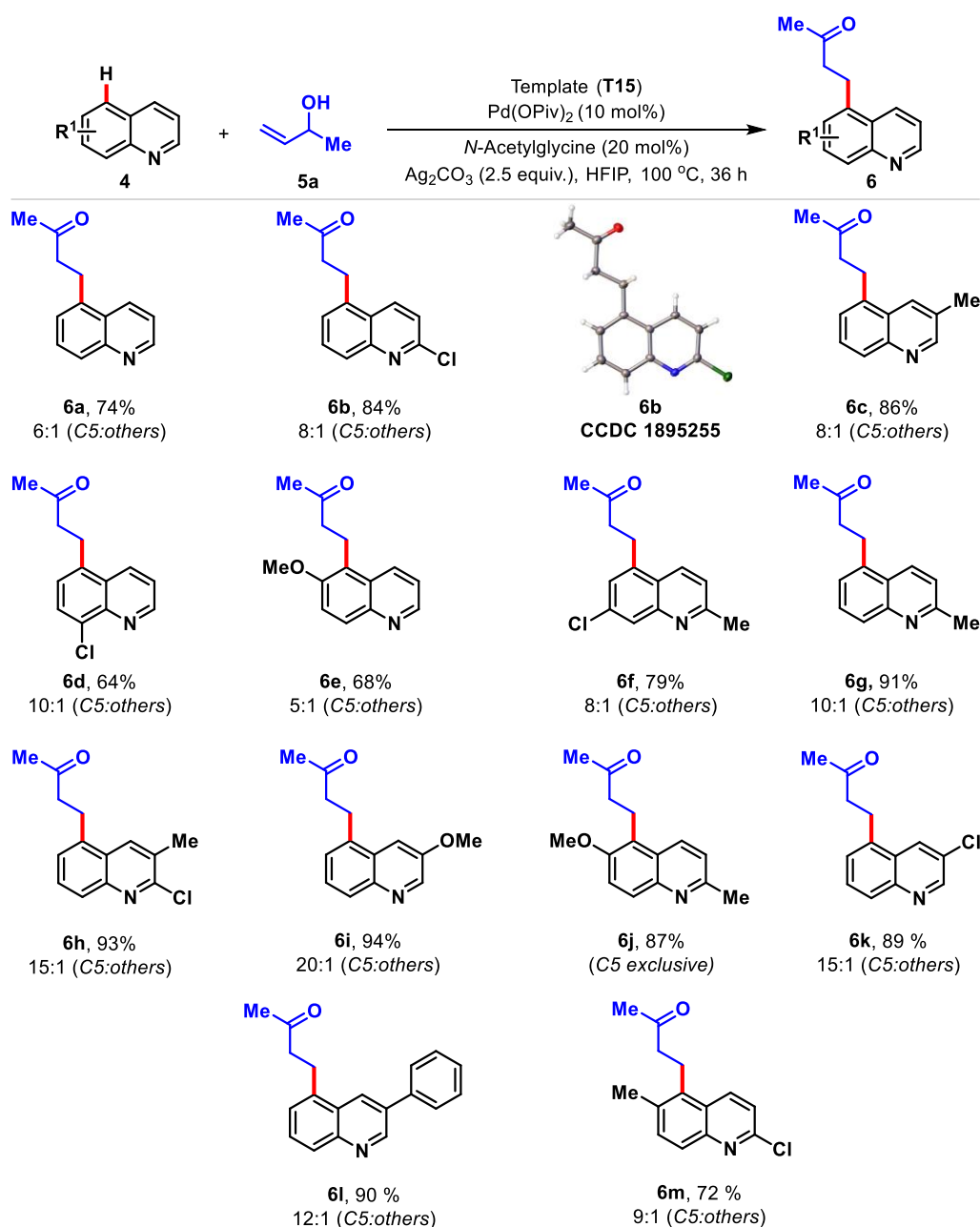
We synthesized bisamide ligands equipped with cyano and pyridine based directing groups. Complexation with palladium in acetonitrile formed the desired template. The fourth coordination site is found to be occupied by a solvent molecule as confirmed by X-ray crystallography. Being superior electron donor, a heterocycle such as quinoline replaces acetonitrile under the reaction condition to form a template-substrate adduct. Initial attempt with symmetrical 3-cyanophenyl and 3-pyridyl DG based templates **T1** and **T2** did not produce any result under standard alkylation condition.^{8e} Shifting to biphenyl cyano based template, **T4** resulted in 43% of the alkylated product at C5 position of quinoline with 4:1 (C5:others) selectivity by employing Pd(OAc)₂ as catalyst in hexafluoroisopropanol (HFIP) solvent. However, electronic manipulation by means of substituent invariably resulted in lower yield as well as loss in selectivity.



Scheme 5.1. Development of templates for distal alkylation of heterocycles

Careful observation revealed dominance of C3 and C4 isomers in the product mixture, presumably owing to the presence of two DGs, each capable of coordinating palladium. This led us to synthesize unsymmetrical templates with DG attached to only one side (**T11**). Enhanced selectivity is observed with **T11** under the reaction condition, albeit loss in product yield. A methoxy substitution found to improve the efficacy of nitrile based biphenyl DG and **T17** has been found to be the best in terms of both C5 selectivity and yield. However attempts to reduce amount of template resulted in decreased yield due to strong coordination of the heterocycle even after functionalization. Thus a relatively stronger Lewis base is required during workup to obtain the free product.

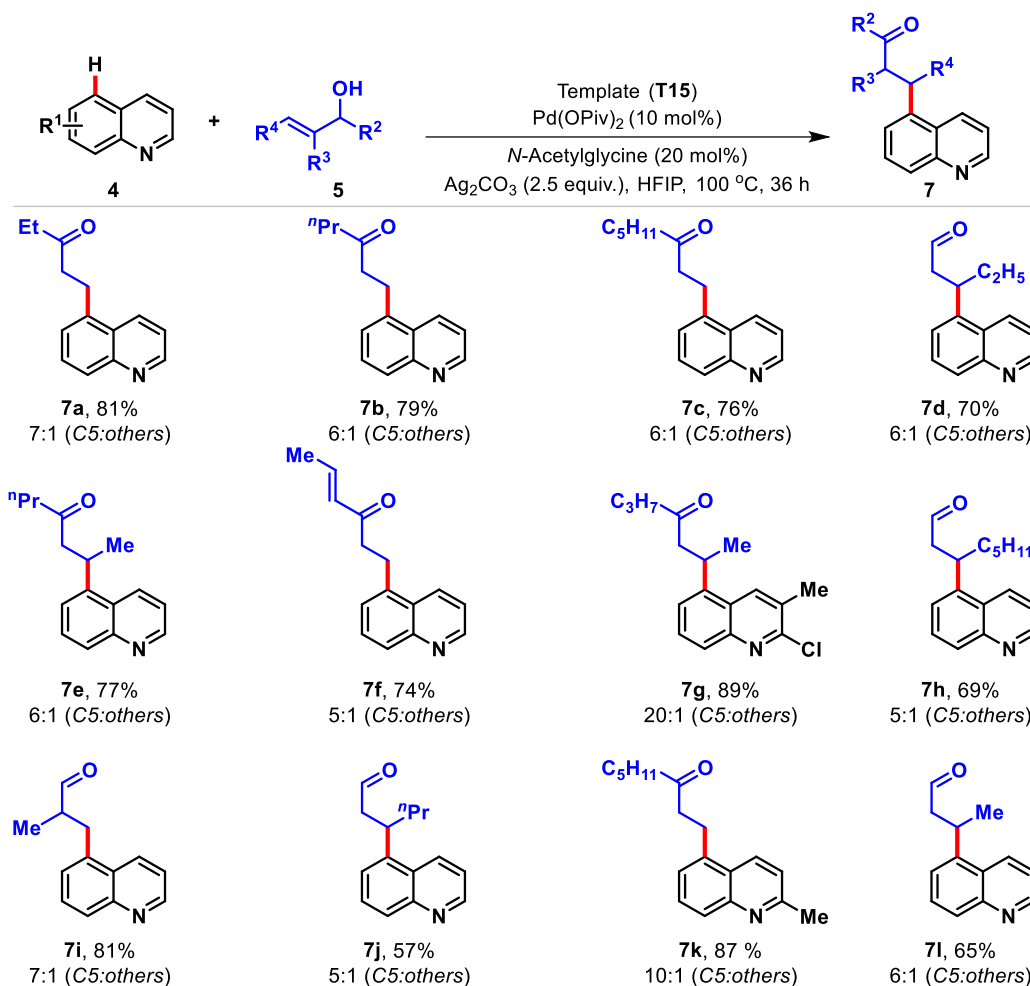
During optimization of the initial reaction condition, palladium pivalate was found to be better catalyst. Amongst the mono protected aminoacid (MPAA) ligands tested, *N*-acetylglycine remained most promising. On contrary, heterocyclic and phosphine based ligands yielded poor results, presumably due to their higher co-ordination tendency towards metal compared to substrate. Although other fluorinated solvents gave promising result, HFIP persisted as the best solvent. It was also observed that change in the oxidant (Ag_2CO_3) equivalence resulted in increased yield. However in presence of certain oxidants, for instance AgBF_4 , the template bound palladium comes out leaving behind free ligand backbone, which was recovered after completion of reaction. Therefore, careful selection of oxidant was believed to be crucial. Intrigued by this observation, a number of oxidants other than silver salts have also been examined, unfortunately none of them improved the yield and selectivity.



Scheme 5.2. Alkylation of quinoline derivatives

With optimized condition in hand, scope of the reaction has been explored. Various substituted quinolines, irrespective of the position of substitution, are found to be compatible with the present strategy (Scheme 5.2). Alkylation of electron withdrawing and donating mono/di substituted derivatives were carried out with moderate to excellent yield as well as selectivity. 3-Phenyl quinoline also provided alkylation at C5 position with good selectivity without

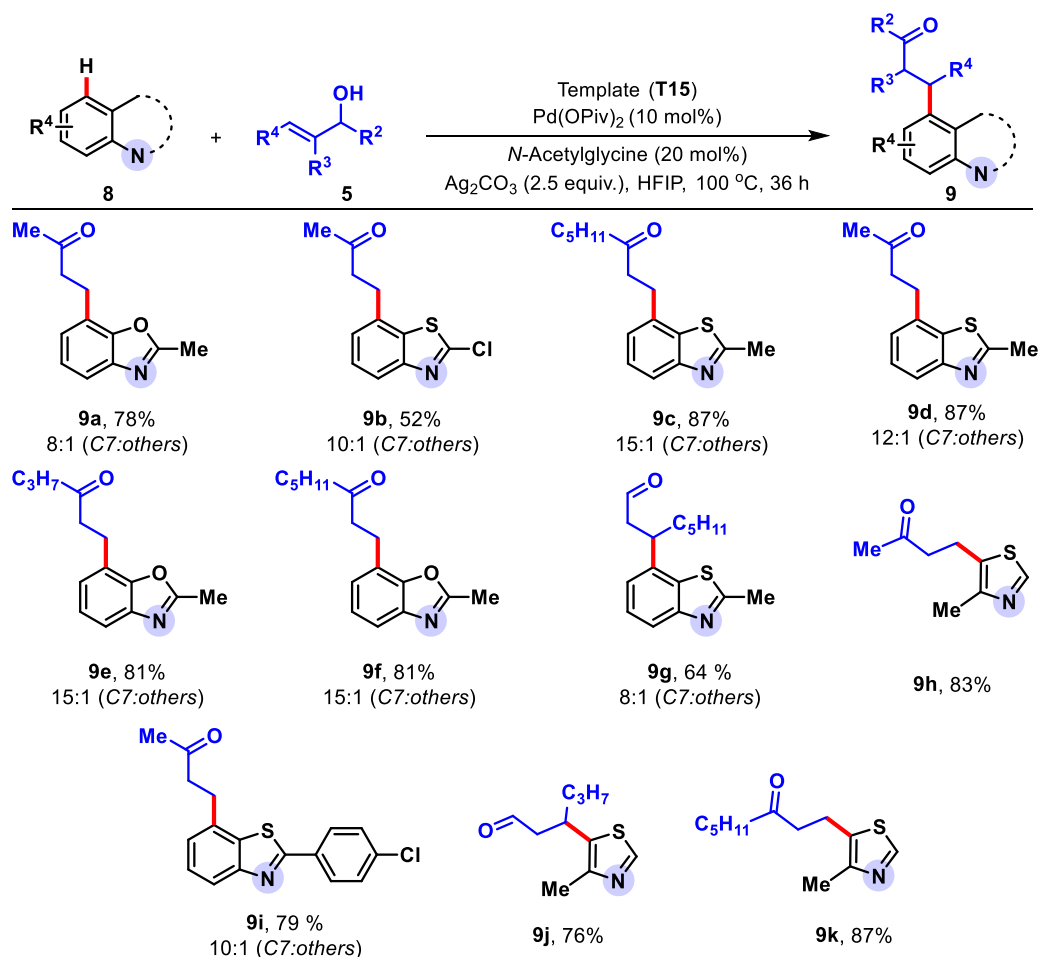
formation of any byproduct functionalized at the phenyl ring (**6l**). The C5 selectivity has been further confirmed by the X-ray crystallography structure of **6b** (CCDC 1895255).



Scheme 5.3. Scope of the reaction with various alkylating agents.

Diverse allyl alcohols have been successfully incorporated as the coupling partners (Scheme 5.3). Only a little change is observed in yield and selectivity upon chain length variation up to eight carbon atoms. Similarly, incorporation of internal allyl alcohols are found to be quite feasible (**7g** and **7h**). Other pharmaceutically relevant heterocycles such as benzoxazole and benzothiazole were found to be amenable as substrate for the protocol (**9a-9g**). Selective alkylation at C7 position of these heterocycles has been observed, which is indicative of heterocycles coordination through the nitrogen center (Scheme 5.4). Interestingly, thiazole

derivatives upon treatment under the reaction condition provided C5 alkylated product in synthetically useful yields (**9h**). Alkyl alcohol partners bearing long aliphatic chains were found to be compatible with benzoxazole, benzothiazoles and thiazoles as well (**9c** and **9f**).



Scheme 5.4. Distal C–H alkylation of different heterocycles.

In order to get insights into the reaction mechanism, several intermediates have been characterized by X-ray crystallography and other spectroscopic techniques. Based on these evidences, a plausible mechanistic pathway has been put forward (Figure 5.3). A square planar palladium complex with tridentate template is the starting scaffold for this alkylation sequence. Addition of heterocyclic substrate leads to the expulsion of weakly coordinating acetonitrile from palladium center. Expectedly, the nitrile group of directing biphenyl moiety interacts with the palladium center to carry out C–H activation at heterocyclic substrate. It is evident from the

crystal structure **E** (CCDC 1891224) that free rotation around M(template)-N(quinoline) single bond allows preferential strain-free interaction of catalyst with C5-hydrogen atom. Subsequent olefin co-ordination followed by insertion/tautomerisation reaction provides alkylated product bound template **G** (CCDC 1889891). Treatment with 4-dimethylaminopyridine (DMAP) in the reaction mixture releases the alkylated product *via* ligand substitution. DMAP co-ordinated complex **H** (CCDC 1889895) regenerates the native complex upon acid treatment in acetonitrile which is further used in the reaction. We were able to recover 90-92% of the template after each cycle. Remarkably, little change has been observed in yield and selectivity of the product, even after fifth cycle (94-91%, **6i**). Further mechanistic investigation is under progress in our laboratory.

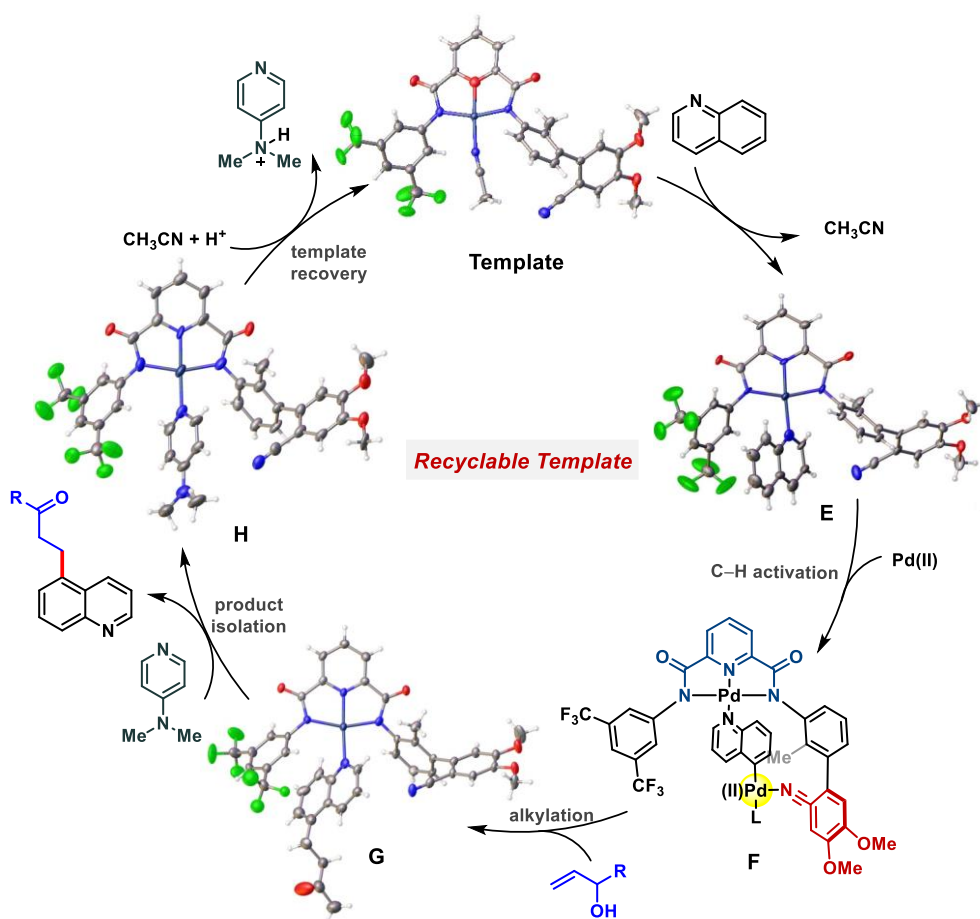


Figure 5.3. Plausible reaction mechanism for distal C–H alkylation.

5.3. Conclusion:

In conclusion, we have developed an efficient and straightforward synthetic protocol for the synthesis of C-5 selective olefination of thiazole derivatives by employing non-covalent interaction. These findings will be useful to the synthetic community for utilization of non-covalent interactions towards regioselective functionalization of small heterocycles and also eventually will be helpful to access diverse array of 5-olefinated bioactive thiazole derivatives. Further exploration of this strategy and application in the synthesis of thiazole containing fluorescent materials are underway in our laboratory.

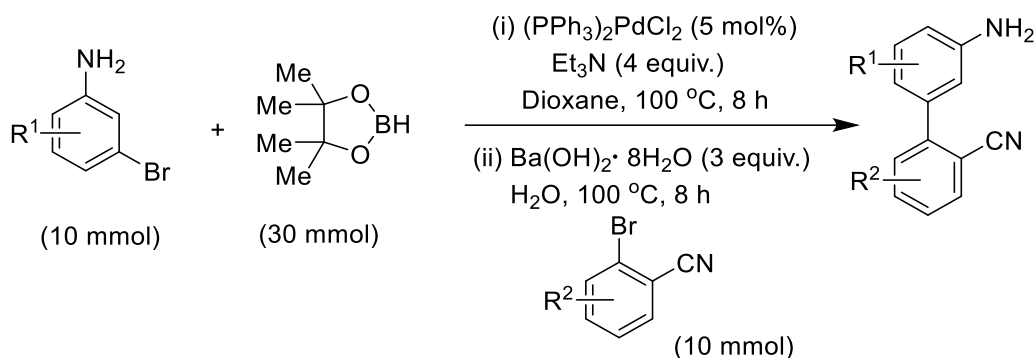
5.4. Experimental Details:

5.4.1. Materials and Methods. Unless otherwise stated, all reactions were carried out using screw cap reaction tubes under aerobic condition. Solvents were obtained from Merck and were used as received. Vinyl alcohols were purchased from TCI and Sigma-Aldrich, India and were used as received. All the other chemicals were bought from Aldrich, TCI-India, and Alfa Aesar. Templates T1 – T14 were prepared and used by the standard literature procedure, for analytical data of T1 – T11, T13 and T14 please follow our earlier report. Compounds were purified by column chromatography using 100-200 mesh silica gel and Petroleum ether/Ethyl acetate solvent mixture as an eluent, unless stated otherwise. Isolated compounds were characterized by ^1H , ^{13}C spectroscopy, IR and HRMS. Unless otherwise mentioned, NMR spectra were recorded on a Bruker 400 MHz and 500 MHz instrument. ^1H and ^{13}C NMR were recorded on 400 MHz (^1H) and 500 MHz (^{13}C) instrument, chemical shifts (δ) are given in ppm. The residual solvent signals were used as references for ^1H and ^{13}C spectra. All ^{13}C NMR spectra were obtained with ^1H decoupling. High-resolution mass spectra (HRMS) were recorded on a micro-mass ESI TOF (time of flight) mass spectrometer.

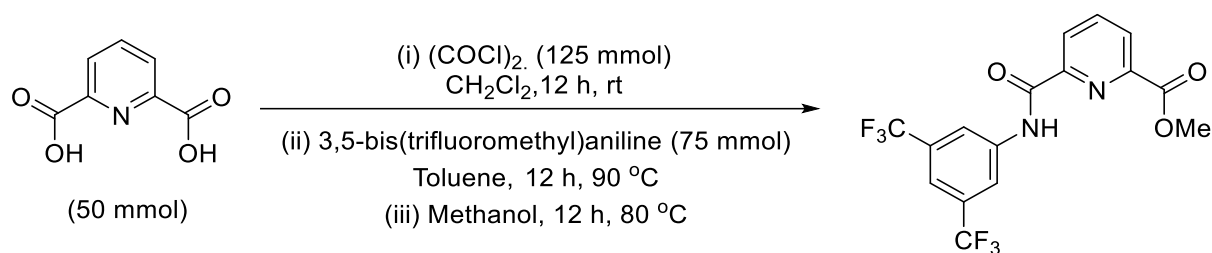
5.4.2. Procedure for synthesis of template:

Synthesis of directing group (DG):

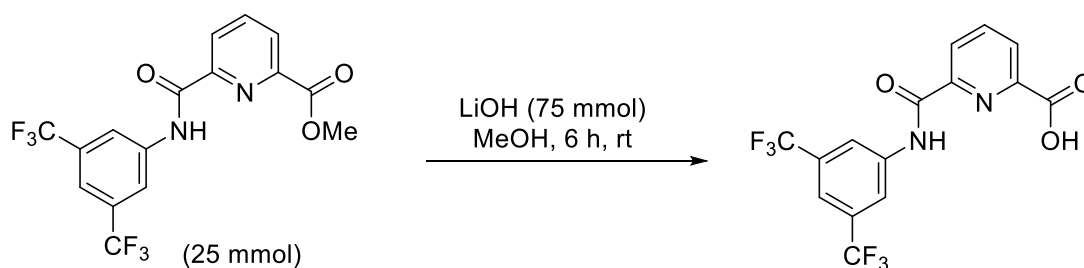
General procedure A:



An oven dried 100 mL reaction tube was charged with 5 mol% of $(\text{PPh}_3)_2\text{PdCl}_2$, corresponding bromo aniline (10 mmol), pinacolborane (3 equiv) and dioxane (35 mL). To this solution Et_3N (4 equiv) and were added. The reaction mixture was stirred at 100 °C for 8 h, then cooled to room temperature, and water (8 mL), $\text{Ba}(\text{OH})_2 \cdot 8\text{H}_2\text{O}$ (3.0 equiv.), and corresponding bromo benzonitrile (10 mmol, 1 equiv) were successively added. Then the mixture was stirred at 100 °C for 8 h. Upon completion, the reaction mixture was cooled to room temperature and quenched with water (50 mL). The mixture was filtered through Celite. The filtrate was extracted with ethyl acetate and the organic layer was dried over Na_2SO_4 . The solvent was removed and the residue was further purified by column chromatography using ethyl acetate/pet ether as an eluent to yield corresponding DG.

Procedure for methyl 6-((3,5-bis(trifluoromethyl)phenyl)carbamoyl)picolinate:

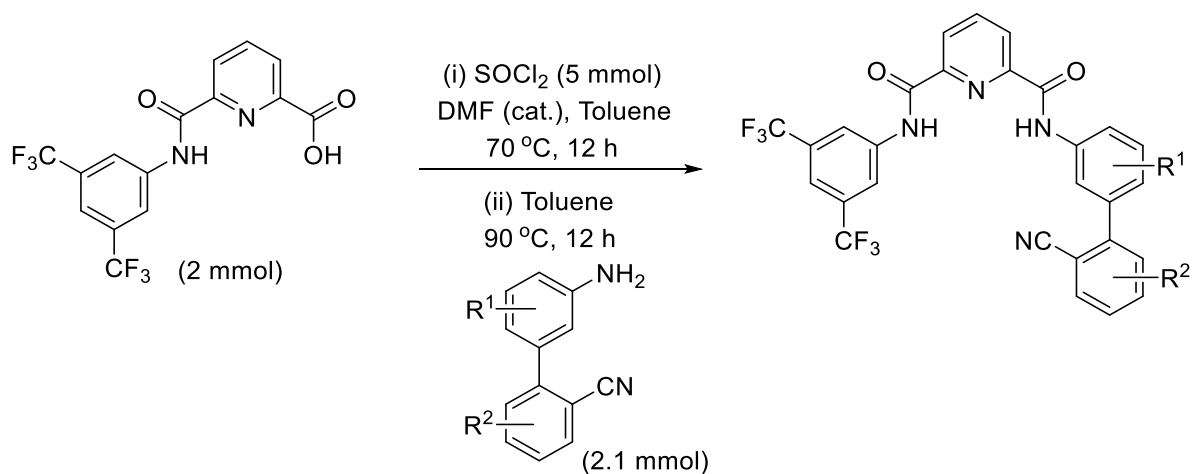
A 500 mL round bottom flask was charged with 2,6-pyridinedicarboxylic acid (8.3 g, 50 mmol), CH_2Cl_2 (150 mL), to this reaction mixture oxalyl chloride (10.7 mL, 125 mmol, 2.5 equiv.) was added at 0 °C, followed by addition of DMF (0.2 mL) the reaction mixture was allowed stir at room temperature for 12 h. Upon completion, the reaction mixture was concentrated under reduced pressure. Next, toluene (300 mL) and 3,5-bis(trifluoromethyl)aniline (11.7 mL, 75 mmol) were added and submerged into an oil bath preheated to 70 °C. Then, the oil bath was heated to 90 °C and the reaction mixture was allowed to stir 12 h. Upon completion, the reaction mixture was cooled down and added 100 mL of methanol. Then the reaction mixture was refluxed for 12 h. Upon completion, the reaction mixture was cooled to room temperature and concentrated under reduced pressure. The white precipitate was recrystallized from hot methanol to give methyl 6-((3,5-bis(trifluoromethyl)phenyl)carbamoyl)-colinate (12.3 g, 62%) as a colorless solid.

Procedure for 6-((3,5-bis(trifluoromethyl)phenyl)carbamoyl)picolinic acid:

To a solution of methyl 6-((3,5-bis(trifluoromethyl)phenyl)carbamoyl)picolinate (9.8 g, 25 mmol) in MeOH (250 mL) was added LiOH monohydrate (3.14g, 75 mmol) in three portions. After completion, the reaction mixture was concentrated under reduced pressure. The crude residue was dissolved in water and acidified by 6 M HCl, then extracted with EtOAc three times. The combined organic phase was dried with anhydrous Na₂SO₄, and concentrated to yield 6-((3,5-bis(trifluoromethyl)phenyl)carbamoyl)picolinic acid (8.4 g, 89%) as a colorless solid.

Procedure for amide formation:

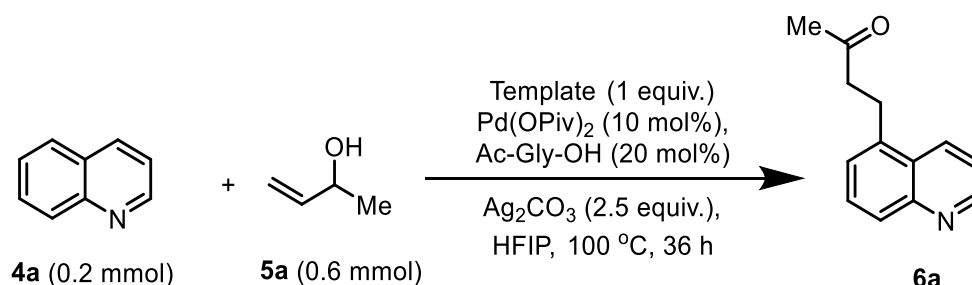
General Procedure B:



To a solution of 6-((3,5-bis(trifluoromethyl)phenyl)carbamoyl)picolinic acid (0.75 g, 2 mmol) in toluene was added thionyl chloride (0.36 mL, 5 mmol) dropwise at room temperature. Then DMF (3 drops) was added and the reaction mixture was stirred at 70 °C. Upon completion, the toluene was evaporated under reduced pressure, amine (2.1 mmol) and 10 mL toluene were added and submerged into an oil bath preheated to 70 °C. Then, the oil bath was heated to 90 °C and the reaction mixture was allowed to stir 12 h. After completion the solid was filtered and washed with toluene and methanol to yield corresponding amide.

General Procedure C: Preparation of metal complex

Corresponding amide (1 mmol) and Pd(OAc)₂ (1 mmol) were taken in 50 mL reaction flask equipped with a stir bar. 10 mL acetonitrile was added to the flask and the resulting mixture was stirred at 60 °C for 6 h. Upon completion, solvent was removed in vacuo. Next the residue was purified by column chromatography on silica gel using CH₂Cl₂/MeOH as the eluent giving the pure template.

General Procedure D: Site-selective C-H olefination of heterocycles with tridentate template

A clean, oven dried reaction tube was charged with **4a** (0.2 mmol), tridentate template (0.2 mmol), magnetic stirring bar and minimal amount of CH₂Cl₂ to dissolve the substrate and template. After 20 min stirring at room temperature, the mixture was concentrated in vacuo. Then Pd(OPiv)₂ (0.02 mmol), *N*-Ac-Gly-OH (0.04 mmol), Ag₂CO₃ (2.5 equiv.), HFIP (2.0 ml) and **5a** (0.6 mmol) were added in the reaction tube in aerobic condition. The reaction tube was sealed and allowed to stir at 100 °C for 36 h. Then the reaction mixture was cooled to room temperature and diluted with EtOAc and filtered through a short pad of celite with additional

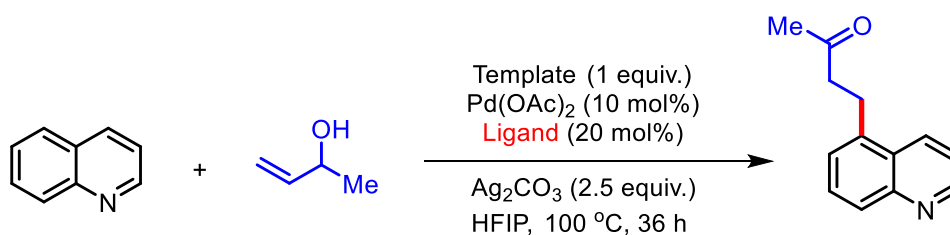
EtOAc. The filtrate was concentrated in vacuo. The residue was dissolved in toluene (3-4 mL) and 2-3 equiv. of DMAP was added to it. The solution was then stirred at 80 °C for 5-10 min. Upon completion, the reaction was cooled to room temperature and the mixture was passed through a short pad of silica using EtOAc/hexanes=1:1 as the eluent to give the product mixture. Finally the compound (**6a**) was purified by column chromatography/on preparative TLC using EtOAc/pet ether solvent mixture as an eluent. (The silica pad was then washed with CH₂Cl₂/MeOH=10:1 to get the crude template solution for the template regeneration.)

5.4.3. Template regeneration

The crude template solution was concentrated in vacuo and the residue was dissolved in acetonitrile. To this solution 2 equiv. of methanesulfonic acid was added and the mixture was placed to a pre-heated oil bath at 60 °C for 2 h. Upon completion, the reaction mixture was cooled to room temperature and the solvent was removed under reduced pressure. Then the residue was dissolved in CH₂Cl₂ and washed with water. The organic layer was dried over anhydrous Na₂SO₄ and concentrated in vacuo. Finally the template was purified by column chromatography (100-200 mesh silica gel) using 10:1 of CH₂Cl₂/Methanol as eluent to obtain 90% of regenerated template **T17** (along with template **T17** we have recovered 7% of ligand **L2**).

5.4.4. Optimization

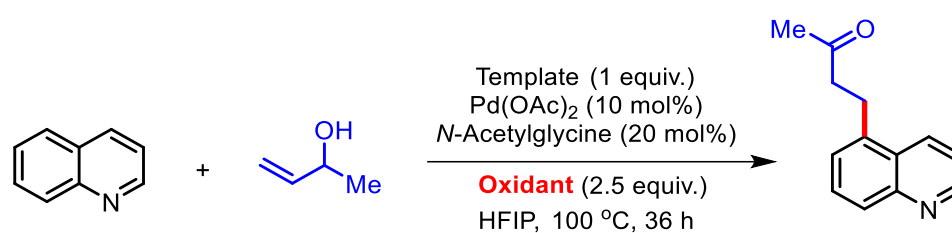
Table 5.1. Ligand optimization for C5-H alkylation of quinoline.



S. No.	Ligand	Yield(%)
1	N-Acetylglycine	56 (4:1)
2	N-Formylglycine	40 (6:1)
3	N-Fmoc-glycine	trace
4	N-Boc-glycine	trace
5	N-Cbz-glycine	-
6	N-Acetyl-DL-tryptophan	-
7	N-Acetyl-4-hydroxy-L-proline	-
8	N-Acetyl-DL-2-phenylglycine	trace
9	N-Acetyl-L-glutamic acid	trace
10	N-Acetyl-L-valine	-
11	N-Acetyl-L-cystine	-
12	N-Acetyl-L-leucine	-
13	N-Cbz-DL-valine	-
14	N-Boc-leucine	trace
15	N-Boc-D-valine	-
16	N-Boc-L-proline	-
17	N-Fmoc-L-methionine	trace
18	Cbz-L-asparagine	-
19	Cbz-L-alanine	15 (2:1)
20	Cbz-glutamine	-
21	N-Fmoc-L-threonine	-
22	N-Fmoc-L-leucine	-
23	Cbz-L-phenylalanine	trace
24	N-Boc-L-phenylglycine	-
25	α -(Boc-amino)isobutyric acid	-
26	N-Boc- β -alanine	-

28	1-(Boc-amino)-cyclopentane carboxylic acid	trace
29	Boc-acetamidomethyl cysteine	-
30	<i>N</i> -Acetyl-L-histidine monohydrate	trace

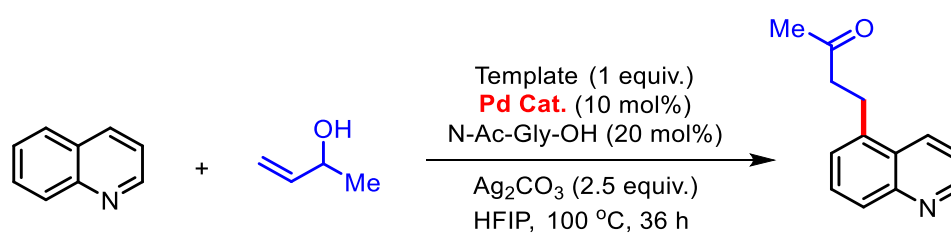
Table 5.2. Oxidant optimization for C5-H alkylation of quinoline.



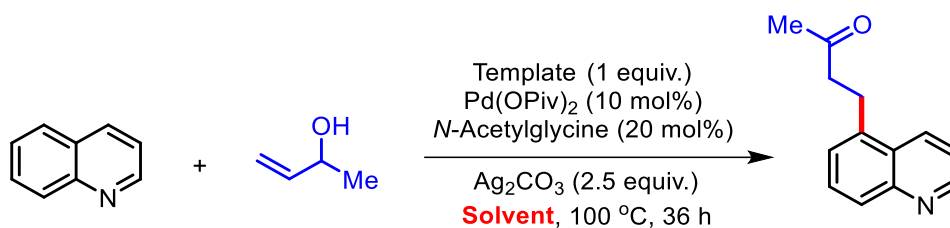
S. No.	Oxidant	Yield(%)
1.	Ag ₂ CO ₃	56 (4:1)
2.	AgOAc	44 (3:1)
3.	AgBF ₄	-
4.	AgNO ₃	36 (3:2)
5.	AgF	-
6.	AgSbF ₆	trace
7.	CF ₃ COOAg	64 (1:1)
8.	Ag ₂ SO ₄	29 (3:1)
9.	AgNO ₂	-
10.	AgI	-
11.	AgBr	-
12.	Ag(OSO ₂ CF ₃)	trace
13.	AgPF ₆	trace
14.	AgN(SO ₂ CF ₃) ₂	-
15.	Cu ₂ CO ₃	-
16.	CuBr	-

17.	Cu(OAc) ₂ ·H ₂ O	-
18.	Cu(TFA) ₂	trace
19.	CuCO ₃	-
20.	Cu(OAc)	-
21.	Cu(OTf) ₂	trace
22.	CuF ₂	trace
23.	Cu ₂ O	trace
24.	CuO	-

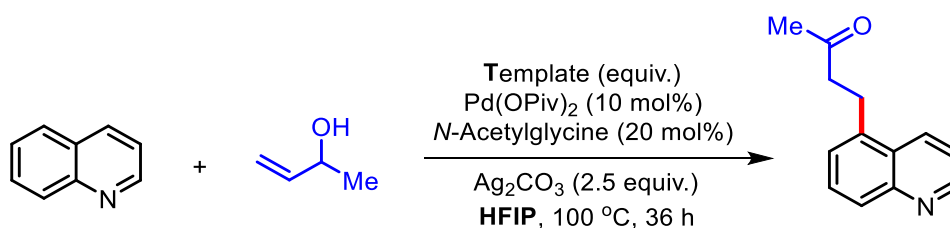
Table 5.3. Catalyst (Pd source) optimization for C5-H alkylation of quinoline.



S. No.	Catalyst	Yield(%)
1.	Pd(OPiv) ₂	74 (6:1)
2.	Pd(CF ₃ COO) ₂	29 (4:1)
3.	Pd(acac) ₂	37 (3:1)
4.	[PdCl(C ₃ H ₅) ₂]	32 (5:1)
5.	Pd ₂ (dba) ₃	23 (5:1)
6.	(PhCN) ₂ PdCl ₂	trace
7.	(CH ₃ CN) ₂ PdCl ₂	-
8.	Pd(dppf)Cl ₂	-
9.	(PPh ₃) ₂ PdCl ₂	-
10.	PdCl ₂	-

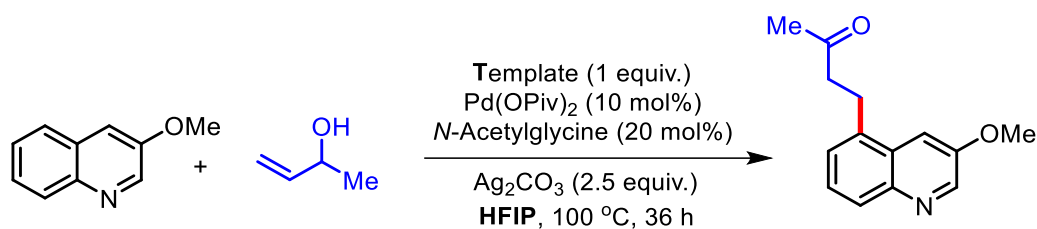
Table 5.4. Solvent optimization for C5-H alkylation of quinoline.

S. No.	Solvent	Yield(%)
1	HFIP	74% (6:1)
2	DCE	trace
3	MeCN	trace
4	TFT	trace
5	TFE	32% (5:1)
6	HFIP:DCE (1:1)	26% (4:1)
7	DMF	-
8	1,4-Dioxane	-
9	Toluene	-
10	HFIP:TFE (1:1)	41% (5:1)

Table 5.5. Template load optimization for C5-H alkylation of quinoline.

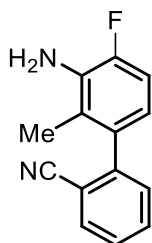
S. No.	Template (equiv.)	Yield(%)
1	0.25	trace
2	0.5	18 (3:2)
3	0.75	43 (3:1)
4	1	74 (6:1)

Table 5.6. Template load optimization for C5-H alkylation of quinoline.



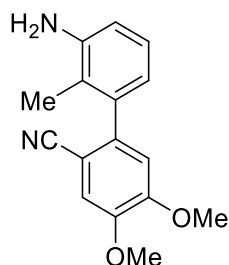
S. No.	Regenerated template	Yield(%)
1	Fresh	94 (20:1)
2	1 st time regenerated	93 (20:1)
3	2 nd time regenerated	93 (20:1)
4	3 rd time regenerated	94 (20:1)
5	4 th time regenerated	92 (20:1)
6	5 th time regenerated	91 (20:1)

5.4.5. Characterization data:



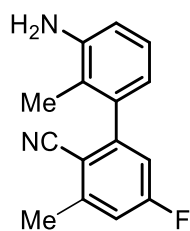
3'-Amino-4'-fluoro-2'-methyl-[1,1'-biphenyl]-2-carbonitrile:

Colorless solid (1.68g, 74% yield); mp 77-79 °C; ¹H NMR (500 MHz, CDCl₃) δ 7.76 (d, *J* = 7.7 Hz, 1H), 7.65 (t, *J* = 7.7 Hz, 1H), 7.47 (t, *J* = 7.7 Hz, 1H), 7.37 (d, *J* = 7.7 Hz, 1H), 6.98 (dd, *J* = 10.2, 8.7 Hz, 1H), 6.62 (dd, *J* = 8.3, 5.3 Hz, 1H), 4.04 – 3.63 (m, 2H), 2.03 (s, 3H); ¹³C NMR (101 MHz, CDCl₃) δ 151.69 (d, *J* = 239.5 Hz), 145.8, 134.5, 133.37 (d, *J* = 12.4 Hz), 132.71 (d, *J* = 32.3 Hz), 130.9, 127.6, 122.91 (d, *J* = 3.7 Hz), 119.4, 119.3, 118.2, 113.3, 112.49 (d, *J* = 19.4 Hz), 14.51 (d, *J* = 2.9 Hz); IR (ATR): 767, 847, 939, 1044, 1098, 1161, 1235, 1301, 1373, 1449, 1479, 1631, 1738, 2228, 2986, 3381, 3476 cm⁻¹.



3'-Amino-4,5-dimethoxy-2'-methyl-[1,1'-biphenyl]-2-carbonitrile:

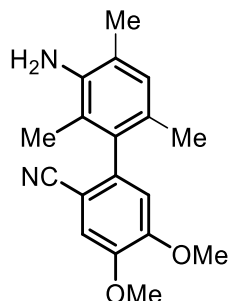
Off-White solid (1.83g, 68% yield); mp 164-166 °C; ^1H NMR (500 MHz, CDCl_3) δ 7.15 (s, 1H), 7.11 (t, $J = 7.7$ Hz, 1H), 6.83 (s, 1H), 6.78 (d, $J = 7.9$ Hz, 1H), 6.69 (d, $J = 7.5$ Hz, 1H), 3.97 (s, 3H), 3.93 (s, 3H), 3.75 (s, 2H), 2.03 (s, 3H); ^{13}C NMR (126 MHz, CDCl_3) δ 152.2, 148.0, 145.2, 140.9, 139.0, 126.4, 120.5, 120.1, 118.7, 115.3, 114.1, 113.2, 104.1, 56.3, 56.2, 14.2.; IR (ATR): 726, 770, 793, 816, 848, 867, 938, 960, 1013, 1045, 1086, 1119, 1155, 1244, 1300, 1352, 1373, 1463, 1515, 1602, 1626, 1737, 2221, 2604, 2851, 2940, 2985, 3244, 3380, 3471 cm^{-1} .



3'-amino-5-fluoro-2',3-dimethyl-[1,1'-biphenyl]-2-carbonitrile:

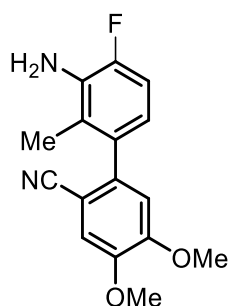
Off-White solid (1.91 g, 79% yield); mp 131-133 °C; ^1H NMR (500 MHz, CDCl_3) δ 7.09 (t, $J = 7.8$ Hz, 1H), 7.01 (dd, $J = 8.9, 1.9$ Hz, 1H), 6.90 (dd, $J = 8.7, 2.2$ Hz, 1H), 6.76 (d, $J = 7.9$ Hz, 1H), 6.62 (d, $J = 7.5$ Hz, 1H), 3.73 (s, 2H), 2.61 (s, 3H), 1.98 (s, 3H); ^{13}C NMR (126 MHz, CDCl_3) δ 164.16 (d, $J = 256.0$ Hz), 149.67 (d, $J = 9.5$ Hz), 145.50 (d, $J = 9.6$ Hz), 145.24, 138.48, 126.62, 120.11, 119.85, 116.71, 116.02 (d, $J = 22.3$ Hz), 115.72, 115.43 (d, $J = 22.3$

Hz), 109.94, 21.18, 14.29; IR (ATR): 724, 790, 871, 939, 985, 1045, 1100, 1133, 1165, 1236, 1294, 1338, 1373, 1466, 1586, 1737, 2225, 2986, 3381 cm^{-1} .



3'-amino-4,5-dimethoxy-2',4',6'-trimethyl-[1,1'-biphenyl]-2-carbonitrile:

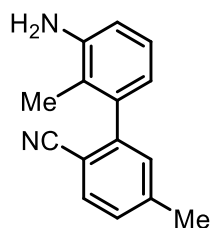
Off-white solid (1.9g, 64% yield); mp 179-181 °C; ^1H NMR (400 MHz, CDCl_3) δ 7.15 (s, 1H), 6.90 (s, 1H), 6.70 (s, 1H), 3.95 (s, 3H), 3.88 (s, 3H), 2.21 (s, 3H), 1.94 (s, 3H), 1.88 (s, 3H); ^{13}C NMR (101 MHz, CDCl_3) δ 152.6, 147.9, 140.8, 140.7, 136.1, 129.6, 125.5, 122.3, 120.4, 118.4, 114.2, 113.1, 104.6, 56.3, 19.8, 17.8, 14.8; IR (ATR): 753, 787, 848, 869, 939, 1011, 1044, 1108, 1239, 1307, 1348, 1373, 1465, 1516, 1566, 1601, 1628, 1737, 2223, 2617, 2861, 2984, 3393, 3472 cm^{-1} .



3'-Amino-4'-fluoro-4,5-dimethoxy-2'-methyl-[1,1'-biphenyl]-2-carbonitrile:

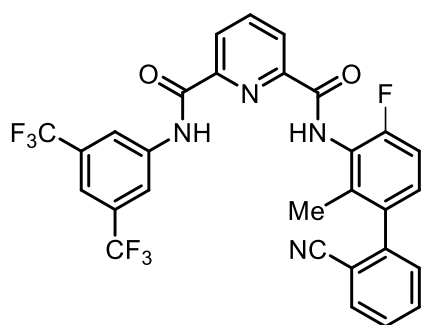
Off-white solid (2.21g, 77% yield); mp 197-199 °C ; ^1H NMR (400 MHz, CDCl_3) δ 7.12 (s, 3H), 6.93 (dd, $J = 10.4, 8.5$ Hz, 3H), 6.76 (s, 3H), 6.59 (dd, $J = 8.4, 5.3$ Hz, 3H), 3.93 (s, 9H), 3.90 (s, 9H), 3.78 (s, 5H), 2.01 (s, 9H); ^{13}C NMR (101 MHz, CDCl_3) δ 152.50, 151.53 (d, $J =$

239.4 Hz), 148.21, 140.21, 134.47 (d, $J = 3.1$ Hz), 133.33 (d, $J = 12.5$ Hz), 123.05 (d, $J = 3.7$ Hz), 119.31 (d, $J = 7.6$ Hz), 118.59, 114.14, 113.34, 112.36 (d, $J = 19.2$ Hz), 104.42, 56.36, 56.26, 14.45 (d, $J = 2.9$ Hz); IR (ATR): 792, 870, 929, 981, 1015, 1082, 1127, 1223, 1268, 1353, 1393, 1453, 1494, 1520, 1602, 1629, 1735, 2222, 2857, 2974, 3389 cm^{-1} .



3'-amino-2',5-dimethyl-[1,1'-biphenyl]-2-carbonitrile:

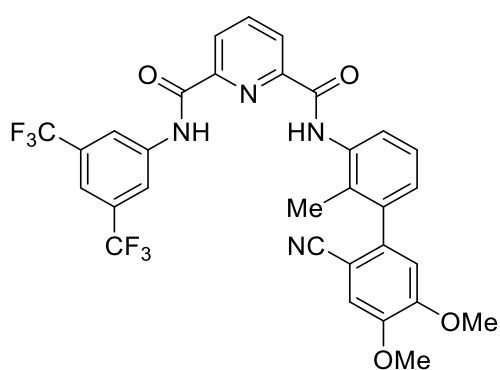
Light Brown solid (1.83 g, 82% yield); mp 63-65 °C ; ^1H NMR (400 MHz, CDCl_3) δ 7.61 (d, $J = 7.9$ Hz, 1H), 7.24 (d, $J = 7.9$ Hz, 1H), 7.18 (s, 1H), 7.09 (t, $J = 7.7$ Hz, 1H), 6.75 (d, $J = 7.9$ Hz, 1H), 6.64 (d, $J = 7.5$ Hz, 1H), 3.73 (s, 2H), 2.44 (s, 3H), 1.98 (s, 3H); ^{13}C NMR (101 MHz, CDCl_3) δ 146.3, 145.2, 143.3, 139.2, 132.6, 131.4, 128.3, 126.4, 120.3, 120.2, 118.6, 115.4, 110.1, 77.5, 77.2, 76.8, 21.9, 14.3; IR (ATR): 725, 789, 847, 939, 1045, 1097, 1236, 1301, 1373, 1464, 1588, 1630, 1738, 2227, 2943, 2986, 3382 cm^{-1} .



***N*²-(3,5-bis(trifluoromethyl)phenyl)-*N*⁶-(2'-cyano-4-fluoro-2-methyl-[1,1'-biphenyl]-3-yl)pyridine-2,6-dicarboxamide:**

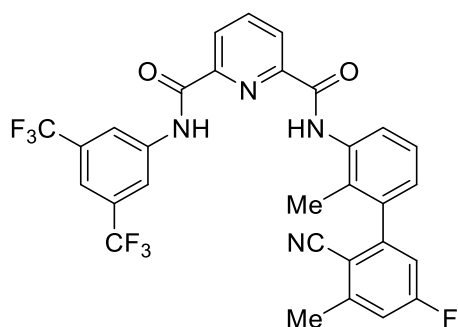
Colorless solid (1.04g, 89% yield); mp 165-167 °C ; ^1H NMR (500 MHz, DMSO) δ 11.32 (s, 1H), 10.94 (s, 1H), 8.54 (s, 2H), 8.43 (dd, $J = 14.8, 7.7$ Hz, 2H), 8.34 (t, $J = 7.3$ Hz, 1H), 7.99 (d, $J = 7.7$ Hz, 1H), 7.83 (dd, $J = 20.0, 12.4$ Hz, 2H), 7.63 (t, $J = 7.6$ Hz, 1H), 7.52 (d, $J = 7.6$

Hz, 1H), 7.46 – 7.27 (m, 2H), 2.10 (s, 3H); ^{13}C NMR (126 MHz, DMSO) δ 162.84, 162.47, 159.51, 157.53, 148.53 (d, $J = 33.9$ Hz), 144.14, 140.57 (d, $J = 51.0$ Hz), 136.99, 135.41, 133.70 (d, $J = 27.4$ Hz), 131.24 (t, $J = 16.4$ Hz), 129.06, 126.28 (d, $J = 9.6$ Hz), 124.77, 124.46 (d, $J = 12.6$ Hz), 122.60, 121.61, 118.34, 117.80, 113.93 (d, $J = 21.6$ Hz), 112.49, 16.01; IR (ATR): 683, 704, 766, 845, 888, 938, 1044, 1134, 1182, 1234, 1279, 1374, 1435, 1474, 1546, 1698, 1738, 2229, 2987, 3301 cm^{-1} .



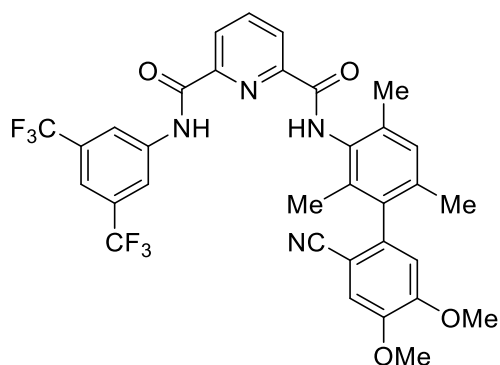
***N*²-(3,5-bis(trifluoromethyl)phenyl)-*N*⁶-(2'-cyano-4',5'-dimethoxy-2-methyl-[1,1'-biphenyl]-3-yl)pyridine-2,6-dicarboxamide:**

Colorless solid (1.16g, 92% yield); mp >232 °C ; ^1H NMR (500 MHz, DMSO) δ 11.46 (s, 1H), 10.98 (s, 1H), 8.60 (s, 2H), 8.44 (d, $J = 7.5$ Hz, 2H), 8.34 (t, $J = 7.6$ Hz, 1H), 7.88 (s, 1H), 7.69 (d, $J = 7.8$ Hz, 1H), 7.49 (s, 1H), 7.43 (t, $J = 7.7$ Hz, 1H), 7.24 (d, $J = 6.9$ Hz, 1H), 7.16 (d, $J = 7.7$ Hz, 1H), 6.98 (s, 1H), 3.87 (d, $J = 4.6$ Hz, 6H), 2.16 (s, 3H); ^{13}C NMR (126 MHz, DMSO) δ 162.54, 161.59, 152.21, 148.32 (d, $J = 110.2$ Hz), 148.14, 140.27, 140.03, 139.20 (d, $J = 51.8$ Hz), 136.03, 136.03, 131.99, 130.79 (q, $J = 32.9$ Hz), 127.94, 126.81, 126.48, 125.88, 125.75, 125.57, 124.31, 122.14, 120.76, 119.97, 118.38, 117.23, 114.67, 113.37, 102.85; IR (ATR): 683, 702, 799, 842, 887, 1015, 1082, 1133, 1182, 1223, 1279, 1353, 1383, 1441, 1474, 1517, 1545, 1602, 1694, 2223, 3323 cm^{-1} .



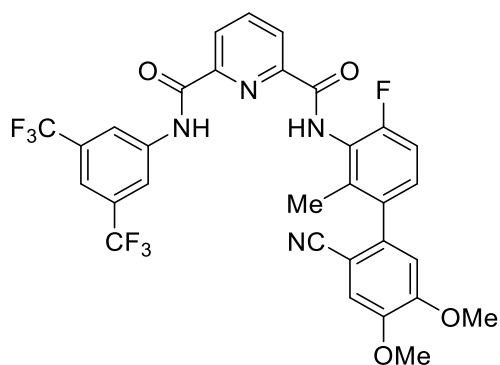
***N*²-(3,5-bis(trifluoromethyl)phenyl)-*N*⁶-(2'-cyano-5'-fluoro-2,3'-dimethyl-[1,1'-biphenyl]-3-yl)pyridine-2,6-dicarboxamide:**

Colorless solid (1045 mg, 87% yield); mp 216-218 °C; ¹H NMR (500 MHz, CDCl₃) δ 10.53 (s, 1H), 10.11 (s, 1H), 8.56 (dd, *J* = 7.8, 3.2 Hz, 2H), 8.39 (s, 2H), 8.20 (t, *J* = 7.8 Hz, 1H), 7.68 (dd, *J* = 7.2, 1.5 Hz, 1H), 7.60 (s, 1H), 7.14 – 6.97 (m, 3H), 6.87 (dd, *J* = 8.4, 2.0 Hz, 1H), 2.57 (s, 3H), 2.07 (s, 3H); ¹³C NMR (126 MHz, CDCl₃) δ 165.47, 163.42, 162.15 (d, *J* = 65.9 Hz), 149.01, 148.50 (d, *J* = 9.6 Hz), 148.32, 146.13 (d, *J* = 9.8 Hz), 139.89, 139.24, 138.95, 135.47, 132.41 (q, *J* = 33.5 Hz), 130.03, 127.41, 126.31 (d, *J* = 8.4 Hz), 126.06, 125.25, 124.24, 122.07, 120.22, 117.94, 117.23 – 116.33, 115.42 (d, *J* = 22.7 Hz), 109.35, 20.99, 15.10; IR (ATR): 890, 936, 1134, 1183, 1227, 1279, 1337, 1383, 1436, 1473, 1546, 1595, 1693, 2224 cm⁻¹.



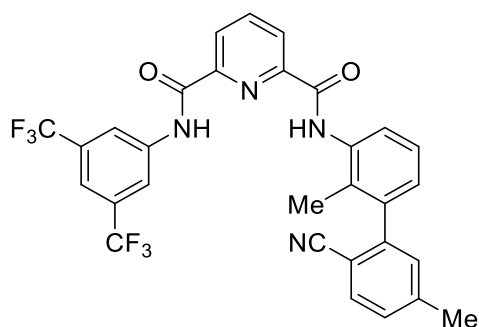
***N*²-(3,5-bis(trifluoromethyl)phenyl)-*N*⁶-(2'-cyano-4',5'-dimethoxy-2,4,6-trimethyl-[1,1'-biphenyl]-3-yl)pyridine-2,6-dicarboxamide:**

Colorless solid (1.12g, 85% yield); mp >232 °C; ^1H NMR (500 MHz, DMSO) δ 11.35 (s, 1H), 10.84 (s, 1H), 8.52 (s, 2H), 8.42 (dd, $J = 14.8, 7.7$ Hz, 2H), 8.32 (t, $J = 7.7$ Hz, 1H), 7.89 (s, 1H), 7.50 (s, 1H), 6.87 (s, 1H), 3.87 (s, 3H), 3.85 (s, 3H), 2.29 (s, 3H), 2.03 (s, 3H), 1.94 (s, 3H); ^{13}C NMR (101 MHz, DMSO) δ 162.41, 161.59, 152.80, 148.33 (d, $J = 108.5$ Hz), 147.99, 140.12, 139.91, 138.49, 136.47, 135.69, 134.84, 134.05, 132.53, 130.77 (q, $J = 32.9$ Hz), 129.18, 127.28, 125.68, 125.45, 124.57, 121.86, 121.19, 119.15, 118.21, 117.29, 114.73, 113.00, 103.05, 56.00, 55.95, 19.89, 18.25, 15.86; IR (ATR): 668, 753, 838, 886, 1046, 1133, 1177, 1217, 1278, 1378, 1466, 1517, 1599, 1620, 1733, 2266, 2944, 3022 cm^{-1} .



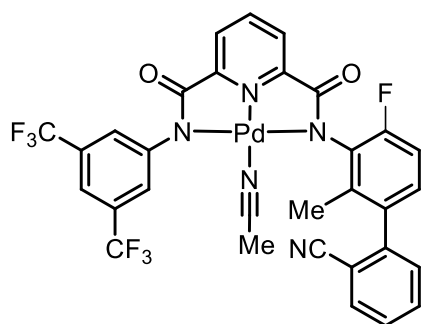
***N*²-(3,5-bis(trifluoromethyl)phenyl)-*N*⁶-(2'-cyano-4-fluoro-4',5'-dimethoxy-2-methyl-[1,1'-biphenyl]-3-yl)pyridine-2,6-dicarboxamide:**

Colorless solid (1.18g, 91% yield); mp 198-200 °C ; ^1H NMR (400 MHz, CDCl_3) δ 10.68 (s, 1H), 9.99 (s, 1H), 8.60 (d, $J = 7.5$ Hz, 1H), 8.51 (d, $J = 9.2$ Hz, 3H), 8.20 (t, $J = 7.6$ Hz, 1H), 7.55 (s, 1H), 7.14 (s, 1H), 7.06 (d, $J = 7.5$ Hz, 1H), 6.82 (s, 1H), 6.66 (t, $J = 8.4$ Hz, 1H), 3.93 (s, 6H), 1.90 (s, 3H); ^{13}C NMR (101 MHz, CDCl_3) δ 162.87, 162.53, 157.88 (d, $J = 250.0$ Hz), 152.91, 148.69, 148.18, 139.73, 139.46, 139.22, 137.16, 135.11, 132.29 (d, $J = 33.5$ Hz), 129.89, 126.38 (d, $J = 40.8$ Hz), 124.50, 123.39, 121.79, 120.55, 119.35, 117.95, 114.20, 113.80 – 112.26 (m), 103.58, 56.49, 15.88; IR (ATR): 757, 785, 847, 937, 1044, 1127, 1235, 1373, 1475, 1517, 1551, 1738, 2222, 2985 cm^{-1} .



***N*₂-(3,5-bis(trifluoromethyl)phenyl)-*N*₆-(2'-cyano-2,5'-dimethyl-[1,1'-biphenyl]-3-yl)pyridine-2,6-dicarboxamide:**

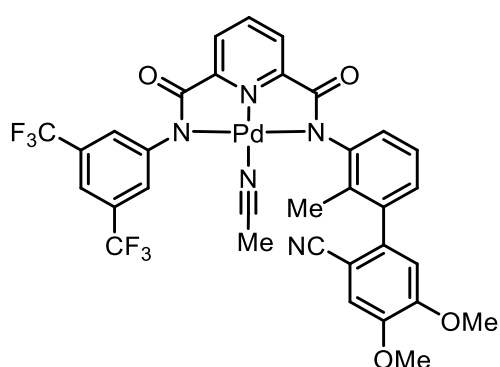
Colorless solid; yield 91% (1063 mg); mp 227-229 °C; ¹H NMR (400 MHz, DMSO) δ 11.41 (s, 1H), 10.96 (s, 1H), 8.57 (s, 2H), 8.42 (t, *J* = 7.0 Hz, 2H), 8.32 (t, *J* = 7.7 Hz, 1H), 7.84 (d, *J* = 7.8 Hz, 2H), 7.71 (d, *J* = 7.8 Hz, 1H), 7.43 (t, *J* = 7.7 Hz, 2H), 7.30 (s, 1H), 7.21 (d, *J* = 7.5 Hz, 1H), 2.44 (s, 3H), 2.12 (s, 3H); ¹³C NMR (101 MHz, DMSO) δ 162.99, 162.02, 148.76 (d, *J* = 86.9 Hz), 144.99, 144.33, 140.60 (d, *J* = 18.6 Hz), 139.80, 136.55, 133.30, 132.05, 131.56, 131.24 (d, *J* = 32.9 Hz), 129.46, 128.04, 127.27, 126.44, 126.19, 126.01, 125.03, 122.31, 121.19, 118.57, 117.61, 109.33, 21.68, 15.45; IR (ATR): 682, 753, 798, 886, 938, 1002, 1133, 1182, 1279, 1383, 1441, 1474, 1545, 1696, 1739, 2228, 2928 cm⁻¹.



Template (12):

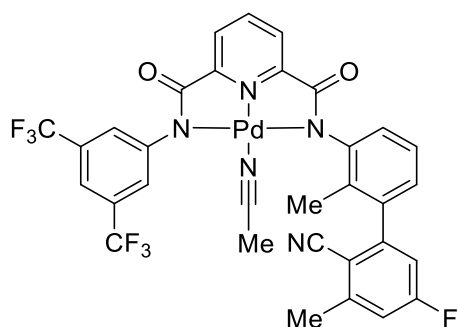
Yellow solid (602, 81% yield); mp/decomposition >232 °C; ¹H NMR (400 MHz, CD₃CN) δ 8.30 (t, *J* = 7.8 Hz, 1H), 7.98 – 7.78 (m, 5H), 7.74 (t, *J* = 7.3 Hz, 1H), 7.66 (s, 1H), 7.55 (td, *J*

= 7.7, 1.0 Hz, 1H), 7.48 (d, $J = 7.7$ Hz, 1H), 7.12 (dd, $J = 10.6, 6.9$ Hz, 2H), 2.17 (s, 3H); ^{13}C NMR (101 MHz, CD_3CN) δ 169.05, 168.23, 158.76, 156.32, 151.90, 150.88, 148.80, 144.83, 142.60, 135.64, 134.85, 133.94, 133.04, 132.79, 131.37 – 130.01 (m), 128.12, 127.80, 127.71, 126.58, 126.49, 126.16, 125.00, 122.30, 118.21, 112.71 (d, $J = 21.6$ Hz), 15.05; IR (ATR): 684, 759, 844, 938, 1045, 1131, 1174, 1236, 1277, 1374, 1447, 1468, 1620, 1738, 2238, 2986 cm^{-1} .

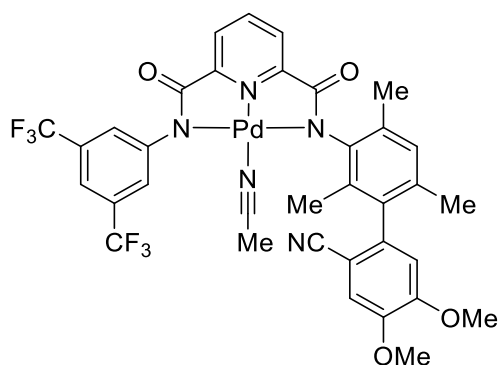


Template (17):

Yellow solid (674 mg, 87% yield); mp/decomposition >232 °C; ^1H NMR (500 MHz, CD_3CN) δ 8.24 (d, $J = 7.8$ Hz, 1H), 7.91 – 7.83 (m, 3H), 7.76 (t, $J = 6.8$ Hz, 1H), 7.63 (s, 1H), 7.31 – 7.23 (m, 3H), 7.10 (d, $J = 7.3$ Hz, 1H), 6.96 (s, 1H), 3.87 (d, $J = 5.5$ Hz, 6H), 2.16 (s, 3H), 1.96 (s, 3H); ^{13}C NMR (126 MHz, CD_3CN) δ 169.97, 168.93, 153.70, 152.78, 149.87, 149.39, 147.54, 143.36, 141.18, 140.28, 133.79, 131.72, 131.46, 131.20, 128.52, 128.02, 127.46, 127.18, 127.02, 126.65, 125.74, 123.58, 119.73, 117.81, 115.35, 114.32, 104.36, 56.91, 56.86, 15.74; IR (ATR): 683, 757, 843, 929, 966, 1013, 1086, 1133, 1175, 1219, 1277, 1379, 1465, 1516, 1600, 1617, 2225, 2272, 2854, 2938, 3020 cm^{-1} .

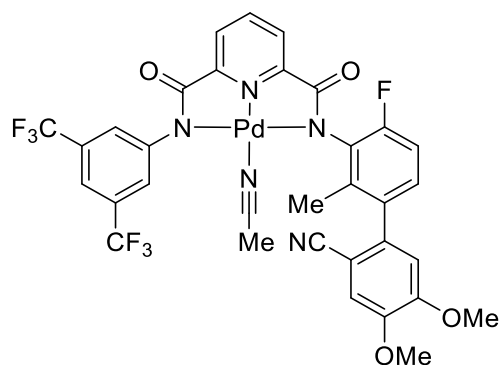
**Template (14):**

Yellow solid (568 mg, 76% yield); mp/decomposition $>232\text{ }^{\circ}\text{C}$; ^1H NMR (500 MHz, CD_3CN) δ 8.27 (dd, $J = 10.0, 5.6$ Hz, 1H), 7.92 – 7.87 (m, 3H), 7.80 (dd, $J = 7.8, 1.2$ Hz, 1H), 7.67 (s, 1H), 7.35 (dd, $J = 7.8, 1.0$ Hz, 1H), 7.29 (t, $J = 7.7$ Hz, 1H), 7.21 (dd, $J = 9.4, 2.1$ Hz, 1H), 7.11 – 6.98 (m, 2H), 2.59 (s, 3H), 2.15 (s, 3H); ^{13}C NMR (126 MHz, CD_3CN) δ 168.96, 167.89, 164.18 (d, $J = 254.1$ Hz), 151.74 (d, $J = 14.4$ Hz), 149.19 – 148.40 (m), 146.45, 145.96 (d, $J = 10.0$ Hz), 142.45, 140.57, 138.56, 132.38, 130.63 (q, $J = 32.7$ Hz), 127.92 (s), 126.51, 126.23 (d, $J = 20.3$ Hz), 125.88, 124.74, 122.58, 116.93, 116.64, 115.60 (dd, $J = 122.4, 22.7$ Hz), 109.72, 20.12, 14.70; IR (ATR): 669, 752, 883, 1134, 1177, 1215, 1278, 1379, 1467, 1625, 1731, 2274, 3021 cm^{-1} .

**Template (18):**

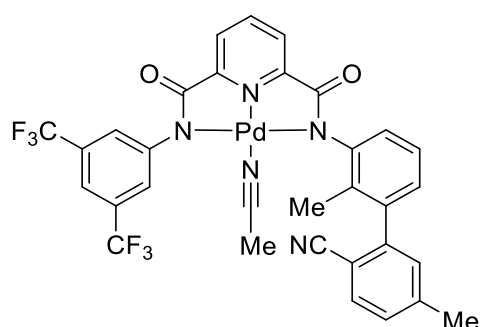
Yellow solid (627 mg, 78% yield); decomposed at $229\text{--}230\text{ }^{\circ}\text{C}$; ^1H NMR (500 MHz, CDCl_3) δ 8.21 (t, $J = 7.8$ Hz, 1H), 7.96 (dd, $J = 20.9, 7.8$ Hz, 2H), 7.82 (s, 2H), 7.55 (s, 1H), 7.15 (s, 1H), 7.05 (s, 1H), 6.84 (s, 1H), 3.96 (s, 3H), 3.91 (s, 3H), 2.48 (s, 3H), 2.10 (s, 3H), 1.98 (s, 3H), 1.90 (s, 3H); ^{13}C NMR (126 MHz, CDCl_3) δ 168.95, 167.86, 153.13, 152.33, 151.90,

148.27, 148.17, 142.05, 141.67, 140.37, 136.20, 134.12, 133.80, 132.45, 131.38, 131.12, 129.10, 126.54, 126.45, 124.63, 122.46, 121.58, 118.86, 117.36, 113.89, 113.24, 103.73, 56.46, 56.34, 20.32, 19.05, 16.11, 2.40; IR (ATR): 668, 753, 838, 886, 1046, 1133, 1177, 1217, 1278, 1378, 1466, 1517, 1599, 1620, 1733, 2266, 2944, 3022 cm^{-1} .



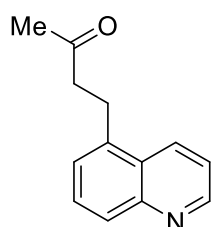
Template (19):

Yellow solid (651 mg, 82% yield); mp/decomposition $>232\text{ }^{\circ}\text{C}$; ^1H NMR (400 MHz, CDCl_3) δ 8.29 – 8.09 (m, 248H), 7.89 – 7.77 (m, 351H), 7.45 (s, 124H), 7.31 – 7.30 (m, 1H), 6.89 – 6.56 (m, 489H), 3.91 (s, 359H), 3.85 (s, 348H), 1.69 (s, 352H); ^{13}C NMR (101 MHz, CDCl_3) δ 169.63, 167.58, 158.47, 156.02, 154.78, 151.83, 150.93, 141.79, 140.40, 134.91, 133.50 (d, $J = 23.9$ Hz), 131.48 (d, $J = 33.2$ Hz), 127.70, 127.49, 127.05, 126.60, 124.50, 122.04 (d, $J = 51.5$ Hz), 117.91, 115.69, 114.24, 112.90, 99.77, 56.54, 56.43, 14.89; IR (ATR): 668, 754, 1000, 1130, 1179, 1215, 1279, 1382, 1487, 1521, 1627, 1732, 2262, 2932, 3021 cm^{-1} .

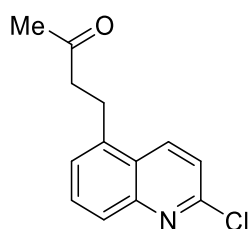


Template (T15):

Yellow solid; yield 85% (621 mg); mp/decomposition >232 °C; ^1H NMR (400 MHz, CD_3CN) δ 8.29 – 8.20 (m, 1H), 7.86 (d, $J = 8.4$ Hz, 3H), 7.78 (d, $J = 6.5$ Hz, 1H), 7.68 (d, $J = 7.4$ Hz, 1H), 7.63 (s, 1H), 7.39 – 7.18 (m, 4H), 7.07 (d, $J = 7.0$ Hz, 1H), 2.43 (s, 3H), 2.11 (s, 3H); ^{13}C NMR (101 MHz, CD_3CN) δ 169.98, 168.97, 152.79, 149.79, 147.41, 146.53, 145.20, 143.40, 140.31, 133.53, 133.44, 132.15, 131.58 (d, $J = 32.6$ Hz), 129.58, 128.69, 128.56, 127.78, 127.44, 127.24, 127.08, 126.77, 125.99, 123.28, 119.52, 21.80, 15.74; IR (ATR): 682, 753, 798, 886, 938, 1002, 1133, 1182, 1279, 1383, 1441, 1474, 1545, 1696, 1739, 2228, 2928 cm^{-1} .

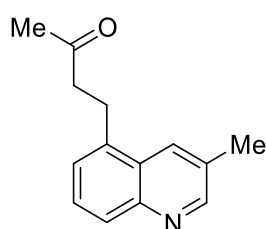
**4-(quinolin-5-yl)butan-2-one (6a):**

Colorless liquid (30 mg, 74% yield); ^1H NMR (400 MHz, CDCl_3) δ 8.90 (dd, $J = 4.2, 1.6$ Hz, 1H), 8.33 (dd, $J = 8.6, 0.8$ Hz, 1H), 7.97 (d, $J = 8.5$ Hz, 1H), 7.60 (dd, $J = 8.4, 7.2$ Hz, 1H), 7.44 – 7.34 (m, 2H), 3.33 (t, $J = 7.7$ Hz, 2H), 2.88 – 2.82 (m, 2H), 2.15 (s, 3H); ^{13}C NMR (126 MHz, CDCl_3) δ 207.5, 150.1, 148.8, 137.6, 132.0, 129.3, 128.4, 126.8, 126.4, 121.0, 44.4, 30.2, 25.9; IR (ATR): 667, 756, 816, 949, 1128, 1160, 1216, 1301, 1380, 1466, 1642, 1763, 2888, 2973, 3614 cm^{-1} ; HRMS-ESI (m/z): $[\text{M}+\text{H}]^+$ calculated (for $\text{C}_{13}\text{H}_{14}\text{NO}$) 200.1075, found 200.1075.

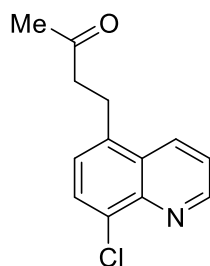


4-(2-chloroquinolin-5-yl)butan-2-one (6b):

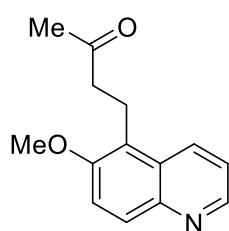
Yellow solid (39.5 mg, 84% yield); ^1H NMR (400 MHz, CDCl_3) δ 8.29 (d, $J = 8.8$ Hz, 1H), 7.87 (d, $J = 8.5$ Hz, 1H), 7.62 (dd, $J = 8.4, 7.3$ Hz, 1H), 7.38 (dd, $J = 7.8, 5.8$ Hz, 2H), 3.30 (t, $J = 7.6$ Hz, 2H), 2.85 (t, $J = 7.6$ Hz, 2H), 2.15 (s, 3H); ^{13}C NMR (101 MHz, CDCl_3) δ 207.2, 150.5, 148.6, 137.9, 135.1, 130.5, 127.5, 126.9, 125.5, 122.2, 44.4, 30.2, 25.9; IR(ATR): 756, 806, 897, 1125, 1163, 1300, 1365, 1402, 1465, 1495, 1588, 1716, 2854, 2924 cm^{-1} ; HRMS-ESI (m/z): $[\text{M}+\text{H}]^+$ calculated (for $\text{C}_{13}\text{H}_{13}\text{ClNO}$) 234.0686, found 234.0682.

**4-(3-methylquinolin-5-yl)butan-2-one (6c):**

Brown color semi solid (37 mg, 86% yield); ^1H NMR (500 MHz, CDCl_3) δ 8.77 (d, $J = 2.0$ Hz, 1H), 8.09 (d, $J = 0.8$ Hz, 1H), 7.94 (d, $J = 8.5$ Hz, 1H), 7.55 (dd, $J = 8.3, 7.2$ Hz, 1H), 7.35 (d, $J = 7.0$ Hz, 1H), 3.35 – 3.29 (m, 2H), 2.90 – 2.84 (m, 2H), 2.55 (s, 3H), 2.17 (s, 3H); ^{13}C NMR (126 MHz, CDCl_3) δ 207.7, 152.1, 147.1, 136.8, 130.7, 130.5, 128.3, 128.2, 126.7, 126.4, 44.5, 30.3, 25.9, 19.2; IR (ATR): 665, 756, 814, 884, 1073, 1162, 1217, 1267, 1364, 1463, 1496, 1576, 1607, 1717, 2853, 2924 cm^{-1} ; HRMS-ESI (m/z): $[\text{M}+\text{H}]^+$ calculated (for $\text{C}_{14}\text{H}_{16}\text{NO}$) 214.1232, found 214.1222.

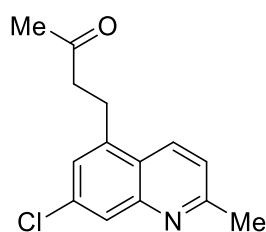
**4-(8-chloroquinolin-5-yl)butan-2-one (6d):**

Light brown color semi solid (45 mg, 64% yield); $^1\text{H NMR}$ (500 MHz, CDCl_3) δ 9.05 (dd, $J = 4.1, 1.5$ Hz, 1H), 8.37 (dd, $J = 8.6, 1.5$ Hz, 1H), 7.75 (d, $J = 7.7$ Hz, 1H), 7.52 (dd, $J = 8.5, 4.1$ Hz, 1H), 7.32 (d, $J = 7.7$ Hz, 1H), 3.32 (t, $J = 7.6$ Hz, 2H), 2.86 (t, $J = 7.6$ Hz, 2H), 2.16 (s, 3H); $^{13}\text{C NMR}$ (126 MHz, CDCl_3) δ 207.2, 150.7, 144.9, 137.0, 132.7, 129.4, 128.2, 126.5, 121.9, 44.3, 30.3, 25.7; IR(ATR): 748, 789, 861, 922, 1042, 1090, 1156, 1265, 1369, 1429, 1477, 1533, 1576, 1614, 1655, 1712, 2855, 2928, 3299 cm^{-1} . HRMS-ESI (m/z): $[\text{M}+\text{H}]^+$ calculated (for $\text{C}_{13}\text{H}_{13}\text{ClNO}$) 234.0686, found 234.0682.



4-(6-methoxyquinolin-5-yl)butan-2-one (6e):

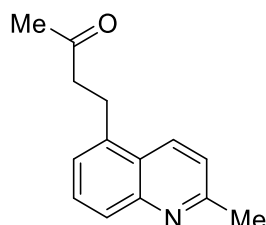
Colorless liquid (29.8 mg, 65% yield); $^1\text{H NMR}$ (500 MHz, CDCl_3) δ 8.78 (dd, $J = 4.1, 1.4$ Hz, 1H), 8.30 (d, $J = 8.6$ Hz, 1H), 8.03 (d, $J = 9.2$ Hz, 1H), 7.49 (d, $J = 9.3$ Hz, 1H), 7.39 (dd, $J = 8.7, 4.1$ Hz, 1H), 3.97 (s, 3H), 3.34 – 3.28 (m, 2H), 2.74 – 2.69 (m, 2H), 2.17 (s, 3H); $^{13}\text{C NMR}$ (101 MHz, CDCl_3) δ 207.8, 153.3, 143.7, 136.3, 127.8, 127.4, 126.9, 126.6, 109.4, 55.8, 44.1, 30.3, 25.9; IR(ATR): 718, 757, 826, 961, 1034, 1093, 1164, 1257, 1325, 1364, 1465, 1507, 1714, 2855, 2925 cm^{-1} ; HRMS-ESI (m/z): $[\text{M}+\text{H}]^+$ calculated (for $\text{C}_{14}\text{H}_{16}\text{NO}_2$) 230.1181, found 230.1175.



4-(7-chloro-2-methylquinolin-5-yl)butan-2-one (6f):

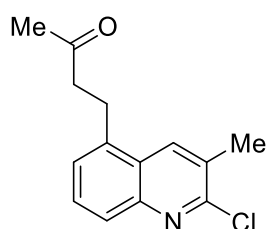
Yellow color semi solid (39.5 mg, 79% yield); $^1\text{H NMR}$ (500 MHz, CDCl_3) δ 8.18 (d, $J = 8.7$ Hz, 1H), 7.88 (d, $J = 1.3$ Hz, 1H), 7.29 (d, $J = 8.7$ Hz, 1H), 7.27 (d, $J = 1.5$ Hz, 1H), 3.27 (t, J

= 7.7 Hz, 2H), 2.85 (dd, $J = 10.1, 5.3$ Hz, 2H), 2.72 (s, 3H), 2.17 (s, 3H); ^{13}C NMR (126 MHz, CDCl_3) δ 207.1, 160.0, 149.0, 139.3, 134.9, 132.1, 126.5, 126.4, 123.5, 122.1, 44.1, 30.2, 25.6, 25.3; IR(ATR): 869, 1088, 1163, 1230, 1277, 1365, 1407, 1505, 1565, 1606, 1718, 2855, 2925 cm^{-1} ; HRMS-ESI (m/z): $[\text{M}+\text{H}]^+$ calculated (for $\text{C}_{14}\text{H}_{15}\text{ClNO}$) 248.0842, 248.0834.



4-(2-methylquinolin-5-yl)butan-2-one (6g):

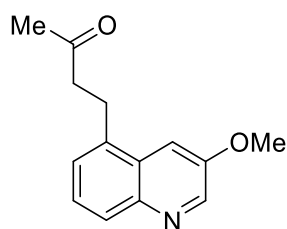
Light yellow liquid (39 mg, 91% yield); ^1H NMR (400 MHz, CDCl_3) δ 8.22 (d, $J = 8.7$ Hz, 1H), 7.88 (d, $J = 8.5$ Hz, 1H), 7.59 – 7.54 (m, 1H), 7.30 (d, $J = 8.2$ Hz, 2H), 3.30 (t, $J = 7.7$ Hz, 2H), 2.87 – 2.81 (m, 2H), 2.73 (s, 3H), 2.15 (s, 3H); ^{13}C NMR (101 MHz, CDCl_3) δ 207.7, 158.7, 148.4, 137.4, 132.1, 129.3, 127.6, 125.6, 125.0, 122.0, 44.5, 30.2, 26.0, 25.3; IR(ATR): 755, 809, 973, 1001, 1163, 1230, 1256, 1312, 1364, 1411, 1509, 1570, 1603, 1714, 2923, 3062 cm^{-1} ; HRMS-ESI (m/z): $[\text{M}+\text{H}]^+$ calculated (for $\text{C}_{14}\text{H}_{16}\text{NO}$) 214.1232, found 214.1222.



4-(2-chloro-3-methylquinolin-5-yl)butan-2-one (6h):

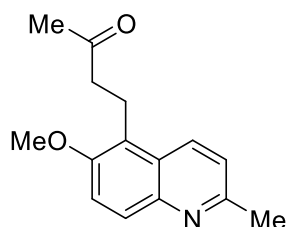
Yellow color semi solid (46 mg, 93% yield); ^1H NMR (500 MHz, CDCl_3) δ 8.13 (s, 1H), 7.84 (d, $J = 8.5$ Hz, 1H), 7.58 – 7.53 (m, 1H), 7.34 (d, $J = 7.1$ Hz, 1H), 3.29 (t, $J = 7.7$ Hz, 2H), 2.87 – 2.83 (m, 2H), 2.55 (s, 3H), 2.17 (s, 3H); ^{13}C NMR (126 MHz, CDCl_3) δ 207.4, 151.8, 147.1, 137.0, 134.0, 130.1, 129.4, 127.1, 126.7, 126.2, 44.3, 30.3, 25.9, 20.5; IR(ATR): 685, 758, 808, 899, 944, 972, 1030, 1090, 1162, 1205, 1365, 1394, 1436, 1482, 1571, 1599, 1717, 2854, 2925,

3065 cm^{-1} ; HRMS-ESI (m/z): $[\text{M}+\text{H}]^+$ calculated (for $\text{C}_{14}\text{H}_{14}\text{ClNNaO}$) 270.0662, found 270.0654.



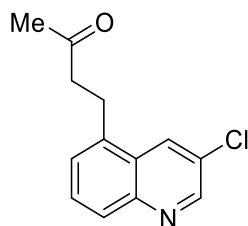
4-(3-methoxyquinolin-5-yl)butan-2-one (6i):

Yellow semi solid (43.5 mg, 93% yield); ^1H NMR (400 MHz, CDCl_3) δ 8.68 (d, $J = 2.8$ Hz, 1H), 7.92 (d, $J = 8.4$ Hz, 1H), 7.53 (d, $J = 2.6$ Hz, 1H), 7.46 (dd, $J = 8.4, 7.1$ Hz, 1H), 7.34 (d, $J = 7.1$ Hz, 1H), 3.97 (s, 3H), 3.33 – 3.26 (m, 2H), 2.91 – 2.84 (m, 2H), 2.17 (s, 3H); ^{13}C NMR (101 MHz, CDCl_3) δ 207.8, 153.2, 144.0, 136.3, 128.1, 127.4, 126.8, 126.4, 108.9, 55.7, 44.1, 30.3, 26.0; IR(ATR): 754, 810, 863, 927, 1031, 1161, 1211, 1261, 1364, 1382, 1412, 1457, 1496, 1607, 1716, 2854, 2926, 3006 cm^{-1} ; HRMS-ESI (m/z): $[\text{M}+\text{H}]^+$ calculated (for $\text{C}_{14}\text{H}_{16}\text{NO}_2$) 230.1181, 230.1176.



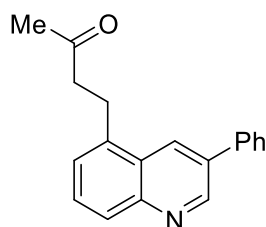
4-(6-methoxy-2-methylquinolin-5-yl)butan-2-one (6j):

Brown color semi solid (42.5 mg, 87% yield); ^1H NMR (400 MHz, CDCl_3) δ 8.19 (d, $J = 8.8$ Hz, 3H), 7.94 (d, $J = 9.2$ Hz, 3H), 7.43 (d, $J = 9.3$ Hz, 3H), 7.33 – 7.18 (m, 4H), 3.95 (s, 9H), 3.39 – 3.16 (m, 8H), 2.76 – 2.62 (m, 15H), 2.15 (s, 9H); ^{13}C NMR (101 MHz, CDCl_3) δ 208.6, 156.3, 154.1, 143.5, 131.9, 128.2, 125.9, 122.4, 122.1, 116.2, 56.4, 43.7, 30.1, 24.8, 19.2; IR(ATR): 669, 753, 818, 929, 1029, 1093, 1162, 1255, 1315, 1362, 1410, 1457, 1504, 1567, 1602, 1712, 2850, 2924 cm^{-1} ; HRMS-ESI (m/z): $[\text{M}+\text{H}]^+$ calculated (for $\text{C}_{15}\text{H}_{18}\text{NO}_2$) 244.1338, found 244.1338.



4-(3-chloroquinolin-5-yl)butan-2-one (6k):

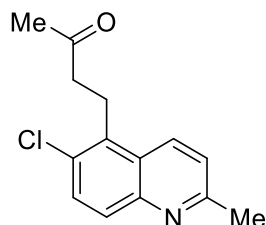
Yellow color semi solid (41.5 mg, 89% yield); ^1H NMR (400 MHz, CDCl_3) δ 8.81 (d, $J = 2.3$ Hz, 1H), 8.32 – 8.28 (m, 1H), 7.95 (d, $J = 8.5$ Hz, 1H), 7.61 (dd, $J = 8.5, 7.2$ Hz, 1H), 7.41 (d, $J = 7.1$ Hz, 1H), 3.29 (t, $J = 7.6$ Hz, 2H), 2.86 (t, $J = 7.6$ Hz, 2H), 2.17 (s, 3H); ^{13}C NMR (101 MHz, CDCl_3) δ 207.2, 149.3, 146.8, 137.0, 130.3, 129.4, 128.6, 128.3, 127.5, 127.2, 44.2, 30.2, 25.7; IR(ATR): 666, 755, 812, 890, 1014, 1062, 1096, 1162, 1287, 1326, 1359, 1409, 1459, 1487, 1590, 1717, 2854, 2926, 3071 cm^{-1} ; HRMS-ESI (m/z): $[\text{M}+\text{H}]^+$ calculated (for $\text{C}_{13}\text{H}_{13}\text{ClNO}$) 234.0686, found 234.0682.



4-(3-phenylquinolin-5-yl)butan-2-one (6l):

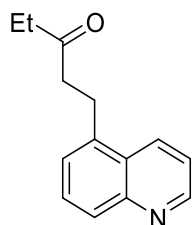
Light brown color semi solid (49.5 mg, 90% yield); ^1H NMR (500 MHz, CDCl_3) δ 9.18 (d, $J = 2.2$ Hz, 1H), 8.46 (d, $J = 1.6$ Hz, 1H), 8.02 (d, $J = 8.5$ Hz, 1H), 7.74 – 7.70 (m, 2H), 7.63 (dd, $J = 8.4, 7.2$ Hz, 1H), 7.55 (dd, $J = 10.5, 4.8$ Hz, 2H), 7.48 – 7.40 (m, 2H), 3.41 (t, $J = 7.7$ Hz, 2H), 2.91 (t, $J = 7.7$ Hz, 2H), 2.17 (s, 3H); ^{13}C NMR (126 MHz, CDCl_3) δ 207.5, 149.7, 147.9, 138.2, 137.8, 133.9, 129.4, 129.3, 129.2, 128.3, 128.2, 127.7, 126.9, 126.6, 44.5, 30.3, 25.9; IR(ATR): 698, 763, 814, 902, 1077, 1162, 1216, 1286, 1364, 1416, 1489, 1600, 1716, 2855,

2927, 3023 cm^{-1} ; HRMS-ESI (m/z): $[\text{M}+\text{H}]^+$ calculated (for $\text{C}_{19}\text{H}_{18}\text{NO}$) 276.1388, found 276.1380.



4-(6-chloro-2-methylquinolin-5-yl)butan-2-one (6m):

Yellow color semi solid (33.2 mg, 67% yield); ^1H NMR (400 MHz, CDCl_3) δ 8.26 (d, $J = 8.9$ Hz, 1H), 7.81 (d, $J = 8.7$ Hz, 1H), 7.54 (d, $J = 8.6$ Hz, 1H), 7.38 (d, $J = 8.9$ Hz, 1H), 3.34 – 3.26 (m, 2H), 2.74 – 2.66 (m, 2H), 2.49 (s, 3H), 2.18 (s, 3H); ^{13}C NMR (101 MHz, CDCl_3) δ 207.5, 149.7, 147.5, 134.9, 134.8, 134.6, 134.1, 127.0, 125.6, 122.2, 43.6, 30.2, 22.3, 20.0; IR(ATR): 820, 907, 967, 1132, 1163, 1303, 1362, 1464, 1498, 1583, 1716, 2854, 2925 cm^{-1} ; HRMS-ESI (m/z): $[\text{M}+\text{H}]^+$ calculated (for $\text{C}_{14}\text{H}_{14}\text{ClNNaO}$) 270.0662, found 270.0656.

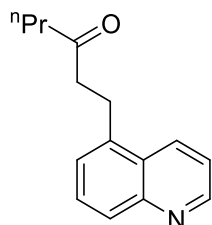


1-(quinolin-5-yl)pentan-3-one (7a):

Colorless liquid (34.5 mg, 81% yield); ^1H NMR (500 MHz, CDCl_3) δ 8.90 (s, 1H), 8.34 (d, $J = 5.7$ Hz, 1H), 8.04 – 7.92 (m, 1H), 7.61 (dt, $J = 11.7, 4.0$ Hz, 1H), 7.41 (ddd, $J = 17.6, 11.2, 8.6$ Hz, 2H), 3.34 (d, $J = 7.2$ Hz, 2H), 2.87 – 2.79 (m, 2H), 2.40 (dd, $J = 8.8, 5.1$ Hz, 2H), 1.11 – 1.02 (m, 3H); ^{13}C NMR (126 MHz, CDCl_3) δ 210.2, 150.1, 148.8, 137.7, 132.0, 129.2, 128.3, 126.7, 126.4, 121.0, 43.1, 36.2, 26.0, 7.8; IR(ATR): 666, 750, 802, 888, 975, 1047, 1068, 1113,

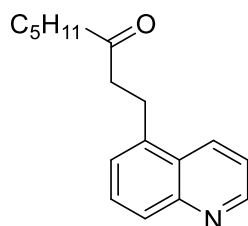
1149, 1216, 1276, 1321, 1363, 1411, 1459, 1503, 1574, 1597, 1712, 2940, 2977, 3021 cm^{-1} ;

HRMS-ESI (m/z): $[\text{M}+\text{H}]^+$ calculated (for $\text{C}_{14}\text{H}_{16}\text{NO}$) 214.1232, found 214.1227.



1-(quinolin-5-yl)hexan-3-one (7b):

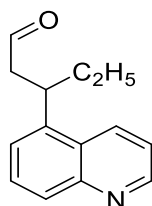
Colorless liquid (36 mg, 79% yield); ^1H NMR (500 MHz, CDCl_3) δ 8.88 (dd, $J = 4.1, 1.5$ Hz, 1H), 8.31 (d, $J = 8.5$ Hz, 1H), 7.95 (d, $J = 8.5$ Hz, 1H), 7.58 (dd, $J = 8.3, 7.3$ Hz, 1H), 7.39 (dd, $J = 8.6, 4.2$ Hz, 1H), 7.35 (d, $J = 7.0$ Hz, 1H), 3.31 (t, $J = 7.7$ Hz, 2H), 2.82 – 2.75 (m, 2H), 2.34 (t, $J = 7.3$ Hz, 2H), 1.56 (dd, $J = 14.8, 7.4$ Hz, 2H), 0.86 (t, $J = 7.4$ Hz, 3H); ^{13}C NMR (126 MHz, CDCl_3) δ 209.8, 150.0, 148.8, 137.7, 132.0, 129.2, 128.3, 126.7, 126.4, 120.9, 45.0, 43.5, 25.9, 17.3, 13.8; IR(ATR): 666, 752, 802, 895, 1014, 1051, 1070, 1125, 1150, 1216, 1321, 1367, 1410, 1459, 1502, 1574, 1596, 1710, 2877, 2963, 3021 cm^{-1} ; HRMS-ESI (m/z): $[\text{M}+\text{H}]^+$ calculated (for $\text{C}_{15}\text{H}_{18}\text{NO}$) 228.1388, found 228.1380.



1-(quinolin-5-yl)octan-3-one (7c):

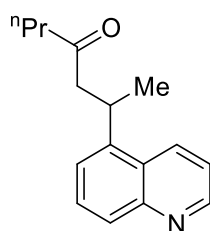
Colorless liquid (39 mg, 76% yield); ^1H NMR (400 MHz, CDCl_3) δ 8.89 (dd, $J = 4.1, 1.5$ Hz, 1H), 8.33 (d, $J = 8.5$ Hz, 1H), 7.96 (d, $J = 8.5$ Hz, 1H), 7.59 (dd, $J = 8.4, 7.2$ Hz, 1H), 7.43 – 7.32 (m, 2H), 3.32 (t, $J = 7.7$ Hz, 2H), 2.80 (t, $J = 7.7$ Hz, 2H), 2.36 (t, $J = 7.4$ Hz, 2H), 1.61 – 1.48 (m, 2H), 1.22 (ddd, $J = 15.5, 11.0, 5.3$ Hz, 4H), 0.84 (t, $J = 7.0$ Hz, 3H); ^{13}C NMR (126

MHz, CDCl₃) δ 210.0, 150.0, 148.8, 137.8, 132.0, 129.3, 128.3, 126.8, 126.5, 121.0, 43.5, 43.2, 31.4, 25.9, 23.6, 22.5, 14.0; IR(ATR): 666, 753, 802, 979, 1080, 1126, 1150, 1215, 1292, 1321, 1364, 1410, 1460, 1502, 1574, 1597, 1712, 2872, 2932, 2956, 3023 cm⁻¹; HRMS-ESI (m/z): [M+H]⁺ calculated (for C₁₇H₂₂NO) 256.1701, found 256.1692.



3-(quinolin-5-yl)pentanal (7d):

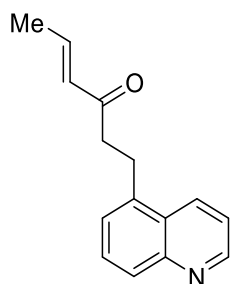
Colorless liquid (30 mg, 70% yield); ¹H NMR (400 MHz, CDCl₃) δ 9.71 (t, *J* = 1.5 Hz, 1H), 8.91 (dd, *J* = 4.1, 1.5 Hz, 1H), 8.53 (d, *J* = 8.7 Hz, 1H), 7.99 (d, *J* = 8.4 Hz, 1H), 7.81 – 7.59 (m, 1H), 7.55 – 7.35 (m, 2H), 4.12 – 3.90 (m, 1H), 2.90 (d, *J* = 7.0 Hz, 2H), 1.83 (dd, *J* = 13.1, 6.8 Hz, 2H), 0.81 (t, *J* = 7.4 Hz, 3H); ¹³C NMR (101 MHz, CDCl₃) δ 201.4, 150.0, 148.7, 140.8, 131.8, 129.3, 128.2, 127.1, 124.1, 121.1, 50.1, 34.7, 29.5, 11.9; IR(ATR): 669, 747, 802, 901, 950, 992, 1051, 1161, 1276, 1317, 1380, 1406, 1461, 1504, 1595, 1721, 2726, 2876, 2931, 2964 cm⁻¹; HRMS-ESI (m/z): [M+H]⁺ calculated (for C₁₄H₁₆NO) 214.1232, found 214.1228.



2-(quinolin-5-yl)heptan-4-one (7e):

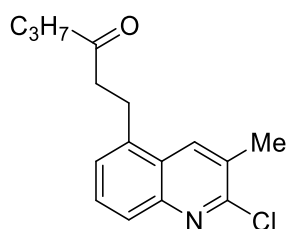
Colorless liquid (37.5 mg, 77% yield); ¹H NMR (400 MHz, CDCl₃) δ 8.89 (dd, *J* = 4.1, 1.4 Hz, 1H), 8.50 (d, *J* = 8.6 Hz, 1H), 7.96 (d, *J* = 8.4 Hz, 1H), 7.65 (dd, *J* = 8.4, 7.4 Hz, 1H), 7.46 – 7.35 (m, 2H), 4.17 (dd, *J* = 13.6, 6.9 Hz, 1H), 2.92 – 2.68 (m, 2H), 2.33 (td, *J* = 7.2, 2.5 Hz, 2H), 1.54 (ddd, *J* = 14.8, 7.5, 1.1 Hz, 2H), 1.36 (d, *J* = 6.9 Hz, 3H), 0.83 (t, *J* = 7.4 Hz, 3H);

^{13}C NMR (101 MHz, CDCl_3) δ 209.7, 150.0, 148.8, 143.2, 131.8, 129.2, 128.1, 126.3, 123.0, 121.0, 50.8, 45.6, 29.0, 21.7, 17.2, 13.7; IR(ATR): 667, 750, 801, 919, 989, 1048, 1127, 1154, 1242, 1314, 1374, 1408, 1457, 1503, 1573, 1595, 1709, 1949, 2876, 2964, 3021 cm^{-1} ; HRMS-ESI (m/z): $[\text{M}+\text{H}]^+$ calculated (for $\text{C}_{16}\text{H}_{19}\text{NNaO}$) 264.1364, found 264.1357.



(E)-1-(quinolin-5-yl)hex-4-en-3-one (7f):

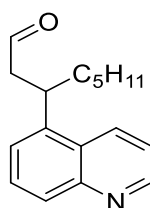
Light yellow semi solid (33.5 mg, 74% yield); ^1H NMR (400 MHz, CDCl_3) δ 8.90 (dd, $J = 4.2$, 1.6 Hz, 1H), 8.36 (ddd, $J = 8.6$, 1.5, 0.9 Hz, 1H), 7.97 (d, $J = 8.5$ Hz, 1H), 7.61 (dd, $J = 8.5$, 7.1 Hz, 1H), 7.48 – 7.35 (m, 2H), 6.91 – 6.74 (m, 1H), 6.12 (dq, $J = 15.8$, 1.6 Hz, 1H), 3.45 – 3.33 (m, 2H), 3.01 – 2.88 (m, 2H), 1.86 (dd, $J = 6.8$, 1.7 Hz, 3H); ^{13}C NMR (101 MHz, CDCl_3) δ 198.96, 150.1, 148.8, 143.3, 137.9, 132.1, 131.9, 129.3, 128.3, 126.9, 126.5, 121.0, 40.8, 26.2, 18.4; IR(ATR): 750, 803, 969, 1059, 1088, 1128, 1187, 1293, 1318, 1363, 1411, 1441, 1502, 1573, 1595, 1631, 1670, 1738, 1951, 2928, 3035 cm^{-1} ; HRMS-ESI (m/z): $[\text{M}+\text{H}]^+$ calculated (for $\text{C}_{15}\text{H}_{16}\text{NO}$) 226.1232, found 226.1224.



1-(2-chloro-3-methylquinolin-5-yl)hexan-3-one (7g):

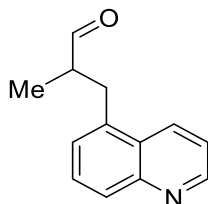
Light brown color semi solid (46.9 mg, 85% yield); ^1H NMR (500 MHz, CDCl_3) δ 8.17 (s, 1H), 7.87 (d, $J = 8.5$ Hz, 1H), 7.58 (dd, $J = 8.4$, 7.2 Hz, 1H), 7.37 (d, $J = 7.1$ Hz, 1H), 3.40 – 3.27 (m, 2H), 2.93 – 2.80 (m, 2H), 2.58 (d, $J = 0.8$ Hz, 3H), 2.41 (t, $J = 7.3$ Hz, 2H), 1.63 (dd,

$J = 14.7, 7.4$ Hz, 2H), 0.92 (t, $J = 7.4$ Hz, 3H); ^{13}C NMR (126 MHz, CDCl_3) δ 209.8, 151.8, 147.2, 137.2, 134.1, 130.1, 129.4, 127.1, 126.7, 126.2, 45.1, 43.4, 29.8, 26.0, 20.5, 17.4, 13.8; IR(ATR): 686, 757, 815, 897, 955, 979, 1011, 1058, 1091, 1125, 1204, 1287, 1366, 1394, 1482, 1571, 1598, 1714, 2928, 2962, 3066 cm^{-1} ; HRMS-ESI (m/z): $[\text{M}+\text{H}]^+$ calculated (for $\text{C}_{16}\text{H}_{19}\text{ClNO}$) 276.1155, found 276.1148.



3-(quinolin-5-yl)octanal (7h):

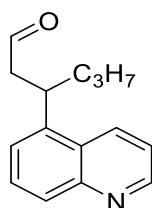
Colorless liquid (35.5 mg, 69% yield); ^1H NMR (400 MHz, CDCl_3) δ 9.69 (s, 1H), 8.91 (dd, $J = 4.0, 1.3$ Hz, 1H), 8.51 (d, $J = 8.6$ Hz, 1H), 7.99 (d, $J = 8.4$ Hz, 1H), 7.68 (t, $J = 7.9$ Hz, 1H), 7.54 – 7.33 (m, 2H), 4.25 – 3.92 (m, 1H), 2.88 (d, $J = 7.0$ Hz, 2H), 1.78 (dd, $J = 14.2, 7.0$ Hz, 2H), 1.29 – 1.11 (m, 6H), 0.79 (t, $J = 6.7$ Hz, 3H); ^{13}C NMR (101 MHz, CDCl_3) δ 201.4, 150.1, 148.8, 141.2, 131.7, 129.3, 128.4, 127.0, 124.0, 121.1, 50.6, 36.7, 31.9, 27.1, 22.6, 14.1; IR(ATR): 669, 750, 929, 1046, 1215, 1375, 1426, 1522, 1732, 3022 cm^{-1} ; HRMS-ESI (m/z): $[\text{M}+\text{H}]^+$ calculated (for $\text{C}_{17}\text{H}_{22}\text{NO}$) 256.1701, found 256.1694.



2-methyl-3-(quinolin-5-yl)propanal (7i):

Colorless liquid (32.5 mg, 81% yield); ^1H NMR (400 MHz, CDCl_3) δ 9.75 (d, $J = 1.4$ Hz, 1H), 8.92 (dd, $J = 4.2, 1.6$ Hz, 1H), 8.32 (d, $J = 8.2$ Hz, 1H), 8.01 (d, $J = 8.5$ Hz, 1H), 7.63 (dd, $J = 8.5, 7.1$ Hz, 1H), 7.43 (dd, $J = 8.6, 4.2$ Hz, 1H), 7.38 (d, $J = 6.9$ Hz, 1H), 3.60 (dd, $J = 14.3,$

5.9 Hz, 1H), 2.94 (dd, $J = 14.3, 8.5$ Hz, 1H), 2.77 (dd, $J = 7.2, 1.2$ Hz, 1H), 1.13 (d, $J = 7.1$ Hz, 3H); ^{13}C NMR (101 MHz, CDCl_3) δ 203.8, 195.0, 150.2, 148.9, 135.5, 131.9, 129.1, 128.8, 127.7, 127.0, 121.1, 47.4, 32.8, 13.9; IR(ATR): 662, 755, 802, 944, 996, 1048, 1083, 1120, 1164, 1248, 1313, 1376, 1404, 1456, 1503, 1573, 1595, 1722, 2727, 2828, 2929, 2967, 3065 cm^{-1} ; HRMS-ESI (m/z): $[\text{M}+\text{H}]^+$ calculated (for $\text{C}_{13}\text{H}_{14}\text{NO}$) 200.1075, found 200.1069.



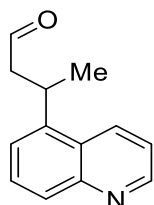
3-(quinolin-5-yl)hexanal (7j):

Colorless liquid (30.5g, 57% yield); ^1H NMR (500 MHz, CDCl_3) δ 9.69 (s, 1H), 8.91 (dd, $J = 4.0, 1.3$ Hz, 1H), 8.51 (d, $J = 8.6$ Hz, 1H), 7.99 (d, $J = 8.4$ Hz, 1H), 7.67 (t, $J = 7.8$ Hz, 1H), 7.53 – 7.35 (m, 2H), 4.15 – 3.98 (m, 1H), 2.88 (d, $J = 6.9$ Hz, 2H), 1.77 (dd, $J = 15.3, 7.6$ Hz, 2H), 1.18 (ddd, $J = 21.0, 13.3, 6.9$ Hz, 2H), 0.84 (t, $J = 7.3$ Hz, 3H); ^{13}C NMR (126 MHz, CDCl_3) δ 201.4, 150.1, 148.8, 141.1, 131.6, 129.2, 128.4, 127.0, 124.0, 121.0, 50.5, 38.9, 20.6, 14.1; IR(ATR): 667, 756, 803, 911, 996, 1051, 1226, 1317, 1379, 1406, 1466, 1504, 1573, 1595, 1723, 2724, 2873, 2930, 2958 cm^{-1} ; HRMS-ESI (m/z): $[\text{M}+\text{H}]^+$ calculated (for $\text{C}_{15}\text{H}_{18}\text{NO}$) 228.1388, found 228.1379.



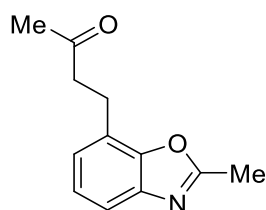
1-(2-methylquinolin-5-yl)octan-3-one (7k):

Light yellow color semi solid (45 mg, 84% yield); ^1H NMR (400 MHz, CDCl_3) δ 8.25 (d, $J = 8.7$ Hz, 3H), 7.91 (d, $J = 8.5$ Hz, 3H), 7.58 (dd, $J = 8.4, 7.2$ Hz, 3H), 7.32 (d, $J = 8.5$ Hz, 6H), 3.38 – 3.25 (m, 6H), 2.89 – 2.79 (m, 6H), 2.75 (s, 10H), 2.38 (t, $J = 7.5$ Hz, 7H), 1.63 – 1.52 (m, 7H), 1.28 – 1.23 (m, 18H), 0.89 – 0.85 (m, 9H); ^{13}C NMR (126 MHz, CDCl_3) δ 210.2, 158.7, 137.6, 132.3, 129.3, 127.5, 125.7, 125.0, 122.0, 43.6, 43.2, 31.5, 29.8, 26.1, 25.2, 23.6, 22.5, 14.0; IR(ATR): 667, 755, 811, 909, 1080, 1126, 1216, 1312, 1372, 1411, 1460, 1509, 1570, 1604, 1714, 2857, 2927 cm^{-1} ; HRMS-ESI (m/z): $[\text{M}+\text{H}]^+$ calculated (for $\text{C}_{18}\text{H}_{24}\text{NO}$) 270.1858, found 270.1851.



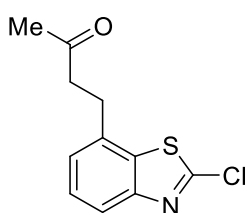
3-(quinolin-5-yl)butanal (7l):

Colorless liquid (26 mg, 65% yield); ^1H NMR (500 MHz, CDCl_3) δ 9.82 (t, $J = 1.4$ Hz, 1H), 8.95 (dd, $J = 4.1, 1.5$ Hz, 1H), 8.50 (d, $J = 8.6$ Hz, 1H), 8.03 (d, $J = 8.5$ Hz, 1H), 7.78 – 7.62 (m, 1H), 7.52 – 7.42 (m, 2H), 4.23 (dd, $J = 13.9, 6.9$ Hz, 1H), 2.92 (dddd, $J = 17.3, 9.9, 7.0, 1.4$ Hz, 2H), 1.47 (d, $J = 6.9$ Hz, 3H); ^{13}C NMR (126 MHz, CDCl_3) δ 201.2, 150.2, 148.9, 142.2, 131.4, 129.3, 128.5, 126.2, 123.3, 121.1, 51.5, 28.1, 22.0; IR(ATR): 669, 748, 802, 902, 991, 1048, 1098, 1161, 1242, 1317, 1374, 1406, 1461, 1504, 1573, 1595, 1722, 2726, 2875, 2931, 2962, 3563 cm^{-1} ; HRMS-ESI (m/z): $[\text{M}+\text{H}]^+$ calculated (for $\text{C}_{13}\text{H}_{14}\text{NO}$) 200.1075, found 200.1067.



4-(2-methylbenzo[d]oxazol-7-yl)butan-2-one (9a):

Light brown color semi solid (32, 78% yield); ^1H NMR (400 MHz, CDCl_3) δ 7.48 (d, $J = 7.8$ Hz, 1H), 7.19 (t, $J = 7.7$ Hz, 1H), 7.08 (d, $J = 7.5$ Hz, 1H), 3.12 (t, $J = 7.7$ Hz, 2H), 2.88 (t, $J = 7.7$ Hz, 2H), 2.63 (s, 3H), 2.16 (s, 3H); ^{13}C NMR (101 MHz, CDCl_3) δ 207.6, 163.6, 149.7, 141.5, 124.6, 124.3, 124.0, 117.5, 43.4, 30.1, 24.2, 14.7; IR: 667, 748, 861, 924, 1041, 1090, 1157, 1216, 1265, 1370, 1430, 1477, 1533, 1574, 1614, 1656, 1711, 2931, 3016 cm^{-1} ; HRMS-ESI (m/z): $[\text{M}+\text{H}]^+$ calculated (for $\text{C}_{12}\text{H}_{14}\text{NO}_2$) 204.1025, found 204.1019.



4-(2-chlorobenzo[*d*]thiazol-7-yl)butan-2-one (9b):

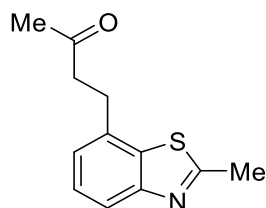
Brown color semi solid (25 mg, 52% yield); ^1H NMR (400 MHz, CDCl_3) δ 7.81 (d, $J = 8.1$ Hz, 1H), 7.42 (t, $J = 7.8$ Hz, 1H), 7.22 (d, $J = 7.6$ Hz, 1H), 3.07 (t, $J = 7.4$ Hz, 2H), 2.89 (t, $J = 7.5$ Hz, 2H), 2.17 (s, 3H); ^{13}C NMR (126 MHz, CDCl_3) δ 206.9, 153.0, 151.5, 136.3, 134.7, 127.1, 125.3, 121.1, 42.7, 30.2, 29.5; IR(ATR): 727, 790, 1014, 1057, 1108, 1163, 1197, 1228, 1289, 1367, 1403, 1477, 1514, 1574, 1719, 2856, 2927 cm^{-1} ; HRMS-ESI (m/z): $[\text{M}+\text{H}]^+$ calculated (for $\text{C}_{11}\text{H}_{11}\text{ClNOS}$) 240.0250, found 240.0246.



1-(2-methylbenzo[*d*]thiazol-7-yl)octan-3-one (9c):

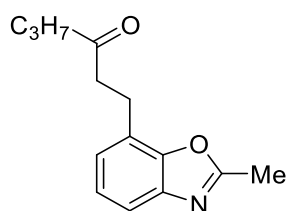
Light yellow color semi solid (53 mg, 87% yield); ^1H NMR (500 MHz, CDCl_3) δ 7.80 (d, $J = 8.1$ Hz, 1H), 7.37 (t, $J = 7.7$ Hz, 1H), 7.15 (d, $J = 7.3$ Hz, 1H), 3.09 (t, $J = 7.6$ Hz, 2H), 2.87 – 2.81 (m, 5H), 2.38 (t, $J = 7.5$ Hz, 2H), 1.59 – 1.51 (m, 2H), 1.29 – 1.19 (m, 4H), 0.86 (t, $J =$

7.1 Hz, 3H); ^{13}C NMR (126 MHz, CDCl_3) δ 209.9, 166.6, 153.8, 135.6, 134.9, 126.4, 124.2, 120.5, 43.1, 41.8, 31.5, 29.9, 23.6, 22.5, 20.3, 14.0; IR(ATR): 731, 754, 790, 994, 1048, 1079, 1127, 1174, 1270, 1314, 1373, 1407, 1458, 1525, 1572, 1714, 2859, 2928 cm^{-1} ; HRMS-ESI (m/z): $[\text{M}+\text{H}]^+$ calculated (for $\text{C}_{16}\text{H}_{22}\text{NOS}$) 276.1422, found 276.1414.



4-(2-methylbenzo[d]thiazol-7-yl)butan-2-one (9d):

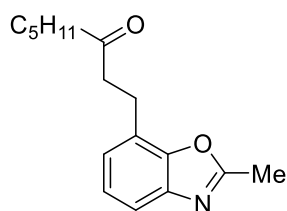
Brown color semi solid (38.5 mg, 87% yield); ^1H NMR (500 MHz, CDCl_3) δ 7.79 (d, $J = 8.1$ Hz, 1H), 7.36 (t, $J = 7.7$ Hz, 1H), 7.14 (d, $J = 7.3$ Hz, 1H), 3.08 (t, $J = 7.6$ Hz, 2H), 2.87 (dd, $J = 8.9, 6.3$ Hz, 2H), 2.83 (s, 3H), 2.15 (s, 3H); ^{13}C NMR (126 MHz, CDCl_3) δ 207.4, 166.5, 153.8, 135.6, 134.6, 126.4, 124.1, 120.5, 42.8, 30.1, 29.8, 20.3; IR(ATR): 731, 753, 791, 982, 1097, 1174, 1270, 1315, 1362, 1407, 1434, 1475, 1525, 1572, 1717, 2854, 2925 cm^{-1} ; HRMS-ESI (m/z): $[\text{M}+\text{H}]^+$ calculated (for $\text{C}_{12}\text{H}_{14}\text{NOS}$) 220.0796, found 220.0793.



1-(2-methylbenzo[d]oxazol-7-yl)hexan-3-one (9e):

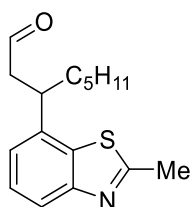
Light yellow semi solid (35 mg, 76% yield); ^1H NMR (500 MHz, CDCl_3) δ 7.48 (d, $J = 7.9$ Hz, 1H), 7.20 (t, $J = 7.7$ Hz, 1H), 7.09 (d, $J = 7.5$ Hz, 1H), 3.14 (t, $J = 7.7$ Hz, 2H), 2.85 (t, $J = 7.7$ Hz, 2H), 2.64 (d, $J = 6.2$ Hz, 3H), 2.40 (t, $J = 7.3$ Hz, 2H), 1.62 (m, 2H), 0.90 (t, $J = 7.4$ Hz, 3H); ^{13}C NMR (126 MHz, CDCl_3) δ 210.0, 163.7, 149.8, 141.4, 124.7, 124.4, 124.2, 117.5, 45.0, 42.5, 24.2, 17.4, 14.7, 13.9; IR(ATR): 667, 755, 1076, 1127, 1177, 1216, 1266, 1374,

1431, 1478, 1539, 1655, 1711, 2927, 2964 cm^{-1} ; HRMS-ESI (m/z): $[\text{M}+\text{H}]^+$ calculated (for $\text{C}_{14}\text{H}_{18}\text{NO}_2$) 232.1338, found 232.1330.



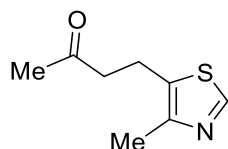
1-(2-methylbenzo[d]oxazol-7-yl)octan-3-one (9f):

Light yellow semi solid (40 mg, 77% yield); ^1H NMR (400 MHz, CDCl_3) δ 7.49 (d, $J = 7.8$ Hz, 1H), 7.20 (t, $J = 7.7$ Hz, 1H), 7.09 (d, $J = 7.5$ Hz, 1H), 3.14 (t, $J = 7.7$ Hz, 2H), 2.85 (t, $J = 7.6$ Hz, 2H), 2.64 (s, 3H), 2.41 (t, $J = 7.5$ Hz, 2H), 1.57 (s, 2H), 1.31 – 1.25 (m, 4H), 0.88 (d, $J = 6.8$ Hz, 3H); ^{13}C NMR (101 MHz, CDCl_3) δ 210.1, 163.7, 149.8, 141.5, 124.7, 124.4, 124.2, 117.5, 43.1, 42.4, 31.5, 24.3, 23.7, 22.6, 14.7, 14.0; IR(ATR): 749, 793, 924, 1047, 1176, 1265, 1379, 1430, 1578, 1614, 1716, 2860, 2928 cm^{-1} ; HRMS-ESI (m/z): $[\text{M}+\text{H}]^+$ calculated (for $\text{C}_{16}\text{H}_{22}\text{NO}_2$) 260.1651, found 260.1644.



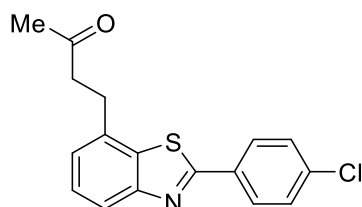
3-(2-methylbenzo[d]thiazol-7-yl)octanal (9g):

Light brown semi solid (35.5 mg, 64% yield); ^1H NMR (400 MHz, CDCl_3) δ 9.67 (t, $J = 1.8$ Hz, 1H), 7.82 (d, $J = 7.9$ Hz, 1H), 7.41 (t, $J = 7.8$ Hz, 1H), 7.17 (d, $J = 7.4$ Hz, 1H), 3.51 – 3.30 (m, 1H), 2.84 (s, 5H), 1.86 – 1.59 (m, 4H), 1.10 (dd, $J = 7.7, 4.8$ Hz, 4H), 0.81 (t, $J = 6.8$ Hz, 3H); ^{13}C NMR (101 MHz, CDCl_3) δ 201.2, 166.6, 154.0, 137.9, 135.4, 126.5, 122.7, 120.9, 49.4, 40.7, 35.3, 31.8, 27.1, 22.5, 20.3, 14.1; IR(ATR): 733, 797, 968, 1049, 1124, 1174, 1271, 1378, 1413, 1466, 1524, 1572, 1725, 2858, 2928 cm^{-1} ; GC-MS (m/z): $[\text{M}]$ calculated (for $\text{C}_{16}\text{H}_{21}\text{NOS}$) 275.1, found 275.1.



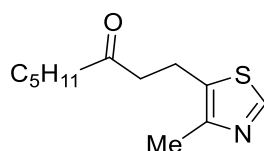
4-(4-methylthiazol-5-yl)butan-2-one (9h):

Colorless liquid (28 mg, 83% yield); ^1H NMR (500 MHz, CDCl_3) δ 8.51 (s, 1H), 2.99 (t, $J = 7.2$ Hz, 2H), 2.73 (t, $J = 7.3$ Hz, 2H), 2.36 (s, 3H), 2.13 (d, $J = 1.4$ Hz, 3H); ^{13}C NMR (126 MHz, CDCl_3) δ 206.7, 149.3, 149.0, 130.3, 44.8, 30.1, 20.2, 14.9; IR(ATR): 749, 792, 841, 888, 940, 1070, 1165, 1239, 1282, 1312, 1366, 1414, 1543, 1714, 2925, 3078 cm^{-1} ; GC-MS (m/z): [M] calculated (for $\text{C}_8\text{H}_{10}\text{NOS}$) 169.05, found 169.1.



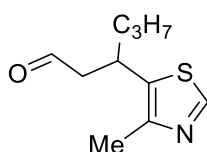
4-(2-(4-chlorophenyl)benzo[d]thiazol-7-yl)butan-2-one (9i):

Yellow color semi solid (50 mg, 79% yield); ^1H NMR (500 MHz, CDCl_3) δ 8.06 – 8.02 (m, 2H), 7.92 (d, $J = 7.7$ Hz, 1H), 7.50 – 7.46 (m, 2H), 7.46 – 7.42 (m, 1H), 7.21 (d, $J = 7.3$ Hz, 1H), 3.17 (t, $J = 7.6$ Hz, 2H), 2.93 (t, $J = 7.6$ Hz, 2H), 2.19 (s, 3H); ^{13}C NMR (101 MHz, CDCl_3) δ 207.3, 166.3, 154.5, 137.2, 135.0, 132.2, 129.4, 128.9, 127.0, 124.9, 121.5, 42.8, 30.2, 29.9; IR(ATR): 727, 789, 834, 1013, 1092, 1162, 1234, 1289, 1365, 1402, 1476, 1509, 1572, 1598, 1717, 2853, 2927, 3064 cm^{-1} ; HRMS-ESI (m/z): $[\text{M}+\text{H}]^+$ calculated (for $\text{C}_{17}\text{H}_{15}\text{ClNOS}$) 316.0563, found 316.0733.



1-(4-methylthiazol-5-yl)octan-3-one (9j):

Colorless liquid (39.5 mg, 87% yield); ^1H NMR (400 MHz, CDCl_3) δ 8.51 (s, 1H), 3.01 (t, $J = 7.3$ Hz, 2H), 2.70 (t, $J = 7.3$ Hz, 2H), 2.42 – 2.32 (m, 5H), 1.54 (dt, $J = 14.8, 7.4$ Hz, 2H), 1.29 – 1.19 (m, 4H), 0.85 (t, $J = 7.1$ Hz, 3H); ^{13}C NMR (101 MHz, CDCl_3) δ 209.3, 149.3, 149.0, 130.5, 43.8, 43.1, 31.4, 23.5, 22.5, 20.3, 14.9, 14.0; IR(ATR): 666, 756, 843, 908, 1031, 1079, 1127, 1216, 1378, 1415, 1543, 1712, 2862, 2931, 2959, 3020 cm^{-1} ; HRMS-ESI (m/z): $[\text{M}+\text{H}]^+$ calculated (for $\text{C}_{12}\text{H}_{20}\text{NOS}$) 225.1, found 225.2.

**3-(4-methylthiazol-5-yl)hexanal (9k):**

Colorless liquid (30 mg, 76% yield); ^1H NMR (400 MHz, CDCl_3) δ 9.67 (t, $J = 1.6$ Hz, 1H), 8.62 (s, 1H), 3.61 – 3.53 (m, 1H), 2.78 – 2.64 (m, 2H), 2.42 (s, 3H), 1.72 – 1.63 (m, 1H), 1.55 – 1.47 (m, 1H), 1.25 – 1.19 (m, 2H), 0.87 (t, $J = 7.3$ Hz, 3H); ^{13}C NMR (101 MHz, CDCl_3) δ 200.5, 150.0, 148.9, 135.5, 51.8, 40.4, 32.0, 20.4, 15.3, 13.9; IR(ATR): 794, 839, 931, 1035, 1107, 1182, 1238, 1311, 1381, 1419, 1458, 1542, 1723, 2725, 2874, 2931, 2959 cm^{-1} ; HRMS-ESI (m/z): $[\text{M}+\text{H}]^+$ calculated (for $\text{C}_{10}\text{H}_{16}\text{NOS}$) 198.0953, found 198.0948.

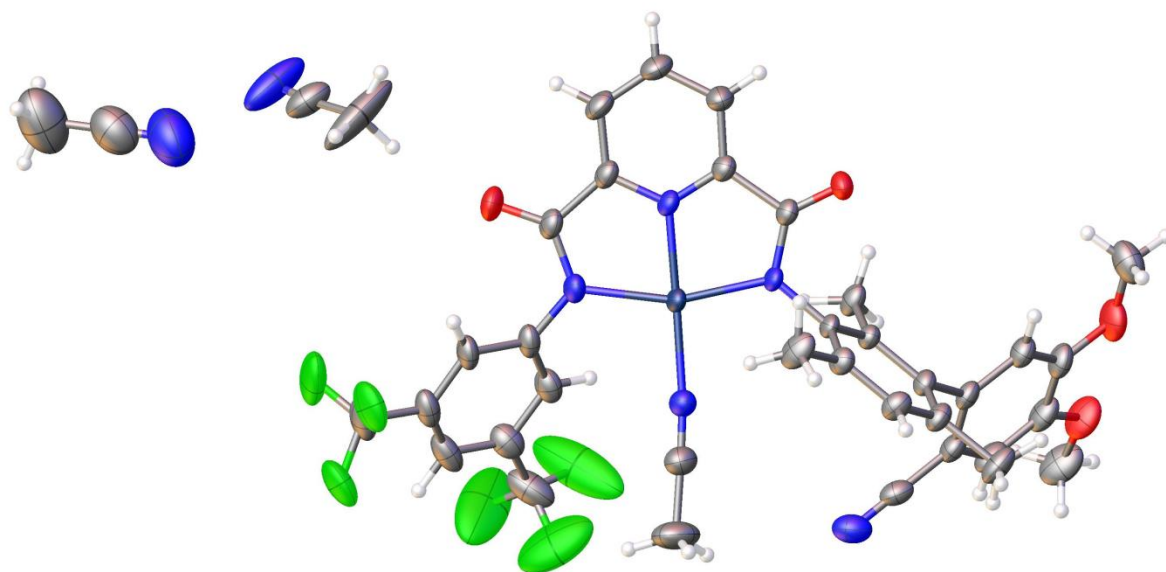


Figure 5.5: Crystal structure of **T18** (Scheme 1) (CCDC 1907082)

Cell:	a= 13.1796(3)	b= 10.8489(3)	c= 27.3741(7)
	alpha= 90	beta= 102.523(2)	gamma= 90
Temperature:	150 K		
Crystal size	0.136 x 0.112 x 0.067 mm ³		
Volume	3820.94(17)		
Space group	P 1 21/c 1		
Hall group	-P 2ybc		
Moiety formula	0.24(C ₃₅ H ₂₇ F ₆ N ₅ O ₄ Pd), 0.47(C ₂ H ₃ N)		
Data completeness=	1		
R(reflections)=	0.0507(6070)		
	Theta(max)= 25.000		
	wR2(reflections)= 0.1538(6721)		

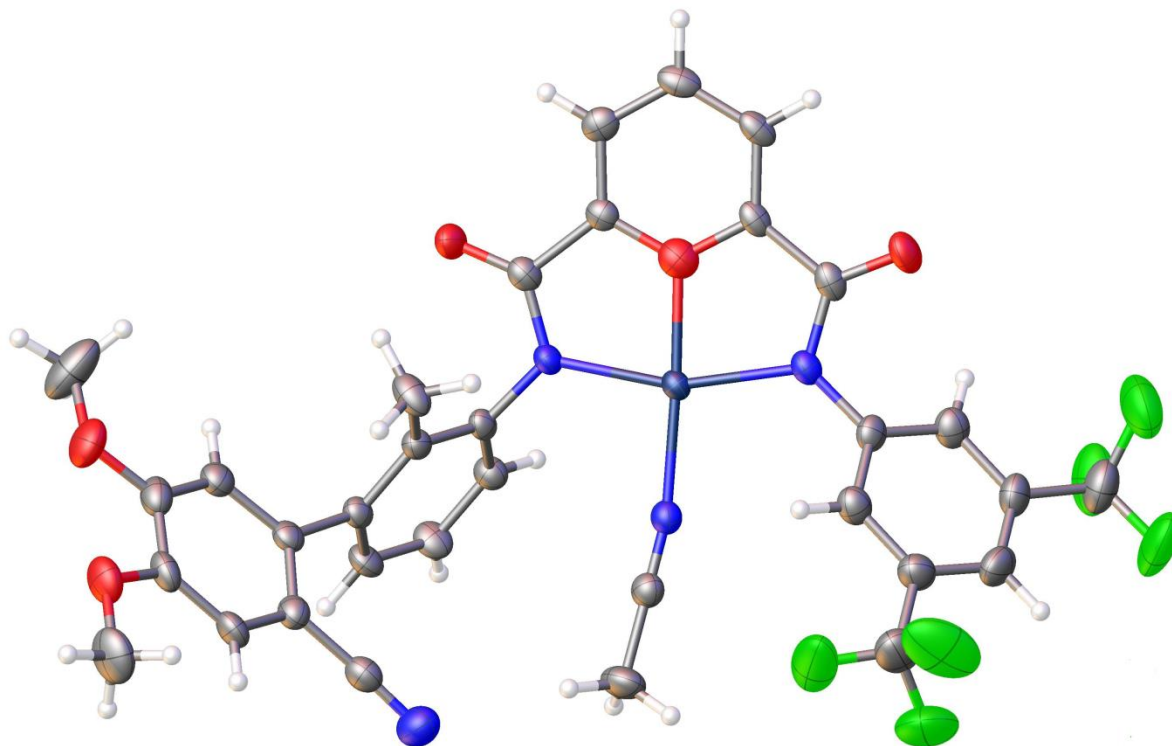


Figure 5.6: Crystal structure of **T17** (Figure 8) (CCDC 1889887)

Cell:	a= 13.6671(3)	b= 18.9509(4)	c= 30.4136(6)
	alpha= 90	beta= 97.736(2)	gamma= 90
Temperature:	150 K		
Crystal size	0.177 x 0.173 x 0.105 mm ³		
Volume	7805.5(3)		
Space group	I 1 2/a 1		
Hall group	-I 2ya		
Moiety formula	C ₃₃ H ₂₃ F ₆ N ₄ O ₅ Pd, C ₂ H ₃ N		
Data completeness=	1.000		
Theta(max)=	24.999		
R(reflections)= 0.0463(5807)	wR2(reflections)= 0.1481(6885)		

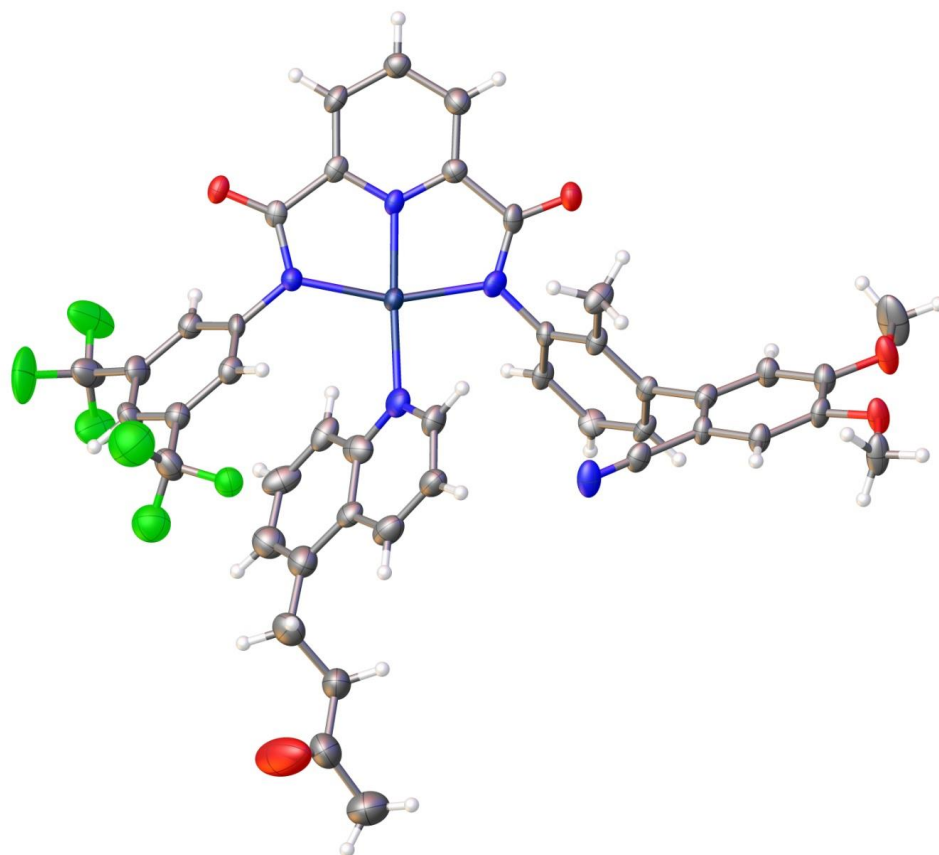


Figure 5.8: Crystal structure of **Intermediate G** (Figure 12) (CCDC 1889891)

Cell:	a= 11.5758(3)	b= 11.6676(3)	c= 15.7946(5)
	alpha= 90.986(2)	beta= 106.836(2)	gamma= 93.328(2)
Temperature:	150 K		
Crystal size	0.158 x 0.112 x 0.053 mm ³		
Volume	2037.09(10)		
Space group	P -1		
Hall group	-P 1		
Moiety formula	C ₄₄ H ₃₃ F _{4.56} N ₅ O ₅ Pd		
Data completeness= 0.999	Theta(max)= 24.999		
R(reflections)= 0.0797	wR2(reflections)= 0.2268(7162)		

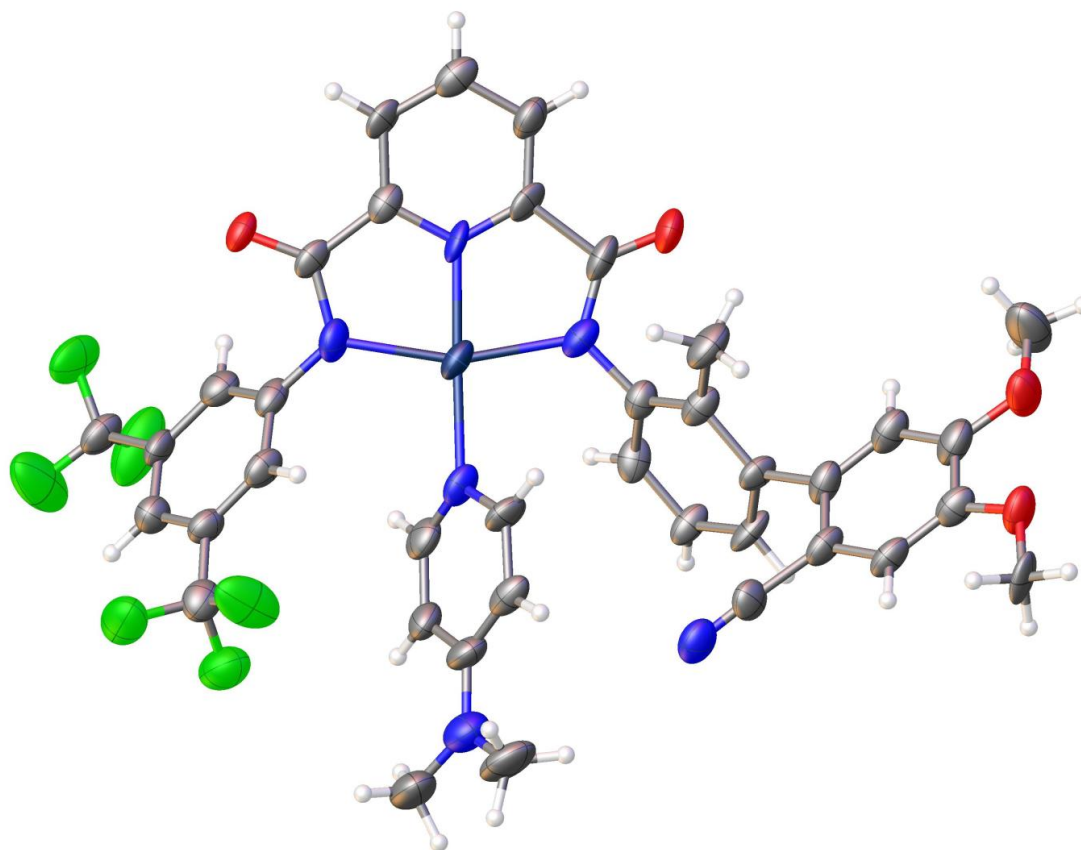
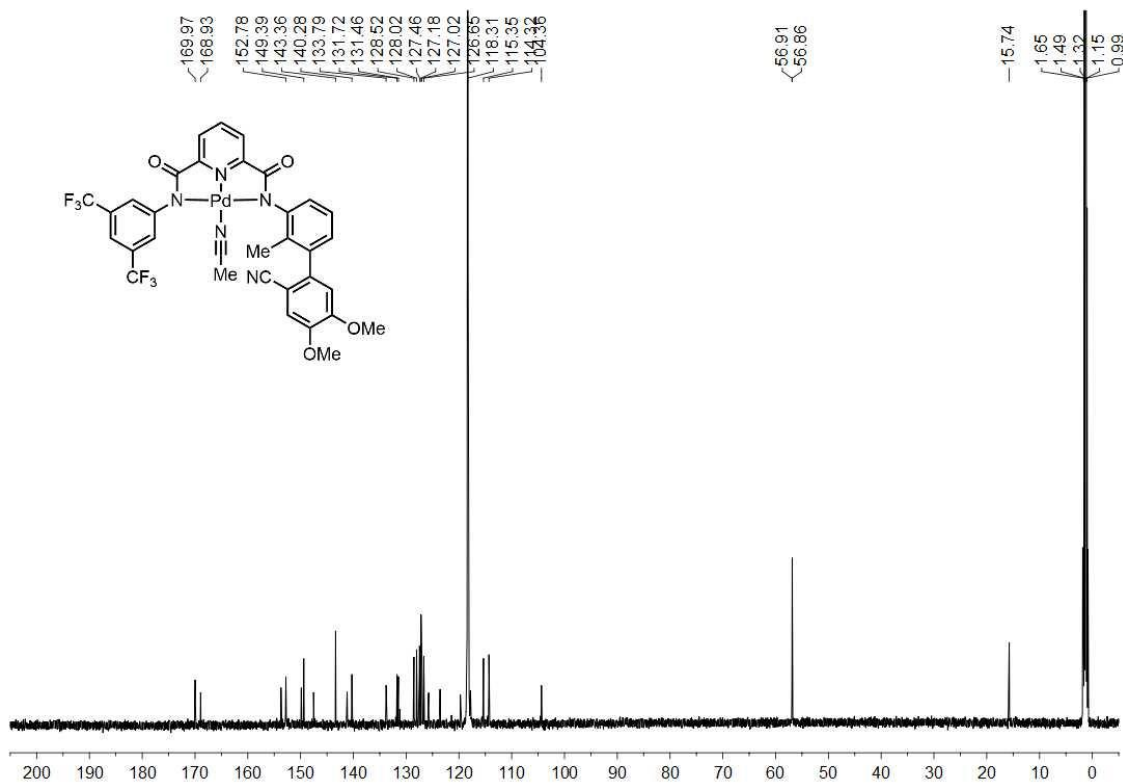
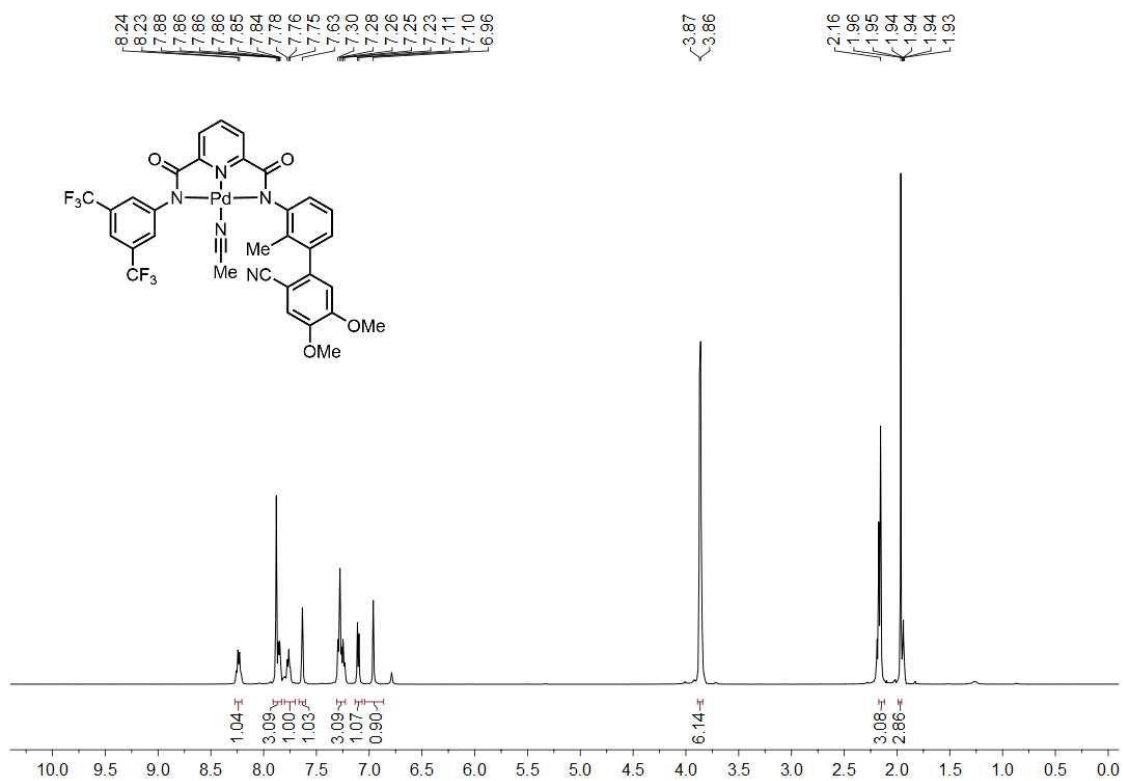
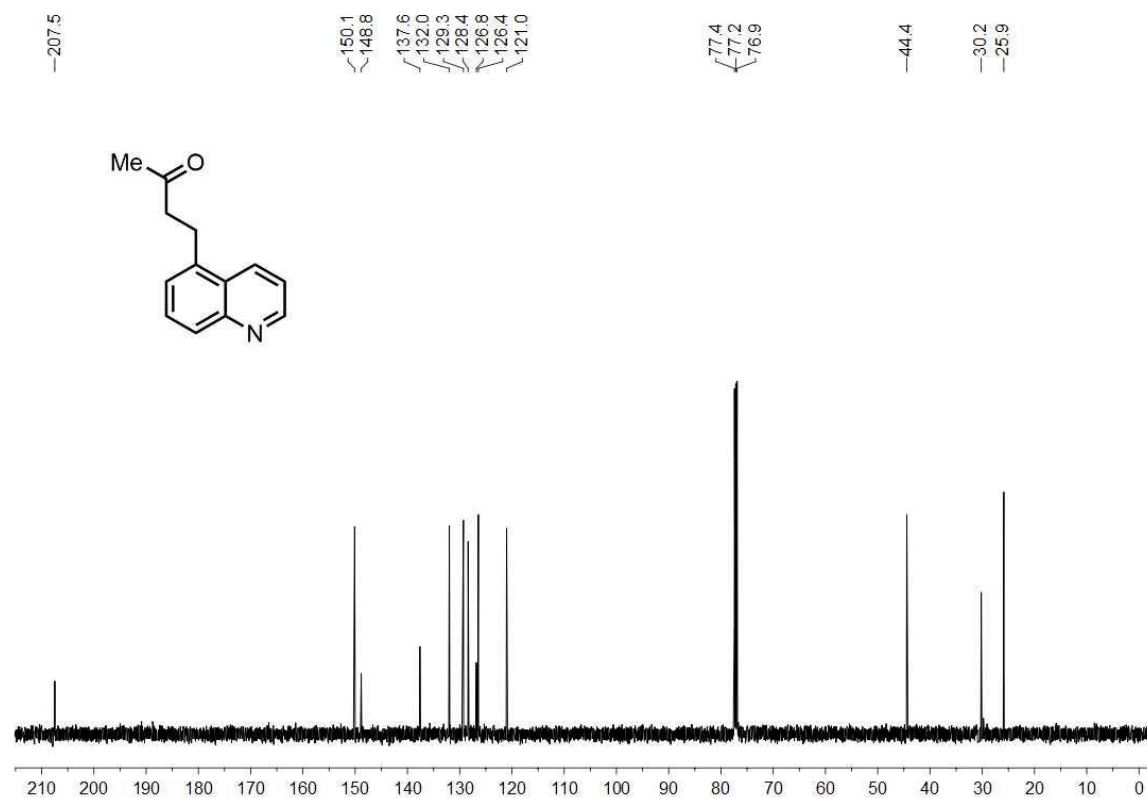
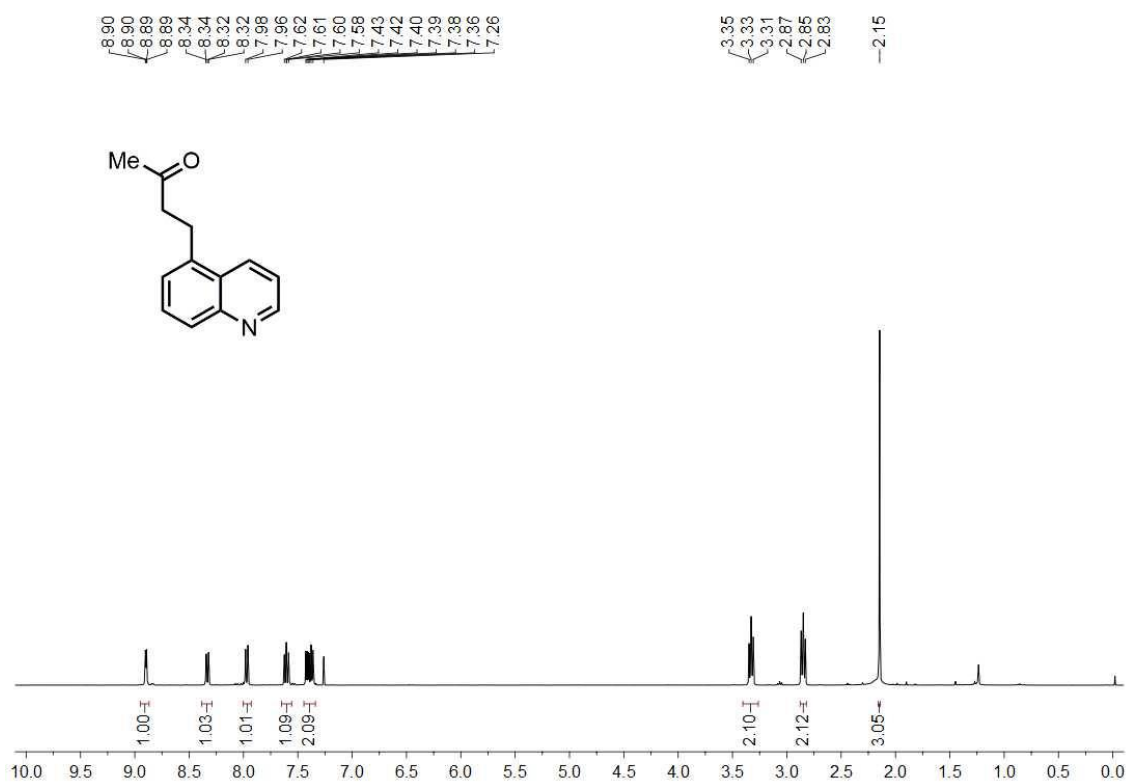


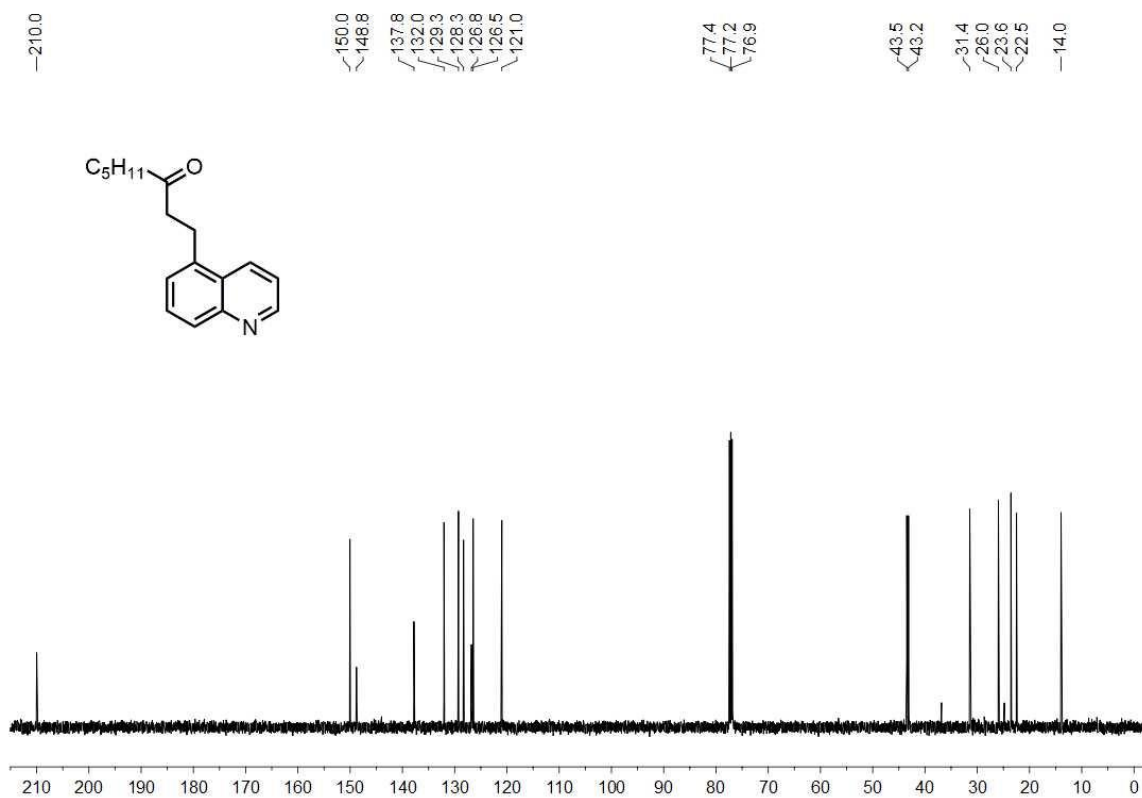
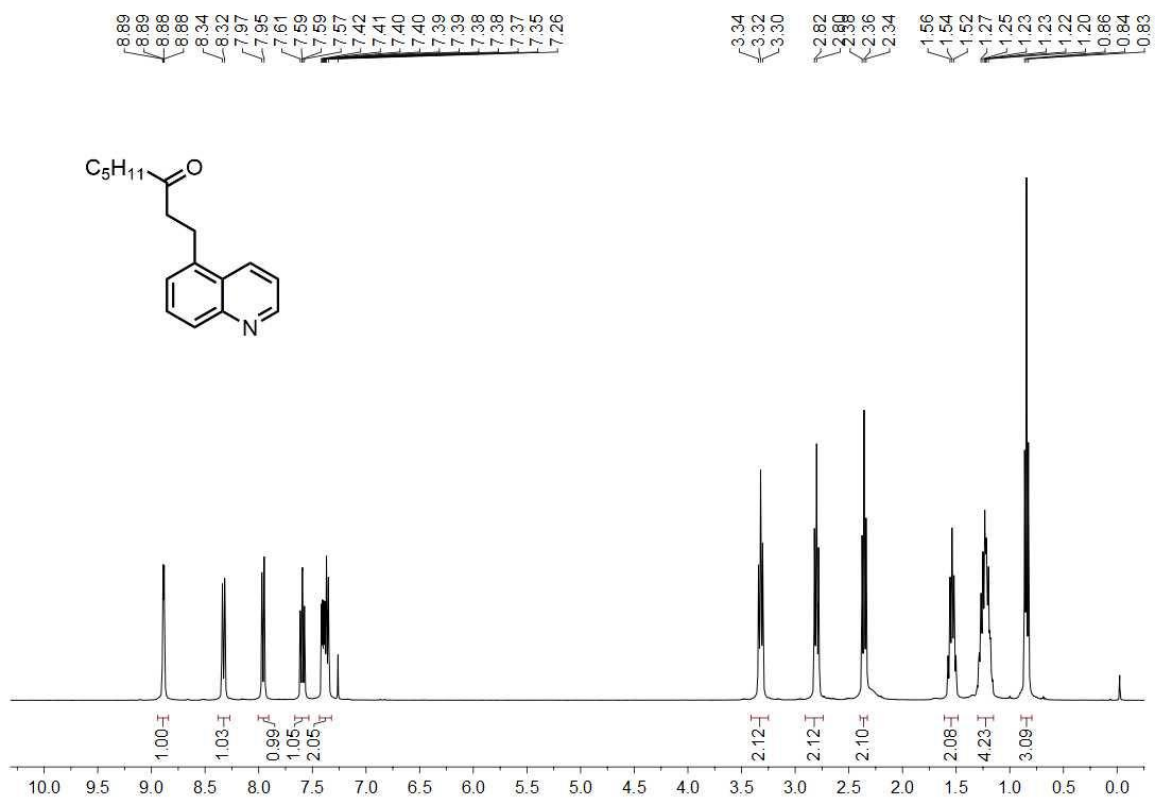
Figure 5.9: Crystal structure of **Intermediate H** (Figure 12) (CCDC 1889895)

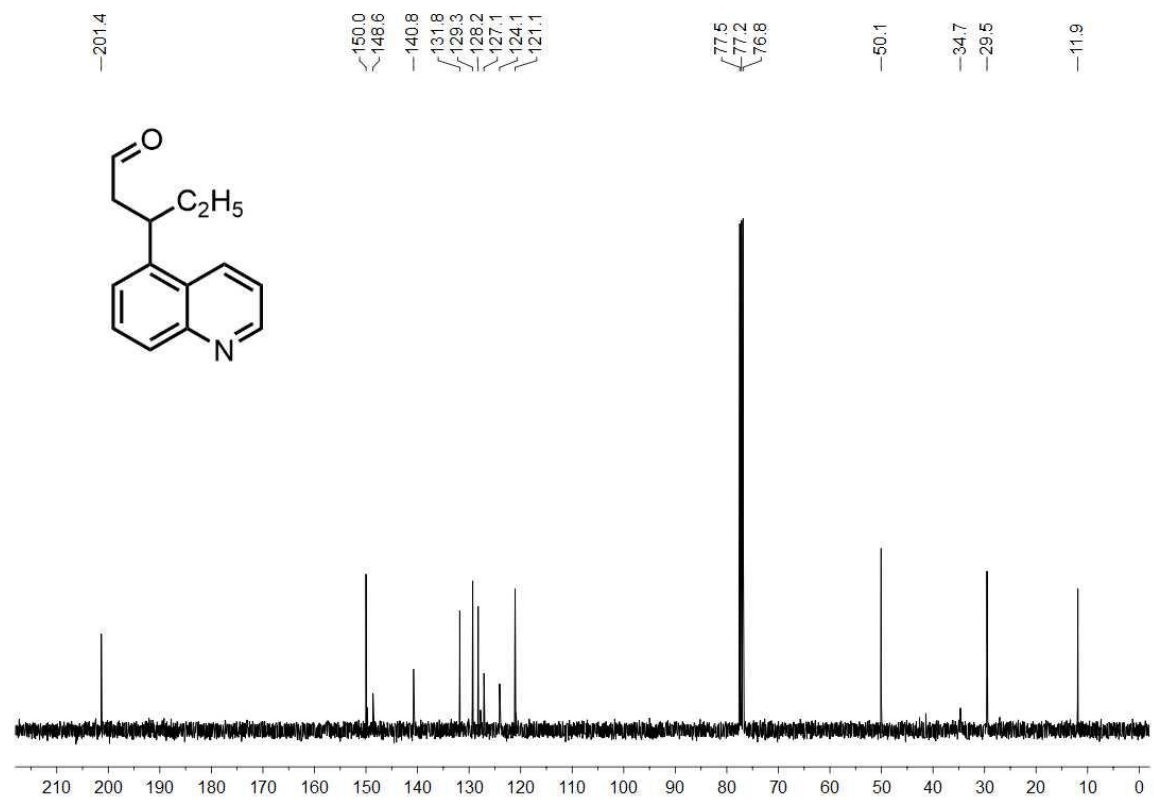
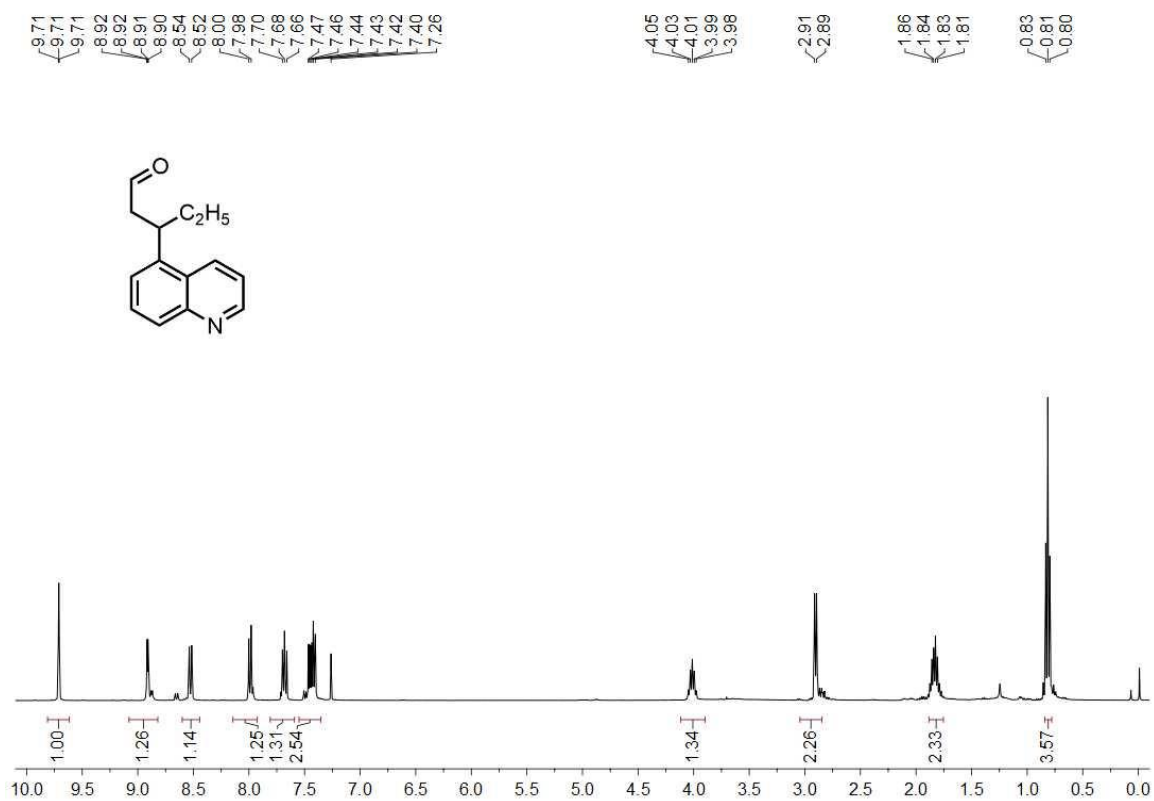
Cell:	a= 11.2235(8)	b= 11.6701(6)	c= 16.2740(12)
	alpha= 108.691(6)	beta= 92.161(6)	gamma= 90.467(5)
Temperature:	150 K		
Crystal size	0.21 x 0.102 x 0.021 mm ³		
Volume	2017.2(2)		
Space group	P -1		
Hall group	-P 1		
Moiety formula	C ₃₈ H ₃₀ F ₆ N ₆ O ₄ Pd		
Data completeness=	0.986		
Theta(max)=	64.997		
R(reflections)=	0.0923		
wR2(reflections)=	0.3357(6755)		

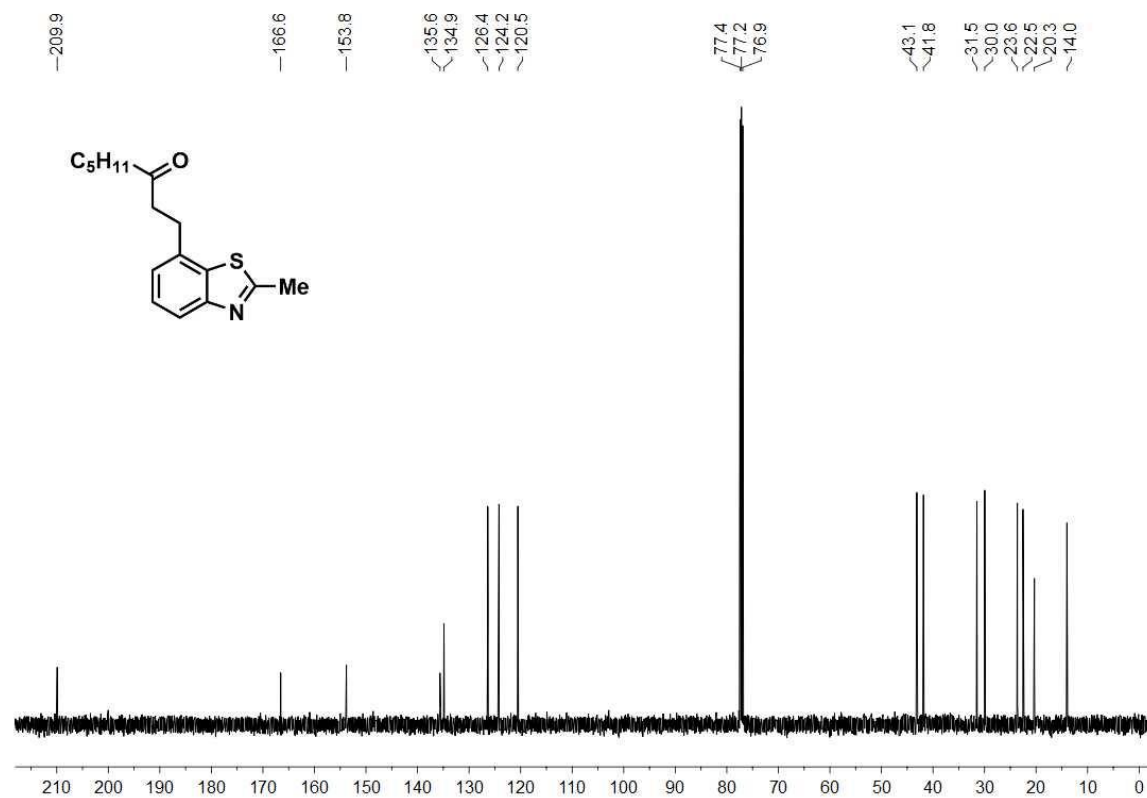
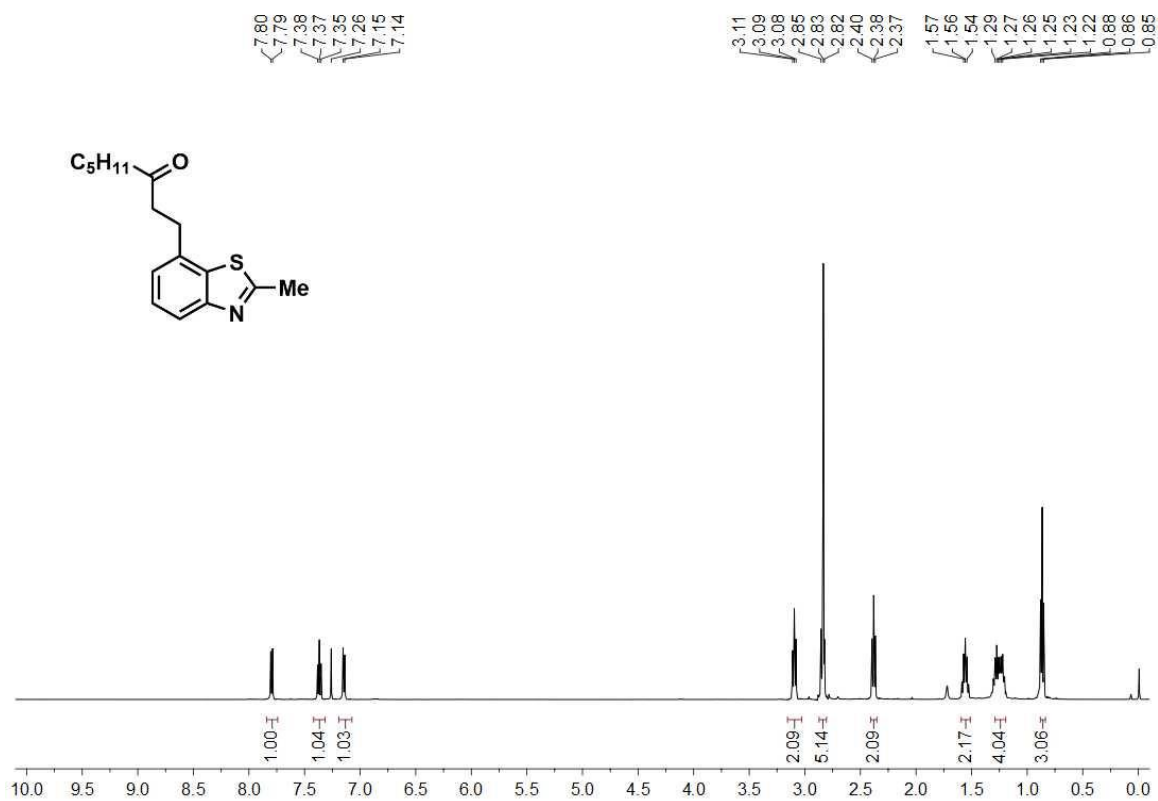
5.4.6. Representative NMR spectra:

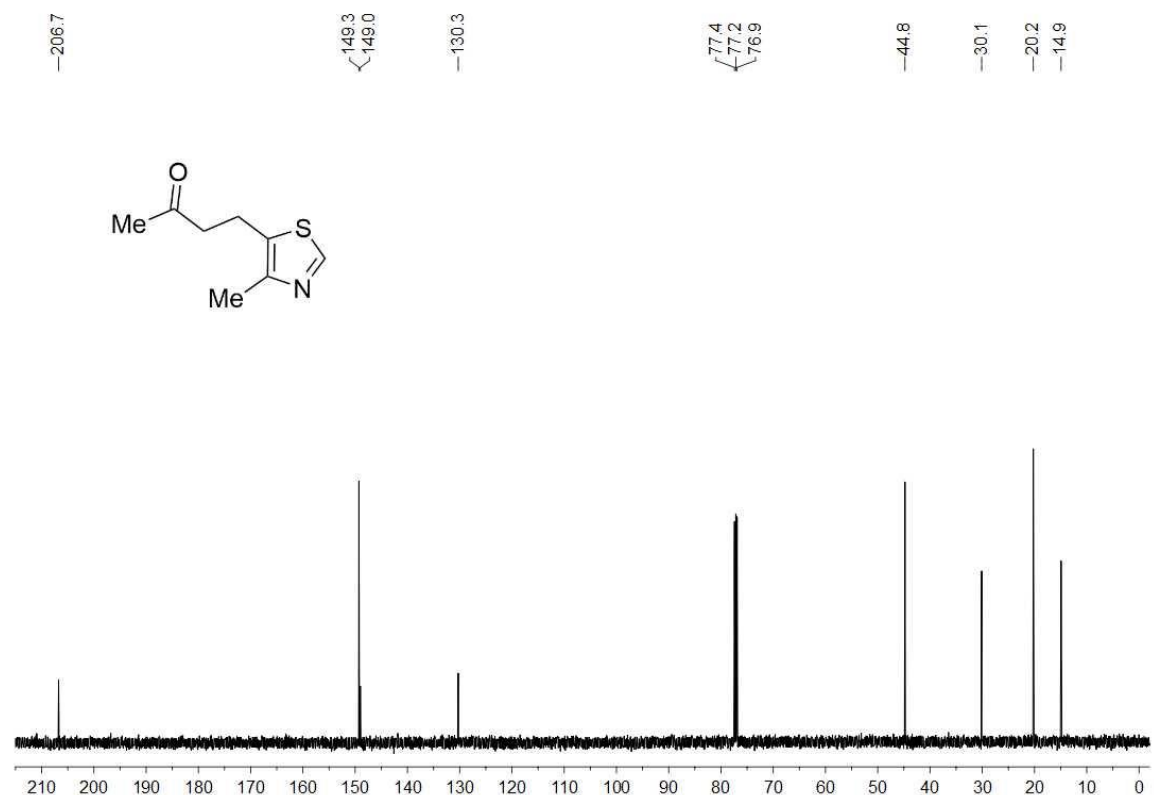
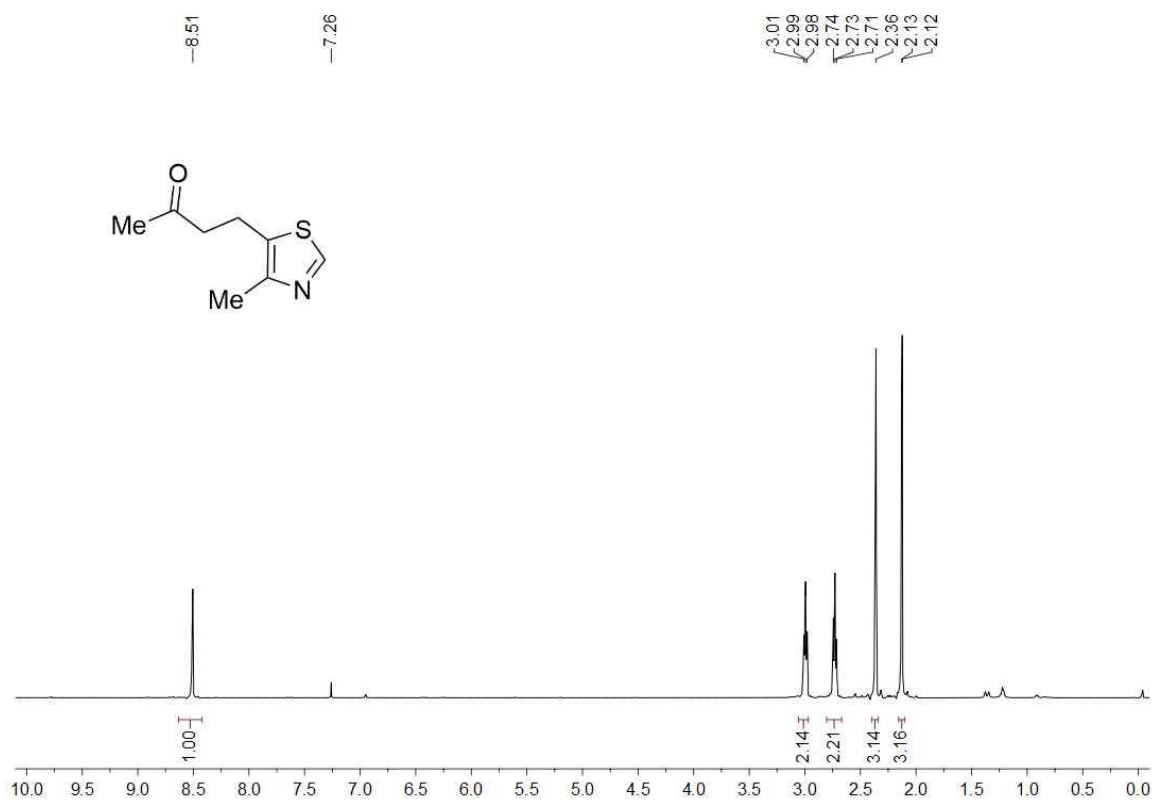












5.5. References:

1. a) J. Yamaguchi, A. D. Yamaguchi, K. Itami, *Angew. Chem. Int. Ed.* **2012**, *51*, 8960–9009; b) J. Wencel-Delord, F. Glorius, *Nat. Chem.* **2013**, *5*, 369-375; c) P. Gandeepan, T. Müller, D. Zell, G. Cera, S. Warratz, L. Ackermann, *Chem. Rev.* **2019**, *119*, 2192-2452.
2. a) L. Fu, D. M. Guptill, H. M. L. Davies, *J. Am. Chem. Soc.*, **2016**, *138*, 5761-5764; b) H. M. L. Davies, D. Morton, *ACS Cent. Sci.* **2017**, *3*, 936–943; c) D. Dailier, R. Rocaboy, O. Baudoin, *Angew. Chem. Int. Ed.* **2017**, *56*, 7218–7222; d) L. Yang, M. Neuburger, O. Baudoin, *Angew. Chem. Int. Ed.* **2018**, *57*, 1394–1398; e) B. Li, X. Li, B. Han, Z. Chen, X. Zhang, G. He, G. Chen, *J. Am. Chem. Soc.* **2019**, DOI: doi.org/10.1021/jacs.9b04221.
3. a) L. Ackermann, R. Vicente, A. R. Kapdi, *Angew. Chem. Int. Ed.* **2009**, *48*, 9792–9826; b) U. K. Sharma, H. P. L. Gemoets, F. Schröder, T. Noël, E. V Van der Eycken, *ACS Catal.* **2017**, *7*, 3818–3823; c) C. Sambigioglio, D. Schönbauer, R. Blicke, T. Dao-Huy, G. Pototschnig, P. Schaaf, T. Wiesinger, M. F. Zia, J. Wencel-Delord, T. Besset, B. U. W. Maes, *Chem. Soc. Rev.* **2018**, *47*, 6603–6743; d) S. Rej, N. Chatani, *Angew. Chem. Int. Ed.* **2019**, DOI: 10.1002/anie.201808159.
4. a) A. Nerush, M. Vogt, U. Gellrich, G. Leitus, Y. Ben-David, D. Milstein, *J. Am. Chem. Soc.* **2016**, *138*, 6985–6997; b) P. Daw, S. Chakraborty, J. A. Garg, Y. Ben-David, D. Milstein, *Angew. Chem. Int. Ed.* **2016**, *55*, 14373–14377; c) B. Shrestha, P. Basnet, R. K. Dhungana, S. KC, S. Thapa, J. M. Sears, R. Giri, *J. Am. Chem. Soc.* **2017**, *139*, 10653-10656; d) P. Basnet, S. KC, R. K. Dhungana, B. Shrestha, T. J. Boyle, R. Giri, *J. Am. Chem. Soc.* **2018**, *140*, 15586-15590; e) W. Wang, M. M. Lorion, J. Shah, A. R. Kapdi, L. Ackermann, *Angew. Chem. Int. Ed.* **2018**, *57*, 14700–14717; f) J. A. L. Urrutia, M. Solà, D. Milstein, A. Poater, *J. Am. Chem. Soc.* **2019**, DOI: 10.1021/jacs.8b11308.
5. For selected examples of sp² C–H activation, see: a) S. Paul, G. A. Chotana, D. Holmes, R. C. Reichle, R. E. Maleczka, M. R. Smith, *J. Am. Chem. Soc.* **2006**, *128*, 15552-15553;

- b) S. M. Preshlock, D. L. Plattner, P. E. Maligres, S. W. Krska, R. E. Maleczka Jr., M. R. Smith III, *Angew. Chem. Int. Ed.* **2013**, *52*, 12915-12919; c) B. Ghaffari, S. M. Preshlock, D. L. Plattner, R. J. Staples, P. E. Maligres, S. W. Krska, R. E. Maleczka, M. R. Smith, *J. Am. Chem. Soc.* **2014**, *136*, 14345-14348; d) A. D. Yamaguchi, K. M. Chepiga, J. Yamaguchi, K. Itami, H. M. L. Davies, *J. Am. Chem. Soc.*, **2015**, *137*, 644-647; e) H. P. L. Gemoets, I. Kalvet, A. V. Nyuchev, N. Erdmann, V. Hessel, F. Schoenebeck, T. Noël, *Chem. Sci.*, **2017**, *8*, 1046-1055; f) B. Li, K. Seth, B. Niu, L. Pan, H. Yang, H. Ge, *Angew. Chem. Int. Ed.* **2018**, *57*, 3401–3405; g) A. Reding, P. G. Jones, D. B. Werz, *Angew. Chem. Int. Ed.* **2018**, *57*, 10610–10614; h) Q. Lu, S. Mondal, S. Cembellín, F. Glorius, *Angew. Chem. Int. Ed.* **2018**, *57*, 10732–10736; i) Y. Shen, Y. Gu, R. Martin, *J. Am. Chem. Soc.* **2018**, *140*, 12200–12209.
6. For selected examples of sp³ C–H activation, see: a) X. Wu, Y. Zhao, G. Zhang, H. Ge, *Angew. Chem. Int. Ed.* **2014**, *53*, 3706–3710; b) K. Liao, S. Negretti, D. G. Musaev, J. Bacsá, H. M. L. Davies, *Nature*, **2016**, *533*, 230-234; c) Yang, Q. Li, Y. Liu, G. Li, H. Ge, *J. Am. Chem. Soc.* **2016**, *138*, 12775-12778; d) K. Yang, Q. Li, Y. Liu, G. Li, H. Ge, *J. Am. Chem. Soc.* **2016**, *138*, 12775–12778; e) H. Wang, H.-R. Tong, G. He, G. Chen, *Angew. Chem. Int. Ed.* **2016**, *55*, 15387–15391; f) Y. Liu, H. Ge, *Nat. Chem.* **2017**, *9*, 26-32; g) W. Wang, M. M. Lorion, O. Martinazzoli, L. Ackermann, *Angew. Chem. Int. Ed.* **2018**, *57*, 10554–10558; h) G. Laudadio, S. Govaerts, Y. Wang, D. Ravelli, H. F. Koolman, M. Fagnoni, S. W. Djuric, T. Noël, *Angew. Chem. Int. Ed.* **2018**, *57*, 4078–4082; i) Y. Gu, Y. Shen, C. Zarate, R. Martin, *J. Am. Chem. Soc.* **2019**, *141*, 127–132; j) B.-B. Zhan,; J. Fan, L. Jin, B.-F. Shi, *ACS Catal.* **2019**, *9*, 3298–3303.
7. A. Dey, S. K. Sinha, T. K. Achar, D. Maiti, *Angew. Chem. Int. Ed.* **2019**, DOI:10.1002/anie.201812116.

8. For selected examples of *meta* C–H activation, see: a) D. Leow, G. Li, T.-S. Mei, J.-Q. Yu, *Nature* **2012**, *486*, 518; b) S. Bag, R. Jayarajan, R. Mondal, D. Maiti, *Angew. Chem. Int. Ed.* **2017**, *56*, 3182–3186; c) Q. Ding, S. Ye, G. Cheng, P. Wang, M. E. Farmer, J.-Q. Yu *J. Am. Chem. Soc.* **2017**, *139*, 417–425; d) Z. Ruan, S.-K. Zhang, C. Zhu, P. N. Ruth, D. Stalke, L. Ackermann, *Angew. Chem. Int. Ed.* **2017**, *56*, 2045–2049; e) R. Jayarajan, J. Das, S. Bag, R. Chowdhury, D. Maiti, *Angew. Chem. Int. Ed.* **2018**, *57*, 7659–7663; f) H.-J. Xu, Y.-S. Kang, H. Shi, P. Zhang, Y.-K. Chen, B. Zhang, Z.-Q. Liu, J. Zhao, W.-Y. Sun, J.-Q. Yu, Y. Lu, *J. Am. Chem. Soc.* **2019**, *141*, 76–79.
9. H. P. L. Gemoets, G. Laudadio, K. Verstraete, V. Hessel, T. Noël, *Angew. Chem. Int. Ed.* **2017**, *56*, 7161–7165.
10. For selected examples of *para* C–H activation, see: a) S. Bag, T. Patra, A. Modak, A. Deb, S. Maity, U. Dutta, A. Dey, R. Kancherla, A. Maji, A. Hazra, M. Bera, D. Maiti, *J. Am. Chem. Soc.* **2015**, *137*, 11888–11891; b) L. Yang, K. Semba, Y. Nakao, *Angew. Chem. Int. Ed.* **2017**, *56*, 4853–4857; c) A. Maji, A. Dahiya, G. Lu, T. Bhattacharya, M. Brochetta, G. Zanoni, P. Liu, D. Maiti, *Nat. Commun.* **2018**, *9*, 3582–3592; d) M. Li, M. Shang, H. Xu, X. Wang, H.-X. Dai, J.-Q. Yu, *Org. Lett.* **2019**, *21*, 540–544.
11. For selected examples of distal aliphatic C–H activation, see: b) A. Deb, S. Bag, R. Kancherla, D. Maiti, *J. Am. Chem. Soc.* **2014**, *136*, 13602–13605; a) S. Guin, P. Dolui, X. Zhang, S. Paul, V. K. Singh, S. Pradhan, H. B. Chandrashekar, S. S. Anjana, R. S. Paton, D. Maiti, *Angew. Chem. Int. Ed.* **2019**, *58*, 5633–5638.
12. H. J. Davis, R. J. Phipps, *Chem. Sci.* **2017**, *8*, 864–877.
13. a) P. C. Roosen, V. A. Kallepalli, B. Chattopadhyay, D. A. Singleton, R. E. Maleczka, M. R. Smith, *J. Am. Chem. Soc.* **2012**, *134*, 11350–11353; b) Y. Kuninobu, H. Ida, M. Nishi, M. Kanai, *Nat. Chem.* **2015**, *7*, 712–717; c) R. Bisht, B. Chattopadhyay, *J. Am. Chem. Soc.* **2016**, *138*, 84–87; d) H. J. Davis, M. T. Mihai, R. J. Phipps, *J. Am. Chem. Soc.* **2016**, *138*,

- 12759–12762; e) H. J. Davis, G. R. Genov, R. J. Phipps, *Angew. Chem. Int. Ed.* **2017**, *56*, 13351–13355; f) M. T. Mihai, H. J. Davis, G. R. Genov, R. J. Phipps, *ACS Catal.* **2018**, *8*, 3764–3769; g) M. E. Hoque, R. Bisht, C. Haldar, B. Chattopadhyay, *J. Am. Chem. Soc.* **2017**, *139*, 7745–7748; h) H. L. Li, Y. Kuninobu, M. Kanai, *Angew. Chem. Int. Ed.* **2017**, *56*, 1495–1499; i) X. Lu, Y. Yoshigoe, H. Ida, M. Nishi, M. Kanai, Y. Kuninobu, *ACS Catal.* **2019**, *9*, 1705–1709; j) R. Bisht, M. E. Hoque, B. Chattopadhyay, *Angew. Chem. Int. Ed.* **2018**, *57*, 15762–15766; k) L. Yang, N. Uemura, Y. Nakao, *J. Am. Chem. Soc.* **2019**, *141*, 7972–7979.
14. a) Z. Zhang, K. Tanaka, J. -Q. Yu, *Nature* **2017**, *543*, 538–542; b) T. K. Achar, K. Ramakrishna, S. Porey, T. Pal, P. Dolui, J. P. Biswas, D. Maiti, *Chem. Eur. J.* **2018**, *24*, 17906–17910; c) T. K. Achar, J. P. Biswas, S. Porey, T. Pal, K. Ramakrishna, S. Maiti, D. Maiti, *J. Org. Chem.* **2019**, DOI: 10.1021/acs.joc.9b01074.

List of publications:

1. **Biswas, J. P.**; Kankanala, R.; Jana, S.; Achar, T. K.; Porey, S.; Maiti, D. *Angew. Chem. Int. Ed.* **2019**, *58*, 13808-13812
2. **Biswas, J. P.**; Ansari, M.; Paik, A.; Sasmal, S.; Paul, S.; Rana, S.; Rajaraman, G.; Maiti, D. *Angew. Chem. Int. Ed.* **2021**, *60*, 14030-14039
3. **Biswas, J. P.**; Guin, S.; Maiti, D. *Coord. Chem. Rev.* **2020**, *408*, 213174
4. Rana, S.; **Biswas, J. P.**; Sen, A.; Clemency, M.; Blondin, G.; Latour, J-M.; Rajaraman, G.; Maiti, D. *Chem. Sci.* **2018**, *9*, 7843-7858
5. Achar, T. K.; Ramakrishna, K.; Pal, T.; Porey, S.; Dolui, P.; **Biswas, J. P.**; Maiti, D. *Chem. Eur. J.* **2018**, *24*, 17906-17910
6. Achar, T. K.; **Biswas, J. P.**; Porey, S.; Pal, T.; Ramakrishna, K.; Maiti, S.; Maiti, D. *J. Org. Chem.* **2019**, *84*, 8315–8321
7. Coin, G; Patra, R.; Rana, S; **Biswas, J.P.**; Dubourdeaux, P; Clémancey, M.; de Visser, S. P.; Maiti, D.; Maldivi, P.; Latour, J-M. *ACS Catal.* **2020**, *10*, 10010–10020
8. Das, J.; Dolui, P.; Ali, W.; **Biswas, J. P.**; Chandrashekar, H. B.; Prakash, G; Maiti, D. *Chem. Sci.* **2020**, *11*, 9697-9702
9. Rana, S.; **Biswas, J. P.**; Paul, S.; Paik, A.; Maiti, D. *Chem. Soc. Rev.* **2021**, *50*, 243-472
10. Basak, S.; **Biswas, J. P.**; Maiti, D. *Synthesis*, **2021**, *53*, 3151-3179
11. Bhagat, K. K.; **Biswas, J. P.**; Dutta, S.; Maiti, D. *Helv. Chim. Acta.* **2022**, *105*, e202100192
12. Sinha, S. K.; Guin, S.; Maiti, S.; **Biswas, J. P.**; Porey, S.; Maiti, D. *Chem. Rev.* **2022**, *122*, 5682–5841

13. Mandal, D.; Roychowdhury, S.; **Biswas, J. P.**; Maiti, S.; Maiti, D. *Chem. Soc. Rev.*, **2022**, *Accepted*
14. **Biswas, J. P.**; Maiti, D. Supramolecular interactions in distal C-H activation of (hetero)arenes. *Wiley-VCH*, **2021**